CHARACTERISATION OF VIRULENCE FUNCTIONS ENCODED BY HUMAN CYTOMEGALOVIRUS

A thesis submitted in candidature for the degree of

DOCTOR OF PHILOSOPHY

By

Melanie Armstrong

July 2007

Department of Medical Microbiology
Cardiff University
Cardiff, CF14 4XX, UK

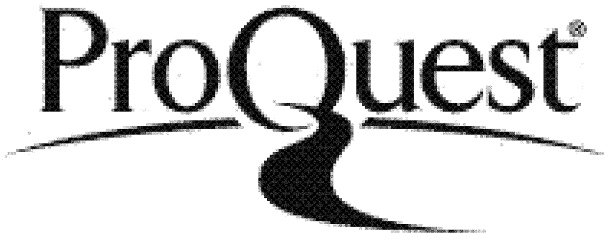

ProQuest LLC
789 East Eisenhower Parkway
P.O. Box 1346
Ann Arbor, MI 48106-1346

DECLARATION

This work has not previously been accepted in substance for any degree and is not concurrently submitted in candidature for any degree.

Signed ..... (Melanie Armstrong)
Date.....

STATEMENT 1

This thesis is the result of my own independent investigation, except where otherwise stated.

Signed ..... (Melanie Armstrong)
Date .....
Signed..... (Professor Gavin Wilkinson)
Date.....

STATEMENT 2

I hereby give consent for my thesis, if accepted, to be available for photocopying and for inter-library loan, and for the title and summary to be made available to outside organisations.

Signed ..... (Melanie Armstrong)
Date .....

ACKNOWLEDGEMENTS

I would firstly like to thank my supervisor, Professor Gavin Wilkinson, whose constant encouragement, advice and hard work has made this project possible, and is greatly appreciated.

I would like to thank my colleagues in the Medical Microbiology and Medical Biochemistry departments for their help, support and friendship throughout this project, and for helping make my PhD a very enjoyable experience. Special thanks goes to Dr Virginie Prod'homme for her work in generating the UL/*b'* RAds and the CD107 NK assays, Dr Peter Tomasec for his work with UL141 and support in generating recombinant adenoviruses, Dr Brian McSharry for his work with UL130 and Dr Richard Stanton for his work in producing the AdZ system and UL14 deletion mutant. Thanks also to Dr Becky Aichler for her patience and support with NK cloning. Their contributions to this study have been invaluable. Thanks also to Dr Eddie Wang, Dr Carole Rickards and Sian Llewellyn-Lacey, for all their advice and support throughout this study and to the MRC for funding me.

I would also like to thank my family, and in particular Robin, for all their understanding and unfailing support over the last three years.

ABSTRACT

HCMV is the largest human virus characterised to date, encoding approximately 165 open reading frames (ORFs). Due to many years of serial passage, laboratory adapted strains of HCMV, such as strain AD169, have lost a 13-15kb region of genome, designated UL/*b'*, compared with HCMV clinical strains (Cha *et al.*, 1996). Loss of this 13-15kb UL/*b'* region is correlated with decreased virulence and increased sensitivity to Natural Killer (NK) cell lysis, leading to the hypothesis that the UL/*b'* region is harbouring one or more NK evasion functions. A comprehensive screen of the UL/*b'* region of HCMV strain Merlin to identify novel NK evasion functions has formed the focus of this study.

The UL/*b'* region encompasses 23 ORFs from UL128 through to UL150. In addition, UL14, a homologue of the UL/*b'* resident ORF UL141, and UL141A, a newly identified UL/*b'* ORF, were included in this study as potential NK evasion functions. Using the AdEasy system and the newly developed AdZ system, the generation of recombinant adenoviruses (RAds) encoding for each of the 24 UL/*b'* ORFs, plus the UL141 homologue, UL14, has been successful and provides a complete resource for the study of these proteins. The majority of the UL/*b'* proteins were previously uncharacterised, and the incorporation of a C-terminal Streptag II has enabled preliminary characterisation of these ORFs. Producing the bank of UL/*b'* RAds has also enabled a functional screen of this region in order to identify novel NK evasion functions.

As a result of the systematic functional NK screen of the UL/*b'* region, two novel NK evasion functions have been identified; the UL141 homologue, UL14 and the UL/*b'* resident ORF, UL135. Their identification brings the total number of NK evasion functions encoded by HCMV up to eight: UL40, UL16, UL18, UL83 (pp65), UL141, UL142, UL14 and UL135. These provide HCMV with an impressive arsenal dedicated to evasion of NK lysis, and are further evidence for the importance of NK cells in the control of HCMV.

Further analysis of the NK evasion function encoded by UL14 revealed that similar to UL141, UL14 encodes an EndoH sensitive glycoprotein and was observed to co-localise with the ER resident protein, calnexin, consistent with gpUL14 being ER-retained. The biochemical similarities of the UL141 and UL14 NK evasion ORFs may be of functional significance, indicating that gpUL14 may also be sequestering an NK activating ligand within the cell similar to gpUL141 (Tomasec *et al.*, 2005).

TABLE OF CONTENTS

LIST OF TABLES

LIST OF FIGURES

SUPPLIERS AND COMPANY ADDRESSES

Abcam, Cambridge, UK
Abnova Corp, Taipai, Taiwan
Alpha Diagnostics, USA
Applied Biosystems, Foster City, USA
ATCC, Teddington, Middlesex, UK
BDH Ltd, Poole, UK
BdBiosciences/ BdPharmingen, Cowley, Oxford, UK
Biochrom AG, Berlin, Germany
BioRad, Hercules, California, USA
Cell Genix, Frieburg, Germany
Cetus Corp, Emeryville, USA
Chemicon, Chandlers Ford, Hampshire, UK
Clontech, Basingstoke, UK
CP Pharmaceuticals Ltd, Clywdd, UK
Dakocytomation, Cambridge, UK
Dynal, Wirral, UK
ECACC, Porton Down, Salisbury, UK
Eurogentec, Southampton, UK
Fisher Scientific, Loughborough, UK
GE Healthcare, Buckingham, UK
Hammatsu, Japan
IBA, Göttingen, Germany
Immunotech, Marseille, France
ImmunoTools, Friesoythe, Germany
Improvision, Coventry, UK
Invitrogen, Paisley, UK
Leica, Germany
Melford, Ipswich, UK
Merck, West Drayton, UK
Molecular Probes, Invitrogen, Groningen, The Netherlands
NEB, Hitchin, UK
Oxoid, Hampshire, UK
Perkin-Elmer, Boston, USA
Pierce, Rockford, USA
Promega, Southampton, UK
Qiagen, Sussex, UK
R&D, Abingdon, Oxford, UK
Welsh Regional Transfusion Centre, Rhydlafar, Llantrisant, UK
Roche, Mannheim, Germany
SantaCruz Biotechnology Inc, Santa Cruz, California, USA
SA Scientific Ltd, San Antonio, Texas, USA
Serotec, (AbD Serotec) Kidlington, Oxford, UK
Sigma-Aldrich, Poole, UK
USB, Cleveland, USA
UVP, Cambridge, UK

ABBREVIATIONS

°C	Degrees Centigrade
µC	MicroCurie
µM	Micromolar
µm	Micromoles
µg	Microgram
µl	Microlitre
l	Litre

A

AB	Human AB Serum
Ad	Adenovirus
Ad5	Adenovirus Serotype-5
ADCC	Antibody Dependent Cellular Cytotoxicity
AD169ΔUL14	HCMV Strain AD169 UL14 Deletion Mutant
AD169ΔUL16	HCMV Strain AD169 UL16 Deletion Mutant
AF594	Alexa Fluor 494
ATCC	American Type Culture Collection
AP	Assembly Protein

B

B_2m	β_2-microglobulin
BAC	Bacterial Artificial Chromosome
BLAST	Basic Local Alignment Search Tool
BTLA	B and T cell Attenuator
bp	Base Pairs

C

CCMV	Chimpanzee Cytomegalovirus
CD	Cluster Determinant
CEACAM1	Carcinoembryonic Antigen Adhesion Molecule 1
CEA	Carcinoembryonic Antigen
CLTs	CMV Latency-Associated Transcripts
CO_2	Carbon Dioxide
CPE	Cytopathic Effect
CPM	Counts Per Minute
crs	*cis* Repression Signal
CTL	Cytotoxic T Lymphocyte

D

D	Donor
DABCO	1,4-Diazabicyclo[2.2.2]octane
DAPI	2-(4-Amidinophenyl)-6-indolecarbamidine dihydrochloride
DMEM	Dulbeccos Modified Eagle's Medium
DMF	N, N-dimethyl formamide
DMSO	Dimethyl Sulphoxide
DNA	Deoxyribonucleic Acid
dNTP	Deoxynucleotide Triphosphate
dsDNA	Double Stranded DNA
ssDNA	Single Stranded DNA

DTT	Dithiothreitol

E

E (β)	Early (gene expression in HCMV)
EC	Endothelial Cell
ECM	Extracellular Matrix
E.coli	Escherichia coli
EDTA	Ethylene Diamine Tetraacetic Acid
ELR	Glutamic Acid-Lysine-Arginine Motif
ER	Endoplasmic Reticulum
E:T	Effector:Target Ratio

F

FACS	Fluorescence Activated Cell Sorter
FASTA	Fast-all Protein Similarity Search
FCS	Foetal Calf Serum
FITC	Fluorescein Isothiocyanate
FSC	Forward Scatter

G

gB	Glycoprotein B
gCI	Glycoprotein Complex I
gCII	Glycoprotein Complex II
gCIII	Glycoprotein Complex III
GCR	G-Protein-Coupled 7-Transmembrane Receptor
GFP	Green Fluorescent Protein
gH	Glycoprotein H
gL	Glycoprotein L
gM	Glycoprotein M
gN	Glycoprotein N
gO	Glycoprotein O
gp	Glycoprotein

H

h	Time in Hours
HA	Haemagluttinin
HCMV	Human Cytomegalovirus
hCAR	Human Cocksackie and Adenovirus Receptor
HFFF	Human Foetal Foreskin Fibroblasts
HIV	Human Immunodeficiency Virus
HLA	Human Leukocyte Antigen
hpi	Hours Post Infection
HRP	Horse Radish Peroxidase
HSPGs	Heparin Sulphate Proteoglycans
Htert	Human Telomerase Reverse Transcriptase
HVEM	Herpes Virus Entry Mediator

I

ICAM-1	Intercellular Adhesion Molecule-1
IE	Immediate Early (gene expression in HCMV)
IE1	Immediate Early Gene 1

IE2	Immediate Early Gene 2
IFN	Interferon
Ig	Immunoglobulin
IL	Interleukin
ILT	Immunoglobulin-like Inhibitory Receptor
IPTG	Isopropyl-beta-D-thiogalactopyranoside
IRS1	Internal Repeat Short
IRL1	Internal Repeat Long
ITAM	Intracellular Tyrosine-based Activatory Motif
ITIM	Intracellular Tryosine-based Inhibitory Motif
IU	International Units

J

JAK1	Janus Kinase 1

K

K562	Human Caucasian Chronic Myelogenous Leukaemia Cells
kb	Kilo Basepairs
kDa	Kilodaltons
KIR	Killer Cell Immunoglobulin-like Receptor
KLRG1	Killer Cell Lectin-like Receptor G1

L

l	Litre
L (γ)	Late (gene expression in HCMV)
LB	Lauria Bertani Agar
LIR-1	Leukocyte Immunoglobulin-like Receptor
LLT1	Lectin-like Transcript 1

M

mAb	Monoclonal Antibody
MAC	Membrane Associated Complex
MCMV	Mouse Cytomegalovirus
MCP	Major Capsid Protein
mCP	Minor Capsid Protein
mCP-BP	Minor Capsid-Binding Protein
MCP-AP	Major Capsid Protein-Assembly Protein Complex
MEM	Minimum Essential Medium
mg	Milligrams
MHC	Major Histocompatibility Complex
MICA	MHC Class I Chain-Related Gene A
MICB	MHC Class I Chain-Related Gene B
MIEP	Major Immediate Early Promoter-Enhancer
ml	Millilitres
MOI	Multiplicity of Infection
MPC	Magnetic Particle Concentrator
mRNA	Messenger Ribonucleic Acid

N

NCBI	National Centre for Biotechnology Information
NCR	Natural Cytotoxicity Receptor

ND10	Nuclear Domain-10
Necl	Nectin-Like Molecule
NK	Natural Killer Cell
NKL	Natural Killer Leukaemia Cell Line
NP40	Nonidet P-40

O

OKT3	CD3 Specific Antibody
ORF	Open Reading Frame
oriLyt	Origin of Replication

P

p	Protein
pp	Phosphoprotein
PAGE	Polyacrylamide Gel Electrophoresis
PBMC	Peripheral Blood Mononuclear Cells
PBS	Phosphate Buffered Saline
PBST	Phosphate Buffered Saline 0.1% Tween 20
PCR	Polymerase Chain Reaction
PE	Phycoerythrin
pfu	Plaque Forming Units
p.i.	Post Infection
pmol	Picomole
PML	Promyelocitic Leukaemia
PMSF	Phenylmethanesulfonyl Fluoride
PTS	Peroxisome Targeting Signal
PVR	Polio Virus Receptor

R

RAd	Recombinant Adenovirus
RANTES	Regulated upon Activation, Normal T cell Expressed and Secreted
RGD	Arginine-Glycine-Aspartamic Acid Cell Attachment Motif
RNA	Ribonucleic acid
RNase	Ribonuclease
RPMI	Roswell Park Memorial Institute
RT	Room Temperature

S

SB	Superbroth
SCGM	Stem Cell Growth Media
SCP	Smallest Capsid Protein
SDS	Sodium Dodecyl Sulphate
SSC	Side Scatter
SUMO	Small Ubiquitin-like Modifier

T

TAE	Tris acetic acid EDTA
TAP	Transporter Associated with Antigen Presentation
$TCID_{50}$	Tissue Culture Infectious Dose
TE	Tris EDTA Buffer

Tet	Tetracycline
TGFβ	Transforming Growth Factor β
Th1/Th2	T Helper Cell 1/ T Helper Cell 2
TM	Transmembrane
TNFR	Tumour Necrosis Factor Receptor
TRL1	Terminal Repeat Long
TRS1	Terminal Repeat Short

U, V, W, X

UL	Unique Long (region of HCMV genome)
ULBP	UL16 Binding Protein
US	Unique Short (region of HCMV genome)
UV	Ultra Violet
V	Volts
v/v	Volume to Volume Ratio
vMIA	Viral Inhibitor of Apoptosis targeting Mitochondria
WASP	Wiscott-Aldrich Syndrome Protein
w/v	Weight to Volume Ratio
x-gal	5-bromo, 4-chloro-3-indolyl-β-D-galactopyranosidase

1. INTRODUCTION

1.1 CYTOMEGALOVIRUSES

Human cytomegalovirus, HCMV, the prototype member of the β-herpesvirus subfamily of herpesviruses, acquired its name from the "giant cell" cytopathic effect (cpe) associated with infection *in vivo*. HCMV infections are also associated with the production of characteristic nuclear and cytoplasmic inclusions, a property shared with other members of the subgroup. Cytomegaloviruses also share several characteristics with other members of the herpesviruses, such as virion structure, DNA replication and the ability to establish persistent and latent infections.

1.2 HUMAN CYTOMEGALOVIRUS STRUCTURE

1.2.1 The genome

HCMV has the largest genome of any characterised human virus, with a 236kb linear genome estimated to encode 165 ORFs (Dolan *et al.*, 2004). Cytomegaloviruses of higher primates, HCMV and Chimpanzee CMV (CCMV), have a class E genome structure, in which two unique regions (unique long, UL and unique short, US) are flanked by inverted direct repeats (terminal repeat long, TRL, internal repeat long, IRL, terminal repeat short, TRS, and internal repeat short, IRS) (Fig 1.1) (Davison *et al.*, 2003a; Westrate *et al.*, 1980). These terminal and internal inverted repeats vary in size depending on the virus strain and passage history. The genome is also terminally redundant, possessing a short region of the genome (the *a* sequence) as a direct repeat at the genome termini and in inverted orientation at the IRL/IRS junction. Genomes can contain multiple copies of the *a* sequence at these locations. The *a* sequence carries cis-signals (*pac-1* and *pac-2*) for cleavage and packaging of the viral genome (Kemble & Mocarski, 1989; McVoy *et al.*, 1998; Mocarski *et al.*, 1987; Spaete & Mocarski, 1985).

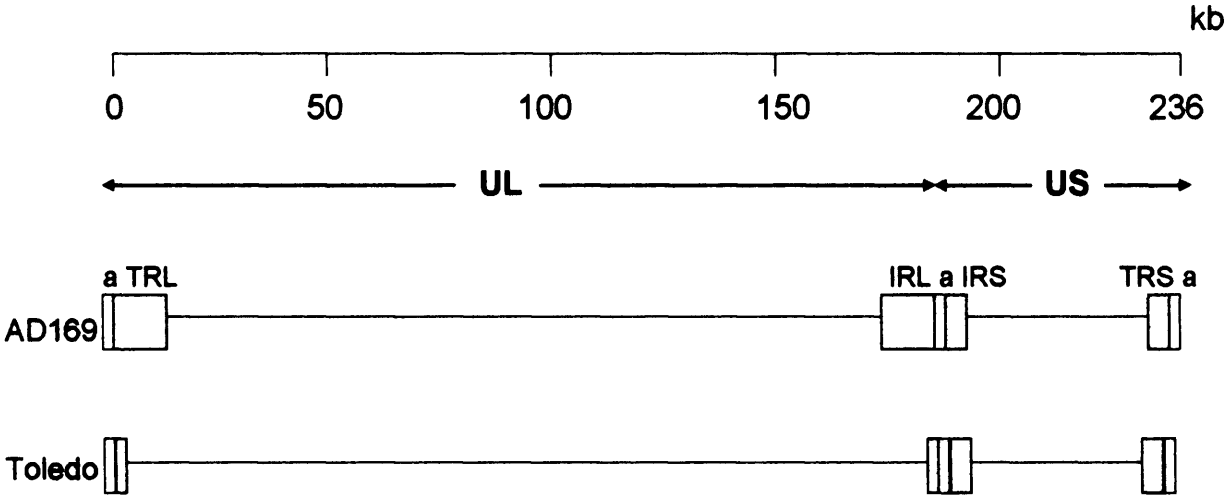

Figure 1.1 HCMV strain AD169 and strain Toledo genome structures
The HCMV genome is split into two unique regions, UL and US. These regions are flanked by terminal and internal inverted repeats denoted TRL, IRL, TRS and IRS. The a sequence is an inverted copy of the direct repeat, and the number of copies can vary between different strains of CMV. Toledo has an additional 15kb at the UL/*b*' end of the genome that has been lost in AD169 by a duplication of ~10kb from the left end of UL to produce a larger IRL. (Adapted from Mockarski & Courcelle, 2001).

HCMV strain AD169 was propagated *in vitro* under conditions designed to attenuate its virulence for use as a live vaccine (Elek & Stern, 1974). When the HCMV AD169 genome was plasmid cloned, it had been subjected to extensive, serial passage in various laboratories over 25 years (Oram *et al.*, 1982; Rowe *et al.*, 1956). The subgenomic strain AD169 clones provided the basis for the generation of the first complete HCMV genome sequence (Chee *et al.*, 1990a). However, during passage the strain AD169 genome (Accession number AF01963) has suffered multiple mutations and deletions that complicate its use as a prototype HCMV sequence (Davison *et al.*, 2003a). For example, a 929bp sequence in the UL42-UL43 region that is carried by all strains of CMV, including certain strain AD169 variants, was deleted in the reported sequence (Dargan *et al.*, 1997; Mocarski *et al.*, 1997). In addition, a large 13-15kb region is absent from AD169, but present in the less attenuated strain, Toledo, and clinical isolates of HCMV, having been replaced in AD169 by an inverted duplication of a 10kb region from the left end of UL (Cha *et al.*, 1996; Fig 1.1).

Deriving the genetic content of the complete HCMV genome has been a drawn-out process (Chee *et al.*, 1990a; Dolan *et al.*, 2004; Dunn, W. *et al.*, 2003; Murphy *et al.*, 2003a, 2003b). Sequence analysis revealed that as HCMV clinical isolates are passaged, they rapidly acquire mutations (deletion, frameshift or termination codon) in small groups of genes to adapt to growth in fibroblasts *in vitro* (Akter *et al.*, 2003; Davison *et al.*, 2003a; Dolan *et al.*, 2004). The low passage strain Merlin is the most genetically intact genome that has been sequenced to date, but does contain a single point mutation in the UL128 ORF that was acquired during its first passage. The sequence and annotation of the strain Merlin defined by Dolan *et al*, 2004 (Fig 1.2) has been designated the prototypic HCMV sequence (Accession no. AY446894). HCMV strain Merlin was estimated to contain 165 ORFs (Fig 1.2) (Dolan *et al.*, 2004), although minor revisions have since increased the number to 167 (Davison, personal

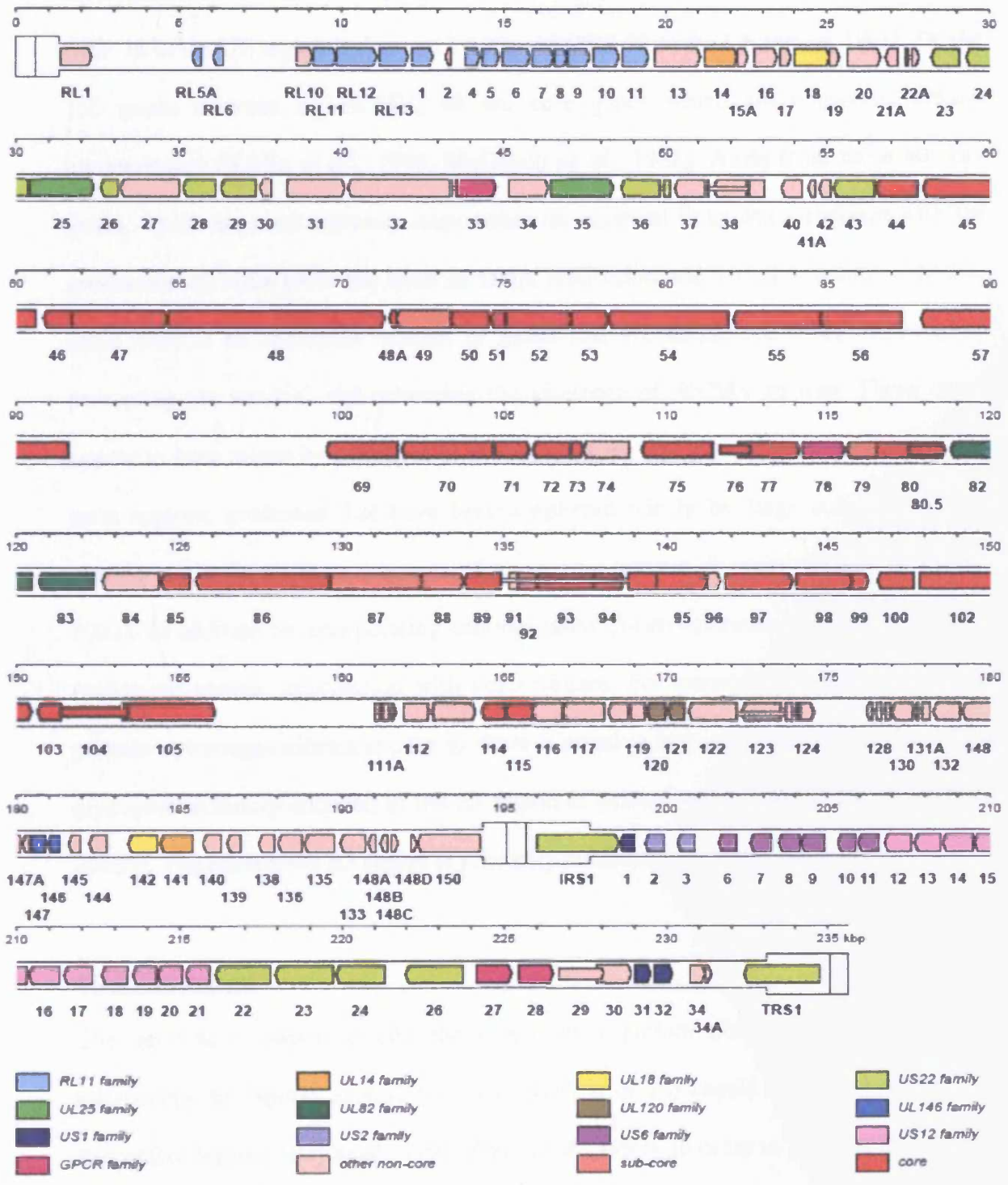

Figure 1.2 Genetic content of wild type HCMV
Annotation of the wild type genome of Merlin, a Cardiff clinical isolate. Protein coding regions are indicated by arrows, with gene nomenclature below (from Dolan *et al.*, 2004).

communication). A nomenclature is used based on gene location within the genome, i.e. ORF 78 in the UL region is denoted UL78, and ORF 22 of the US region, US22. Of the 165 genes encoded by HCMV, 40 are core genes which are conserved among herpesviruses (Karlin *et al.*, 1994; McGeoch *et al.*, 1988). Aside from these 40 core genes, which are predominantly responsible for essential functions associated with the production of virus particles, such as DNA replication and virion structural proteins, there remains an enormous number of genes that are anticipated to be dedicated to promoting the survival and enhancing the virulence of, HCMV *in vivo*. These genes appear to have arisen by a number of evolutionary events, such as gene duplication and gene capture, processes that have been employed widely by large eukaryotic DNA viruses and their hosts as a means of generating genetic diversity (Prince & Picket, 2002). In addition to incorporating cellular genes, β-herpesviruses also appear to have exchanged genetic information with other viruses. For example, the RL11 family of primate cytomegaloviruses appear to share a putative immunoglobulin domain with a glycoprotein family encoded in the E3 region of primate adenoviruses (Davison *et al.*, 2003b). The adenovirus E3 region is primarily involved in immune modulation.

1.2.2 The capsid

The genome is packaged into the capsid in a pattern observed by cryo-electron microscopy to "spool" around the inner surface of the capsid and wind inwards in successive layers (Booy *et al.*, 1991; Zhou *et al.*, 1999). In order to package its genome, HCMV has evolved tighter DNA packaging than smaller herpesviruses such as HSV-1 (Bhella *et al.*, 2000) and has a larger 130nm diameter capsid, compared to the 125nm diameter of smaller herpesviruses (Butcher *et al.*, 1998). There are three capsid forms; A, B and the mature C-type capsid, representing different stages in virion morphogenesis (Gibson, 1996; Irmiere & Gibson, 1983; Lee *et al.*, 1988; Trus *et al.*,

1999). Type A capsids lack DNA or scaffold and accumulate because of a failure to stably package the viral genome. Type B capsids are found predominantly in the nucleus as precursors of mature capsids, lacking DNA but containing the viral scaffold cores, and Type C capsids represent the mature HCMV virion (Butcher *et al.*, 1998; Lee *et al.*, 1988).

The capsid consists of a number of proteins, encoded by genes distributed within the herpesvirus-common core set of genes. There are four major structural proteins; the major capsid protein (MCP), encoded by UL86, forms the chief constituent of capsid hexamers and pentamers; the less abundant capsid proteins are the minor capsid protein (mCP), encoded by UL85, the minor capsid-binding protein (mCP-BP) encoded by UL46 and the smallest capsid protein (SCP) encoded by UL48A (Gibson, 1996; Gibson *et al.*, 1996a; Gibson *et al.*, 1996b; Irmiere & Gibson, 1985; Sedarati & Rosenthal, 1988). The major structural components of the capsid are the capsomeres, termed pentons and hexons. These structures are composed primarily of 5 and 6 copies of MCP, respectively, with a total of 150 hexons and 12 pentons in the capsid. The hexon tips are decorated by SCP, which also directs tegumentation (Yu *et al.*, 2005). The other structural proteins, mCP and mCP-BP, associate in a 2:1 ratio to form triplexes, major surface structures that interconnect hexons and pentons. The triplexes are critical for capsid morphogenesis, and link together the capsomeres in the procapsid, directing assembly and stabilising the structure prior to virion maturation. There are also two different UL80-derived proteins, generated by posttranslational processing, which carry out distinct functions in capsid assembly. An assembly protein is derived from the carboxy-terminus of UL80 by autocatalytic cleavage, mediated by a serine-like protease called assemblin, which is itself embedded in the amino-terminal portion of this ORF (Baum *et al.*, 1993; Gibson *et al.*, 1990). This produces the minor capsid scaffold protein (pUL80), which together with the major capsid scaffold protein (pUL80.5),

associates with the capsid and directs formation of the capsid shell (Oien *et al.*, 1997; Wood *et al.*, 1997).

1.2.3 The tegument

Between the capsid shell and the envelope, HCMV has an extensive network of highly ordered icosahedral tegument (Chen *et al.*, 1999; McGavran & Smith, 1965; Wright *et al.*, 1964). The tegument contains a number of proteins, many of which are phosphorylated and highly immunogenic. For example, pp65 is a broadly recognized viral antigen that is detected by 85-90% of CMV-seropositive human sera. As many tegument proteins play a role in the early stages of virus infection they are therefore packaged within the virion to ensure their presence upon infection of a new host (Roby & Gibson, 1986). The most prominent tegument proteins are the major tegument protein, pp150 (UL32) which is O-glycosylated (Benko *et al.*, 1988) and binds directly to the capsid through its N-terminus (Baxter & Gibson, 2001); the lower matrix protein, pp65 (UL83); the upper matrix protein, pp71 (UL82); the associated myristylated protein, pp28 that is essential for envelopment (UL99; Sanchez *et al.*, 2000a); the high molecular weight tegument protein, ppUL48, and its binding protein, UL47 (reviewed in Mocarski & Courcelle, 2001). Over time, a number of additional HCMV-encoded proteins have been identified to be tegument constituents; these include the phosphoprotein ppUL69, pTRS1/pIRS1 (Liu & Stinski, 1992; Romanowski *et al.*, 1997; Winkler *et al.*, 1995; Winkler & Stamminger, 1996), the viral DNA polymerase (Mar *et al.*, 1981), the UL97 kinase (Wolf *et al.*, 1998), pUL36 (Patterson & Shenk, 1999) and pp130 (ppUL56) (Bogner *et al.*, 1998).

1.2.4 The virion envelope

The genome, capsid and tegument of the HCMV particle are enveloped in a host lipid bilayer carrying a large number of virus-encoded glycoproteins (Brit & Mach, 1996; Spaete *et al.*, 1994). The envelope, and its associated glycoproteins, is derived from intracellular membranes, acquired from both nuclear and cytoplasmic sites. The most abundant envelope proteins are distributed among three complexes, gCI, gCII and gCIII (Gretch *et al.*, 1988). gCI is composed of homodimers of glycoprotein B (gB, UL55), recognized as a major envelope constituent, and is the most highly conserved glycoprotein in mammalian herpesviruses. Glycoprotein B is a heparan sulphate proteoglycan-binding glycoprotein, and a type I integral membrane protein (Cranage *et al.*, 1986). gCII comprises two proteins, gM (UL100), a type III membrane protein, and gN (UL73), a type I membrane protein (Kari *et al.*, 1994; Mach *et al.*, 2000). Both gCI and gCII mediate cell attachment and entry, a two step process that involves initial attachment to heparan sulphate, followed by a stabilising interaction with another receptor (Boyle & Compton, 1998). gCI and gCII also target progeny virus to apical membranes for release from polarized cells (Tugizov *et al.*, 1998). The third complex, gCIII is a heterotrimer of gH (gpUL75), gL (UL115) and gO (UL74) (Huber & Compton, 1998; Kaye *et al.*, 1992; Li *et al*, 1997; Spaete *et al.*, 1993). gCIII is involved in mediating fusion of viral and host cell membranes in concert with gCI. It is likely that the gH/gL/gO complex is vital in cell entry, and it is also possible that components of this heterotrimeric complex, or other associated proteins may have a role in cell tropism (Keay & Baldwin, 1991; Wang *et al.*, 1998). The gH/gL complex may also facilitate transport to the cell surface (Kaye *et al.*, 1992; Spaete *et al.*, 1993).

There are several additional viral glycoproteins that are likely to be minor envelope constituents, but are not apparently associated with any major glycoprotein complexes. The glycoproteins, gp48 (gpUL4) and TRL10 have been identified as virion envelope

components (Chang *et al.*, 1989; Spaderna *et al.*, 2002), and UL33, a homologue of seven-transmembrane receptors (Chee *et al.*, 1990b) is also likely to be carried in the virion envelope. The presence of over 60 ORFs with the sequence characteristics of integral membrane glycoproteins in HCMV (Cha *et al.*, 1996; Chee *et al.*, 1990a; Dolan *et al.*, 2004) suggests that additional functions for less abundant envelope glycoprotein constituents will continue to emerge.

1.2.5 Additional virion components

In addition to viral proteins, a number of host cell proteins have also been observed to associate with purified virions. For example, β2-microglobulin has been detected in the tegument (Stannard, 1989), suggesting a way that CMV attaches to cells (Grundy *et al.*, 1987), and the inclusion of an actin-like protein suggests a means of cytoplasmic transport (Baldick & Shenk, 1996). Other virion components contributed by the host cell include annexin II (Wright *et al.*, 1995), phospholipase A2 (Allal *et al.*, 2004) and the complement control proteins CD55, CD46 and CD59 which are associated with the virion envelope (Spear *et al.*, 1995; Spiller *et al.*, 1997).

In addition to the genome, two small RNA molecules are present in the core of the virion, hybridized with the origin of replication (*ori*Lyt) in packaged genomes and may play a role in initiating DNA replication (Prichard *et al.*, 1998). There are also a number of mRNAs found within the tegument that are expressed after entry into cells, for example RNAs specified by UL22A and RL13 (Bresnahan & Shenk, 2000). Translation of certain of these RNAs could ensure targeting of encoded proteins to the endoplasmic reticulum and Golgi network, before the viral genome becomes transcriptionally active. Alternatively, these molecules may be modulators of cellular immunity or structural components of the tegument. However, the incorporation of viral and cellular mRNAs can occur non-specifically, and care must be taken when assessing the biological

significance of the presence of these mRNAs in the virion (Greijer *et al.*, 2000; Terhune *et al.*, 2004).

There are no histone-like proteins present in herpesvirions to counteract the negative charge of packaged DNA. Instead, alongside a single copy of the tightly packed DNA with RNA at the *ori*Lyt, the core of the human CMV virion contains the polyamines spermine and spermidine, at a ratio approximately 2:1, which play a role in virion assembly (Gibson *et al.*, 1984).

Mass spectrometric methods have enabled HCMV virion proteins to be catalogued, including a number of viral proteins that had been undetected, and a large array of cellular proteins (Varnum *et al.*, 2004). However, caution must be exercised as proteins detected in low abundancy may not be biological relevant due to contamination with non-virion material.

1.3 HCMV VIRUS GROWTH

1.3.1 Infection and the viral life cycle

HCMV infection exhibits a highly restricted host range in cell culture, with efficient productive infection best achieved by "adapted" viruses in primary human fibroblasts, although significant virus production can also be achieved in endothelial and differentiated myeloid cells as well as certain astrocyte cell lines (Ibanez *et al.*, 1991; Nowlin *et al.*, 1991). *In vivo*, HCMV can infect a wide variety of cell types, including: fibroblasts, epithelial cells, endothelial cells, monocytes/macrophages, smooth muscle cells, stromal cells, neuronal cells, neutrophils and hepatocytes (Ibanez *et al.*, 1991; Myerson *et al.*, 1984; Sinzger *et al.*, 1995; Sinzger *et al.*, 2000). This extended *in vivo* tropism may contribute to the diverse nature of the symptoms and diseases associated with this virus.

The replication cycle of HCMV is summarised in Figure 1.3, although many aspects are only partially understood. The ability of HCMV to enter such a wide range of cells, and the fact that attachment and penetration at the cell surface is rapid and efficient in permissive cell types suggests that receptors for HCMV are widely distributed, with either broadly expressed receptors, or multiple cell specific receptors for HCMV entry. Virus attachment is likely a multistep process, typically involving a number of envelope glycoproteins interacting with a series of cell surface molecules that serve as receptors and co-receptors (Fig 1.3a). An initial engagement of HCMV with cell surface heparan sulphate proteoglycans (HSPGs) is thought to play a crucial role in the recruitment of virions to the cell surface, and is also thought to enhance the engagement of other receptors to result in membrane fusion (Boyle & Compton, 1998; Compton *et al.*, 1993). The attachment to the cell surface is then likely followed by receptor activated conformational changes that result in membrane fusion of the virion envelope and the cell surface to deliver the viral nucleocapsid to the cytoplasm of the host cell (Fig 1.3b) (Boehme & Compton, 2006). The nucleocapsids are then able to make their way to the nucleus, and expression of gene products follows shortly thereafter (Fig 1.3c). Productive replication follows a pattern of coordinate expression with viral genes assigned to different kinetic classes, referred to as α or immediate-early (IE), β or early (E) and γ or late (L).

1.3.2 IE gene expression and gene products

Four regions of IE gene expression have been mapped on the HCMV genome, IE1/IE2 (UL122-123), UL36-38, TRS1-IRS1 and US3. The IE genes play a number of important roles in transcriptional regulation (*ie*1/*ie*2 products), counteracting the interferon response (TRS1/IRS1), inhibition of apoptosis (UL36 and UL37) and modulation of host cell MHC I expression (US3) (Child *et al.*, 2004; Colberg-Poley, 1996; Spector,

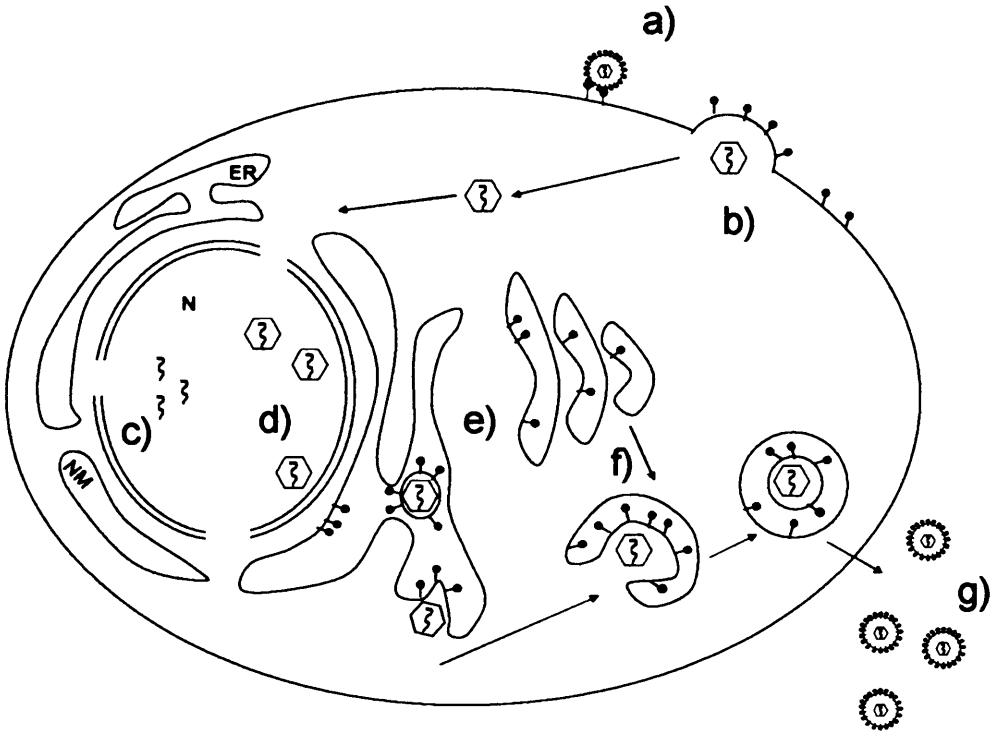

Figure 1.3 HCMV life cycle
Virus binding to the cell a) is followed by nucleocapsid entry into the cell b). The nucleocapsid then makes its way to the nucleus (N), where expression of immediate early genes follows. Following DNA replication, c), genomes are then packaged into capsids in the nucleus to form nucleocapsids, d), which bud into the perinuclear membrane (NM) and then undergo a process of envelopment and de-envelopment as they traverse nuclear and cytoplasmic membranes (NM/ER), e). The maturing virus particles obtain their tegument in cytoplasmic compartments, termed tegusomes, and finally bud into Golgi-derived cytoplasmic compartments, gaining their lipid membrane and envelope proteins, f), before exiting the cell as a mature virion, g).

1996; Stenberg, 1996; Wilkinson *et al.*, 1984). The *ie*1/*ie*2 promoter-enhancer is also known as the major immediate early promoter-enhancer, or MIEP, and comprises a dense collection of host transcription factor binding sites (Akrigg *et al.*, 1985; Boshart *et al.*, 1985; Thomsen *et al.*, 1984). Shortly after infection, several transcription factors (NFKB, AP1, CREB, Sp1) are induced and activate expression from the *ie*1/*ie*2 promoter-enhancer (reviewed in Sinclair & Sissons, 2006). Transcription from the *ie*1/*ie*2 promoter-enhancer gives rise to differentially spliced and polyadenylated transcripts encoding two major products, the nuclear phosphoproteins, IE1 and IE2, which share a common 85 amino acid N-terminal but splice either to UL123 for IE1 or UL122 for IE2 (reviewed in Mocarski & Courcelle, 2001). These phosphoproteins are thought to play key roles in initiating and maintaining HCMV gene regulation pathways during infection. IE1 is thought to have very little activity on its own as a transactivator (Ahn & Hayward, 1997). However, in addition to it's cooperation with IE2, IE1 has been suggested to directly influence gene expression via a number of different transcription factors, including NFκB (Sambucetti *et al.*, 1989), CCAAT box-binding protein (Hayhurst *et al.*, 1995), and E2F (Azizkhan *et al.*, 1993). IE1 is observed to associate with chromatin (LaFemina *et al.*, 1989) and PML nuclear bodies, disrupting their integrity (Ahn *et al.*, 1998; Ahn & Hayward, 1997; Ishov *et al.*, 1997; Kelly *et al.*, 1995; Korioth *et al.*, 1996; Wilkinson *et al.*, 1998). These PML nuclear bodies, or nuclear domain 10 (ND10) structures, function as sites of organisation for viral transcription and DNA replication, but may be antiviral. Specifically, a component of ND10 structures, Daxx, is reported to mediate repression of HCMV IE genes by recruiting chromatin-modifying enzymes to the MIEP (Hollenbach *et al.*, 2002; Murphy *et al.*, 2002; Woodhall *et al.*, 2006). It is therefore possible that HCMV employs a number of mechanisms during immediate-early times of infection to overcome this repression mediated by Daxx in order to activate gene expression. The disruption of

ND10 structures by IE1 is likely to be one such mechanism (Ahn & Hayward, 2000; Woodhall *et al.*, 2006). The tegument protein, pp71 (UL82), also accumulates at ND10 structures in a process that is mediated by Daxx (Hofmann *et al.*, 2002; Ishov *et al.*, 2002). pp71 mediates the degradation of Daxx, providing another mechanism for HCMV to overcome the transcriptional repression mediated by Daxx.

IE2 is a major regulatory protein with two established core functions. Firstly, it controls the activation of, and switch from, immediate-early to early and late gene expression during productive infection (Hermiston *et al.*, 1987; Pizzorno *et al.*, 1988), with IE1 acting as an accessory protein in this process, and secondly, it regulates its own promoter via binding to a cis-repression sequence (*crs*) located near the MIEP start site (Cherrington *et al.*, 1991; Lang & Stamminger, 1993; Liu *et al.*, 1991). Alternative forms of IE2, known as IE2p55 and γIE2 (or late IE2) retain different subsets of activation and repression functions (Jenkins *et al.*, 1994; Stenberg, 1996).

TRS1 and IRS1 are two members of the US22 family, distributed in both the nucleus and the cytoplasm of infected cells (Chee *et al.*, 1990a; Romanowski *et al.*, 1997) and are also found in the virion (Romanowski *et al.*, 1997). TRS1 and IRS1 proteins play an important role in the block of interferon-induced host cell protein synthesis shut-off, by reducing the phosphorylation of eIF-2α by PKR, and therefore removing the inhibition of translation initiation (Child *et al.*, 2004).

The US3 region encodes a number of related, integral membrane glycoproteins (Jones & Muzithras, 1992). US3 encodes an endoplasmic reticulum (ER)-targeted protein that blocks the egress of peptide loaded MHC I proteins, and therefore represents one of several viral gene products that down modulate MHC I expression (Ahn *et al.*, 1996, Jones *et al.*, 1995; Jones *et al.*, 1996). This is discussed in further detail in Section 1.5.

UL37 from the UL36-UL38 genomic region is a mitochondrial localized protein, and encodes an inhibitor of apoptosis (vMIA), that appears to be functionally similar to Bcl-

2 as it inhibits Fas-mediated apoptosis, blocking apoptosis at a point downstream of caspase 8 but prior to cytochrome c release from mitochondria (Goldmacher *et al.*, 1999). UL36 encodes a non-glycosylated cytoplasmic protein (Patterson & Shenk, 1999), and is also involved in the inhibition of apoptosis, but its mechanism of cell-death suppression is different from that of vMIA (Skaletskaya *et al.*, 2001). The UL36 gene product inhibits Fas-mediated apoptosis by complexing with pro-caspase-8, suppressing its proteolytic activation, and as such UL36 has been designated a viral inhibitor of caspase-8-induced apoptosis (vICA) (Skaletskaya *et al.*, 2001). The UL36 protein is rendered inactive by a point mutation in HCMV laboratory strains including certain AD169 variants (Skaletskaya *et al.*, 2001), and as such, laboratory strains of HCMV may rely more directly on UL37 gene products than pUL36 to prevent apoptosis. As many of the counter-assaults mounted by the immune system incorporate activation of the apoptotic pathway as a mechanism to restrict viral replication, it is interesting to note that HCMV encodes genes that prevent apoptosis, enhancing replication of the virus. The HCMV IE1 and IE2 proteins have also been demonstrated to block apoptosis, mediated by TNF-α (Zhu *et al.*, 1995).

1.3.3 Early and late gene expression and gene products

Both early (β) and late (γ) gene expression requires prior expression of IE gene products, and hence early and late gene expression is delayed. Although it is difficult to define these kinetic classes temporally, early gene transcription can operationally be defined as those genes that are transcribed in the presence of an inhibitor of DNA replication, whereas late genes are not. Two abundantly expressed early genes are the β1.2 and β2.7 transcripts, encoding 1.2kb and 2.7kb proteins respectively. β1.2 and β2.7 map to adjacent positions and represent 20% and 40% of total viral transcription from early times of infection respectively (Spector, 1996). The β2.7 gene encodes the single

most abundant viral early or late transcript in infected cells (Greenaway & Wilkinson, 1987; McSharry *et al.*, 2003). Other early gene products include US11, a β1 gene encoding an ER resident protein that is involved in immune modulation (see Section 1.5) (Ahn *et al.*, 1996; Hengel *et al.*, 1996; Shamu *et al.*, 1999; Wiertz *et al.*, 1996a), UL112-UL113, which encode a family of phosphoproteins that regulate the expression of core DNA replication genes (Iwayama *et al.*, 1994; Wright *et al.*, 1988), and the DNA polymerase (UL54) (Chee *et al.*, 1990a).

1.3.4 Genome maturation and virion morphogenesis

Genome maturation occurs in the nucleus of infected cells, with most newly replicated DNA maturing into virions that are released 48 hours after synthesis (Penfold & Mocarski, 1997). Virion maturation commences in the nucleus, beginning with the formation of capsids which is initiated and controlled by an MCP-AP (major capsid protein-assembly protein) precursor complex (Gibson, 1996; Wood *et al.*, 1997). In the nucleus, an AP precursor domain facilitates the formation of hexons, pentons, and high order structures that form the capsid (described in Section 1.2). The association of SCP on the outer capsid surface and a series of assemblin-mediated protease cleavage steps separate AP from MCP, inactivating the protease and separating the scaffold from the inside surface of the capsid. This completes the formation of B capsids into which the linear HCMV genome is packaged, using the cleavage and packaging signals *pac*1 and *pac*2 sites. Once the genome is packaged, scaffold components are removed to complete the formation of mature C-capsids (Irmiere & Gibson, 1985). Progeny nucleocapsids bud into the perinuclear cisternae and are then thought to undergo a process of envelopment and de-envelopment as they traverse the nuclear and cytoplasmic membranes (Gibson, 1996; Fig 1.3d, e). The maturing virion acquires its tegument in cytoplasmic compartments termed tegusomes (Sanchez *et al.*, 2000a, 2000b; Tooze *et*

al., 1993), and finally capsids bud into Golgi-derived cytoplasmic compartments (Homman-Loudiyi *et al.*, 2003) (Fig 1.3f), gaining their lipid membrane and envelope glycoproteins in the process, before exiting the cell by the exocytotic pathway (Fig 1.3g).

Three types of virus particles are produced in HCMV-infected cells: virions, non-infectious enveloped particles and dense bodies (Gibson, 1996; Irmiere & Gibson, 1983). Non-infectious enveloped particles are readily differentiated from virions because they lack a DNA core (Gibson, 1996; Irmiere & Gibson, 1983). Non-enveloped particles consist of nucleocapsid with DNA, and have been observed free in the cytoplasm as well as budding into cytoplasmic vesicles. Dense bodies lack both a nucleocapsid and viral DNA, consisting solely of several tegument proteins, predominately pp65 (ppUL83), surrounded by an envelope derived from cytoplasmic membranes. These abundant particles mature exclusively at cytoplasmic sites (Craighead *et al.*, 1972; Irmiere & Gibson, 1983; Landini *et al.*, 1987; Sarov & Abady, 1975).

1.4 PATHOGENESIS, LATENCY AND REACTIVATION

HCMV exhibits a ubiquitous distribution in populations throughout the world. Primary infection is normally subclinical in the immunocompetent individual, being controlled by a combination of adaptive and innate immune responses. However, although primary infection is controlled, the virus is not cleared and a persistent, lifelong infection is established. Pathogenesis of CMV disease is directly linked to the immune status of the host, and the occurrence of primary infection, lifelong latency, and intermittent shedding of this virus without any marked disease consequences highlights the remarkable balance HCMV has with its host. Serious disease results from primary infection, as well as reactivation from latency in the immuno-compromised host, which

includes transplant recipients, transfusion patients and HIV infected individuals. Infection in these individuals can result in central nervous system damage, viral retinitis and pneumonia, as well as graft rejection or transplant dysfunction in transplant patients. In addition, HCMV is a significant cause of congenital birth defects. Approximately 10% of infants born with HCMV infection suffer severe congenital defects such as abnormal muscle tone, pneumonia, mental retardation, hearing and vision loss. HCMV is a clinically relevant disease and as such it is regarded among the top priority category for vaccine development (Arvin *et al.*, 2004).

1.4.1 Pathogenesis of HCMV

Primary infection starts with replication in mucosal epithelium as a result of direct contact with infectious secretions from an infected individual. A systemic phase of infection disseminates virus in the host that may last several months (Revello *et al.*, 1998; Zanghellini *et al.*, 1999). The distribution of virus during infection in immuno-competent individuals includes a range of endothelial, epithelial and haematopoietic cells, with myeloid-lineage haematopoietic cells as important targets for lifelong persistence (Larsson *et al.*, 1998; Mendelson *et al.*, 1996; Taylor-Weideman *et al.*, 1991; Stainer *et al.*, 1992) and neutrophils suggested to act as the vehicle to disseminate infectious virus (Gerna *et al.*, 2000). Systemic replication of virus leads to seeding of the ductal epithelia where replication releases virus into secretions, leading to persistent virus shedding in urine, saliva, breast milk, semen and cervical secretions, which become important sources for transmission between hosts. Although an initial persistent infection is often observed, clearance of acute infection is the norm in all immunocompetent individuals. Reactivation of the virus is correlated with a slow rise in cell-mediated immunity that acts to control the virus (Zanghellini *et al.*, 1999).

1.4.2 Latent infection

The ability to establish lifelong persistence within the host is common to all herpesviruses. Latent infection is defined as the persistence of the virus genome in the absence of the production of infectious virus. With HCMV, peripheral blood (PB) monocytes have been identified as the major site of carriage of HCMV DNA in healthy seropositive individuals (Larsson *et al.*, 1998; Stanier *et al.*, 1992; Taylor-Weidmann *et al.*, 1991). Monocytes represent a short-lived population of cells, and are subject to constant renewal from myeloid precursors, $CD34^+$ stem cells, residing in the bone marrow (Katz *et al.*, 1985; Metcalf, 1989). Analysis of these $CD34^+$ progenitor cells showed that they harbour HCMV genomes in naturally infected individuals (Kondo *et al.*, 1996; Mendelson *et al.*, 1996) and thus represent an important reservoir for HCMV latency *in vitro* (Sinclair & Sissons, 2006).

During latency, the HCMV genome is maintained as a circular plasmid in the nucleus of peripheral blood (PB) mononuclear cells (Bolovan-Fritts *et al.*, 1999) and it is thought that chromatin remodelling of the MIEP may control latency and reactivation of lytic gene expression (Reeves *et al.*, 2005a; Reeves *et al.*, 2005b; Sinclair & Sissons, 2006). Viral gene expression in latently infected cells is restricted to latency-associated transcripts (or CLTs) (Hahn *et al.*, 1998; Kondo *et al.*, 1996), small viral transcripts that may be involved in the establishment or maintenance of latency. These transcripts originate from both DNA strands in the *ie*1/*ie*2 region (Kondo *et al.*, 1996), with four ORFs (ORF55, ORF42, ORF45, and ORF94) predicted to be uniquely encoded by sense CLTs, and three ORFs (ORF59, ORF154 and ORF152/UL124) present on antisense CLTs. Antibodies to the ORFs from sera of healthy seropositive individuals suggests that these ORFs are expressed during natural infection (Landini *et al.*, 2000). However, many of the transcripts were also detected in infected cells in culture (Lunetta & Weidemann, 2000), and hence the role for CLTs in virus latency and reactivation *in vivo*

has not yet been clearly established (Sinclair & Sissons, 2006). Similarly, transcripts encoded by the UL111.5A region of HCMV have been detected in latently infected granulocyte-macrophage progenitors (Jenkins *et al.*, 2004). The UL111.5A is predicted to encode a viral homologue of IL-10, suggesting a function for this transcript in immune modulation during latency. However, as yet, no direct role for the UL111.5A transcript during latency has been assigned (Jenkins *et al.*, 2004; Sinclair & Sissons, 2006).

1.4.3 Reactivation

Both primary infection and reactivation of latent HCMV are responsible for serious disease in the immuno-compromised host (Adler, 1983; Rubin, 1990). The myeloid progenitors that carry viral DNA do not produce infectious virus or express viral lytic genes to any appreciable extent (Mendelson *et al.*, 1996; Taylor-Wiedeman *et al*, 1993). However, the pattern of latent gene expression, and the ability to support IE gene expression has been observed to change as these cells differentiate into monocytes/ macrophages or dendritic cells (Hahn *et al.*, 1998), potentially becoming productive as a result of differentiation under proinflammatory conditions, although the precise factors that control this process are not clear (Meier & Stinski, 1996; Soderberg-Naucler & Neslon, 1999; Soderberg-Naucler *et al.*, 1997; Sinclair & Sissons, 2006). Recent analysis by Reeves *et al.*, 2005b has indicated that induction of HCMV IE gene expression from latent virus upon differentiation of myeloid cells to dendritic cells occurs as a result of chromatin remodelling around the MIEP. HCMV present in latently infected dendritic cell precursors is in a closed, transcriptionally silent, chromatin confirmation. In contrast, differentiation of these precursors to dendritic cells resulted in specific chromatin remodelling of the MIEP, resulting in an open, transcriptionally active confirmation. These investigations indicate that virus reactivation is likely to be

the result of chromatin remodelling of the MIEP during cell differentiation, which results in the induction of IE gene expression (Reeves *et al.*, 2005b).

1.5 IMMUNE MODULATION BY HCMV

HCMV has a huge genetic capacity, encoding 165 ORFs. However, there are only 45 essential genes in HCMV (Dunn W., *et al.*, 2003; Fig 1.2), leaving more than 120 ORFs encoded by HCMV that are dispensable for virus replication. These genes are likely to be dedicated to optimizing virus growth, dissemination, tissue tropism, pathogenesis and evasion of the host immune response. This study is particularly concerned with the interplay between HCMV and the immune system, with specific interest in the modulation of the innate immune system by evasion of Natural Killer (NK) cells (Section 1.6).

Through various mechanisms, host cells can sense the presence of a virus, and attempt to trigger cell death to prevent viral replication. Interferons (IFNs) released by the cell upon virus infection signal the presence of virus to the cellular immune system, whose initial innate response includes NK cells, with a second wave of cellular attack from $CD8^+$ T cells (cytotoxic T cells, CTLs). Resistance to HCMV infection depends on the successful collaboration between these innate and adaptive immune systems, which are required to control primary virus infection and reactivation (Borysiewicz *et al.*, 1985; Riddell & Greenberg, 1997; Rook, 1988). The importance for this collaboration is reinforced by the observation that individuals with deficiencies in cellular immunity exhibit the highest risk for HCMV disease (Biron *et al.*, 1989; Li *et al.*, 1994; Reusser *et al*, 1991).

However, despite these controls, the immune response is subjected to a range of HCMV-encoded immunomodulatory mechanisms, which act to evade, modify and regulate the immune response to ends that benefit the virus.

1.5.1 Down-modulation of MHC class I

Cytotoxic T lymphocytes (CTLs) recognize virus-derived peptides in the antigen binding-site of major histocompatibility complex (MHC) class I molecules present on the surface of infected cells (Fig 1.4a) (Zinkernagel, 1979; Zinkernagel, 1996). Viral mRNAs are translated using the normal translation machinery of the cell, and like other proteins, cytosolic viral gene products are degraded as part of normal protein turnover. Among the cellular proteases that degrade these viral proteins is the multi-subunit catalytic protease complex called the proteasome (Fig 1.4a) (Coux *et al.*, 1996). Degradation of viral proteins in the cytoplasm leads to the formation of polypeptides that are then transported to the lumen of the endoplasmic reticulum (ER) by the transporter associated with antigen presentation (TAP) complex (Fig 1.4a), which consists of two subunits; TAP1 and TAP2 (Heemels & Ploegh, 1995). In the ER, these peptides assemble with the membrane-bound heavy chain of the MHC class I molecules and the light chain β2 microglobulin (β2m). The binding of peptide stabilizes the interactions of the MHC class I heavy and light chain and as a result, a trimolecular complex of MHC class I heavy chain, β2m and peptide is formed (Fig 1.4a) (Heemels & Ploegh, 1995; Townsend & Bodmer, 1989). Peptide-loaded MHC complexes are then transported from the ER, through the Golgi to the cell surface (Fig 1.4a) where they are available for surveillance by CTLs (Jorgensen *et al.*, 1992). Upon recognition of the MHC-foreign peptide complex, the CTLs lyse the infected cell by receptor and granule-mediated pathways (Barry & Bleackley, 2002). MHC-I restricted CTL play an important role in the maintenance of the HCMV-host equilibrium, and in the clearance of virus-infected cells (Reusser *et al.*, 1991; Quinnan *et al.*, 1982). In order to reduce the impact of CTL immunity, HCMV expresses four genes (US2, US3, US6 and US11) that are responsible for the downregulation of MHC class I (Fig 1.4b) (Hengel *et al.*, 1996; Jones *et al.*, 1995; Wiertz *et al.*, 1997). Efficient downregulation of cell surface MHC

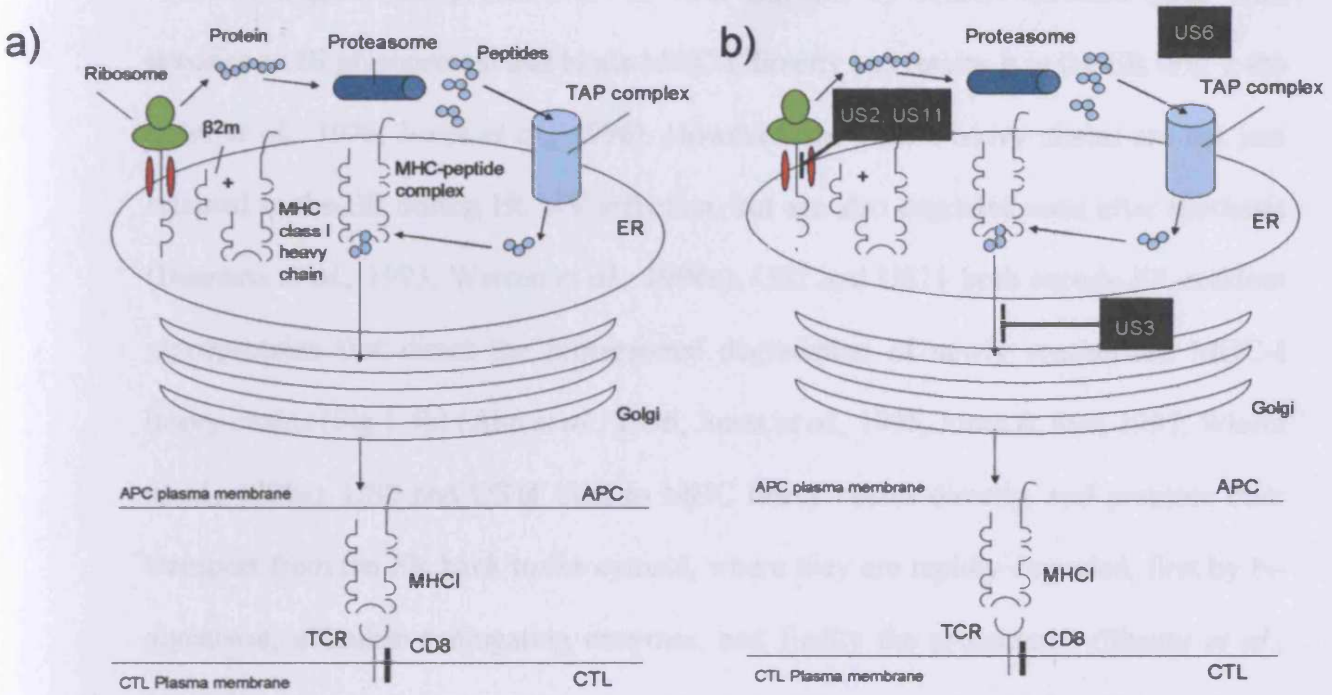

Figure 1.4 HCMV encodes four proteins responsible for the downregulation of MHC-I from the cell surface

The MHC class I-restricted antigen processing and presentation pathway is depicted in a). To evade lysis by CTLs, HCMV encodes four proteins that are responsible for the downregulation of MHC-I in infected cells b). US2 and US11 direct the proteasomal degradation of newly synthesised MHC-I heavy chains. US6 prevents peptide translocation via TAP and US3 binds MHC-I directly, retaining it in the ER (adapted from Wiertz *et al.*,1997).

class I abrogates the presentation of viral antigens by HCMV-infected cells. US3 encodes an IE glycoprotein that binds MHC-I directly and retains it in the ER (Fig 1.4b) (Ahn *et al.*, 1996; Jones *et al.*, 1996). However, the class I heavy chains are not just retained in the ER during HCMV infection, but are also degraded soon after synthesis (Beersma *et al.*, 1993; Warren *et al.*, 1994a). US2 and US11 both encode ER-resident glycoproteins that direct the proteasomal degradation of newly synthesised MHC-I heavy chains (Fig 1.4b) (Ahn *et al.*, 1996, Jones *et al.*, 1995, Jones & Sun, 1997, Wiertz *et al.*, 1996a). US2 and US11 bind to MHC heavy chains directly, and promote their transport from the ER back to the cytosol, where they are rapidly degraded, first by N-glycanase, ubiquitin-conjugating enzymes, and finally the proteasome (Shamu *et al.*, 1999; Shamu *et al.*, 2001; Story *et al.*, 1999; Wiertz *et al.*, 1996b). This pathway resembles the mechanism by which mammalian cells dispose of misfolded proteins. A mammalian protein, Derlin-1, has also recently been identified as the partner essential for US11 to perform its function (Lilley & Ploegh, 2004), and required for the dislocation of misfolded proteins from the ER to the cytosol for degradation. US6 is an ER resident glycoprotein, and prevents viral peptide translocation (Ahn *et al.*, 1997; Hengel *et al.*, 1997; Lehner *et al.*, 1997). US6 binds to the luminal side of the TAP complex (Ahn *et al.*, 1997; Hengel *et al.*, 1997, Lehner *et al.*, 1997), inhibiting the binding of ATP to TAP1 of the TAP complex, preventing translocation of peptides (Hewitt *et al.*, 2001). The inability of MHC class I to bind TAP-dependent peptides leads to retention of MHC class I in the ER, and a corresponding downregulation of MHC I on the cell surface.

Whilst HCMV encodes multiple mechanisms to suppress MHC-I mediated antigen presentation, cytokines released at the site of infection appear capable of overcoming viral immune evasion. Interferon γ (IFNγ), type I IFN, or tumour necrosis factor α

(TNFα) treatment of HCMV infected cells can restore antigen presentation by upregulating MHC-I expression. As the HCMV-encoded functions for suppressing MHC-I expression become saturated, the surplus MHC-I molecules escape to restore efficient presentation of viral peptides (Hengel *et al.*, 1998). As such, CTL-mediated immune clearance remains an important component of the immune response contributing to viral clearance (Hengel *et al.*, 1998; Riddell & Greenberg, 1997).

1.5.2 Down-modulation of MHC class II

Where MHC I molecules present peptides to $CD8^+$ CTLs, MHC class II molecules present antigenic peptides to $CD4^+$ T helper cells. These $CD4^+$ T cells are involved in the activation of B cells to produce an immune response. Unlike MHC class I, where the peptides presented are usually derived from proteins endogenously synthesised by the cell, MHC class II molecules generally present antigenic peptides derived from endocytosed, soluble proteins that have been degraded in cellular lysosomal compartments.

Although not as well studied as MHC-I downregulation, multiple mechanisms appear to control MHC-II modulation during HCMV infection. For example, HCMV can inhibit cytokine-induced MHC II expression by blocking the induction of transcription activator, CTAII, a target of the janus kinase I (JAK1) pathway (Miller *et al.*, 1998, Miller & Sedmak, 1999). In addition, US3 is also known to bind to newly synthesised class II molecules (alpha/beta complexes), reducing the association with the invariant chain and causing mis-localisation of class II complexes (Johnson & Hegde, 2002; Misaghi *et al.*, 2004). This reduces the accumulation of class II complexes in peptide-loading compartments, therefore reducing peptide loading and surface expression of MHC II (Johnson & Hegde, 2002). A US2 dependent degradation system also contributes to reduction in MHC-II levels (Tomazin *et al.*, 1999), by binding

specifically to both class I heavy chains and MHC class II DRα and DMα chains, triggering their degradation by proteosomes (Hegde & Johnson, 2003).

An additional mechanism of MHC class II downregulation may result from the induction of IL10. IL10 has several immunosuppressive activities that potentially could be favourable to HCMV. As well as downregulation of MHC-II, IL10 can downregulate MHC-I, interfere with antigen presentation and inhibit the production of inflammatory cytokines (Kotenko *et al.*, 2000). As an example of its uses, Mouse CMV (MCMV) induces host IL10 during infection of macrophage-lineage cells, suppressing even constitutive MHC-II expression (Redpath *et al.*, 1999). HCMV also encodes a functional viral IL10 (vIL10) homologue, encoded by UL111A (Kotenko *et al.*, 2000; Lockridge *et al.*, 2000). Although vIL10 has been shown to be ineffective at down-modulating HCMV peptide presentation by MHC-I (Pepperl-Klindworth *et al.*, 2006), it may contribute to MHC-II downregulation, in addition to the impact of cellular IL-10 and other viral gene products.

1.5.3 Manipulation of cytokine responses

Cytomegaloviruses may exploit the host cytokines to promote virus replication and modulate immune responses. Transforming growth factor β (TGFβ) is a cytokine that has a major impact on inflammatory and immunological responses; primarily through suppressing the generation of T-helper type 2 (Th2) cells, $CD8^+$ CTL and NK cells by counteracting IL2, TNF and IL1 function, and by depressing polyclonal antibody production (Hengel *et al.*, 1998). HCMV induces TGFβ synthesis in infected fibroblasts (Michelson *et al.*, 1994), and consequently TGFβ suppresses T cell proliferation (Hengel *et al.*, 1998; Michelson *et al.*, 1994).

HCMV also encodes four genes (UL33, UL78, US27, and US28) that are homologues of G-protein coupled receptors (GCR), expressed at both early and late times of

infection (Chee *et al.*, 1990a; Davis-Poynter *et al.*, 1997). Members of the GCR superfamily of receptors transduce signals through the cell membrane by activating G proteins, and are triggered by chemokines, which can be subdivided into four groups, CXC, CC, C and CX3C. The HCMV gene, US28, is the best studied member of the HCMV GCR proteins and encodes a G-protein-coupled receptor that binds several CC chemokines (Gao & Murphy, 1994; Kuhn *et al.*, 1995), stimulating intracellular calcium mobilization (Neote *et al.*, 1993). US28 also selectively binds a CXC3 chemokine (Kledal *et al.*, 1998). Chemokines not only mediate inflammatory processes by recruiting leukocytes (chemotaxis), but also stimulate the effector mechanisms of lymphocytes (Zlotnik & Yoshie, 2000), and it is thought US28 may function as a chemokine "sink" (Bodaghi *et al.*, 1998) or mediate intracellular signalling (Billstrom *et al.*, 1998), influencing chemotaxis and chemokinesis (Alcami, 2003; Streblow *et al.*, 1999). By altering the trafficking of infected cells, the HCMV GCRs may also affect virus dissemination (Hengel *et al.*, 1998).

In addition to the G-protein coupled receptor homologues, HCMV also encodes a soluble CC chemokine receptor, pUL21.5 (Wang *et al.*, 2004). HCMV pUL21.5 mRNA is packaged into virions, implying a role for the encoded protein before the viral genome reaches the nucleus and is transcribed (Wang *et al.*, 2004). The soluble pUL21.5 CC chemokine receptor selectively binds RANTES, a CC proinflammatory chemokine with a broad range of activities. It is generated by a variety of cell types, including $CD8^+$ T cells, epithelial cells, fibroblasts, and platelets and its receptors reside in monocytes, dendritic cells, T cells, NK cells, neutrophils, and eosinophils (Wang *et al.*, 2004). In addition to its chemotactic activity, oligomerized RANTES is also thought to be responsible for T cell activation (Appay *et al.*, 1999; Appay & Rowland-Jones, 2001). By blocking the ability of RANTES to bind to its receptor, pUL21.5 may inhibit the ability of RANTES to mediate T cell activation.

1.5.4 Viral chemokine homologues

Virus encoded chemokines can also influence the behaviour of leukocytes during infection. Two other HCMV genes, UL146 and UL147, exhibit homology to the CXC chemokine IL-8, with UL146 encoding a fully functional IL-8 like chemokine denoted vCXC1 (Penfold *et al.*, 1999), but no function is yet assigned to UL147. vCXC1 is secreted, and induces chemotaxis of neutrophils via the human chemokine receptor CXCR2. By attracting neutrophils and/or other CXCR2-positive myeloid cells to the site of infection, vCXC1 may play a role in the dissemination of the virus. Neutrophils attracted to the sites of infection by UL146 may then be susceptible to infection by HCMV. In MCMV, the CC chemokine homologue, MCK, increases the level of monocyte-associated viraemia during infection by increasing the size and composition of the inflammatory response at sites of infection, attracting host monocytes that carry virus into the bloodstream (MacDonald *et al.*, 1999; MacDonald *et al.*, 1997; Saederup *et al.*, 1999).

1.5.5 Additional immune-modulators encoded by HCMV

Immune evasion precedes *de novo* virus-encoded gene expression, being mediated by proteins delivered during infection released from input virions. Virions release into infected cells the RANTES-binding protein, ppUL21.5 (section 1.5.3), pTRS1/pIRS1 and pp65. pTRS1/pIRS1 evade the antiviral cellular response by preventing activation of interferon-response genes by the protein kinase R (PKR) pathway. The IFN pathway is a key component in the innate immune response to HCMV infection, and IFN is synthesised in response to viral infection. IFN binds to cognate receptors on target cells to activate a signalling pathway that leads to the induction of IFN-responsive genes, many of which have anti-viral activity. The pTRS1/pIRS1 proteins prevent the phosphorylation of eukaryotic translation initiation factor (eIF-2α) by PKR, which in

turn inhibits translation initiation (Child *et al.*, 2004). The virion protein pp65 is also involved in blocking the induction of IFN-responsive genes (Browne & Shenk, 2003), although its mechanism remains unclear (Abate *et al.*, 2004; Shenk, 2006).

The complement system is a first-line immunological defence, and includes proteolytic enzymes, inflammatory proteins, cell surface receptors and proteins that cause cell death through the formation of a membrane-associated complex (MAC). Antibody-activated complement mediated cytolysis and virolysis are general immune effector mechanisms. Accordingly, a broad range of host cells express several complement inhibitory mechanisms to modulate the complement response and protect tissues from complement-mediated cytolysis. Although there are no HCMV-encoded virus complement inhibitor homologues, the cell surface expression of two complement control proteins, CD46 and CD55, is drastically enhanced following HCMV infection and shown to protect infected cells from complement-mediated attack (Spiller *et al.*, 1996). The host-derived complement control proteins, CD55, CD59 and CD46 are also found incorporated into HCMV virions, where they may provide potential mechanisms for escape of complement-mediated virolysis (Spear *et al.*, 1995; Spiller *et al.*, 1997).

HCMV also induces IgG Fc γ receptors (MacCormac & Grundy, 1996; Xu-Bin *et al.*, 1989) that are thought to be encoded by TRL11/IRL11 (Lilley *et al.*, 2001) and gpUL119-UL118 (Atalay *et al.*, 2002). FcγR homologues encoded by HSV-1 and varicella-zoster viruses protect the virus from antibody neutralisation and virus-infected cells from lysis mediated by antibody and complement (Dowler & Veltri, 1984; Dubin *et al.*, 1991; Frank & Friedman, 1989; Friedman *et al.*, 1984). It was thought that the cytomegalovirus FcγR homologue may also have similar protective effects. However, the MCMV m138 encoded IgG Fc receptor (Thale *et al.*, 1994) function is antibody independent (Crnkovic-Mertens *et al.*, 1998), and the function of HCMV induced IgG Fc receptors remains unknown.

In contrast to the stimulation of host cell gene expression observed in HCMV infection, that presumably favours viral DNA replication and virion production, HCMV also downregulates a number of molecules. Both integrin α1β1 cell surface expression (Warren *et al.*, 1994b) and fibronectin expression (Pande *et al.*, 1990) have been shown to decrease upon HCMV infection, but the mechanism and reasons for this remain unknown. The cellular aminopeptidase proteins, CD10 and CD13, have also been shown to be downregulated during HCMV infection (Philips *et al.*, 1998).

1.6 HCMV ENCODES NATURAL KILLER CELL EVASION FUNCTIONS

1.6.1 Natural Killer cells

This study is particularly concerned with the interplay between HCMV and Natural Killer (NK) cells. NK cells play a vital part in the control of CMV infection, shown in MCMV infection of mice (Bukowski *et al.*, 1984; Scalzo *et al.*, 1992) and highlighted in patients with NK deficiencies (Biron *et al.*, 1989) where recurrent herpesvirus infection, in particular HCMV infection, is very problematic. NK cells play an important role in early defence against virus infection. During acute virus infections, peak NK responses of cytotoxicity and IFN-γ production occur within the first several hours to days of infections, whereas adaptive T and B cell responses take up to a week to develop.

1.6.1.1 NK cell activating and inhibitory receptors

NK cells constitute a heterogenous population that express a wide range of activatory and inhibitory receptors (Table 1.1) (Biassoni *et al.*, 2001; Moretta & Moretta, 2004). The balance between the activating and inhibiting signals determines the outcome of the NK response to the target cell (Fig 1.5). Klaus Karre's 'Missing Self Hypothesis' led to an appreciation of the important role played by the interaction between NK inhibitory

Table 1.1 Human NK receptors and co-receptors involved in the regulation of NK-mediated functions
(From Biassoni *et al.*, 2001; Lanier, 1998; Lanier, 2005; Moretta & Moretta, 2004)

Gene Name	Receptor Name	Function	Ligand Specificity
KIR2DL1	CD158a	Inhibitory	HLA-Cw2, 4, 5, 6
KIR2DL2	CD158b1	Inhibitory	HLA-Cw1, 3, 7, 8
KIR2DL3	CD158b2	Inhibitory	HLA-C
KIR2DL4	CD158d	Inhibitory/ Activating	HLA-G?
KIR2DL5A	CD158f	Inhibitory	unknown
KIR2DL5B		Inhibitory	unknown
KIR3DL1	CD158e1	Inhibitory	HLA-Bw4
KIR3DL2	CD158k	Inhibitory	HLA-A3, -A11
KIR3DL3	CD158z	Inhibitory	unknown
KIR3DL4	p49	Inhibitory (?)	HLA-G
LIR1/ILT2	LIR1/ILT2	Inhibitory	HLA-G and broad HLA class I specificity, CMV UL18
LIR2 ILT4	LIR2 ILT4	Inhibitory (?)	HLA-F
CD94	a	a	a
NKG2A	CD94/NKG2A	Inhibitory	HLA-E
KIR2DS1	CD158h	Activating	HLA-Cw2,4, 5, 6
KIR2DS2	CD158j	Activating	HLA-Cw1, 3, 7, 8
KIR2DS3		Activating	unknown
KIR2DS4	CD158i	Activating	unknown
KIR2DS5	CD158g	Activating	unknown
KIR3DS1	CD158e2	Activating	unknown
NKG2C	CD94/NKG2C	Activating	HLA-E
LAIR1	p40/LAIR1	Inhibitory	unknown
IRC1	IRp60	Inhibitory	unknown
CMRF35	CMRF35	?	unknown
AIRM1	p75/AIRM1	Inhibitory	unknown (sialic acid dependent)
NKp46	NKp46	Activating	viral hemagglutinin
1C7 NK-A1	NKp30	Activating	HCMV pp65
NKp44	NKp44	Activating	viral hemagglutinin
NKG2D	NKG2D	Activating	MICA, MICB, ULBPs 1-4
2B4	2B4	Activating	CD48
KLRF-1	NKp80	Activating	AICL
	NTB-A	Activating	unknown
CD226	DNAM-1	Activating	CD155 (PVR)/CD112 (Nectin-2)
CD96	TACTILE	Activating	CD155 (PVR)
KLRC3	NKG2E	unknown	unknown
KLRC4	NKG2F	unknown	unknown
KLRB1	NKR-P1A/ CD161	unknown	unknown
FcγRIII	CD16	Activating	IgG
	CD2	Activating	CD58 (LFA-3)
	CD28 (only fetal NK cells)	Activating	CD80/ CD86

a Forms heterodimers with different members of the NKG2 family, including NKG2A and NKG2C

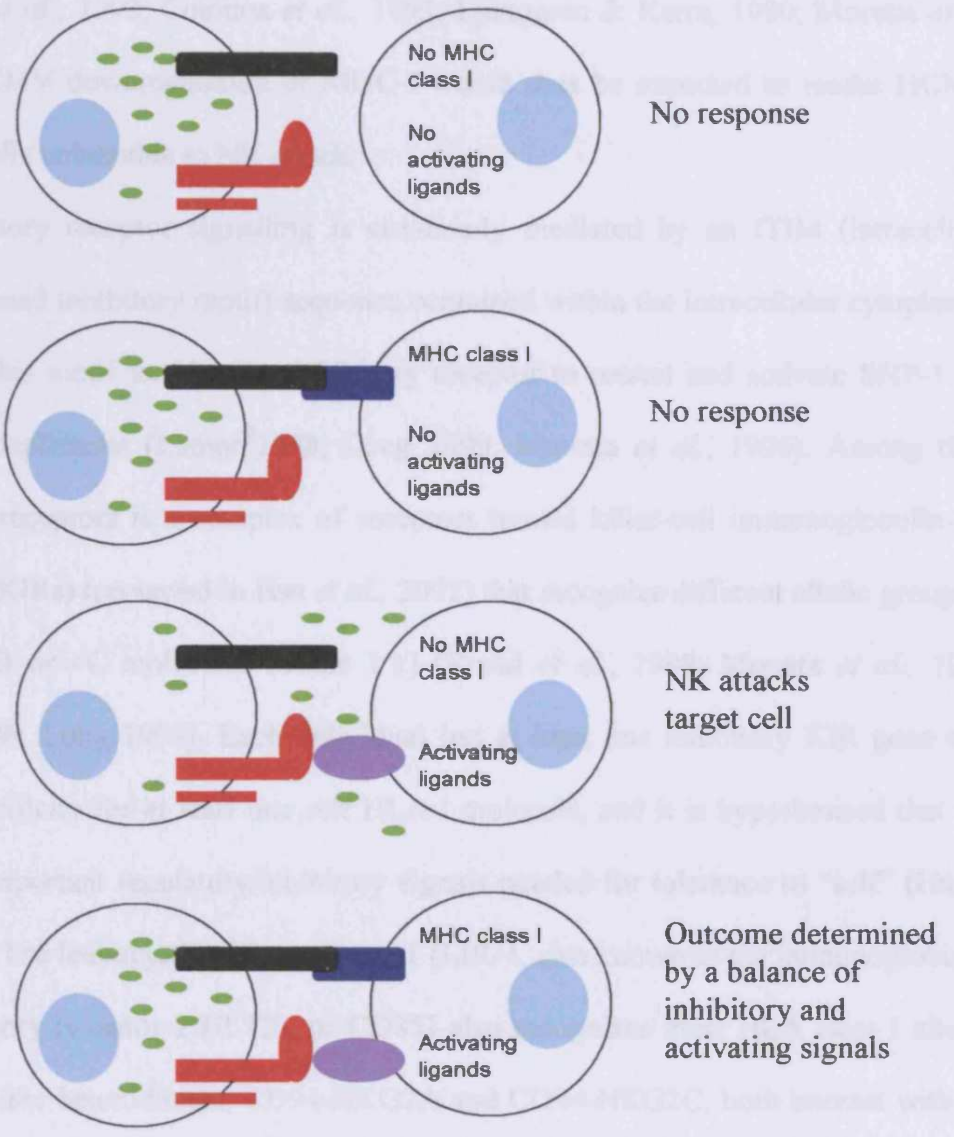

Figure 1.5 The "missing-self" hypothesis
A graphic depiction of the interaction between NK and target cells, and the possible outcomes. When interacting target cells express ligands for both inhibitory and activatory receptors, the outcome is determined by the summation of the strength of the signals. The numbers of activating and inhibiting receptors on the NK cell surface, of ligands on the target cell, as well as qualitative differences in the signals transduced, determine the extent of the NK cell response (from Lanier, 2005).

cells and matched MHC-I molecules in suppressing killing of normal autologous cells (Ciccone *et al.*, 1992; Colonna *et al.*, 1993; Ljunggren & Karre, 1990; Moretta *et al.*, 1993). HCMV downregulation of MHC-I would thus be expected to render HCMV-infected cells vulnerable to NK attack.

NK inhibitory receptor signalling is commonly mediated by an ITIM (intracellular tyrosine-based inhibitory motif) sequence contained within the intracellular cytoplasmic domain. This motif enables the inhibitory receptor to recruit and activate SHP-1 and SHP-2 phosphatases (Lanier 1998; Long 1999; Moretta *et al.*, 1996). Among these inhibitory receptors is a complex of receptors termed killer-cell immunoglobulin-like receptors (KIRs) (reviewed in Hsu *et al.*, 2002) that recognize different allelic groups of HLA-A, -B or –C molecules (Table 1.1) (Braud *et al.*, 1998; Moretta *et al.*, 1996; Lanier 1998; Long 1999). Each individual has at least one inhibitory KIR gene with ligand specificity for at least one self HLA-I molecule, and it is hypothesised that this provides important regulatory/inhibitory signals needed for tolerance to "self" (Hsu *et al.*, 2002). The leukocyte Ig-like receptor-1 (LIR-1, also known as the immunoglobulin-like inhibitory receptor 2 (ILT2), or CD85J also recognizes most HLA class I alleles. The lectin-like heterodimers, CD94-NKG2A and CD94-NKG2C, both interact with the non-polymorphic, non-classical HLA molecule, HLA-E (Braud *et al.*, 1998; Lee *et al.*, 1998). Interestingly, the CD94-NKG2A heterodimer is an inhibitory ligand, whereas CD94-NKG2C forms an activating ligand, each triggering distinct intracellular pathways (Houchins *et al.*, 1997). The lectin-like transcript 1 (LLT1) was also recently shown to bind CD161, an interaction which inhibits NK cell-mediated cytoxicity and IFN-γ production, whilst also enhancing CD3-triggered IFN- γ production by T-cells (Aldemir *et al.*, 2005).

NK activating receptors signal via an intracellular tyrosine-based activating motif (ITAM) contained within its cytoplasmic domain that activates NK cells. On

phosphorylation of the tyrosine motif within the ITAM domain, a signalling cascade is initiated that activates the NK cell. Among the NK activating receptors identified are the natural cytotoxicity receptors (NCRs), NKp30, NKp44, NKp46 and NKp80 (Table 1.1). Viral haemagglutinin (HA) binds and activates NKp44 and NKp46, but not NKp30 or NKp80 (Arnon *et al.*, 2004; Arnon *et al.*, 2001; Mandelboim *et al.*, 2001). The HCMV tegument protein, pp65, has recently been identified to interact with the natural cytotoxicity receptor, NKp30, preventing NK activation via this receptor (Arnon *et al.*, 2005). NKp80 has also recently been identified to bind to the genetically linked orphan receptor, AICL (Welte *et al.*, 2006). AICL is defined as a myeloid-specific activating receptor, and is upregulated by Toll-like receptor stimulation. Binding of AICL to NKp80 stimulates NK lysis of malignant myeloid cells (Welte *et al.*, 2006). In addition to the NCRs, a subset of KIR genes also encodes activating receptors (Table 1.1), which mediate their activation by association with the ITAM-bearing molecule DAP12, although ligand specificity for these activating KIRs remains unknown. Of the other NK activating receptors identified, a number of receptor-ligand interactions are now known (Table 1.1). For example, binding of CD2 family members such as CD3 and LFA-3 (CD58) (Davis *et al.*, 1998) and 2B4 with CD48 (Mathew *et al.*, 2005) results in NK activation. CD226 (DNAM-1) binding to both CD155 (PVR) and CD112 (Nectin-2) (Bottino *et al.*, 2003) also results in NK activation. NK cells can also recognise CD155 through CD96 (TACTILE), which promotes NK cell adhesion to the target cell and stimulates NK cytotoxicity (Fuchs, *et al.*, 2004). NK cells are also able to recognise the stress induced molecules MICA, MICB and UL16 binding proteins via the NKG2D receptor, which leads to activation of NK cells (Bauer *et al.*, 1999; Cosman *et al.*, 2001; Kubin *et al.*, 2001).

1.6.1.2 Cytokine modulation of NK responses

Cytokines also play a major role in coordinating and modulating NK responses to viral infection (reviewed in Biron *et al.*, 1999). The type I interferons (α/β) induced by cells upon virus infection enhance NK cell-mediated cytotoxicity. Other cytokines that influence NK cell responses include IL12, TNFα, IL1α, IL1β, IL6, IL10, TGFβ, IL15 and IL18. These cytokines function to regulate NK cell cytotoxicity, cytokine production and proliferation, and their activities are summarised in Table 1.2 (Biron *et al.*, 1999). A primary function of NK cells is to secrete proinflammatory cytokines, including IFNγ, TNF and a range of beta chemokines (Biron, 1997; Biron *et al.*, 1999; Bluman *et al.*, 1996; Oliva *et al.*, 1998). NK cell-produced IFNγ plays an important role in antiviral defence by the direct inhibition of replication in infected cells (Biron *et al.*, 1999; Lucin *et al.*, 1994) and increasing the expression of MHC-I on the infected cell surface.

1.6.1.3 The NK cell response

The outcome of the NK cell response is determined by a balance between its activating and inhibitory ligands, and by the cytokine and chemokine environment. Activation of NK cells results in release of proinflammatory cytokines and NK cells also mediate direct killing of target cells by the release of cytotoxic granules containing perforin and granzymes, or by binding to apoptosis-inducing receptors on the target cell (Fas-Fas ligand system). Thus, NK cells can mediate powerful effector functions, but these are effectively regulated by the host cell under normal circumstances.

1.6.2 HCMV evasion of NK cells

HCMV has developed a number of mechanisms to regulate the recognition of the infected cell by NK cells. These mechanisms can be divided into four main categories:

Table 1.2 Innate cytokine and chemokine regulation of NK cell function (From Biron *et al.*, 1999)

Cytokine	Direct and indirect effects on NK cells
Cytokines	
IFNα/β	Induce cell trafficking and cytoxicity; stimulate proliferation *in vivo*; inhibit IL12 production; stimulate expression of IL15
IL12	Stimulates IFNγ production; induces cytotoxicity; induces expression of MIP-1α in synergy with IL15; vital for non-viral, but not viral, NK responses
TNF	Synergizes with IL12 to induce IFNγ production
IL1α,β	Synergizes with IL12 to induce IFNγ production
IL15	Promotes cell growth and maturation; induces IFNγ and MIP-1α production/ expression in synergy with IL12
IGIF	Stimulates IFNγ production; induces cytotoxicity; synergizes with IL12 for IFN-γ production and cytotoxic activity
IL10	Inhibits IL12 production
TGFβ	Inhibits IFNγ production; inhibits IL12 production; blocks proliferation and cytotoxicity
Chemokines	
MIP-1α	Induces chemotaxis in culture and following infection in vivo
MIP-1β	Induces chemotaxis in culture
MCP-1,2,3	Induces chemotaxis in culture
RANTES	Induces chemotaxis in culture

the expression of virus-encoded MHC I homologues; selective modulation of endogenous MHC I; virus-mediated inhibition of activating receptors and production of virokines or cytokine-binding proteins. The HCMV functions that fall into these categories are summarised in Table 1.3, and described in more detail below (Braud *et al.*, 2002; Orange *et al.*, 2002).

The downregulation of MHC class I by HCMV encoded US2, US3, US6 and US11 proteins may render HCMV infected cells more susceptible to NK lysis. However, HCMV encodes an MHC class I heavy chain homologue, UL18 (Beck & Barrell, 1988), which can act as a decoy receptor for NK cells to evade lysis (Fig 1.6) (Reyburn *et al.*, 1997). UL18 binds β2 microglobulin (Browne *et al.*, 1990) and peptides (Fahnestock *et al.*, 1995) in a similar manner to MHC class I, and interacts with the NK inhibitory receptor, LIR-1. LIR-1, initially identified by its interaction with UL18 (Cosman *et al.*, 1997), is an inhibitory receptor that binds a wide range of MHC class I molecules (HLA-A, -B, -C, -E, -F and –G) (Chapman *et al.*, 1999; Lepin *et al.*, 2000; Shiroishi *et al.*, 2003). LIR-1 is found on myeloid cells, B cells, and subpopulations of T and NK cells (Young *et al.*, 2001), and is thought to contact common structural features in the UL18 and MHC a-3 domains and β2-m (Chapman *et al.*, 1999; Willcox *et al.*, 2003). LIR-1 has more than a 1000-fold higher affinity for UL18 than endogenous MHC class I molecules, so the presence of only a small amount of UL18 on the cell surface may be able to compete with MHC class I (Chapman *et al.*, 1999). Historically, there has been some conflict over the role of UL18 as an inhibitory receptor, with experimental results both supporting (Kim *et al.*, 2004; Reyburn *et al.*, 1997) and questioning (Leong *et al.*, 1998; Odeberg *et al.*, 2002) its role in NK inhibition (Cosman *et al.*, 1999). Work performed in this laboratory provides strong evidence that UL18 both inhibits LIR-1^+ NK cells through a direct interaction whilst also being able to activate LIR-1^- NK cells (Griffin *et al.*, 2005; Prod'homme *et al.*, 2007).

Table 1.3 HCMV-encoded mechanisms for evasion of NK cell responses
(From Orange *et al.*, 2002)

Viral Protein	Mechanism of action	Effects on NK cells
	Homologues of MHC class I	
UL18	Binds to LIR-1	Inhibits cytotoxicity in certain NK cell types (Reyburn *et al.*, 1997; Beck & Barrell, 1988; Leong *et al.*, 1998; Cosman *et al.*, 1997)
	Selective retention of MHC class I expression	
US2, US11	Cytosolic degradation of MHC class I, but not HLA-C or HLA-E	Presence of HLA-C and HLA-E thought to inhibit NK cell functions (Machold *et al.*, 1997; Lopez-Botet *et al.*, 2001)
UL40	Enhanced surface expression of HLA-E	Inhibits NK cell cytotoxicity (Tomasec *et al.*, 2000; Wang *et al.*, 2002)
	Interference with activation and cognate ligand interactions	
UL16	Blocks surface expression of NKG2D ligands	Inhibits NK cell cytotoxicity (Sutherland *et al.*, 2001; Kubin *et al.*, 2001, Cosman *et al.*, 2001)
ppUL83 (pp65)	Direct binding to NKp30	Binding results in dissociation of CD3ζ chain from NKp30 resulting in inhibiton of NK activation via NKp30 (Arnon *et al.*, 2005)
	Modulation of cytokine pathways relevant to NK cells	
vIL10 (UL111A)	Agnostic viral IL-10 homologue	Similar function to human IL10, inhibitory effect on NK cells (Kotenko *et al.*, 2000)

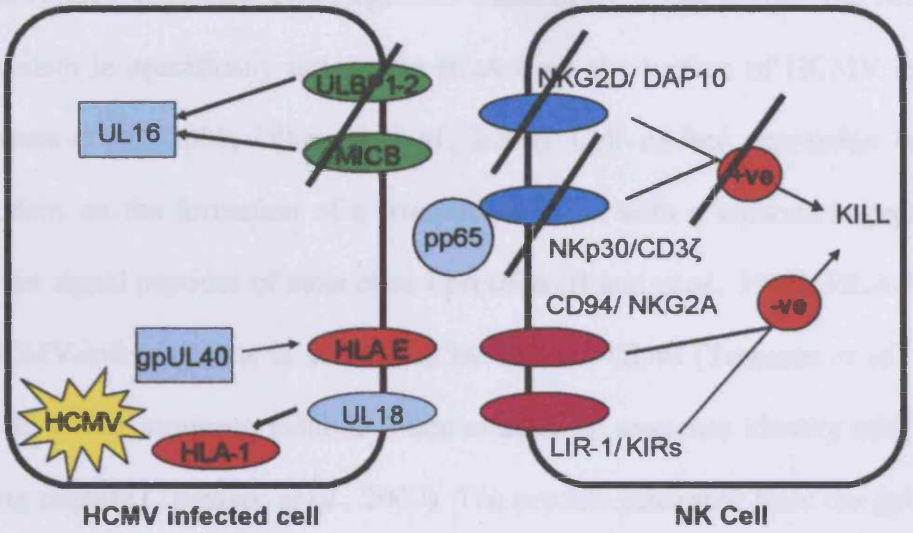

Figure 1.6 NK evasion mechanisms encoded by HCMV
HCMV encodes an MHC-class I homologue, UL18, that is thought to replace host MHC-I on the cell surface where it can interact with the inhibitory receptor LIR-1, to prevent NK lysis. In addition, the HCMV protein, UL40, enhances the expression of HLA-E at the cell surface, again enabling interaction with NK inhibitory receptors (CD94/NKG2A) to prevent NK cell attack. A third HCMV protein, UL16, acts to inhibit the cell surface expression of NK activating receptor ligands. The stress-induced ULBP1, ULBP2 and MICB molecules are retained in the ER by UL16, preventing their interaction with NKG2D/DAP10 activating NK receptor. The virion protein, pp65, binds to the NK activating receptor, NKp30, causing the CD3ζ side chain to dissociate from the receptor, preventing NK activation.

Whilst HCMV efficiently downregulates classical HLA I molecules, the virus encodes a mechanism to specifically upregulate HLA-E on the surface of HCMV infected cells (Tomasec *et al.*, 2000; Ulbrecht *et al.*, 2000). Cell surface expression of HLA-E is dependent on the formation of a trimeric complex with a nonameric peptide derived from the signal peptides of most class I proteins (Braud *et al.*, 1998). HLA-E expression on HCMV-infected cells is stimulated by HCMV UL40 (Tomasec *et al.*, 2000). The gpUL40 leader sequence exhibits 9 amino acids of sequence identity with the HLA-E binding peptide (Tomasec *et al.*, 2000). The peptide generated from the gpUL40 leader sequence binds to HLA-E in a TAP-independent manner, bypassing the HCMV MHC I downregulation protein, US6. Peptide-binding is essential for HLA-E maturation and transport to the cell surface, where it interacts with the NK inhibitory receptor CD94/NKG2A (Fig 1.6) (Wang *et al.*, 2002).

HCMV also evades NK recognition by suppressing the expression of activating NK ligands. A major activating receptor on NK cells is NKG2D, whose ligands include the MHC class I-like molecules (MIC) A and B, and the UL16-binding proteins (ULBP) 1 to 3 (Bauer *et al.*, 1999; Cosman *et al.*, 2001; Kubin *et al.*, 2001). These closely related molecules are stress-induced, and are upregulated on the cell surface during virus infection (Dunn C. *et al.*, 2003; Groh *et al.*, 1996; Welte *et al.*, 2003). UL16 was identified by Cosman *et al.* (2001) as an NK evasion function. UL16 binds to the NKG2D ligands MICB, ULBP 1 and ULBP2 (Cosman *et al.*, 2001) and retains them in the ER (Dunn C. *et al.*, 2003; Welte *et al.*, 2003), preventing their expression at the surface and the activation of NK cells by NKG2D (Fig 1.6).

A recent study by Arnon *et al.* (2005) has also shown that the HCMV virion protein, pp65, inhibits NK cytotoxicity by dissociating the linked CD3ζ chain from the NK activating receptor, NKp30 (Fig 1.6). pp65 was found in the supernatants of infected

cells, indicating that it may be the release of soluble pp65 from infected cells that can bind to NKp30 to inhibit NK cytotoxicity (Arnon *et al.*, 2005).

As antiviral cytokines are produced by NK cells, and NK cell activity is modulated by cytokines and chemokines, there is a potential for a number of virus evasion mechanisms to counter these cytokine/chemokine functions. For example, the HCMV gene, pp65, in addition to its role in inactivating the NK receptor NKp30, has been implicated in the prevention of type I interferons, which activate NK cells (Section 1.5.5, Browne & Shenk, 2003). HCMV may also influence over-production or encode homologues of other cytokines that have an inhibitory effect upon NK cells. For example, the viral IL10 homologue encoded by the HCMV UL111A gene (Section 1.5.2, Kotenko *et al.*, 2000; Lockridge *et al.*, 2000), may directly inhibit NK cell IFNγ production and cytotoxicity by inhibiting the function of IL12, which can induce IFNγ (Table 1.2). HCMV also encodes a soluble RANTES receptor, UL21.5 (Wang *et al.*, 2004), and the IL8 homologues, UL146 and UL147 (Penfold *et al.*, 1999), which may interfere with the recruitment of NK cells to the sites of HCMV infection.

HCMV has evolved a number of mechanisms by which it subverts NK cell-mediated cytolysis of the infected cell. The number and intricacy of these evasion mechanisms are further examples for the importance of NK cells in the control of HCMV.

1.6.3 The UL/*b'* region is responsible for increased virulence and resistance to NK cytolysis

A range of HCMV strains are used in research laboratories worldwide, including highly passaged laboratory-adapted strains such as AD169, and low passage strains such as Toledo or Merlin. HCMV strain AD169 has suffered multiple genetic changes during passages, including a large deletion (15kb) in the UL sequences that has been

compensated for by an 11kb expansion of *b* sequence repeats (TRL/IRL repeats; Fig 1.1) (Cha *et al.*, 1996; Prichard *et al.*, 2001). This 15kb deleted sequence will be referred to as UL/*b'*. Strain Towne (passage 125), also used extensively in HCMV research (Plotkin *et al.*, 1975), has also suffered a comparable deletion (13kb) affecting the UL/*b'* region, although less extensive than that of AD169. Serial passage of HCMV was carried out at a high MOI with the aim of attenuating virulence of HCMV so as to create vaccine candidates. A marked difference in virulence is seen between these highly passaged strains and low passage or clinical strains of HCMV (Quinnan *et al.*, 1984). In addition to this observation of reduced virulence of laboratory strains, an increase in infected cell lysis by NK cells has also been observed in laboratory strains versus clinical strains (Cerboni *et al.*, 2000; Wang *et al.* 2002) that is not correlated with reduced HLA-1 expression levels (Cerboni *et al.*, 2000). This observation was explored further by this laboratory using chromium release assays (Tomasec *et al.*, 2005). Although strain AD169 induced an inhibition of NK cell lysis in comparison to mock infected targets, almost complete protection was elicited by the low passage strains Toledo, 6397 and Merlin (Fig 1.7a). Thus, the loss of UL/*b'* from laboratory strains of HCMV was therefore associated with reduced virulence and increased susceptibility to NK cell lysis. However, strains AD169 and Towne had suffered genetic alteration additional to the UL/*b'* deletion (Davison *et al.*, 2003a). Resistance to NK cell attack was restored in a HCMV recombinant virus, T/T11 1.1, which is a strain Towne virus containing 13kb of UL/*b'* region from strain Toledo (Fig 1.7b) (Mocarski *et al.*, 1996; Tomasec *et al.*, 2005). The experiment provided a strong indication that one or more NK resistance functions are encoded by UL/*b'*. These observations provided the rationale for focussing this study on the UL/*b'* sequence.

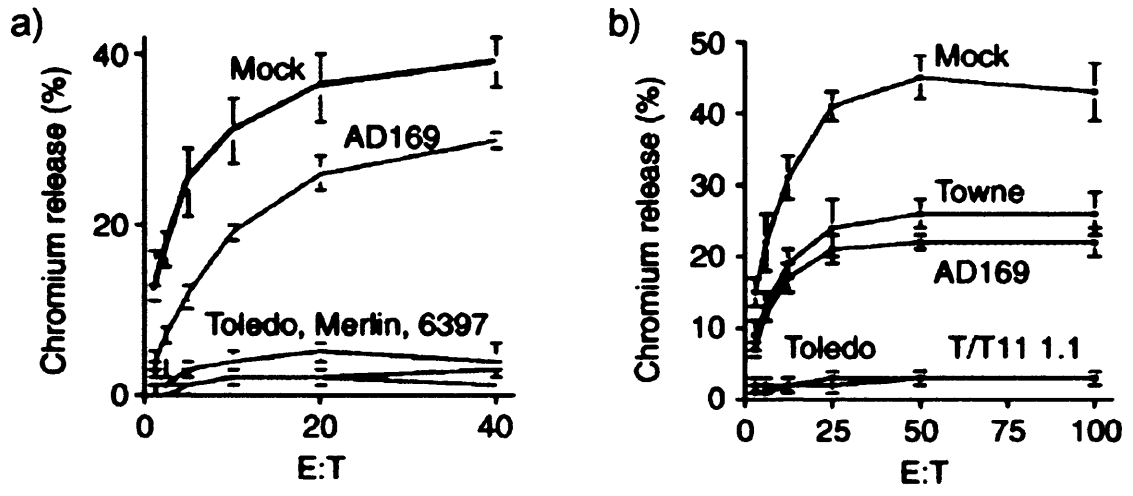

Figure 1.7 Increased resistance to NK cell lysis lies with the UL/*b'* region
a) Fibroblasts were infected with various HCMV strains, or mock infected as a negative control for 72h. Infected cells were used as targets in an allogeneic chromium release assay with NKL. The percent specific lysis is a readout of the percentage of infected cells killed by NK cells (from Tomasec *et al.*, 2005). b) Fibroblasts were infected with the laboratory adapted HCMV strains AD169 and Towne, the clinical strain Toledo, the HCMV mutant T/T11 1.1, or mock infected as a negative control for 72h. Infected cells were used as targets in an allogeneic chromium release assay with NKL. The T/T11 1.1 strain is the result of the restoration of HCMV strain Towne with the UL/*b'* region of HCMV strain Toledo (Mocarski *et al.*, 1996). From Tomasec *et al.* (2005).

1.6.4 The UL/*b'* region

The low passage strain Merlin has been designated the prototypic HCMV sequence on GenBank. It has the most complete sequence and annotation of any HCMV strain (Dolan *et al.*, 2004) and thus was selected for use throughout this study. The UL/*b'* region of Merlin was predicted to encode 23 open reading frames (ORFs), from UL128 at the left end of the UL/*b'*, through to UL150 at the right hand end, as defined by Dolan *et al.* (2004) (Figs 1.2 and 1.8). Although the majority of the 23 UL/*b'* ORFs are previously uncharacterised, there are a number of important genes encoded within the UL/*b'* that are involved in immuno-modulation of HCMV, further highlighting the importance of this region to the virulence of HCMV clinical strains. Beginning at the 'left hand' end of the UL/*b'* region is the UL128-UL131A locus (UL128, UL130 and UL131A) that is required for endothelial cell (EC) tropism and virus transfer to leukocytes (Hahn *et al.*, 2004). Although HCMV can infect a broad range of cell types *in vivo* (Plachter *et al.*, 1996), the adaptation of clinical isolates to fibroblasts in culture results in the inability to replicate efficiently in ECs or monocytes (Kahl *et al.*, 2000; MacCormac & Grundy, 1999; Revello *et al.*, 2001; Singzer *et al.*, 1999; Waldman *et al.*, 1989) or to transfer virus to leukocytes (Hahn *et al.*, 2004; Revello *et al.*, 2001). In searching for the genetic determinants of HCMV EC tropism and transfer to leukocytes, the UL/*b'* region appeared as a prime candidate (Prichard *et al.*, 2001). Subsequent studies have shown that all fibroblast-adapted, non-endotheliotropic laboratory strains contain mutations in the UL128-UL131A locus (Akter *et al.*, 2003, Hahn *et al.*, 2004), therefore making the presence of an intact UL128-UL131A locus essential for endotheliotropism and transfer to leukocytes (Hahn *et al.*, 2004). They are thought to play a role in the entry process (Hahn *et al.*, 2004) and recent studies have revealed that UL128, UL130 and UL131A are virion constituents. UL128 and UL130 form a

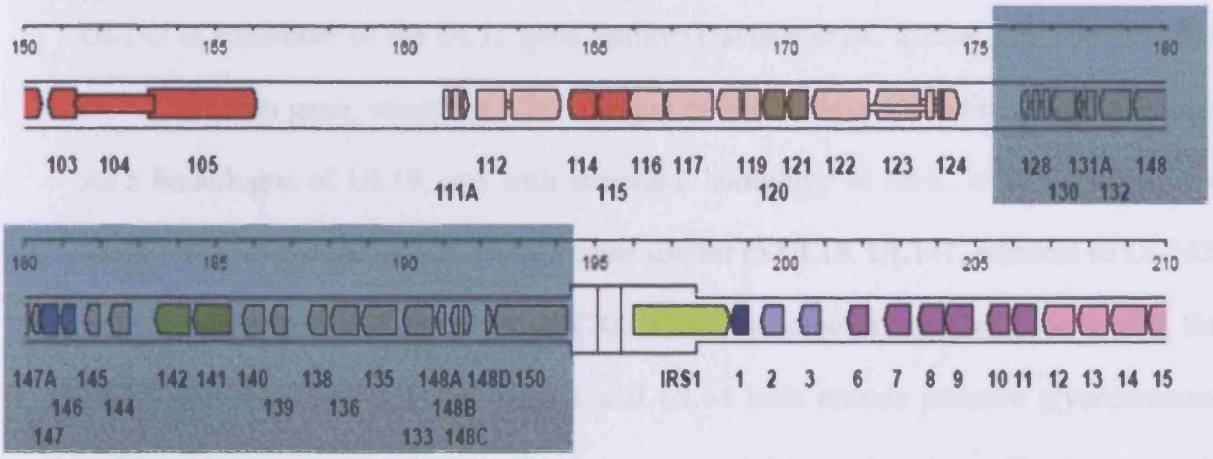

Figure 1.8 The UL/*b'* region encoded by HCMV strain Merlin
The UL/*b'* region of Merlin, highlighted by the shaded area, encodes 23 ORFs, UL128 to UL150. From Dolan *et al.* (2004)

complex with the viral envelope proteins gH and gL (Wang & Shenk, 2005) and UL131A has been found in a complex with gH (Adler *et al.*, 2006).

UL142 is a member of the UL18 gene family (Davison *et al.*, 2003a; Fig 1.9). UL18 is an NK evasion gene, encoding a homologue of MHC class I (Section 1.6.2, Fig 1.6). As a homologue of UL18, and with structural homology to MHC class I, UL142 is a likely target to encode an NK evasion gene similar to UL18. UL141, adjacent to UL142, was also described by Davison *et al.* (2003a) as a member of another gene family, the UL14 gene family (Fig 1.10). UL141 and UL14 both encode putative glycoproteins, making them potential targets for immune-modulatory functions (Davison *et al.*, 2003a).

In addition to UL142's homology to MHC class I, a number of other UL/*b'* ORFs are also described as homologues to components of the immune system. A tumour necrosis factor receptor superfamily (TNFR) homologue is encoded by ORF UL144 (Cha *et al.*, 1996). TNFRs are known as death receptors, and can trigger apoptosis upon binding of their ligands. However, the gpUL144 itself does not bind any known TNF ligands, suggesting its action is intracellular and differs from other known TNFR immune evasion strategies (Benedict *et al.*, 1999). Recent analysis has indicated that UL144 plays an important role in the evasion of immune surveillance. UL144 was found to inhibit T cell proliferation by binding the B and T cell attenuator (BTLA) (Cheung *et al.*, 2005), and recent analysis by Poole *et al.* (2006) revealed an additional function for UL144, showing UL144 activates NFκB-induced transcription, resulting in enhanced expression of CCL22. CCL22 is a chemokine which attracts Th2 and regulatory T cells. By attracting Th2 cells, it is thought that an efficient antiviral Th1 will not be induced (Poole *et al.*, 2006).

Also within the UL/*b'* region are the ORFs UL146 and UL147, that encode homologues of the IL8 chemokine (Section 1.5.4). UL146 and some of the RL11 family are among

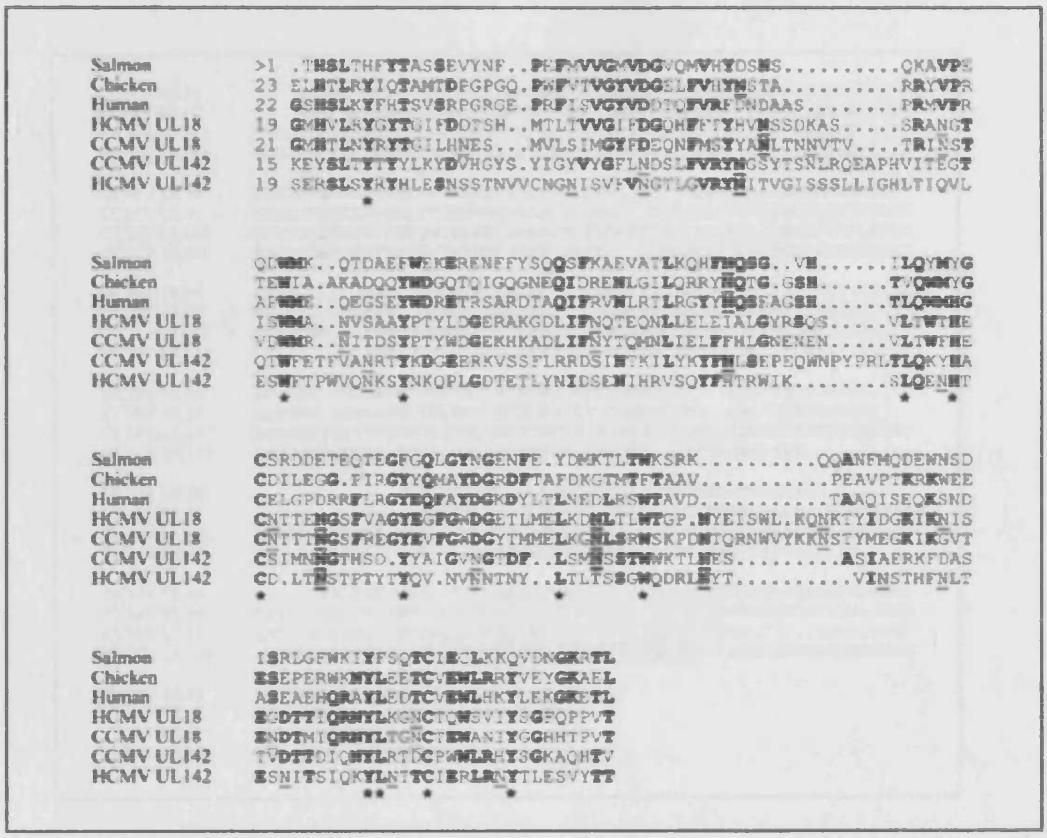

Figure 1.9 Amino acid sequence alignment of the UL18 and UL142 proteins of HCMV (strain Toledo) and CCMV with the conserved MHC-I domain
Alignment of UL18 and UL142 with the conserved MHC class I domain as represented by a diverse range of sequences from human HLA-E (AAH02578), chicken MHC-I (P15979) and salmon MHC-I (AAL60588). Potential *N*-linked glycosylation sites are underlined, and residues conserved in three or more sequences are in bold. Residues conserved in human HLA-E and all the viral sequences (including two disulphide-linked C residues in the MHC-I domain) are asterisked. From Davison *et al.* (2003).

Figure 1.10 UL141 is a member of the UL14 gene family
The HCMV genes UL141 and UL14 are members of the same gene family. The HCMV genes also show distinct conservation with their Chimpanzee CMV (CCMV) homologues. Underlined regions indicate putative transmembrane region. Bold type indicates fully conserved residues. From Davison *et al.* (2003).

the most variable in HCMV strains, illustrating a more recent, rapid evolution of these genes (Dolan *et al.*, 2004; Hassan-Walker *et al.*, 2004; Murphy *et al.*, 2003b; Pignatelli *et al.*, 2004).

1.7 CLONING THE UL/*b'* REGION: ADENOVIRUS AND ADENOVIRUS VECTORS

Before commencement of this study, the predicted ORFs from the UL/*b'* region of Toledo had been individually cloned into a mammalian expression plasmid as GFP fusion constructs, transfected into 293 cells and GFP positive cells selected. However, a number of problems were soon identified with this approach. Considerable variation was observed within repeats in NK assays when using 293 cells, making a functional read out for each ORF problematic. Such 293 cell lines could not be used to analyse the ORFs in an autologous setting, and sequence errors and sub-optimal annotation of the strain Toledo sequence meant a significant number of ORFs were missing or mis-identified. As a result of this preliminary study, it was felt a different approach was required. Strain Merlin is the prototypic HCMV sequence on GenBank, and the annotation of HCMV gene useage has been upgraded with its analysis (Dolan *et al.*, 2004), overcoming any issues with Strain Toledo. Primary human skin fibroblasts are to be used as targets for natural killer cells in functional assays, as they are permissive for HCMV and enable the use of autologous systems. However, plasmid DNA transfection of fibroblasts is difficult and inefficient; for NK cytolysis assay gene expression in 100% of target cells is preferable. To characterise the expression of the predicted UL/*b'* ORFs and to screen each UL/*b'* ORF for novel NK evasion function, an expression system that could give high levels of transgene expression, and could be used to provide efficient expression in fibroblasts was sought. The Adenovirus (Ad) vector was chosen to fulfil all these requirements.

Ad is a non-enveloped virus containing an approximately 36kb linear dsDNA genome (Fig 1.11). There are over 40 Ad subtypes, most causing benign respiratory infections (Shenk, 2001). Of these subtypes, species C serotype 5 has been most commonly used as a vector. Ad is a popular mammalian expression vector that is exploited for a wide range of applications, including an important role in gene therapy (reviewed in Benihoud *et al.*, 1999). Many features make Ad the vector of choice. Ads infect a broad spectrum of cell types, and infection is not dependant on active cell division. In addition, Ad can be grown to high titres, and high expression levels of transgenes are generally obtained (Horwitz, 2001). Briefly, the wild type genome contains an IE transcript, E1A, early-transcriptional units, E1B, E2A, E2B, E3 and E4, which are known to encode RNA processing, replication and immune evasion functions, and late genes which encode mostly structural proteins (Fig 1.11, Shenk, 2001). The most widely used Ad vectors are deleted in E1 and E3 (Horwitz, 2001; Shenk, 2001). The E3 region of Ad contains a number of genes involved in immune evasion and is dispensable for growth *in vitro*. E1A activates transcription and induces cell cycle progression in the host cell, while E1B acts to inhibit apoptosis. Deletion of the E1 gene from the genome renders the vector replication deficient (He *et al*, 1998, Horwitz, 2001). The removal of these genes creates approximately 7.5kb of space in the vector that can be replaced by transgenes (He *et al.*, 1998; Hosfield & Eldridge, 2000), which is more than sufficient for any of the UL/*b'* ORFs. In order to produce recombinant virus, mammalian packaging cell lines (911 or 293s) are used as these cell lines provide E1 *in trans* (Graham *et al*, 1977). A replication-deficient Ad ΔE1 ΔE3 vector system type will be used to clone the UL/*b'* ORFs in order to screen these ORFs for novel NK evasion functions.

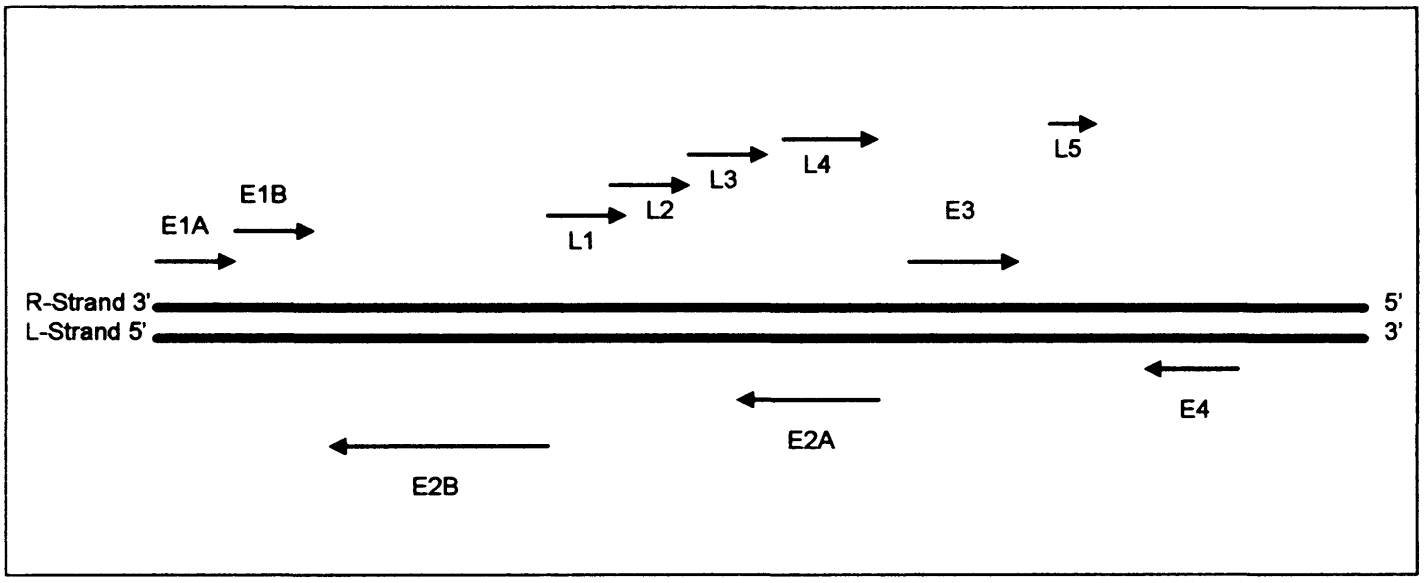

Figure 1.11 Simplified transcription map of an Ad wild type genome (Not to scale). The 36kb dsDNA genome contains an immediate early gene E1A, early genes E1B, E2A, E2B, E3 and E4 and late genes L1-L5 (adapted from Shenk, 2001)

1.8 AIMS

The aim is to identify novel HCMV-encoded NK evasion functions. To this end I had the following objectives:

1) To clone each of the HCMV UL/*b'* ORFs with an epitope tag into an Ad vector. Due to its homology with the UL/*b'*-encoded UL141, UL14 will be included in this study in parallel with the UL/*b'* ORFs.
2) To characterise expression of the UL/*b'* and UL14 ORFs in cells infected with the library of Ad recombinants by using immunofluorescence and western blot analysis.
3) To screen the UL/*b'* and UL14 ORFs for novel NK evasion functions.

2. MATERIALS AND METHODS

2.1 SOLUTIONS

Ampicillin stock — Ampicillin (Sigma-Aldrich, Poole, UK) was dissolved in water at 50mg/ml and stored in aliquots at -20°C.

Chloramphenicol stock — Chloramphenicol (Sigma-Aldrich) was dissolved in ethanol at 12.5mg/ml and stored in aliquots at -20°C.

DABCO — 2% (w/v) 1,4-Diazabicyclo[2.2.2]octane (DABCO) (Sigma-Aldrich) and 10% (v/v) phosphate buffered saline (PBS) in glycerol (Fisher Scientific, Loughborough).

DNA loading buffer — 30% glycerol in water with bromophenol blue (0.25%) (Sigma-Aldrich) and xylene cyanol FF (0.25%) (Sigma-Aldrich).

0.5M EDTA, pH8.0 — 186.1g Ethylene diamine tetraacetic acid (EDTA) (Sigma-Aldrich) dissolved in 1l water with approximately 20g sodium hydroxide (Fisher Scientific) to dissolve and adjust pH to 8.0.

Freezing Mixture — 90% (v/v) foetal calf serum (FCS) (Invitrogen, Paisley) mixed with 10% (v/v) dimethyl sulphoxide (DMSO) (Sigma-Aldrich).

IPTG stock — 23.8mg Isopropyl-beta-D-thiogalactopyranoside (IPTG) (Melford, Ipswich) was dissolved in 1ml water to generate a 1mM stock solution.

Iodoacetamide stock — 37.0mg iodoacetamide (Sigma-Aldrich) was dissolved in 1ml water to generate a 5mM stock solution.

Kanamycin stock — Kanamycin (Roche, Mannheim, Germany) was dissolved in water to generate a 50mg/ml stock solution which was stored in aliquots at -20°C.

Luria Bertani (LB) agar	As for LB, but additional agar (Fisher Scientific) was added to 1.5% (w/v) before autoclaving. Antibiotics were added as required once cooled to 50°C, before setting in plates.
LB broth	1% (w/v) tryptone (Fisher Scientific), 1% (w/v) NaCl (Sigma-Aldrich) and 0.5% (w/v) yeast extract (Sigma-Aldrich) were dissolved in water and autoclaved.
LB X-gal plates	40µl of X-gal stock solution was spread on pre-warmed LB agar plates and allowed to dry at room temperature (RT).
LB IPTG plates	40µl of IPTG stock solution was spread on pre-warmed LB agar plates and allowed to dry at RT.
NP40 lysis buffer	0.876g sodium chloride was dissolved in 5ml 1M Tris-Cl pH7.5 with 1ml 5mM EDTA and 1% Nonidet P-40 (v/v) (Sigma-Aldrich) and made up to a total volume of 100ml with water. Prior to use, 1x protease inhibitor cocktail was added (Sigma-Aldrich). For immunoprecipitations, Iodoacetamide (25µl) and PMSF (10µl) were also added per 1ml lysis buffer before use.
PBS	Phosphate buffer solution (PBS) was prepared by dissolving 1 PBS tablet (Oxoid, Hampshire) per 100ml water to generate buffer containing 8% (w/v) sodium chloride, 0.2% (w/v) potassium chloride, 1.15% (w/v) disodium hydrogen phosphate and 0.2% (w/v) potassium dihydrogen phosphate at pH7.3.
PBST	PBS, 0.1% (v/v) Tween-20 (USB, Cleveland, USA)
PMSF stock	34.8mg phenylmethanesulfonyl fluoride (PMSF) (Sigma-Aldrich) was dissolved in 1ml 95% ethanol (Fisher Scientific) at 37°C to generate a 2mM solution.

5XSDSPAGE sample buffer - reducing

0.225M Tris-Cl, pH6.8, 50% glycerol (v/v), 5% SDS (w/v) (Fisher Scientific), 0.05% bromophenol blue (w/v), 0.25M dithiothreitol (DTT) (Sigma-Aldrich) and 1% 2-mercaptoethanol (Sigma-Aldrich) were mixed in PBS to generate 5XSDSPAGE sample buffer.

5XSDSPAGE sample buffer – non reducing

Buffer made as for reducing 5XSDSPAGE sample buffer, omitting DTT and 2-mercaptoethanol.

Semi-dry transfer buffer

3g Tris base (USB), 11.3g glycine (Fisher Scientific) and 100ml methanol (Fisher Scientific) were mixed in 1l water.

SOC

2% (w/v) tryptone, 0.5% yeast extract and 0.05% sodium chloride were dissolved in water. To this solution potassium chloride (Sigma-Aldrich) and magnesium chloride (Fisher Scientific) were added to final concentrations of 2.5mM and 10mM respectively. The solution was autoclaved and after cooling, filter sterilized glucose (Sigma-Aldrich) added to a final concentration of 20mM.

3M sodium acetate

2.49g sodium acetate (Fisher Scientific) was dissolved in 10ml water to generate a 3M solution.

35% sodium-tartrate buffer

35g sodium tartrate (Sigma-Aldrich) was dissolved in 100ml sodium phosphate buffer.

15% sodium-tartrate/ 30% glycerol buffer

15g sodium tartrate was dissolved in 30ml glycerol and 70ml sodium phosphate buffer.

Sodium phosphate buffer

4.8g sodium dihydrogen phosphate (BDH Ltd, Poole) was dissolved in 1l water to generate a 0.04M solution. 5.7g disodium hydrogen phosphate (Sigma-Aldrich) was dissolved in 1l water to generate a 0.04M solution. Each solution was mixed to generate a buffer with final concentrations of 7.6mM sodium dihydrogen phosphate and 0.032M disodium hydrogen phosphate.

Superbroth (SB) 3% (w/v) tryptone, 2% (w/v) yeast extract and 5% sodium chloride were mixed with water, pH 7.5 and autoclaved. 1% sterile filtered glucose was added after autoclaving.

TAE (50x) 242g Tris base, 57.1ml glacial acetic acid (Fisher Scientific) and 100ml 0.5M EDTA, pH8.0 were mixed with water in a final volume of 1l.

0.8% TAE Agarose gel

0.8g agarose (Invitrogen) was dissolved in 100ml TAE buffer by heating. The liquid was poured into a gel mould and left at RT to set.

Townsend wash buffer

4.38g sodium chloride was dissolved in 2.5ml NP40, 5ml 5mM EDTA and 25ml 50mM Tris pH7.5 and made up to a total volume of 500ml with water.

Tris buffer (TE) 10ml of a 1M Tris-Cl solution, pH7.4 was mixed with 2ml 0.5M EDTA, pH 8.0 and water added to a final volume of 1l.

1M Tris-Cl	121.1g Tris base was dissolved in 1l water and adjusted to desired pH with a hydrogen chloride solution.
X-gal stock	5-bromo-4-chloro-3-indoyl-β-D-galactopyranoside (X-gal) (Melford, Ipswich) was dissolved in N, N-dimethyl formamide (DMF) (Sigma-Aldrich) to generate a 40mg/ml stock solution. Aliquots were stored at -20°C.

2.2 MEDIA

2.2.1 Tissue culture media

Cells were cultured in either Dulbecco's modified Eagle Medium (DMEM) (Invitrogen), Minimum Essential Medium (MEM) (Invitrogen), Roswell Park Memorial Institute (RPMI) 1640 (Invitrogen) or CellGro Stem Cell Growth Media (SCGM) (Cell Genix, Frieburg, Germany) supplemented with L-glutamine (2mM) (Invitrogen), penicillin ($1x10^5$ IU/ml) (Invitrogen), streptomycin (100mg/ml) (Invitrogen) and either 10% (v/v) FCS (Invitrogen), or 5% (v/v) human AB serum (obtained from Dr R. Aichler). Media was warmed to 37°C before use. A list of media and the varying constituents used is provided in Table 2.1.

Serum free media, referred to as DMEM-wash or RPMI-wash and PBS (Invitrogen) were used to wash cells where necessary.

2.3 CELL CULTURE

All cell lines were screened for mycoplasma by S. Llewellyn-Lacey using the VenorGeM™ Mycoplasma PCR detection kit (Biochrom AG, Berlin, Germany), which screens samples of cell lines for mycoplasma using PCR. Only mycoplasma negative cell lines were used in this study.

Table 2.1 Media used for cell culture

Media	Constituents
DMEM-wash[1]	DMEM
RPMI-wash[1]	RPMI
DMEM-10[2]	DMEM, 10% FCS (v/v)
MEM-10[2]	MEM, 10% FCS (v/v)
RPMI-10[2]	RPMI, 10% FCS (v/v)
RPMI-AB5[2]	RPMI, 5% human AB serum (v/v)
SCGM-AB5[2]	SCGM, 5% human AB serum (v/v)

(1) No supplements added to media

(2) Supplemented with 2mM L-glutamine, $1x10^{5}$ IU/ml penicillin and 100mg/ml streptomycin

2.3.1 Established cell lines

Human foetal foreskin fibroblasts (HFFF) (kindly provided by Dr G. Farrar, Porton Down) were immortalised with human telomerase reverse transcriptase (HFFF-htert) by S. Llewellyn-Lacey as described in McSharry *et al.* (2001). HFFF-htert, HFFF-htert expressing human Cocksackie and adenovirus (CAR) receptor (HFFF-hCAR) (kindly provided by Dr B. McSharry), human caucasian glioblastoma-astrocytoma, U373 (kindly provided by Dr M. Wills, Cambridge University), retinal pigment epithelial cells, ARPE-19 (ATCC), and human embryonic retinal cells, 911 cells (Crucell, Leiden) were maintained in 175cm^2 tissue culture flasks in DMEM-10. 293 cells (kindly provided by F. Graham, McMaster University) and 293 T-REx^{TM} cells (Invitrogen) were maintained in 175cm^2 flasks in MEM-10. Human caucasian chronic myelogenous leukaemia cells, K562 (ATCC) were maintained in 25cm^2 flasks in RPMI-10 and the natural killer leukaemia cell line, NKL (Robertson *et al.*, 1996) in RPMI-10 supplemented with 1000IU/ml IL2 (Cetus Corp, Emeryville, USA). All cell lines were grown in incubators at 37°C in 5% CO_2.

Primary skin fibroblasts were obtained from donors D7, D8 and D9 by skin biopsy performed by Dr S. Siebert (Siebert *et al.*, 2005), and cell lines established by Dr E. Wang before immortalization by S. Llewellyn-Lacey as described in McSharry *et al.* (2001). Immortalized primary skin fibroblasts were maintained in 175cm^2 tissue culture flasks in DMEM-10.

2.3.2 Passage of cell lines

Confluent layers of adherent cells were passaged by removing medium, washing the cell layer with PBS and incubating cells in 1-5mls Trypsin/EDTA (Invitrogen) until cells fell into suspension. Cells were resuspended in DMEM-10 or MEM-10, and split between 1:2 and 1:5. For non-adherent cell cultures, K562 and NKL, cells were

passaged by dividing the culture 1:2 and replacing with fresh RPMI-10 medium to maintain the culture at $1x10^6$ cells/ml.

2.3.3 Activation of NKL

Before use in functional assays, NKL were activated to kill over a 10 day period by gradually decreasing the serum concentration to 1-2% FCS and the IL2 concentration to 125-250IU/ml (Robertson *et al.*, 1996).

2.3.4 Isolation of polyclonal NK cells from PBMC

Polyclonal NK cells were isolated from PBMC obtained from fresh donor blood or buffy coat (Welsh Regional Transfusion Centre, Rhydlafar, Lllantrisant) by Histopaque density centrifugation. Fresh blood was collected into tubes containing heparin (Monoparin, CP Pharmaceuticals Ltd., Clywdd) (5IU/ml blood) and layered onto Histopaque-1077 (Invitrogen) in a 1:1 ratio. Blood obtained from buffy coat was first diluted 1:3 with PBS before layering onto Histopaque-1077 in a 1:1 ratio as above. Tubes were centrifuged for 20min at 1100 g without braking. The interfacing layer of mononuclear cells was removed into a universal container and diluted with PBS. The cells were washed first at 1100 g for 7min, followed by two slower washes of 350 g for 5min. The cells were resuspended in RPMI-10, counted and diluted to the required concentration for use. $1x10^5$ PBMC were usually collected per ml blood from healthy donors.

NK cells were enriched from PBMC by negative selection using immunomagnetic beads. PBMC isolated from fresh blood or buffy coat by Histopaque density centrifugation were washed in 4°C PBS/2% FCS (v/v) for 3min at 300 g, and then incubated with a CD3-FITC antibody (Serotec, Oxford, UK) (25µl per 50ml blood) at

4°C for 30min in the dark. M-450 sheep anti-mouse IgG Dynalbeads (Dynal, Wirall, UK) were prepared by washing three times in PBS/2% FCS (v/v). Cells were then washed twice in PBS/2% FCS by centrifugation for 4min at 300 g and a sample collected for flow cytometric analysis. The cells were added to the prepared M-450 sheep anti-mouse IgG Dynalbeads and incubated for 2h at 4°C in the dark, with regular agitation. The mixture was then placed in a Magnetic Particle Concentrator (MCP) (Dynal) to draw bead: cell conjugates to the side of the container. The supernatant was collected and the process repeated to remove as many bead:cell conjugates as possible. The cells were counted and a sample collected for flow cytometric analysis. The cells were resuspended at a concentration of $1x10^6$ cells/ml in RPMI-10, and as there is little NK activity in the absence of stimulation, the polyclonal NK bulk cultures were incubated overnight at 37°C in 5% CO_2 with interferon alpha (IFNα) (1000IU/ml) (Roferon, Roche) and IL2 (200IU/ml) to induce cytotoxicity (Borysiewicz *et al.*, 1985). The efficiency of CD3 depletion and the number of NK cells obtained were checked by flow cytometric analysis (Section 2.10) after staining pre-Dynalbead and post-Dynalbead samples with a CD56-PE antibody (Serotec).

2.3.5 NK cell cloning

The method described by Morris *et al.* (2005) was used to generate and culture NK clones. The process is summarised in Figure 2.1. Briefly, NK clones were isolated from fresh PBMC by single cell sorting using the MoFlo™ High-Performance Cell Sorter (Dako): $1x10^6$ PBMC in 200µl PBS-FCS were incubated with CD3-FITC and CD56-PE antibodies for 30min at 4°C. The cells were then washed once in 10ml PBS-FCS and once in 5ml SCGM-AB5, filtered with a 40µm cell strainer and resuspended at a final concentration of $1x10^6$ cells/ml in SCGM-AB5. $CD3^-CD56^+$ cells were sorted by the dedicated Central Biotechnology Services technician using the MoFlo cell sorter into

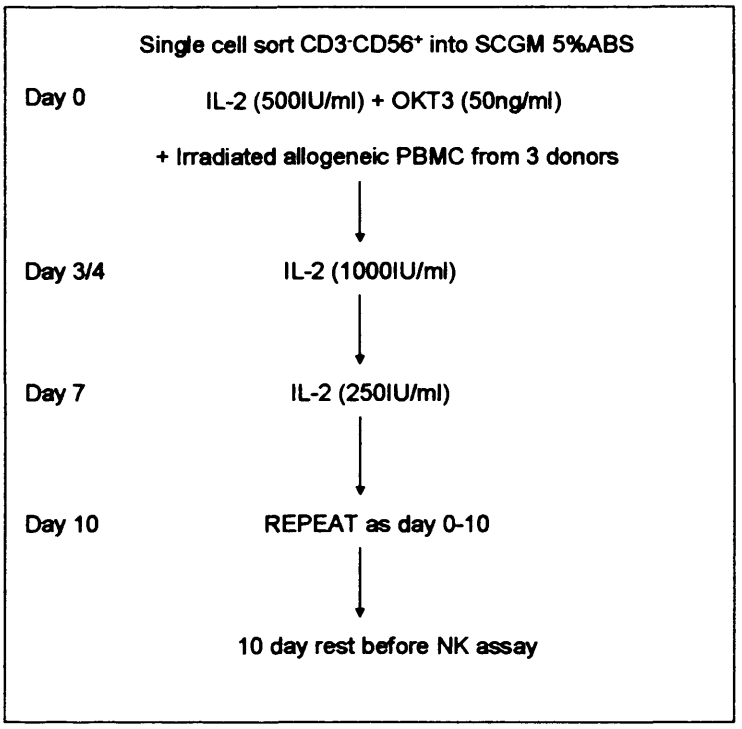

Figure 2.1 Summary of NK cloning method
NK clones were single cell sorted from PBMC into 96 well plates and cultured at 37°C, 5% CO_2 in SCGM 5% ABS (v/v) supplemented with 500IU/ml IL2, 50ng/ml OKT3 and $5x10^4$ irradiated PBMC from three allogeneic individuals for 4 days. On day 4, half the medium was removed and replaced with fresh medium containing 1000IU/ml IL2. On day 7, half the medium was removed and replaced with fresh medium containing 250IU/ml IL2. Clones were restimulated every 10 days with irradiated PBMC, IL2 and OKT3. Clones were maintained up to 8 weeks, and assayed from week 5-8 (Morris *et al.*, 2005).

single wells of a 96-well U bottom plate, and cultured for 4 days at 37°C, 5% CO_2 in SCGM-AB5 medium containing IL2 (500IU/ml), a CD3 specific antibody (OKT3 at 50ng/ml; ATCC) and irradiated feeder cells ($5x10^4$ cells), obtained from PBMC of three allogeneic donors. On day 4, half the culture media was removed and replaced with fresh SCGM-AB5 containing IL2 (1000IU/ml). The NK clones were cultured for up to 7-8 weeks, and re-stimulated every 7-10 days with irradiated feeder cells, IL2 and OKT3 as described above. Clones were moved to larger culture volumes as cell numbers expanded.

2.3.6 Cryopreservation of cells

Adherent cells were put into suspension as described in Section 2.3.2. Suspended cells were then recovered by centrifugation and resuspended in 1ml of freezing mix. The 1ml aliquot was transferred to a cryovial and placed in a Nalgene 5100 Cryo 1°C freezing container (Merck, West Drayton, UK) which contained isopropanol at RT. This was then transferred to a -70°C freezer for 24h before transferring to liquid nitrogen for storage.

To resurrect cells from liquid nitrogen storage, they were rapidly thawed, resuspended in warmed DMEM containing 50% FCS (10ml) and transferred to a 15ml centrifuge tube. Cells were centrifuged at 250 g for 5min, resuspended in normal culture medium (7ml) and incubated at 37°C, 5% CO_2 in a $25cm^2$ tissue culture flask.

2.3.7 Cell counting

A 10µl aliquot of cell suspension was diluted 1:1 with Trypan Blue (Sigma-Aldrich) and cells were counted on a glass haematocytometer (Sigma-Aldrich) under white light. Viable cells were identified by the exclusion of the blue dye. The number of cells per ml was determined using the following:

Number of cells/ml = [(no of cells in grid) x ($1x10^4$)] x 2

2.4 VIRUSES

2.4.1 Propagation of Human Cytomegalovirus (HCMV) stocks

HCMV was grown in HFFF-htert cells in 175cm^2 flasks. Once HFFF-hterts reached ~70% confluency, they were infected with HCMV at a MOI of 0.1 in a minimal volume of media (5ml) for 2h at 37°C in a rocking incubator. After this incubation, the inoculum was removed, cells washed with PBS, and 25ml fresh DMEM-10 added. After approximately 10 days, once a cytopathic effect (cpe) was observed, the media was collected and stored at -70°C. This process was repeated until all the cells showed cpe. To prepare HCMV virions, aliquots were defrosted and centrifuged at 600 g for 10min to remove cellular debris. The supernatant was decanted into a 250ml Sorvall centrifuge pot and centrifuged at 23000 g (GSA Sorvall) for 120min at RT. The supernatant was removed and the pellet resuspended in RPMI. Aliquots of approximately 100µl were transferred to -70°C for storage. For this study, a stock of HCMV strain Merlin and the deletion mutant AD169ΔUL14 (generated by Dr R. Stanton) were prepared using the method described above. HCMV strain AD169 used in this study was obtained from Dr P. Tomasec.

Prior to extracting HCMV strain Merlin DNA, a sample of HCMV Merlin virions was purified using the glycerol-tartrate gradient method (Talbot & Almeida, 1977). Media was collected from infected cell flasks and centrifuged as described above to remove cell debris. The supernatant was transferred to ultracentrifugation tubes and centrifuged (Beckman L8-60M ultracentrifuge with SW28 rotor) at 44600 g, 4°C for 70min. During centrifugation, gradients were prepared in ultracentrifuge tubes using a gradient mixer with 35% sodium-tartrate (4ml) and 15% sodium-tartrate/30% glycerol (5ml). After centrifugation, the pellet was resuspended in sodium phosphate buffer (1-2ml) and

overlayed onto the prepared gradients. Ultracentrifugation at 44600 g was repeated for 45min at 4°C and the virion band, formed at the interfacing layer of the two gradients, was collected using a 20G needle inserted into the centrifuge tube. Virions were collected into fresh ultracentrifuge tubes, diluted with sodium phosphate buffer, and centrifugation repeated for a further 60min at 4°C, 44600xg. The pellet was resuspended in 100µl sodium phosphate buffer and stored at -70°C.

2.4.2 Propagation of recombinant adenovirus (RAd) stocks

RAd stocks were generated by propagation in 293 or 911 cells. Cells were grown in 175cm^2 flasks to 80% confluency before infection with the RAd virus at a MOI of 0.1 in 20ml DMEM-10 or MEM-10 overnight. The inoculum was replaced the following day with fresh media, and thereafter as necessary. Cell monolayers were checked for cpe, and once 100% cpe was observed, cells were detached from the flask by gentle tapping and resuspended in media. Infected cells were recovered by centrifugation at 450 g for 5min and the cell pellet resuspended in PBS (5-8ml). Arklone P or tetrachloroethylene (Fisher Scientific) was added to the cells at a 1:1 ratio and mixed vigorously before centrifuging at 900 g for 5min. The aqueous phase, containing the RAd virus, was removed and divided into ~500µl aliquots that were transferred to -70°C for storage.

2.4.3 Titre of virus stocks

HCMV and RAd virus stock titres were determined using limiting dilution assay. HFFF-hterts (HCMV) or 293s (RAd) from a confluent 175cm^2 flask were trypsinised (Section 2.3.2) and split between 72 wells of 3 x 24 well plates (HCMV) or 80 wells of a flat-bottom 96 well plate (RAd) and left overnight to adhere. Serial dilutions of the virus stock from 10^{-2} to 10^{-10} were made and 1ml (HCMV) or 100µl (RAd) of each dilution was used to infect cells. The media was replaced 24hpi, and thereafter as

necessary. At 4 weeks (HCMV) or 10-12 days (RAd), cpe was marked where it appeared in each well. The virus titre was calculated as tissue culture infectious dose ($TCID_{50}$) units using the formula of Reed and Meunch (Reed & Meunch, 1938). $TCID_{50}$ units were converted to pfu/ml for convenience, using the accepted conversion factor: [1 $TCID_{50}$ = 0.7 infectious units] (Davis *et al.*, 1990).

2.4.4 Infection of cells for assays

HFFF-hterts were normally infected with HCMV at a MOI of 10 pfu/cell or with RAds at a MOI of 100 for use in western blot and functional assays. HFFF-hCAR cells were infected with both HCMV and RAds at a MOI of 10 for use in western blot, FACS and functional assays. For immunofluorescence studies, HFFF-hCAR were infected at a MOI of 50 (RAds). Immortalized primary human skin fibroblasts used in functional assays were infected with HCMV at a MOI of 10 and RAd at a MOI of 500.

Cells were seeded at the required density 24h prior to infection. The cell media was removed and cells were washed in PBS before adding virus in the minimal, yet consistent, volume of media. Cells were incubated with virus for 2h in a rocking incubator at 37°C, 5% CO_2, after which time the inoculum was removed, cells washed once in PBS, and media replaced. For western blots, the replacement media contained forskolin (1μg/ml) (Sigma-Aldrich).

2.4.5 Isolation of HCMV and RAd DNA

HCMV and RAd DNA was purified using the QIAmp blood kit (Qiagen, Sussex, UK). Briefly, an aliquot of virus was pre-digested with RNAse (1mg) (Sigma-Aldrich) for 30min at RT. The supplied protease and lysis buffer (Qiagen) were added, and the mixture incubated at 70°C for 10min. Finally, a QIAmp column was used to capture

viral DNA from the lysate mixture. The column was washed to remove impurities before eluting the viral DNA by centrifugation.

2.5 STANDARD MOLECULAR BIOLOGY

2.5.1 PCR

PCR reactions were carried out using a *Taq* DNA polymerase (Sigma-Aldrich and Roche) with the manufacturers supplied buffer containing magnesium sulphate, dNTPs (1μM) (Sigma-Aldrich) and 20pmol of each primer (made to order by Invitrogen). Unless otherwise stated, the following thermocycling reaction was used:

Denaturation	95°C 2min	
Denaturation	95°C 15s	x 30 cycles
Annealing	58°C 30s	
Elongation	72°C 30s	
Hold	4°C	

2.5.2 Agarose gel electrophoresis

Separation of DNA fragments by size was performed by electrophoresis with a 0.8% (w/v) TAE agarose gel. DNA samples were mixed with DNA loading buffer (6x) before adding to wells of the pre-set agarose gel. Samples were electrophoresed at 75V for approximately 1h depending on the resolution required. The gel was stained with an ethidium bromide buffer for approximately 15min before visualization of DNA bands under ultra violet light, 365nm.

2.5.3 Isolation of DNA from agarose gel

To isolate DNA from agarose gel, the QIAquick gel extraction kit (Qiagen) or GFX™ PCR and Gel Band Purification kit (GE Healthcare, Buckingham, UK) were used according to the manufacturer's instructions. The kits work on the principle that DNA adsorbs to a silica gel membrane in the presence of high salt, while contaminants pass through. The membrane was washed before finally eluting the DNA in Tris buffer or water. The DNA was then stored at -20°C until use.

Electroelution was also used to isolate DNA from agarose gel. In this method, the gel containing the DNA fragment of interest was added to a small piece of dialysis membrane containing TAE buffer (500µl). The gel was placed in an electrophoresis tank containing TAE buffer and an electric current (100V) passed through which moves the DNA from the agarose gel slice into the TAE buffer. The DNA was extracted from the buffer by adding an equal volume phenol:chloroform:isoamyl alcohol (24:25:1) (Sigma-Aldrich), vortexing briefly and centrifuging for 5min at 10000 g. The uppermost layer containing DNA was removed. DNA was precipitated by adding 1ml 95% (v/v) ethanol and 50µl 3M sodium acetate solution and incubating at -20°C overnight. The solution was centrifuged at 10000 g for 20min at 4°C, the supernatant removed and the DNA pellet washed in 70% (v/v) ethanol by centrifuging for a further 20min at 4°C. The DNA pellet was air dried before resuspending in Tris buffer and storing the DNA at -20°C.

2.5.4 TOPO TA cloning®

PCR products were cloned into a pCR2.1 TOPO® vector by TOPO TA cloning® (Invitrogen) according to the manufacturers' instructions. Amplification with *Taq* polymerase generates PCR products with a single overhanging 3' deoxyadenosine (A). The TOPO TA cloning® principle exploits this overhanging base, and the linearised

pCR2.1 TOPO® vector contains a single overhanging 3' deoxythymidine (T) residue, which enables efficient ligation of the PCR product with the vector. Briefly, the cloning process involved mixing the PCR product (2µl) with TOPO vector (0.5µl) and the supplied salt solution (0.5µl), and incubating for 5 – 30min at RT for ligation to occur. Following this incubation, the TOPO reaction (1µl) was added to a vial of TOP10 bacterial cells, and incubated on ice for 15min. The DNA was transformed into the TOP10 cells by heat shock at 42°C (Section 2.5.8). The cells were allowed to recover in SOC medium for 1-2h at 37°C before plating onto LB plates containing ampicillin (50µg/ml) and X-gal solution (40µl) and incubating at 37°C overnight.

2.5.5 Plasmid DNA minipreps

Small scale plasmid preparations were performed using Qiagen spin miniprep kits according to the manufacturer's instructions (Qiagen). The kit is based on the alkaline lysis of bacterial cells and the adsorption of DNA to a silica gel membrane in the presence of high salt. DNA is then washed and eluted into Tris buffer. Bacterial cells containing the plasmid of interest were harvested from an overnight culture (1-5ml) by centrifugation at 10000 g. The bacterial cells were resuspended in the manufacturers supplied buffer (250µl) and mixed with an equal volume of lysis buffer (250µl). This solution was incubated for 5min at RT and lysis stopped by the addition of a neutralisation buffer (350µl). The resulting precipitate was cleared by centrifugation at 10000 g for 10min, and the supernatant removed to a DNA separation column. The DNA was adsorbed onto the silica-based membrane of the column by centrifugation at 10000 g for 1min, washed by further centrifugation with a wash buffer, and finally eluted into 50µl Tris buffer. DNA was then stored at -20°C until further use.

2.5.6 Plasmid purification by maxiprep

QIAfilter plasmid maxiprep kits (Qiagen) were used for large scale plasmid DNA preparation and to generate transfection-quality DNA. For this procedure, bacteria are subject to alkaline lysis, followed by binding of plasmid DNA to the Qiagen resin under the appropriate salt and pH conditions. Impurities are removed by a medium salt wash, and plasmid DNA is eluted in a high salt buffer. Plasmid DNA is then concentrated and desalted by isopropanol precipitation. For large scale plasmid purification, a colony of bacteria containing the plasmid of interest was used to inoculate 250ml LB media and incubated overnight at 37°C in a shaking incubator. Bacterial cells were recovered by centrifugation at 6000 g for 15min, and resuspended in the manufacturers supplied buffer (10ml) containing RNAse. Similar to miniprep procedure, bacteria were lysed by the addition of an equal volume of lysis buffer and incubated for 5min at RT before the addition of neutralisation buffer (10ml). The resulting solution and precipitate were then transferred to a QIAfilter cartridge, through which the solution was filtered to remove the precipitate. The solution was then transferred to a Qiagen tip-500 and passed through the column by gravity flow where DNA bound to the resin of the Qiagen tip-500 column. The resin was washed with a wash buffer and the DNA eluted with elution buffer (15ml) into a fresh centrifuge tube. To precipitate DNA, 0.7 volumes of isopropanol (10.5ml) were added to the eluate, and the solution was centrifuged at 15000 g, 4°C for 30min. The DNA precipitate was washed with 70% (v/v) ethanol by centrifugation at 15000 g, 4°C for 10min and the DNA pellet air dried before resuspending in Tris buffer.

2.5.7 Estimation of DNA concentration

To estimate DNA concentration, DNA from plasmid preparations was analysed by spectrophotometer (Biopharmacia Biotech Ultrospec 3000). Using the

spectrophotometer, absorbance of a DNA solution at 260nm was compared with that of a control sample. DNA concentration can be very low after gel purification of a PCR or restriction enzyme digest product. In these cases, the purified DNA product was electrophoresed in a 0.8% agarose TAE gel alongside a SmartLadder marker (Eurogentec, Southampton, UK). Concentration of DNA can be estimated by comparison with the ladder, which contains DNA fragments of defined size and amount.

2.5.8 Restriction enzyme digestion

All restriction enzymes used in this study were purchased from NEB (Hitchin, UK), and each enzyme reaction was carried out according to the manufacturers' instructions. Reaction mixtures were set up in volumes of 50µl, containing DNA template, 5µl reaction buffer (supplied by manufacturer, NEB), 0.5µl restriction enzyme and distilled water as required. Restriction digests were incubated at 37°C for 1-16h. Following digestion, DNA fragments were separated by agarose gel electrophoresis (Section 2.5.2) and purified by either gel extraction kit (Qiagen, GE Healthcare) or electroelution (Section 2.5.3). Following digestion of vector DNA to linearise, small DNA fragments were removed by dialysis in TE buffer for 4h at 4°C.

2.5.9 Ligation

For ligation of inserts with linearised vector DNA, DNA concentrations of each were first estimated by agarose gel electrophoresis (Section 2.5.7). Approximately 100ng of linearised vector was mixed with sufficient insert to give molar ratios of insert:vector of 3:1 according to the equation:

$$\frac{(100ng\ vector \times size\ of\ insert,\ kb)}{(size\ of\ vector,\ kb)} \times \frac{3}{1} = ng\ insert\ to\ add\ to\ 100ng\ vector$$

Ligations were carried out using Quick T4 ligase (NEB). To the insert:vector mix, distilled water was added to a total volume of 10µl, followed by Quick T4 ligase (2µl) and the manufacturers' supplied ligation buffer (10µl). The reaction was incubated for 5min at RT, and stopped by cooling on ice.

The quick ligation was used directly to transform *E.coli* strain JM109 (Promega, Southampton, UK) by heat shock (Section 2.5.10) or alternatively, used to transform *E.coli* strain XL-1 blue bacteria by electroporation (Section 2.5.10) once DNA had been precipitated by ethanol/sodium acetate precipitation (Section 2.5.3) to remove excess salts.

2.5.10 Transformation of *E.coli* JM109 and *E.coli* XL-1 blue

Plasmids were transformed into *E.coli* JM109 by heat shock. Ligation mixture (2µl) was added to a vial of *E.coli* JM109 and was incubated on ice for 15min. Bacteria were heat shocked by incubation in a 42°C water bath for 40s. Transformed bacteria were then allowed to recover in SOC media for 1-2h at 37°C before plating onto LB-selective plates and incubating overnight at 37°C.

Plasmids were transformed into electrocompetent *E.coli* XL-1 blue by electroporation. Briefly, DNA (1µl) was added to a vial of *E.coli* XL-1 blue (50µl) and incubated on ice for 15min. Bacteria were then electroporated at 2.3V using an electroporator (BioRad Gene Pulser™), and allowed to recover in SOC media at 37°C for 1-2h. After recovery, bacteria were plated onto LB selective plates and incubated overnight at 37°C.

2.5.11 Glycerol stocks

Plasmids of interest were stored as glycerol stocks, generated by mixing 500µl of an overnight bacterial culture with an equal volume of 80% (v/v) glycerol in a cryovial. Glycerol stocks were stored at -70°C.

2.5.12 DNA Sequencing

DNA samples were sequenced using the "Big Dye" terminator cycle sequencing kit (Perkin-Elmer, Boston, USA) and dideoxy terminator cycle sequencing. To set up a sequencing reaction, plasmid DNA (200ng) was mixed with terminator ready reaction mix (4µl) and distilled water to a total reaction volume of 10µl. Except where stated, the following thermocycling reaction was used:

Denaturation	96°C 30s	} x 25 cycles
Annealing	50°C 15s	
Elongation	60°C 4min	

Following the thermocycling reaction, DNA was precipitated by ethanol/sodium acetate precipitation (Section 2.5.3) and the sequencing products separated on an ABI model 377 sequencer (Applied Biosystems, Foster City, USA) by a dedicated technician in Central Biotechnology Services (Cardiff University).

2.6 GENERATION OF RECOMBINANT ADENOVIRUSES BY AdEASY

2.6.1 Generating TOPO clones

An overview of the AdEasy method for generating recombinant adenoviruses (RAds) is provided in Figure 2.2. Each UL/*b*' ORF was amplified from HCMV strain Merlin DNA by PCR with a C-terminal epitope tag, Streptag (Section 2.5.1). The C-terminal

Streptag was incorporated into the specific reverse PCR primer for each gene. A list of the primers used is provided in Table 2.2.

PCR products were separated by agarose gel electrophoresis (Section 2.5.2) to check for correct product size. PCR products were purified from agarose gel (Section 2.5.3) and inserted into the pCR2.1TOPO vector (Fig 2.3a) by TOPO TA cloning® (Section 2.5.4). TOPO clones were selected by ampicillin resistance and blue-white screening and purified by plasmid miniprep (Section 2.5.5). The presence of a correct UL/*b'* insert and its orientation in the vector was checked by *Eco*RI restriction enzyme digest followed by agarose gel electrophoresis. Clones containing the correct inserts were then sequenced to check for mutations before purifying plasmid DNA by maxiprep (Section 2.5.6).

2.6.2 Sub-cloning to pShuttleCMV

UL/*b'* ORFs were removed from the TOPO vector by restriction enzyme digest (Section 2.5.8) using asymmetric sites according to their orientation in the vector. The sites used are summarised in Figure 2.3b, c. The digested UL/*b'* ORF product was separated from the TOPO vector by agarose gel electrophoresis and purified from the gel by electroelution (Section 2.5.3). The pShuttleCMV adenovirus transfer vector (kindly donated by Dr B.Vogelstein) was similarly digested (Fig 2.3b, c) and purified by dialysis in TE buffer at 4°C for 4h. Linearised vector DNA and the digested UL/*b'* product were extracted in phenol:chloroform and precipitated by ethanol/ sodium acetate precipitation (Section 2.5.3). The DNA concentrations of the digested UL/*b'* product and the vector were estimated by agarose gel electrophoresis alongside a Smartladder marker (Section 2.5.6). Vector and insert were then ligated using T4 Quick ligase at molar ratios of 3:1 (Section 2.5.9).

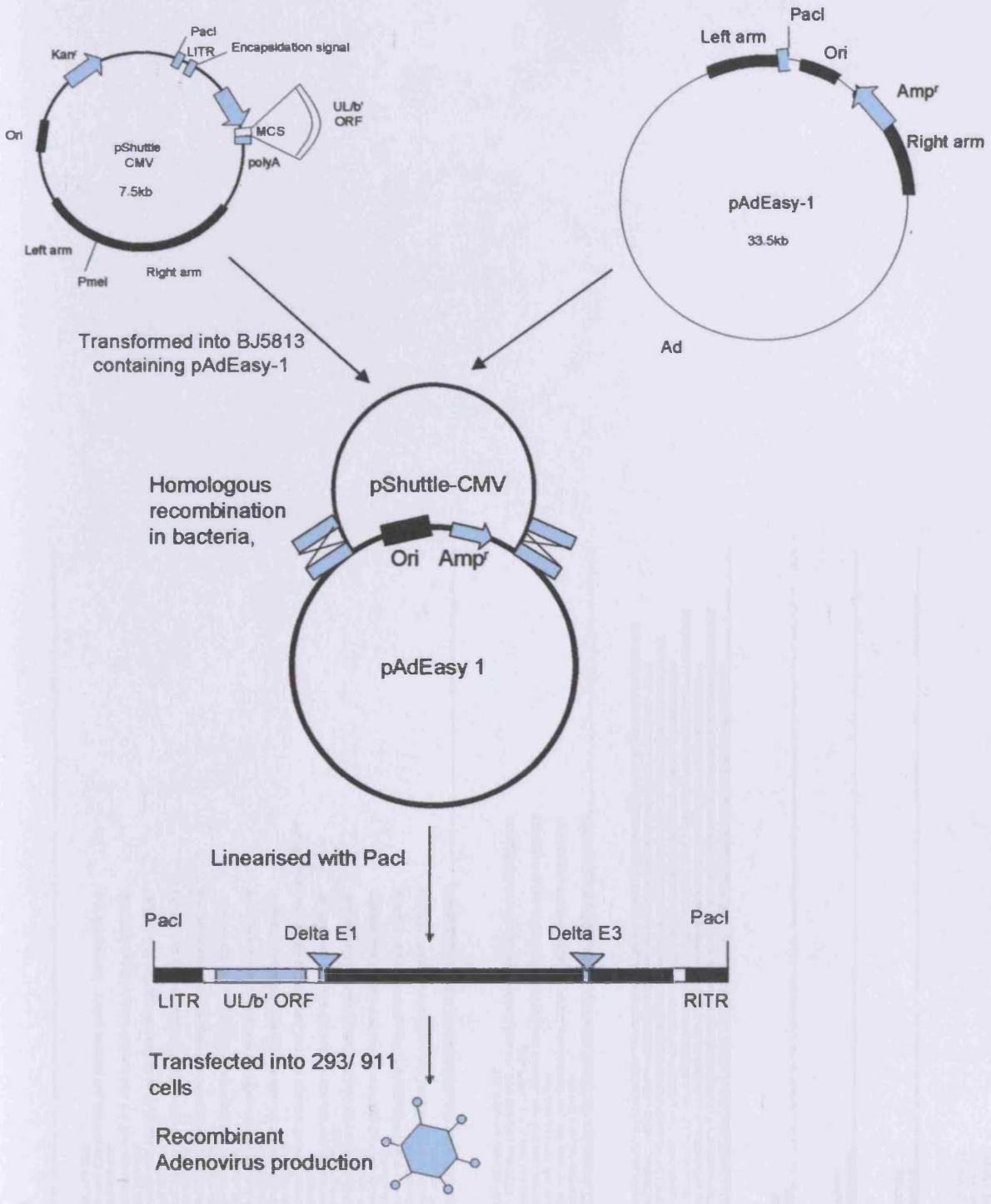

Figure 2.2 Generation of Ad recombinants by homologous recombination in bacteria: The AdEasy system (not to scale)

The UL/*b*' ORFs were individually cloned into the pShuttleCMV transfer vector. This vector was then transformed into *E.coli* BJ5813 cells that contained the pAdEasy-1 adenoviral backbone. Homologous recombination occurred between the arms of homology of the pShuttleCMV transfer vector and pAdEasy-1 in BJ5813s and the recombinant Ad DNA was extracted and linearised with *Pac*I before transfecting mammalian packaging cells (293 or 911). Recombinant Ad was extracted from these cells using ArkloneP.

Table 2.2 Primers used for RAd cloning and sequencing

Name	Primer
For AdEasy via TOPO cloning	
UL132 down	CGC CAC GTC TCG AGA ATG CCG
UL132 up + Strep	TTA TTT TTC GAA CTG CGG GTG GCT CCA AGC GCT GTC GTA CTC GGG ATC TCT GAG
UL133 down	GAG AAC GCA GTA GCA ATG GGT
UL133 up + Strep	TTA TTT TTC GAA CTG CGG GTG GCT CCA AGC GCT CGT TCC GGT CTG ATG CTG CTG
UL135 down	GGA GAG AAG ATC ATG GTG TGG
UL135 up + Strep	TTA TTT TTC GAA CTG CGG GTG GCT CCA AGC GCT GGT CAT CTG CAT TGA CTC GGC
UL136 down	AGA GAG AAA GAG AGT ATG TCA GTC
UL136 up + Strep	TTA TTT TTC GAA CTG CGG GTG GCT CCA AGC GCT CGT AGC GGG AGA TAC GGC GTT
UL139 down	GTA ACG AAC ATG CTG TGG ATA
UL139 up + Strep	TTA TTT TTC GAA CTG CGG GTG GCT CCA AGC GCT CCG AGG CGG AGG TGG AAA TGA
UL141 down	ATC ATG TGC CGC CGG GAG TCG
UL141 up + Strep	TTA TTT TTC GAA CTG CGG GTG GCT CCA AGC GCT CCT CTT CAT CTT TTT AAC ACC
UL141A down	TCC GAG GTA GCA ATG AGA CAG
UL141A up + Strep	TTA TTT TTC GAA CTG CGG GTG GCT CCA AGC GCT ACA GCA CCC AGA ACA GCC ACG
UL142 down	TAT GCG GAT TGA ATG GGC GTG
UL142 up + Strep	TTA TTT TTC GAA CTG CGG GTG GCT CCA AGC GCT CTG ACC GCG CCA TAC TTC GTA
UL144 down	GGC ATG AAG CCT CTG GTG ATG
UL144 up + Strep	TTA TTT TTC GAA CTG CGG GTG GCT CCA AGC GCT CCA AGC GCT CAG GGT GCG GTA GAA AAT TTT
UL145 down	ATG TAC GGC GTC CTG GCT CA
UL145 up + Strep	TTA TTT TTC GAA CTG CGG GTG GCT CCA AGC GCT ATC TTC ACT TCC ACC CAT CGG
UL146 down	ATA ATG CGA TTA ATT TTT GGT GCG
UL146 up + Strep	TTA TTT TTC GAA CTG CGG GTG GCT CCA AGC GCT TTC CTT CAG ACC TAC TAG GGT
UL147 down	TTC AAT ATG TTG CTA ACA TGG
UL147 up + Strep	TTA TTT TTC GAA CTG CGG GTG GCT CCA AGC GCT CCA GCG CAG TCT AAA GTA GTG
UL148 down	AGC ATG TTG CGC TTG CTG TTC
UL148 up + Strep	TTA TTT TTC GAA CTG CGG GTG GCT CCA AGC GCT CCG ACG CCG CGA CAC CAG GTA
UL148B down	AAC GGG ATG GCG CTG GAT ACG
UL148B up + Strep	TTA TTT TTC GAA CTG CGG GTG GCT CCA AGC GCT AAG TCG CGT GTG GTA GAT CTC
UL150 down	CAT ACA GCT ATG CTC ACA CTC
UL150 up + Strep	TTA TTT TTC GAA CTG CGG GTG GCT CCA AGC GCT CAG CTC CAA GCG CCG TAG CCG
For AdEasy direct cloning	
UL133 down plus KpnI	GCGC GGTACC GAG AAC GCA GTA GCA ATG GGT
UL133 up plus Strep and XbaI	GGCC TCTAGA TTA TTT TTC GAA CTG CGG GTG GCT CCA AGC GCT CGT TCC GGT CTG ATG CTG CTG
UL136 down plus KpnI	GCGC GGTACC AGA GAG AAA GAG AGT ATG TCA GTC
UL136 up plus Strep and XbaI	GGCC TCTAGA TTA TTT TTC GAA CTG CGG GTG GCT CCA AGC GCT CGT AGC GGG AGA TAC GGC GTT
UL147down plus KpnI	GCGC GGTACC TTC AAT ATG TTG CTA ACA TGG
UL147 up plus Strep and XbaI	GGCC TCTAGA TTA TTT TTC GAA CTG CGG GTG GCT CCA AGC GCT CCA GCG CAG TCT AAA GTA GTG
UL148 down plus KpnI	GCGC GGTACC AGC ATG TTG CGC TTG CTG TTC
UL148 up plus Strep and XbaI	GGCC TCTAGA TTA TTT TTC GAA CTG CGG GTG GCT CCA AGC GCT CCG ACG CCG CGA CAC CAG GTA
For AdZ recombineering	
UL131A down	AACCGTCAGATCGCCTGGAGACGCCATCCACGCTGTTTTGACCTCCATAGAAGACACCGGGACCGATCCAGCCCACCATGCGGCTGTGTCGGGTGTGGC
UL131A up + Strep	TATAACATAGAGTATAATATAGAGTATACAATAGTGACGTTTATTTTTCGAACTGCGGGTGGCTCCAAGCGCTGTTGGCAAAGAGCCGCACGCT
UL128 down	AACCGTCAGATCGCCTGGAGACGCCATCCACGCTGTTTTGACCTCCATAGAAGACACCGGGACCGATCCAGCCACCGCGCGTCATGAGTCCCAAAGA
UL128 up + Strep	TATAACATAGAGTATAATATAGAGTATACAATAGTGACGTTTATTTTTCGAACTGCGGGTGGCTCCAAGCGCTATAGGGAACGCTGCCAGCGGC
UL132 down	AACCGTCAGATCGCCTGGAGACGCCATCCACGCTGTTTTGACCTCCATAGAAGACACCGGGACCGATCCAGCCTGGATCCCCACGTCTCGAGAATGCCGGC
UL132 up + Strep	TATAACATAGAGTATAATATAGAGTATACAATAGTGACGTTTATTTTTCGAACTGCGGGTGGCTCCAAGCGCTGTCGTACTCGGGATCTCTGAG
UL148 down	AACCGTCAGATCGCCTGGAGACGCCATCCACGCTGTTTTGACCTCCATAGAAGACACCGGGACCGATCCAGCCTGGATCCACCCGCGCAGCATGTTGCGCT
UL148 up + Strep	TATAACATAGAGTATAATATAGAGTATACAATAGTGACGTTTATTTTTCGAACTGCGGGTGGCTCCAAGCGCTCCGACGCCGCGACACCAGGTA
For sequencing TOPO clones	
M13 For	GTAAAACGACGGCCAG
M13 Rev	CAGGAAACAGCTATGAC
For sequencing direct pShuttle clones	
pShuttle For	GGTCTATATAAGCAGAGCTG
pShuttle Rev	GTGGTATGGCTGATTATGATCAG
For sequencing AdZ clones	
CMV For	CGCCATCCACGCTGTTTTGA
PolyA rev	TTGAGTAGGATTACAGAGTA
For RAd screening by duplex PCR	
Kan For	CAA GAT GGA TTG CAC GCA GG
Kan Rev	AAG GCG ATA GAA GGC GAT GC
Ad For	GGC TGC TCT GCT CGG AAG AC
Ad Rev	GGC ATA CGC GCT ACC CGT AG

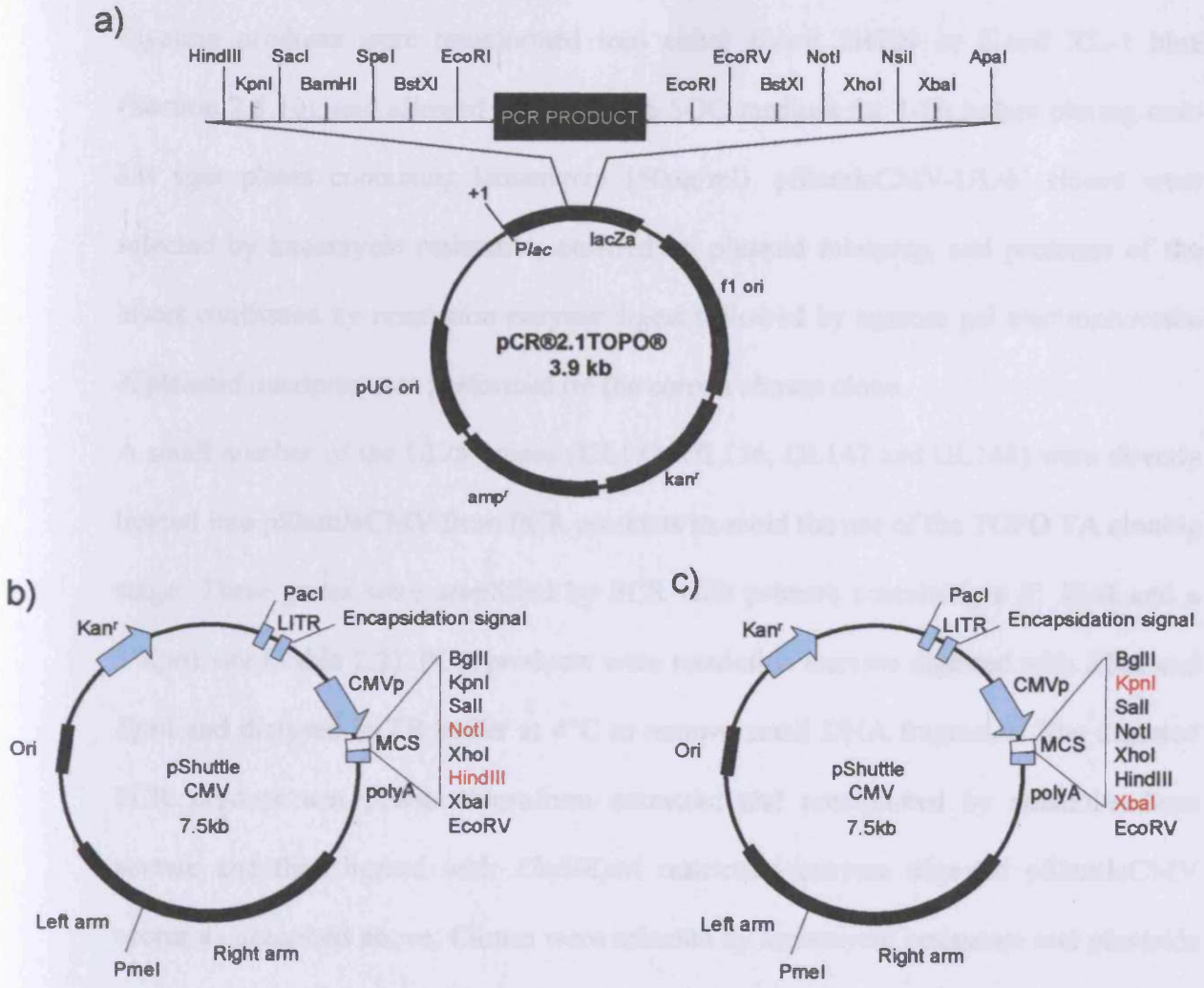

Figure 2.3 Cloning UL/*b*' ORFs into the AdEasy transfer vector, pShuttleCMV (not to scale)

Each UL/*b*' ORF PCR product was cloned directly into the TOPO cloning vector, pCR®2.1-TOPO® (Invitrogen) (a). The UL/*b*' ORF was subcloned from the UL/*b* 'ORF-TOPO vector into pShuttleCMV using various restriction enzyme digest sites. UL/*b*' ORFs cloned into TOPO vector in the incorrect orientation were subcloned into pShuttle-CMV on a *Not*I/*Hin*dIII fragment (b), with the exception of UL135, which was subcloned into pShuttleCMV on a *Xho*I/*Hin*d III fragment. UL/*b*' ORFs cloned into TOPO vector in the correct orientation were subcloned into pShuttleCMV on a *Kpn*I/ *Xba*I fragment (c), with the exception of UL14, subcloned into pShuttle-CMV on a *Hin*dIII/ *Eco*RV fragment, and UL148, subcloned into pShuttleCMV on a *Kpn*I/ *Not* I fragment. The UL/*b*' ORFs that were directly cloned (UL133, UL136, UL147) into pShuttleCMV were amplified from Merlin with primers containing *Kpn*I (5' end) and *Xba*I (3' end) restriction sites and were also cloned into a *Kpn*I/*Xba*I digested pShuttleCMV vector.

Ligation products were transformed into either *E.coli* JM109 or *E.coli* XL-1 blue (Section 2.5.10), and allowed to recover in SOC medium for 1-2h before plating onto LB agar plates containing kanamycin (50μg/ml). pShuttleCMV-UL*b'* clones were selected by kanamycin resistance, purified by plasmid miniprep, and presence of the insert confirmed by restriction enzyme digest followed by agarose gel electrophoresis. A plasmid maxiprep was performed on the correct chosen clone.

A small number of the UL*b'* genes (UL133, UL136, UL147 and UL148) were directly ligated into pShuttleCMV from PCR products to avoid the use of the TOPO TA cloning stage. These genes were amplified by PCR with primers containing a 5' *Xba*I and a 3'*Kpn*I site (Table 2.2). PCR products were restriction enzyme digested with *Xba*I and *Kpn*I and dialysed in TE buffer at 4°C to remove small DNA fragments. The digested PCR product was phenol:chloroform extracted and precipitated by ethanol/sodium acetate and then ligated with *Xba*I/*Kpn*I restriction enzyme digested pShuttleCMV vector as described above. Clones were selected by kanamycin resistance and plasmids purified by miniprep. Ligation was checked by restriction enzyme digest and agarose gel electrophoresis. The insert DNA was sequenced to ensure no mutations had occurred during amplification and a plasmid maxiprep was performed on the correct chosen clone.

2.6.3 AdEasy recombination

The pShuttleCMV transfer vector containing the transgene (25ng) was cleaved with *Pme*I for 1h and purified using a GFX PCR and Gel Band Purification column (Section 2.5.3). The digested shuttle vector was then transformed into *E.coli* BJ5813 containing pAdEasy-1 (kindly provided by Dr B. Vogelstein) by electroporation. pAdEasy-1 contains an ampicillin resistance marker, whereas pShuttleCMV contains a kanamycin resistance gene. Recombination between the shuttle vector and pAdEasy-1 in BJ5813

results in a recombinant Ad (RAd) plasmid that contains the kanamycin resistance gene. Bacteria were therefore plated out onto SB agar plates containing kanamycin (50μg/ml) and kanamycin resistant clones were selected and plasmid purified by miniprep. The plasmid DNA preparation was split into two samples, digested with either *Pac*I or *Hin*dIII, and separated by agarose gel electrophoresis to test for recombination. *Hin*dIII digestion resulted in a familiar fragmentation pattern of the RAd which could be compared with a *Hin*dIII digested RAd control. *Pac*I digest of a RAd resulted in the production of a large ~30kb fragment with a smaller 3kb or 4.5kb fragment, and was therefore diagnostic of recombination. Duplex PCR was used as an alternative method to identify recombinants (Antolovic *et al.*, 2005). A RAd contains both the kanamycin gene and the adenovirus backbone. Identification of these components by PCR can therefore be used to diagnose recombination. Briefly, kanamycin resistant clones were added to a PCR reaction mix that contained PCR primers for both the kanamycin gene and a section of the adenovirus backbone (Table 2.2). Samples were denatured for 10min at 95°C before commencing the usual PCR reaction (Section 2.5.1). PCR products were separated by agarose gel electrophoresis. Two diagnostic fragments of 384bp and 768bp were produced for recombinant clones.

2.6.4 Generation of RAd virus

Once identified by restriction enzyme digest or duplex PCR, a recombinant clone was expanded overnight in SB media (200ml) containing kanamycin (50μg/ml). Bacteria were recovered by centrifugation at 6000 g for 10min at 4°C, and resuspended in a resuspension buffer (10ml) (Buffer P1, Qiagen). Bacteria were lysed by the addition of an equal volume of lysis buffer (Buffer P2, Qiagen) and this reaction stopped by the addition of an equal volume of neutralisation buffer (Buffer P3, Qiagen). The mixture was incubated on ice for 15min, during which time a precipitate formed. The solution

was cleared by centrifugation at 10000 g for 30min at 4°C and recombinant plasmid DNA recovered using a 20/G column or Qiagen tip-500 column (Qiagen), passing the supernatant through the column so that DNA adsorbed to the column resin. DNA was washed with a medium salt wash buffer (Qiagen) and eluted in elution buffer heated to 50°C (Buffer QF, Qiagen). To precipitate plasmid DNA, 10.5 volumes of isopropanol were added and the solution centrifuged at 10000 g for 30min at 4°C. The DNA pellet was washed by repeating centrifugation with 70% (v/v) ethanol. The DNA pellet was air dried and resuspended in 300µl Tris buffer.

Before transformation of packaging cells, the recombinant plasmid DNA was first digested with *Pac*I to release the viral genome. This was then purified using a GFX column (GE Healthcare) and the DNA resuspended in Tris buffer (30µl). The linearised DNA was transfected into 911 or 293 packaging cells at 70% confluency in a 25cm^2 flask using Polyfect (Qiagen) according to the manufacturers' instructions. Briefly, recombinant Ad DNA (4µg) was diluted in DMEM-wash to a total volume of 150µl. To this mixture, Polyfect reagent (40µl) was added and the solution incubated for 10min at RT. Following this incubation, 1ml DMEM-10 was added and the whole mixture transferred drop-wise to cells into a total volume of 4ml DMEM-10. Cells were incubated overnight at 37°C, 5% CO_2, after which the media was replaced with fresh DMEM-10, and thereafter when required. Viral plaques were observed at approximately 7-10 days post-transfection, and the presence of virus checked using an Ad antibody test kit (SAScientific, Texas, USA). The virus was extracted using ArkloneP (Section 2.4.2) and stored at -70°C until used to inoculate multiple 175cm^2 flasks to generate virus stocks (Section 2.4.2).

2.7 GENERATION OF RECOMBINANT ADENOVIRUSES BY AdZ

The AdZ system was developed by Dr R. Stanton as a more efficient alternative to AdEasy for the generation of RAds (Stanton *et al.*, unpublished). The principle of this system lies in the ability to directly clone PCR products into a recombinant adenovirus vector by homologous recombination, bypassing the need for multiple sub-cloning steps. An overview of this cloning process is provided in Figure 2.4, and for a direct comparison of AdZ with the AdEasy Ad cloning method, a flow diagram is included in Figure 2.5. Briefly, the UL/*b'* genes UL128, UL131A, UL132 and UL148 were amplified by PCR using specific primers containing 50bp homology to the CMV promoter (For) or polyA tail plus a C-terminal Streptag II (Rev) required for homologous recombination with the adenovirus vector (Table 2.2). Amplification products were separated by agarose gel electrophoresis to ensure the correct size product was produced, and DNA was purified by GFX column (GE Healthcare). *E.coli* SW102 (kindly donated by Dr N. Copeland) containing the adenovirus vector pAL942 were grown overnight at 32°C in a shaking incubator in LB (5ml) containing ampicillin (50μg/ml) and chloramphenicol (12.5μg/ml). The next day, a sample of the overnight culture (1ml) was inoculated into LB (50ml) containing ampicillin (50μg/ml), and incubated at 32°C until the culture reached an optical density, $O.D_{600}$, of 0.6. Once this O.D. was reached the culture was split into two equal portions, with one incubated at 42°C for 15min in a water bath to induce the lambda red genes, while the other fraction remained at 32°C as a control. After this incubation, both fractions were cooled on ice for 20min then centrifuged at 4500 g for 5min at 0°C. The supernatant was removed and the cells washed twice in ice cold water by centrifugation at 4500 g to remove salts, making the bacteria electocompetent. The bacterial cell pellet was resuspended in distilled water (~1ml) and an aliquot (25μl) of each induced and non-induced bacteria was transferred to a pre-cooled cuvette for electroporation with 4μl each of the PCR

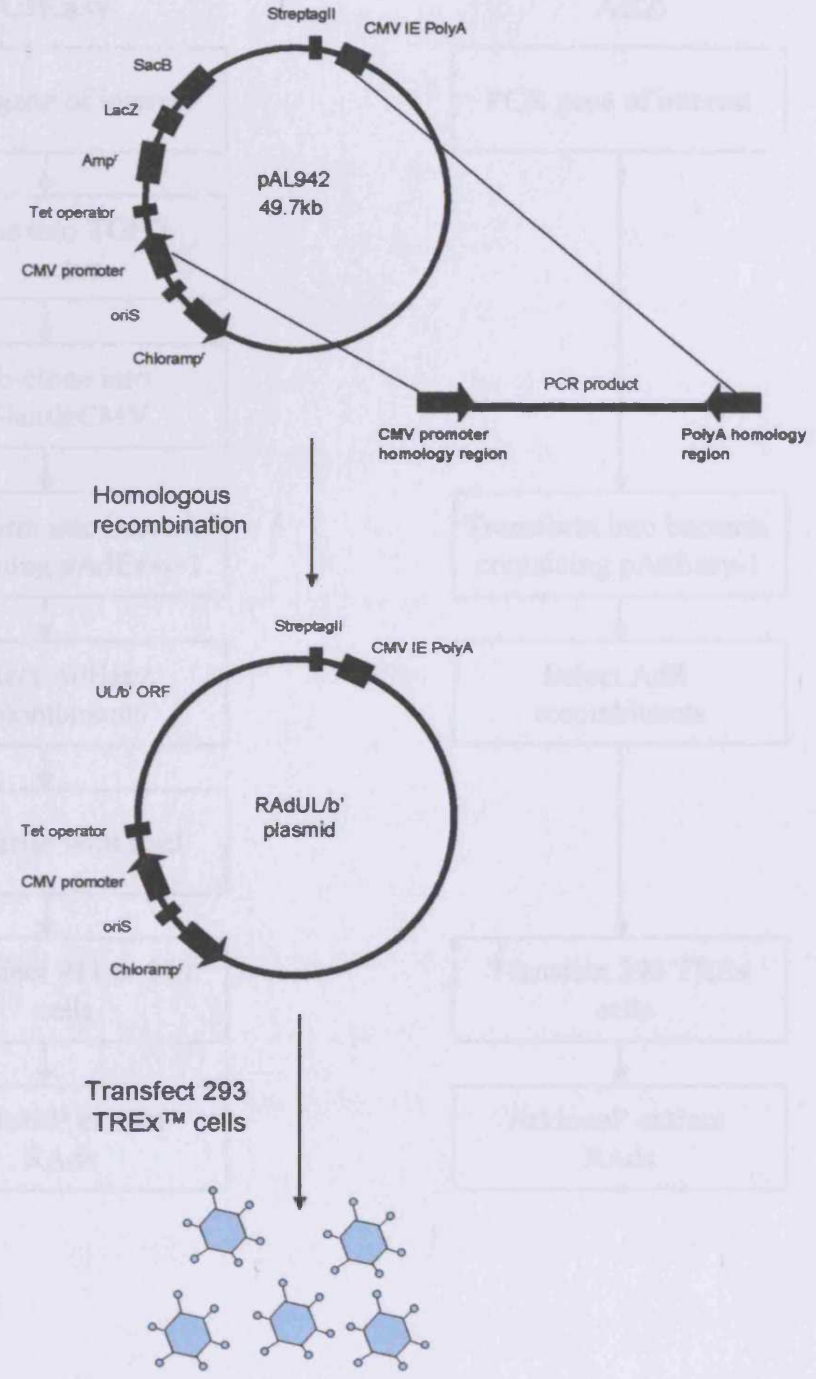

Figure 2.4 The AdZ system: Ad recombinant generation with zero cloning steps (not to scale)

The UL/*b*' ORF was amplified by PCR with primers containing homology to the CMV promoter region (promoter and Tet operator) and the CMV PolyA region (StreptagII and PolyA). Homologous recombination between the RAd vector and PCR product occurred in *E.coli* strain SW102. The resulting RAd plasmid vector was transfected directly into 293 T-REx™ cells to produce recombinant Ad.

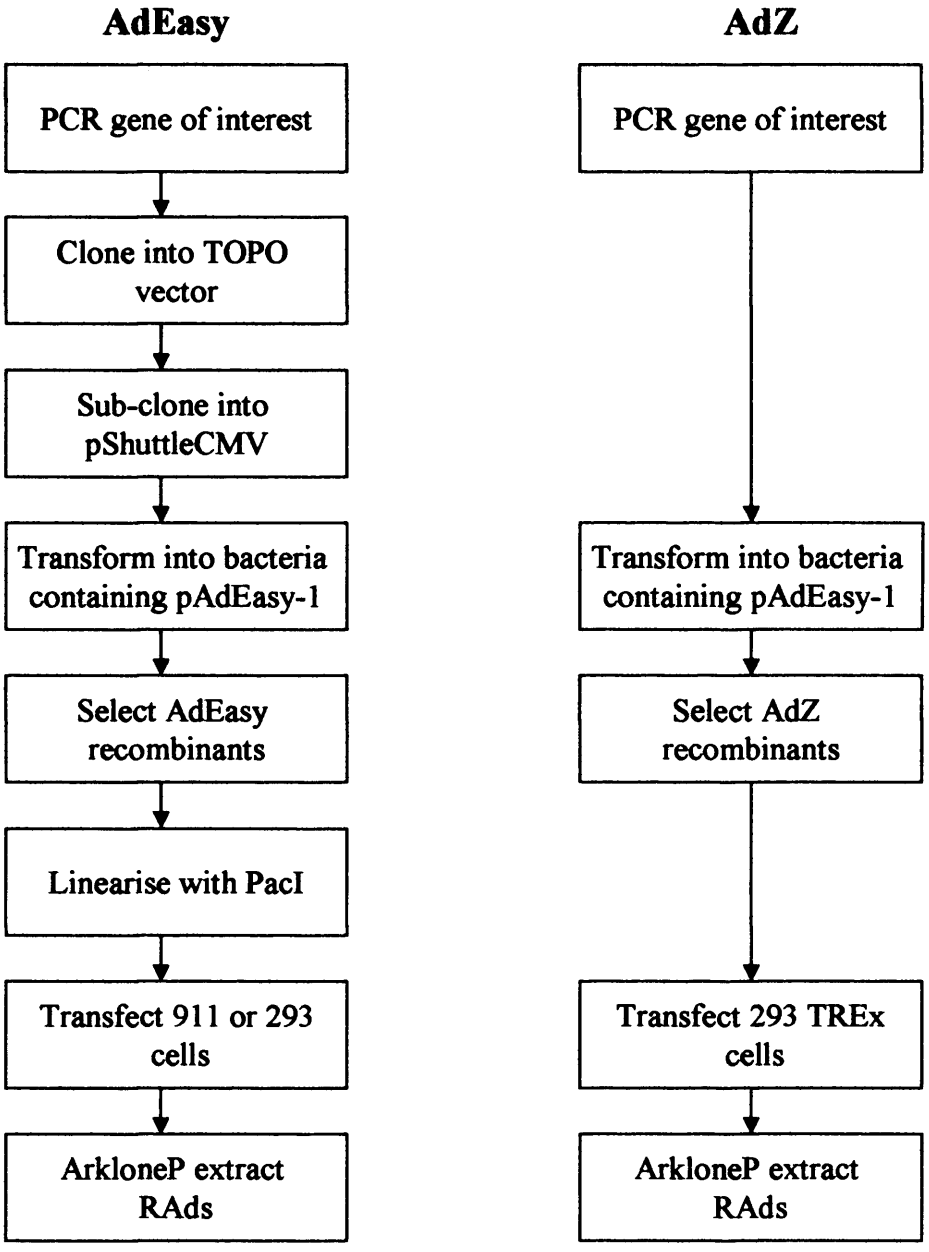

Figure 2.5 Flow diagram of recombinant Ad generation: AdEasy v's AdZ
A brief outline of the cloning steps required for the generation of Ad recombinants via the AdEasy or AdZ cloning systems.

product (2.3V). After electroporation, the bacteria were recovered for 3-4h in LB at 32°C before plating onto LB plates containing 5% (w/v) sucrose, chloramphenicol (12.5μg/ml), 40% (v/v) X-gal and IPTG. Plates were incubated at 32°C for 48h. White colonies were selected after this incubation time and grown overnight in LB (5ml) containing chloramphenicol (12.5 μg/ml). Cells were recovered by centrifugation at 4000 g for 5min, and plasmid purified by alkaline lysis using the Qiagen miniprep kit (Qiagen), followed by isopropanol precipitation of the purified DNA. The DNA pellet was washed once in 70% (v/v) ethanol, air dried and resuspended in Tris buffer (30μl). *Hin*dIII digestion was performed on a sample of DNA (8μl) to ensure the correct banding patterns for the RAd were observed when compared with a *Hin*dIII digested RAd control. Recombinants were sequenced to ensure no mutations were present in the PCR product, using a modified version of the sequencing reaction described in Section 2.5.12 as very little DNA is obtained from the single copy Ad5 genome vector. To the 4μl of Big Dye sequencing reaction mix, 1μl primer (Table 2.2) and 5μl DNA were added. The thermocycling sequencing reaction was performed as normal (Section 2.5.12), but with 100 cycles. The low template concentration results in a low signal and a high amount of unincorporated dye terminators. These dye terminators were minimised by the addition of 2μl 150mM EDTA to the ethanol/sodium acetate precipitation mix. Once the sequence had been confirmed for the gene of interest, the correct clone was inoculated into LB media (500ml) containing chloramphenicol (12.5μg/ml) and grown overnight at 32°C. A Nucleobond® BAC-100 kit (Clontech, Basingstoke) was used for plasmid purification according to the manufacturer's instructions. DNA was eluted into 50°C elution buffer (200μl), and the DNA concentration measured by spectrophotometer. As the pAL942 vector is self-excising, the recombinant plasmid was transfected directly into 293 T-REx® helper cells, using Polyfect or Effectene (Qiagen) according to the manufacturers' instructions. The 293 T-

REx® helper cells produce the Tet repressor, which suppresses transgene expression from the Ad recombinant during virus production due to the presence of Tet operator sites in pAL942. Similar to the AdEasy method, a viral plaque is produced 7-10 days post-transfection. The virus can then be extracted by ArkloneP or tetrachloroethylene and viral stocks generated as described in Section 2.4.2.

A summary of the methods used to generate each UL/*b*' RAd is provided in Table 2.3.

2.8 WESTERN BLOTTING

Proteins separated by SDSPAGE were detected by western blotting. Pre-set 12.5% acrylamide gels of 12 or 20 wells (Invitrogen) were used in conjunction with the Invitrogen electrophoresis kit. To prepare reduced cell samples, either HFFF-htert or HFFF-hCAR ($5x10^5$ – $1x10^6$ cells) were seeded into $25cm^2$ flasks and infected with RAd at a MOI of 100 or a MOI of 10 respectively, or with HCMV at a MOI of 10 (Section 2.4.4). At 72hpi, cells were washed once with ice cold PBS and then resuspended in ice cold PBS (5ml). Cells were recovered by centrifugation at 400 g for 3min, washed in ice cold PBS and centrifugation repeated. Cells were resuspended in PBS and 5xSDSPAGE sample buffer to a total volume of 50-100µl. To prepare non-reduced cell samples for western blot, cells were prepared as described above, but resuspended in PBS plus 5xSDSPAGE sample buffer containing no DTT or 2-mercaptoethanol reducing agents.

Samples were then denatured at 99°C for 10min before loading 10µl into wells of the 12.5% acrylamide gel alongside a 10µl sample of Rainbow marker (GE Healthcare). Gels were placed in an electrophoresis tank and covered with the manufacturer's supplied SDSPAGE running buffer (Invitrogen). Proteins were separated by SDSPAGE at 100V for 2-3h, depending on the resolution required. Gels were removed from the electrophoresis tank and layered onto nitrocellulose (GE Healthcare) that had been pre-

Table 2.3 Summary of UL/*b'* ORF RAd cloning methods

ORF	Recombination method	Epitope tag	Cell type generated in	Generated by
UL128	AdZ	Strep	293 TREx	M. Armstrong
UL130	AdEasy	FLAG	293	B. McSharry
UL131A	AdZ	Strep	293 TREx	M. Armstrong
UL132	AdEasy	Strep	293	M. Armstrong
UL133	AdEasy	Strep	293	M. Armstrong
UL135	AdEasy	Strep	911	M. Armstrong
UL136	AdEasy	Strep	911	M. Armstrong
UL138	AdEasy	Strep	293	V. Prod'Homme
UL139	AdEasy	Strep	911	M. Armstrong
UL140	AdEasy	Strep	911	V. Prod'Homme
UL141	AdEasy	Strep	911	M. Armstrong
UL141A	AdEasy	Strep	911	M. Armstrong
UL142	AdEasy	Strep	911	M. Armstrong
UL144	AdEasy	Strep	911	M. Armstrong
UL145	AdEasy	Strep	293	M. Armstrong
UL146	AdEasy	Strep	911	M. Armstrong
UL147	AdEasy	Strep	911	M. Armstrong
UL147A	AdEasy	Strep	911	V. Prod'Homme
UL148	AdEasy	Strep	293	M. Armstrong
UL148A	AdEasy	Strep	911	V. Prod'Homme
UL148B	AdEasy	Strep	293	M. Armstrong
UL148C	AdEasy	Strep	911	V. Prod'Homme
UL148D	AdEasy	Strep	911	V. Prod'Homme
UL150	AdEasy	Strep	911	M. Armstrong
UL14	AdEasy	Strep	911	M. Armstrong

soaked in transfer buffer. Proteins were transferred from the gel onto the nitrocellulose by semi-dry transfer for 1h at 10V. Nitrocellulose blots were washed twice in 10ml distilled water and incubated with Miser Antibody extender solution (Pierce, Rockford, USA) for 10min at RT. Following this incubation, blots were washed a further 5 times in distilled water. The position of the Rainbow markers™ were marked on the blot using an Antigen-Antibody (Mouse) Pen™ (Alpha Diagnostics, USA) before incubating the blot in a 5% (w/v) milk powder/PBST blocking buffer overnight at 4°C. Primary antibody was incubated with the blot for 1h at RT, or overnight at 4°C, in 5% (w/v) milk/PBST blocking buffer (20ml). Table 2.4 lists the antibodies and the dilutions used for western blot during this study. Following primary antibody incubation, blots were washed in 5% (w/v) milk/PBST blocking buffer for 1h at RT, and then incubated with a HRP-tagged secondary antibody (Table 2.4) for 1h in 5% (w/v) milk/PBST. Blots were finally washed in PBST buffer for 1h before incubation with a HRP substrate solution (Supersignal® West Pico chemiluminescent substrate, Pierce). Protein bands were visualized either by exposure to film, or with Chemidoc (UVP, Cambridge) which produces a digital image of the blot.

To re-probe a blot, blots were washed in PBST then stripped by incubating with ReStore (Pierce) stripping buffer for 2h at RT. Blots were washed twice in PBST before re-blocking in 5% (w/v) milk/PBST overnight at 4°C. The antibody incubation process was then carried out as described above.

2.8.1 Preparation of deglycosylated samples for western blot

Cells infected with RAds (72hpi) were resuspended in ice cold PBS, washed as described (Section 2.8), then recovered by centrifugation (400 g) before being resuspended in NP40 lysis buffer and lysed on ice for 30min. The lysate was cleared by centrifugation at 10000 g for 20min at 4°C, after which the supernatant was removed

Table 2.4 Antibodies used in western blotting

Antibody	Dilution	Isotype	Company
Primary Antibodies			
α-Streptag monoclonal	1:1000	Mouse IgG1	IBA
α-MICA	1:500	Mouse IgG2b	R&D
α-MICB	1:500	Mouse IgG2b	R&D
α-MICA/B	1:500	Rabbit IgG	SantaCruz
α-ULBP1	1:500	Mouse IgG2a	R&D
α-ULBP2	1:500	Mouse IgG2a	R&D
α-ULBP3	1:500	Mouse IgG2a	R&D
α-ULBP3	1:500	Goat IgG	SantaCruz
α-Nectin 1	1:500	Mouse IgG1	SantaCruz
α-Nectin 2	1:500	Mouse IgG1	Serotec
α-Nectin 3	1:500	Goat IgG	SantaCruz
α-Nectin 4	1:500	Goat IgG	SantaCruz
α-UL141 monoclonal (MAB1, MAB3)	1:10000 each	Mouse IgG1	Tomasec *et al*. (2005)
α-UL135 polyclonal (PAb1, PAb2, PAb3)	1:2000 each	Mouse Ig	n/a
α-Necl2	1:500	Mouse IgG2b	Abnova
α-CD90 (Thy-1)	1:300	Mouse IgG1	Serotec
α-E-Cadherin	1:500	Mouse IgG1	Serotec
α-CD66a (CEACAM-1)	1:500	Mouse IgG1	Abcam
α-CD29	1:500	Mouse IgG1	Immunotools
α-CD31	1:500	Mouse IgG1	Immunotools
α-CD43	1:500	Mouse IgG1	Immunotools
α-CD54	1:500	Mouse IgG2a	Immunotools
α-CD56	1:500	Mouse IgG2a	Immunotools
α-CD58	1:500	Mouse IgG1	Immunotools
α-CD147	1:500	Mouse IgG1	Immunotools
α-Actin	1:2000	Rabbit IgG	Sigma
Secondary Antibodies			
Goat α-rabbit IgG HRP	1:2000	Goat IgG	BioRad
Goat α-mouse IgG HRP	1:1000	Goat IgG	BioRad
Chicken α-goat IgG HRP	1:2000	Chicken IgG	SantaCruz
Donkey α-goat IgG HRP	1:2000	Donkey IgG	SantaCruz

and split into 3 fractions. A 1x denaturation buffer (supplied with deglycosylase enzyme, NEB) was added and the samples denatured at 99°C for 10min. After denaturation, one fraction was left untreated as a control, one treated with PNGaseF (NEB) and one with EndoH (NEB) according to the manufacturer's instructions, and incubated overnight at 37°C. 5xSDSPAGE loading buffer was added and the sample heated to 99°C for 5min before loading 10µl of each onto a 12.5% acrylamide gel for western blotting, as described above.

2.8.2 RAd592 and RAdIL10 controls

As a positive control for preliminary western blots with the Streptag antibody, a RAd encoding for a Strep-tagged version of HCMV vIL10 (designated RAdIL10, generated by Dr P. Tomasec) was included in western blots. As a negative control for the Ad recombinants, a control RAd was generated by Dr P. Tomasec using the AdEasy system, whereby pShuttleCMV containing no transgene was recombined with pAdEasy-1 to generate an "empty" RAd vector, designated RAd592. RAd592 was included as an Ad control in all western blot, immunofluorescence, FACS and functional assays.

2.9 MICROSCOPY

2.9.1 Preparation of cells

HFFF-hCAR cells were seeded onto coverslips in a 12 well plate ($1x10^6$ cells/ plate) and infected the next day at a MOI of 50. At 72-96hpi, cells were washed in PBS and fixed in 2% paraformaldehyde for 20min at RT. To permeabilize cells, coverslips were washed twice in PBS then incubated with 0.1% Triton-X-100 for 20min at RT. When formaldehyde fixation gave poor results, immersion in acetone/methanol (1:1) for 30s was used as an alternative method to fix/ permeabilize cells (used for RAdUL139 and

RAdUL148C immunofluorescence). Both solvents remove lipid structures from the cell, which could potentially help antibody recognition of Strep-tagged proteins that may be residing in vesicular compartments or other lipid structures in the cell. Coverslips were allowed to dry before cells were reconstituted by immersion in PBS for a further 30s prior to antibody staining (Section 2.9.2).

2.9.2 Immunofluorescence

Cells were incubated with primary antibody diluted in PBS at 37°C for 1h in a humidified chamber. Table 2.5 lists the antibodies and their dilutions used for immunofluorescence during this study. Coverslips were washed with PBS and incubated with secondary antibody (Table 2.5) at 37°C for a further 1h in a humidified chamber. After staining, cells were washed in PBS to remove excess antibody before mounting coverslips onto glass slides using 2% (w/v) DABCO mounting medium. Immunofluorescence was visualised using a Leica DM IRBE microscope (Leica, Germany) with a Hamamatsu ORCA-ER camera (Hamamatsu, Japan) and Improvision Openlab 3 software (Improvision, Coventry, UK).

2.9.3 Actin staining by coumarin phallacidin

To stain for cellular actin filaments, RAd infected cells were prepared as described in Section 2.9.1. After fixing and permeabilizing, coverslips were incubated with coumarin phallacidin (Molecular Probes, Invitrogen) (5µl in 200µl PBS) for 20min at RT. Coverslips were washed twice in PBS and mounted onto slides using 2% (v/v) DABCO. Cells were visualised by microscopy as described above.

Table 2.5 Antibodies used for immunofluorescence microscopy studies

Antibody	Dilution	Isotype	Company
Primary antibodies			
α-Streptag monoclonal	1:100	Mouse IgG1	IBA
α-human Bcl-2	1:100	Mouse IgG1	BDBiosciences
α-human calnexin	1:100	Mouse IgG1	Chemicon
α-UL135, UL14, UL144, UL146 and UL147 polyclonal sera	1:50	Mouse Ig	n/a
Mouse IgG1	1:100		Sigma
Secondary antibodies			
Goat α-mouse IgG AlexaFluor 594	1:1000	Goat IgG	Molecular Probes
Sheep α-mouse IgG FITC	1:100	Sheep IgG	Sigma
Other			
Streptavidin-AlexaFluor 594	1:100	n/a	Molecular Probes
Coumarin Phallacidin	6.6μM	n/a	Molecular Probes

2.10 FLOW CYTOMETRY (FACS)

2.10.1 General cell surface staining procedure

To prepare cell samples, HFFF-hCAR or HFFF-htert cells infected with RAds or HCMV in 25cm^2 flasks (Section 2.4.4) were trypsinised at 72hpi and cells recovered by centrifugation at 400 g for 3min. Cells were plated in a 200µl volume into 96 well U bottom plates and washed twice in 2% FCS (v/v)/PBS (200µl) by centrifugation at 400 g for 3min. For FACS analysis of NK clones, cells were prepared by washing the cell suspension twice in 2% FCS (v/v)/PBS by centrifugation at 400 g for 3min before moving to a FACS tube in a 200µl volume.

For staining with pre-conjugated antibodies, cells were incubated with a suitable concentration of antibody in a 50µl volume for 30min at 4°C in the dark. A list of antibodies used in FACS analysis is provided in Table 2.6. The stained samples were washed twice in 2% FCS (v/v)/PBS (200µl) before analysing by flow cytometry. For staining with unconjugated antibodies, cell samples were incubated with the appropriate concentration of unconjugated antibody in a 50µl volume of 2% FCS (v/v)/PBS for 30min at 4°C in the dark, washed twice in 200µl 2% FCS (v/v)/PBS and then incubated with an isotype specific fluorochrome conjugated secondary antibody for 30min at 4°C in the dark. Cells were washed twice in 2% FCS (v/v)/PBS before analysing by flow cytometry. FACS analysis was performed using the FACSCalibur (Dakocytomation, Cambridge, UK). Cells were selected by standard forward scatter and side scatter criteria before analysis of fluorochromes using the appropriate laser excitation.

2.10.2 General intracellular staining procedure

To analyse intracellular proteins by FACS, cell samples were fixed and permeabilized prior to antibody incubation. Cell samples were prepared as described above into 96 well U bottom plates. Cells were fixed in 4% (v/v) paraformaldehyde/PBS for 15min at

Table 2.6 Antibodies used for FACS analysis

Antibody	Dilution	Isotype	Company
Unconjugated antibodies			
α-CD66a (CEACAM-1)	1:100	Mouse IgG1	Abcam
α-CD90 (Thy-1)	1:100	Mouse IgG1	Serotec
α-Cadherin	1:100	Mouse IgG1	Serotec
α-ULBP1	1:100	Mouse IgG2a	R&D
α-ULBP2	1:100	Mouse IgG2a	R&D
α-ULBP3	1:100	Mouse IgG2a	R&D
α-MICA	1:100	Mouse IgG2b	R&D
α-MICB	1:100	Mouse IgG2b	R&D
α-Necl-2	1:100	Mouse IgG2b	Abnova
α-Nectin 1	1:100	Mouse IgG1	SantaCruz
α-Nectin 2	1:50	Mouse IgG1	Serotec
α-UL135 polyclonal	1:100	Mouse Ig	n/a
Mouse IgG1	1:100		Sigma
Mouse IgG2a	1:100		Sigma
Mouse IgG2b	1:100		R&D
Conjugated antibodies			
α-mouse IgG PE	1:100	Goat Ig	BDPharmingen™
α-CD56 PE	1:100	Mouse IgG1	Immunotech
α-CD3 FITC	1:100	Mouse IgG1	Serotec
StrepTactin PE	1:100	n/a	IBA

RT and washed in PBS by centrifugation at 400 g for 3min. Cells were permeabilised by incubating with 2% (v/v) saponin/PBS for 15min at RT and washed in PBS before staining as described in Section 2.10.1 and analysing by flow cytometry.

2.11 IMMUNOPRECIPITATION

To perform immunoprecipitation, cells were first labelled with ^{35}S methionine and cysteine. HFFF-hCAR cells were seeded in a 75cm^2 flask and infected with RAd (Section 2.4.4). At 72hpi, media was removed and cells were washed twice in PBS before replacing with methionine and cysteine-free MEM (5% (v/v) FCS, 1% (v/v) glutamine) (Invitrogen) and incubating at 37°C for 1h. After this incubation, ^{35}S *in vitro* cell labelling mix (200μCi) (Promix, GE Healthcare) was added and incubated with the cells for a further 4h. The media was removed and the cells washed 3 times with ice cold PBS. The cells were trypsinised and recovered by centrifugation at 400 g for 5min. The cell pellet was washed in PBS, resuspended in NP40 lysis buffer containing iodoacetatamide (1mg/ml) and PMSF (0.35mg/ml) (Sigma-Aldrich), then incubated at 4°C for 20min. The lysate was centrifuged at 10000 g, 4°C for 15min, and the supernatant mixed with 100μl protein A (Sigma-Aldrich) with rotation overnight at 4°C. To separate the insoluble protein A the mixture was centrifuged at 10000 g, 4°C for 15min and aliquots of the supernatant taken according to the number of antibodies required for immunoprecipitation. An appropriate concentration of antibody (2-5μl) was added to each aliquot and the antibody/lysate mixture was rotated at 4°C for 90min before adding protein A Sepharose beads (Sigma-Aldrich) (~200μl/ aliquot) and 10% (v/v) BSA to each aliquot and rotating for a further 45min. Samples were washed 4 times with Townsend wash buffer and the supernatant removed. 2xSDSPAGE sample buffer (10μl) was added to the beads and boiled at 99°C for 10min. The sample was then centrifuged at 10000 g for 1min before loading the cleared sample onto a pre-cast

12.5% acrylamide gel. SDSPAGE was carried out as described in Section 2.8. Following SDSPAGE, the gel was removed from the electrophoresis apparatus and fixed in 25% (v/v) isopropanol/10% (v/v) acetic acid for 30min. The gel was washed and incubated with Amplify (GE Healthcare) for 30min before placing in a film cassette with an X-ray film (GE Healthcare). The cassette was stored at -70°C for 4-7 days before developing the film as standard to visualize metabolically labelled ^{35}S proteins.

2.12 FUNCTIONAL ASSAYS

2.12.1 Chromium release cytotoxicity assay for NK cells

HFFF-htert, HFFF-hCAR and immortalized skin fibroblast cells were infected with RAd and HCMV as described in Section 2.4.4. Targets were assayed at 72hpi by chromium release cytotoxicity assay. Briefly, infected cells (targets) were trypsinised and recovered by centrifugation at 400 g for 5min. The target cells were resuspended in sodium chromate (150μC) (GE Healthcare) and incubated for 1h at 37°C. The cells were washed with RPMI-10 to remove excess sodium chromate, fresh RPMI-10 added and the cells left to leach for a further 30-60min at 37°C. Finally target cells were washed twice in RPMI-wash, counted and resuspended in RPMI-AB5 to the appropriate concentration for plating into a 96 well U bottom plate at $1.5x10^3$ – $2x10^3$ targets/well in a volume of 100μl. These prepared target cells were added to NK (effector) cells that had been pre-plated in the 96 well plates. In the case of NK clones, effector cells were prepared by harvesting $4.5x10^4$ – $6x10^4$ NK clones from culture, which were washed in RPMI-wash before resuspending in RPMI-AB5 to give an E:T ratio of 30:1 in a volume of 100μl/ well. For polyclonal NK cells obtained from PBMC, NK cell numbers were estimated by flow cytometry, gating on $CD3^-CD56^+$ cells. Cells were harvested and washed in RPMI-wash before resuspending in RPMI-AB5 to give a final E:T ratio of

40:1. NKL cells were harvested from culture, counted and prepared as above, to give final E:T ratios ranging from 40:1 to 2.5:1.

Target cells and effector cells were incubated together in 96 well U bottom plates for 4h at 37°C. Spontaneous sodium chromate release for each target was determined by incubating target cells with medium only. The maximum sodium chromate release for each target was determined by the addition of 5% (v/v) Triton-X-100. After the incubation time, a 25µl sample of the supernatant was removed from each well and added to a beta plate containing scintillation fluid (150µl) (Perkin-Elmer). The plates were agitated for 15min and counted in a 1450 Microbeta Trilux Liquid Scintillation counter (Perkin-Elmer).

As a measurement of cytotoxicity, the mean specific sodium chromate released for each E:T ratio was calculated using the standard equation:

$$\% \text{ specific lysis} = \frac{(\text{mean test cpm}) - (\text{mean spontaneous cpm})}{(\text{mean max cpm}) - (\text{mean spontaneous cpm})} \times 100$$

3. EXPRESSING THE UL/*b'* ORFS: PRODUCTION OF RECOMBINANT ADENOVIRUSES

3.1 BIOINFORMATICS

At the start of this study, the majority of the UL/*b'* ORFs existed only as uncharacterised computer predictions. Sequence analysis programmes can be readily accessed to help scrutinise DNA and protein coding sequences. Specific programmes are designed to identify motifs associated with post-translational modification or intracellular trafficking within protein-coding sequences. Database search engines can also be exploited to identify homology or sequence similarity with any known protein or DNA sequence. Sequence analyses can thus place an uncharacterised protein into a specific family, reveal sequence or structural similarity to known proteins, and even provide insight into function. Each UL/*b'* ORF predicted in the original characterisation of the HCMV strain Merlin genome (Dolan *et al.*, 2004) was therefore first analysed *in silico* in order to identify homologies and motifs that may give insight into their possible function.

3.1.1 Sequence similarities identified by BLAST and FASTA searches

NCBI protein FASTA (Pearson, 1990; Pearson & Lipman, 1988) and protein BLAST (Altschul *et al.*, 1990) were used to search Uniprot and Swissprot databases with all UL/*b'* ORF protein sequences. Table 3.1 gives a summary of these homology searches, and also includes general sequence information for each ORF. The results of this bioinformatic analysis supported information known about these genes prior to this study, for example; UL146 and UL147 were identified as chemokine homologues; UL142 exhibited low level homology to UL18 and MHC-I, whilst UL144 was found to be a TNF receptor homologue (Table 3.1).

Table 3.1 General sequence information for the UL/*b'* ORFs and summary of homology searches

ORF[1]	Coding Region[1]	Protein ID[1]	Homology[2]	Notes[3]
UL128	complement (join 176309..176402, 176523..176657, 176781..176944)	AAR31668.1		Truncated owing to single base mutation in Merlin. Involved in cell tropism
UL130	complement (176984..177628)	AAR21669.1		Involved in cell tropism
UL131A	complement (join 177649..177802, 177911..178146)	AAR31670.1		Involved in cell tropism
UL132	complement (178252..179064)	AAR31671.1		Putative membrane protein
UL133	complement (189949..190722)	AAR31685.1	WASP (Proline-rich proteins)	Putative membrane protein
UL135	complement (188846..189772)	AAR31684.1	WASP (Proline-rich proteins)/ EVH1 domain	Putative secreted protein
UL136	complement (188033..188755)	AAR31683.1		Putative membrane protein
UL138	complement (187441..187950)	AAR31682.1		Putative membrane protein
UL139	complement (186462..186878)	AAR31681.1	CD24	Putative membrane glycoprotein
UL140	complement (185705..186280)	AAR31680.1		Putative membrane protein
UL141	complement (184396..185412)	AAR31679.1	UL14 gene family member	Membrane glycoprotein
UL141A	complement (185345..185666)	-		Unpublished potential ORF
UL142	complement (183406..184323)	AAR31678.1	UL18 (MHC I)	Membrane glycoprotein
UL144	complement (182206..182736)	AAR31677.1	TNFR	Putative membrane glycoprotein
UL145	complement (181573..181965)	AAR31676.1		
UL146	complement (180930..181292)	AAR31675.1	IL-8/ CXC	Secreted glycoprotein
UL147	complement (180390..180869)	AAR31674.1	IL-8/ CXC	Putative secreted glycoprotein
UL147A	complement (180160..180387)	AAR31673.1		Putative membrane protein
UL148	complement (179141..180091)	AAR31672.1		Putative membrane glycoprotein
UL148A	complement (190818..191060)	AAR31686.1		Putative membrane protein, unrelated to UL148
UL148B	complement (191190..191432)	AAR31687.1		Putative membrane protein, unrelated to UL148
UL148C	191522..191755	AAR31688.1		Putative membrane protein, unrelated to UL148
UL148D	192137..192325	AAR31689.1		Putative membrane protein, unrelated to UL148
UL150	complement (192341..194260)	AAR31690.1	Mucin-like proteins	Putative secreted protein
UL14	21229..22212	AAR31579.1	UL14 gene family member	Putative membrane protein

1 Nomenclature and sequence information obtained from GenBank Merlin sequence AY446894 (Dolan *et al.*, 2004)
2 Homology searches performed using NCBI protein Fasta (http://www.ebi.ac.uk/fasta33/) (Pearson, 1990; Pearson & Lipman, 1988) and protein BLAST (http://www.ebi.ac.uk/blastall/) (Altschul *et al.*, 1990). Both search tools used UniProt and Swiss-prot databases
3 Observations from Dr A.Davison, personal communication

Few novel homologues were revealed for the remaining UL/*b'* ORFs. Although no functional data exists for UL139, it was found to share sequence similarity with the B-cell maturation factor, CD24 (Table 3.1). UL133 and UL135 do not possess any distinct homologues, but both showed some similarity to a number of proline-rich proteins, in particular WASP and WASP-related proteins. UL150 exhibits similarity to mucin-like proteins (Table 3.1), and in this context it is interesting to note UL150 has been identified as a potentially secreted protein (A. Davison, personal communication). UL141 was revealed to contain an Ig-like β sandwich domain (Table 3.1). As previously described by Dolan *et al* (2003) and confirmed in this bioinformatics search, UL141 is a homologue of the HCMV protein UL14, and together they comprise the UL14 gene family. UL14 is also found to contain an Ig-like β sandwich domain (Table 3.1), and with the exception of its homologue, UL141, does not show any sequence identity to other known proteins.

In addition to the 23 ORFs of the UL/*b'* region, UL141A was proposed as another potential ORF by Dr P. Tomasec (Table 3.1). No homologues to UL141A were revealed by this bioinformatics search, but it has been included in this study as a putative UL/*b'* region ORF.

3.1.2 Post-translational modifications

An interface for a number of different protein modification analysis tools called PredictProtein (Rost *et al.*, 2003) was used to gather the majority of motif pattern information for each UL/*b'* ORF. The results are described in Table 3.2. Prosite (Bairoch *et al.*, 1997) details all possible post-translational motif patterns from a protein sequence and was also used, via PredictProtein, to run a more detailed analysis of the UL/*b'* ORFs.

Table 3.2 Summary of post-translational modifications predicted for the UL/*b'* ORFs

ORF[1]	Amino Acids[1]	Signal Peptide[2]	Transmembrane domain[3]	N-Glycosylation[4a]	O-Glycosylation[5]	Phosphorylation[4b]	N-Myristoylation[4c]	SUMOylation[4d]	Other[4e]
UL128	130	Y (1-27)	-	-	-	PKC x1 CK2 x1 TYR x1	2	-	
UL130	214	Y (1-25)	-	3	4	PKC x1 CK2 x4	-	Low probability x1 High probability x1	
UL131A	129	Y (1-18)	-	1	-	CAMP x1 PKC x2 TYR x2	-	Low probability x1	
UL132	270	Y (1-27)	Y (84-106)	4	10	CAMP x1 PKC x4 CK2 x5 TYR x1	4	Low probability x1 High probability x1	
UL133	257	Y (1-39)	Y (13-35 potential N-term signal, 45-67)	-	14	PKC x3 CK2 x2	1	Low probability x1	Glycosaminoglycan attachment site, prokaryotic lipoprotein attachment site
UL135	302	Y (1-22)	Y (4-26 potential N-term signal)	2	42	CAMP x1 PKC x8 CK2 x3	3	Low probability x8	Pro rich region
UL136	240	-	Y (65-87)	-	-	CAMP x1 PKC x2 CK2 x4	3	-	
UL138	169	Y (1-28)	Y (10-32 potential N-term signal, 33-52)	-	9	CAMP x1 PKC x6 CK2 x1 TYR x1	1	-	
UL139	138	Y (1-16)	Y (62-84)	4	9	CK2 x3	4	-	
UL140	191	- (signal anchor)	Y (26-48)	2	-	CAMP x2 PKC x2 CK2 x2	1	Low probability x1	
UL141	338	Y (1-29)	Y (279-301)	3	3	CAMP x1 PKC x2 CK2 x3 TYR x1	3	-	Prokaryotic lipoprotein lipid attachment site, YXXL (YRRL) motif, Ig like β sandwich domain
UL141A	102	-	-	-	-	CAMP x3 PKC x4 CK2 x2	2	Low probability x2	Bipartite nuclear signal sequence
UL142	305	Y (1-19)	Y (57-75, 270-289)	17	9	PKC x4 CK2 x5	5	Low probability x1	
UL144	171	Y (1-20)	Y (129-151)	7	1	PKC x4	2	Low probability x1 High probability x1	TNFR signature, YXXL (YTRL) motif
UL145	130	-	Y (69-90)	-	-	PKC x1 CK2 x1	-	Low probability x1	
UL146	120	Y (1-22)	Y (1-18 potential N-term signal)	1	2	TYR x1	1	Low probability x1	ELR motif
UL147	159	- (signal anchor)	Y (20-42)	-	-	PKC x1 CK2 x1 TYR x1	-	-	
UL147A	73	Y (1-23)	Y (7-25 potential N-term signal, 57-75)	-	-	CK2 x1	1	-	
UL148	316	Y (1-20)	Y (206-308)	2	-	CAMP x1 PKC x1 CK2 x1	1	High probability x1	RGD cell attachment sequence, Lectin legume beta domain
UL148A	80	- (signal anchor)	Y (10-32)	-	-	CK2 x1	-	High probability x1	
UL148B	80	Y (1-18)	Y (10-32)	-	2	CK2 x1	2	-	Prokaryotic membrane lipoprotein attachment site, peroxisome targeting signal
UL148C	77	Y (1-29)	Y (10-32, 39-61)	-	1	-	1	-	
UL148D	62	- (signal anchor)	Y (30-52)	1	-	-	-	-	Glycosaminoglycan attachment site
UL150	639	Y (1-16)	-	1	1	CAMP x3 PKC x17 CK2 x10	6	Low probability x4 High probability x1	
UL14	327	Y (1-23)	Y (266-289)	2	-	PKC x5 CK2 x4	3	Low probability x1	Ig-like β sandwich domain, YXXL (YRRL) motif

1 Nomenclature and sequence information obtained from GenBank Merlin sequence AY446894 (Dolan *et al.*, 2004)

2 Potential signal peptide predictions obtained from database SignalP 3.0 (http://www.cbs.dtu.dk/services/SignalP/) (Bendtsen *et al.*, 2004). Signal anchor denotes previously named uncleaved signal peptide

3 Predicted transmembrane regions, obtained from database TMHMM (http://www.cbs.dtu.dk/services/TMHMM-2.0/) (Krogh *et al.*, 2001) and TMPred (http://www.ch.embnet.org/software/TMPRED_form.html) (Hofmann & Stoffel, 1993). Brackets indicate the amino acid residues the domain lies within.

4 Potential protein motifs detected using various tools via the PredictProtein database (http://cubic.bioc.columbia.edu/predictprotein/) (Rost *et al.*, 2003)

4a Asparagine glycosylation prediction obtained via PredictProtein from Prosite (http://www.expasy.ch/prosite) (Bairoch *et al.*, 1997)

4b Phosphorylation motif predictions obtained from Prosite via PredictProtein.

PKC: a protein kinase C phosphorylation site

CAMP: a cAMP and cGMP - dependent protein kinase phosphorylation site

CK2: a casein kinase 2 phosphorylation site

TYR: a tyrosine kinase phosphorylation site

4c N-Myristoylation prediction obtained from Prosite, via PredictProtein.

4d SUMO modification sites predicted based on the motif Ψ-K-x-D/E by SumoPlot™ (Abgent; www.abgent.com/doc/sumoplot)

4e Other modifications, motifs predicted by Prosite, via PredictProtein, and structure homology predicitions by Phyre (http://www.sbg.bio.ic.ac.uk/phyre)

5 Database NetOGlyc (http://www.cbs.dtu.dk/services/NetOGlyc/) (Julenius *et al.*, 2005) was used to predict O-glycosylation (mucin type glycosylation)

NOTE: Although a motif for O-glycosylation may be present in a sequence, it is unlikely to take place unless the protein possess a signal peptide and is processed via the correct cellular route through the Golgi.

O-glycosylation will not take place in transmembrane regions or cytoplasmic portions of protein.

Most of the UL/*b'* ORFs were found to contain common protein motifs (Table 3.2), for example for phosphorylation and N-myristoylation, a lipid anchor modification. An additional common motif predicted for some of these proteins is the SUMOylation motif. SUMO modification is the covalent attachment of a small, 11kDa ubiquitin-like molecule. It has been implicated in the regulation of a number of mammalian molecules, such as TNFR and viral proteins like CMV IE1 and IE2, and also may stabilize proteins and affect their subcellular localisation. SUMO modification sites were predicted for a number of the UL/*b'* ORFs using SUMOPlot™ (Abgent) (Table 3.2). Of particular interest are the high probability sites predicted for UL130, UL132, UL144, UL148, UL148A (a non-overlapping, individual ORF unrelated to UL148; this applies to each of the UL148A, UL148B, UL148C and UL148D ORFs) and UL150. The remaining ORFs are predicted either low probability sites, which are motifs with amino acids of similar hydrophobicity to the consensus sequence, or possess no SUMOylation motif.

Less common modifications were also predicted for some of the UL/*b'* ORFs. Both UL133 and UL148D are predicted to contain an attachment site for the carbohydrate modification, glycosaminoglycan (Table 3.2), and UL133, UL141 and UL148B are predicted to contain a prokaryotic membrane lipoprotein lipid attachment site, a type of lipid anchor for lipoproteins that may provide membrane fixation for the modified lipoprotein in prokaryotes. UL148B is predicted to encode a peroxisome targeting signal (PTS). There are many variations of the PTS, but it is prototypically Ser-Lys-Leu, which is encoded by UL148B in the centre of its sequence. The PTS targets the peroxisomal protein to a PTS1 receptor, which then directs the protein into the peroxisome. UL141A is predicted to contain a nuclear signal sequence (Table 3.2). A YXXL motif is found in UL141, UL14 and UL144 (Table 3.2). YXXL defines the immunoreceptor tyrosine-based activation motif (ITAM) motif which is associated with

binding of SH2 domain-containing proteins including the tyrosine-kinase Syk and other adaptor proteins involved in multiple cell signalling processes. The presence of this motif may affect the constitutive or inducible signalling of UL144, UL141 and UL14. It is also possible the YXXL motif may be required for protein binding. UL16 is described as an ER resident protein that binds and sequesters the ULBP1, ULBP2 and MICB stress-induced molecules, evading NK lysis. A YXXL motif in UL16 (YQRL) has been found to be necessary for its retention of MICB (Wu *et al.*, 2003).

The ELR motif identified in UL146 is involved in the binding of IL8 chemokines to the receptor CXCR1 (specific for IL-8) and CXCR2, a more general receptor for ELR-containing chemokines. The fact that the ELR motif is present in UL146 but not UL147 suggests these HCMV virokines may be functionally distinct. UL148 is predicted to be a membrane associated glycoprotein that possesses an RGD cell attachment motif. This RGD motif is often found in extracellular matrix (ECM) proteins where it forms a specific interaction with integrins. Integrins are found on the plasma membrane as a non-covalently linked heterodimer consisting of an α and β subunit, which convey specificity in cell-cell as well as cell-ECM attachment, immune cell recruitment, extravasation and signalling. In addition, it was recently shown that the integrins α2β1, α6β1 and αVβ3 are involved in the HCMV entry pathway (Feire *et al.*, 2004).

The signal peptide sequence plays a key role in targeting the translation of proteins to the ER. The signal peptide is responsible for expression in the ER, and is a pre-requisite for trafficking through the Golgi to the cell surface or other secretory vesicles. SignalP (Bendstenn *et al.*, 2004) was used to predict the presence of potential signal peptides, and their possible cleavage sites, for each of the UL/*b'* ORFs (Table 3.2). With the exception of UL136, UL141A and UL145, the UL/*b'* ORFs all possess signal peptides. UL140, UL147, UL148A and UL148D are predicted to contain a signal peptide in the

centre of the protein that is not cleaved. This is described in Table 3.2 as a signal anchor, or uncleaved signal peptide, describing proteins that are sorted by the signal peptide, but may not follow on through the secretory pathway. This data indicates that most of the UL/*b'* ORFs are potentially secretory or sorted to membrane locations within the cell.

3.1.3 A number of the UL/*b'* ORFs encode potential glycoproteins

Glycosylation is an important post-translational modification that provides insight into cellular location and potential function; many glycoproteins are expressed on the cell surface where they can play vital roles in intercellular communication and receptor interaction. Two different types of glycosylation have been defined; N-glycosylation and O-glycosylation. N-glycosylation is initiated in the ER, with the formation of more complex carbohydrates being the result of further processing through the Golgi. O-glycosylation tends to be initiated in the Golgi. N-glycosylation involves the addition of N-linked oligosaccharides to asparagine via N-acetylglucosamine. Potential N-glycosylation sites were identified via Predict Protein (Rost *et al.*, 2003) based on the sequence motif NXS/T, where X can be any amino acid except proline. O-glycosylation involves the addition of O-linked oligosaccharides to serine or threonine residues via N-acetylgalactosamine, and was predicted using the program, NetOGlyc (Julenius *et al.*, 2005).

Sequence analysis indicated only 7/24 of the predicted UL/*b'* ORFs (UL128, UL136, UL141A, UL145, UL147, UL147A and UL148A) did not encode a potential glycosylation motif. The remaining 17 ORFs were predicted to contain both types of glycosylation motifs, which implies the majority of proteins encoded by the UL/*b'* region may be glycoproteins (Table 3.2). A number of very highly glycosylated proteins have been predicted (Table 3.2). In particular UL144 and UL142 are predicted to

contain the most N-glycosylation sites, with 7 and 17 sites predicted respectively. UL142 is a homologue of UL18, which is also predicted to contain 13 N-glycosylation sites and was recently confirmed by Griffin *et al* (2005) to encode a highly glycosylated protein. UL142 is also predicted to contain 9 O-glycosylation sites and, most remarkably, the UL135 ORF is predicted to contain some 42 O-glycosylation sites (Table 3.2).

3.1.4 A number of UL/*b'* ORFs encode potential transmembrane proteins

Protein topology was predicted using a number of different programs. Although variation can occur in the exact placing of transmembrane regions, predictions for transmembrane domains from most programs concur. Table 3.2 gives the transmembrane region for each ORF predicted by TMPred (Hoffman & Stoffel, 1993) and TMHMM (Krogh *et al.*, 2001). With the exception of UL128-UL131A, UL141A and UL150, most of the UL/*b'* proteins are predicted to contain transmembrane regions. A number of UL/*b'* ORFs have been predicted to contain two transmembrane regions, although care must be taken with these results, as some of the regions are predicted at the N-terminus of the protein, encompassing a signal peptide that may be cleaved.

In addition to secondary structure predictions, the program Phyre was also used to compare predicted protein folds of the UL/*b'* ORFs that may match other known secondary structures. Both 1D and 3D sequence profiles, coupled with secondary structure and solvation potential information are used to predict similarity to other structures. Although less successful than the BLAST and FASTA searches, it was felt necessary to look at this level for any homology. Of the UL/*b'* ORFs, both UL14 and UL141 were predicted to contain Ig-like β sandwich domains, and UL142 was successfully matched to MHC-I structures (Table 3.2).

3.2 GENERATING RECOMBINANT ADENOVIRUSES

3.2.1 AdEasy system for generating recombinant adenovirus

To screen the UL/*b'* ORFs in functional assays and to characterise their expression, each UL/*b'* ORF was cloned into a replication deficient Ad vector. A commonly used method in the construction of recombinant Ads (RAds) involves homologous recombination in mammalian cells capable of complementing the E1 defective Ad. One such system is the commercially available Admax system (Microbix) in which the gene of interest is cloned into a transfer vector, which is then co-transfected into a mammalian packaging cell line with a plasmid containing the Ad backbone (ΔE1, ΔE3). Homologous recombination occurs between the two transfected plasmids in the mammalian cells, and the expression cassette from the transfer vector is inserted into the original E1 region of the adenoviral genome. E1 is provided in trans in mammalian packaging cells such as 293s (Graham *et al.*, 1977) and 911s (Fallaux *et al.*, 1996) to produce the RAd. However, this method is time-consuming as it requires multiple plaque purifications to isolate and identify the RAd.

Further developments in the production of RAds have been made based on the finding that homologous recombination can be carried out in *E.coli*, resulting in a more efficient system for RAd production as it obviates the need for plaque purification (Chartier *et al.*, 1996; He *et al.*, 1998; Zeng *et al.*, 2001). AdEasy is one of these faster and more efficient systems for generating RAds (He *et al.*, 1998; Fig 2.2). This system also involves insertion of the gene of interest into a transfer vector, pShuttleCMV, so that the gene of interest is under the control of the CMV major IE promoter. The CMV major IE promoter gives high expression of transgenes from the Ad vector (Wilkinson & Akrigg, 1992). pShuttleCMV is then linearised with *Pme*I, and transformed into *E.coli* BJ5813 containing the adenoviral backbone vector, pAdEasy-1 (Fig 2.2). *E.coli* BJ5813 are recombination-competent and homologous recombination occurs between the two

plasmids. The resulting recombinant adenovirus DNA produced in these cells is then purified, linearised with *Pac*I and transfected into mammalian packaging cells, where E1 is complemented *in vivo* to produce RAds (Fig 2.2; He *et al*, 1998; Hosfield & Eldridge, 2000).

A number of RAds that could not be made by the Admax system were generated using AdEasy. With the Admax system, recombination occurs under high transgene expression, and therefore if this gene is not fully compatible with efficient Ad replication, it reduces the chances of obtaining a recombinant. The AdEasy system, on the other hand, involves recombination in bacteria, where transgene expression is not an issue in the generation of RAds, increasing the chances that a recombinant will be produced. In addition, plaque purification of progeny virus is essential in the Admax system, whereas in the AdEasy system, a single clone is already selected before RAd production in 293 or 911 cells, obviating the need for plaque purification. AdEasy was therefore chosen as the most efficient available system for the generation of RAds encoding the UL/*b'* ORFs.

3.2.2 Epitope tag (Streptag II)

Specific antibodies for individual UL/*b'*-encoded proteins were not available for this study; indeed, most of the associated ORFs were previously uncharacterised. To test whether expression was being achieved, it was therefore considered necessary to incorporate a C-terminal epitope tag during PCR amplification. As the primary aim in cloning the UL/*b'* ORFs was to investigate their function, a tag was selected that would provide maximum potential utility, whilst minimising any potential affect on protein structure. GFP is a relatively large molecule (26.9kDa), that could potentially hinder the structure, intracellular trafficking or activity of the UL/*b'* proteins. Instead, a small epitope tag was used, called Streptag II (IBA). The Streptag technology was developed

to provide a highly efficient protein purification system, and is based on the strong binding of biotin and streptavidin. The manufacturers have optimised the tag sequence and have engineered the biotin-binding pocket of streptavidin to produce StrepTactin, a form of streptavidin that possesses 100x the affinity for the Streptag sequence. Streptag II is 8 amino acids in length (Trp-Ser-His-Pro-Gln-Phe-Glu-Lys) and has a balanced amino acid composition, making it unlikely to affect protein structure or activity. Reagents are available commercially that facilitate purification of Strep-tagged proteins and the detection of Streptag II in western blot, ELISA and immunofluorescence. The Streptag sequence was cloned onto the C-terminus of the UL/*b'* ORFs by PCR using specific primers coding for Streptag (Table 2.2).

3.3 CONSTRUCTION OF RECOMBINANT ADENOVIRUSES VIA THE AdEASY SYSTEM

3.3.1 Cloning UL/*b'* ORFs into the AdEasy transfer vector, pShuttleCMV

Each UL/*b'* ORF, amplified by PCR with a C-terminal Streptag, was cloned into a RAd vector using the AdEasy system, either via TOPO® cloning (Invitrogen) or by direct cloning into pShuttleCMV. Briefly, TOPO® cloning is a plasmid vector system that exploits the single base extension generated by *Taq* polymerase to enable efficient, direct, cloning of PCR products. Using this approach, UL/*b'* ORFs were inserted into the TOPO plasmid, pCR2.1-TOPO® (Fig 2.3a). From the TOPO vector, the UL/*b'* ORFs were then excised by restriction endonuclease digestion using asymmetric sites and sub-cloned into pShuttleCMV (Fig 2.3b,c). Although TOPO cloning is an efficient system, it creates an extra step in the process of inserting transgenes into pShuttleCMV. To remove this step from the process, some of the genes (UL133, UL136, UL147 and UL148) were cloned directly into pShuttleCMV. Each ORF was amplified by PCR from Merlin DNA with primers containing the restriction sites *Kpn*I (5') and *Xba*I (3'), which

were then used to directly ligate the digested PCR product into pShuttleCMV (Fig 2.3c). Each step in the cloning system was checked by sequencing and restriction digest to ensure the presence and integrity of the transgenes.

3.3.2 Generation of recombinant Ad plasmids

To generate RAds, the UL/*b'* ORF-pShuttleCMV transfer vectors were transformed into *E.coli* BJ5813 carrying the pAdEasy-1 vector. pAdEasy-1 should lose its ampicillin resistance selectable marker following homologous recombination with pShuttle-CMV, and the recombinant plasmid gain kanamycin resistance from the pShuttleCMV plasmid (Fig 2.2). Recombinants were selected by kanamycin resistance, and screened by *Pac*I and *Hin*dIII restriction enzyme digest. *Hin*dIII restriction enzyme digest was used to check the pAdEasy-1 restriction endonuclease digestion pattern against a RAd control to check the adenovirus backbone was intact. *Pac*I restriction enzyme was used for classification of recombination. There are two different sites of recombination between pAdEasy-1 and pShuttleCMV. Normally, recombination will occur between the right and left arms of homology that are present in the transfer vector, but can also be seen between the replication of origin (ORI) and the right arm of homology. This results in two different fragment combinations with *Pac*I digest, consisting of a large fragment ~ 30kb, and a smaller fragment of either 3kb if recombination occurred at the left arm or 4.5kb if recombination occurred at the ORI (Hosfield & Eldridge, 2000). During the cloning of the UL/*b*' genes, recombination at the ORI was more frequent, producing a 4.5kb fragment. Both types of recombination are correct, yielding recombinant adenoviral DNA. An example is provided in Figure 3.1a, where clone 1 shows the correct banding pattern for a recombinant clone. The banding patterns for clones 2-6 are unknown, as they do not correspond to either pAdEasy-1 or pShuttleCMV *Hin*dIII or *Pac*I digested plasmids (Fig 3.1a).

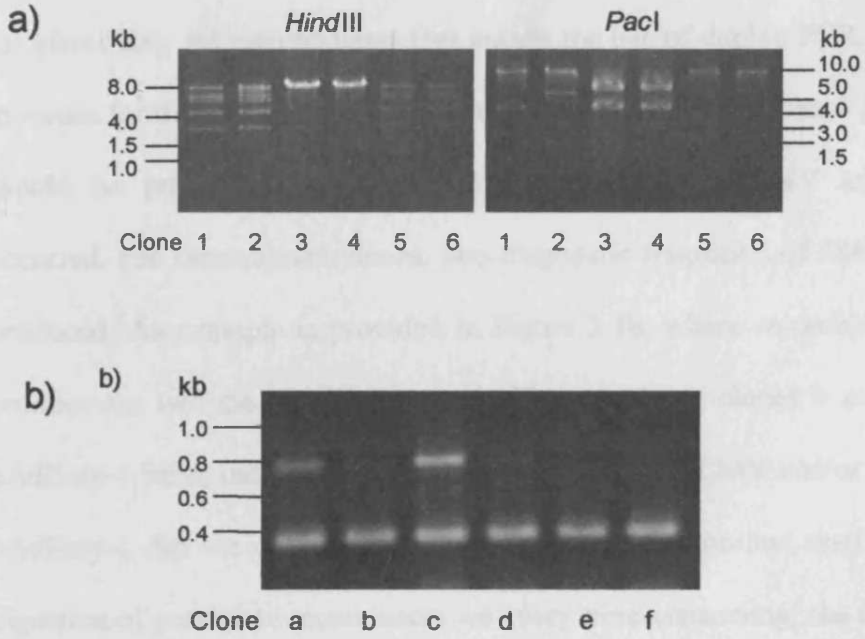

Figure 3.1 Screening for recombination between pAdEasy-1 and pShuttleCMV by restriction enzyme digest and duplex PCR
a) UL14 RAds were screened by *Pac*I/*Hin*dIII restriction enzyme digest and 0.8% agarose gel electrophoresis. UL14-pShuttleCMV recombination with pAdEasy-1 produces a large fragment of approximately 30kb, plus a smaller 4.5kb or 3kb fragment by *Pac*I restriction enzyme digest. *Hin*dIII restriction enzyme digest produces a 5 band pattern that can be compared with a RAd control (not shown) and indicates the pAdEasy-1 backbone is intact. b) UL/*b*' ORF-pShuttleCMV recombination was also screened by duplex PCR (Antolovic *et al.*, 2005) with primers for the kanamycin gene and a portion of the Ad backbone. Duplex PCR of correct Ad recombinants produces 2 bands of 784bp and 384bp respectively.

During the production of these RAds, Antolovic *et al.* (2005) described a rapid method for identifying Ad recombinants that entails the use of duplex PCR. Primers were used to screen for the adenoviral backbone and the kanamycin resistance gene, both of which should be present if recombination between pShuttle-CMV and pAdEasy-1 has occurred. For recombinant clones, two diagnostic fragments of 384bp and 768bp were produced. An example is provided in Figure 3.1b, where recombinant clones a and c produce the two diagnostic fragments. The remaining clones b and d-f show only a pAdEasy-1 band, indicating transformation of pShuttleCMV and/or recombination with pAdEasy-1 did not occur. As plasmid DNA preparation and restriction endonuclease digestion of potential recombinants was very time-consuming, the duplex PCR method for screening recombinants was adopted.

3.3.3 Generation of recombinant Ad particles

Once insertion of the HCMV ORF into the AdEasy-1 vector has been demonstrated by restriction endonuclease digestion or duplex PCR, the clone was expanded overnight. The recombinant plasmid is very large (>30kb), and large scale culture must be performed rapidly to avoid additional recombination events. The recombinant DNA was extracted, purified and digested by *Pac*I, necessary to release the viral genome for viral particle production. The recombinant DNA was then transfected into 293 or 911 cells using Polyfect (Qiagen).

It is possible to produce virus in both cell lines, and each has certain advantages and disadvantages. Early on in the production of the UL/*b*' viruses, 911 cells were transfected to produce the virus, as the plaques in these cells are easier to recognise. The 911 cells also grow slower than 293s, an advantage when producing slow growing viruses as cells do not become too confluent too quickly, whereas 293 cells become over-confluent and detach before the virus has produced recognisable plaques.

However, there were a number of recombinant plasmids that did not produce virus in the 911 cells (UL128, UL131A, UL132, UL133, UL138, UL145, UL148 and UL148B). Repeating the transfections in 293 cells resulted in the production of most of these problematic RAds (UL132, UL133, UL138, UL145, UL148 and UL148B). Perhaps, the faster growth rate of 293 cells allowed certain viruses to be produced before the cells could be affected by potential toxicity of the expressed transgene.

Virus plaques were usually seen approximately 7 to 10 days after transfection of RAd DNA. As identification of virus plaques could be ambiguous, virus production was also confirmed using an Ad antibody test kit (SAScientific). Once a virus was produced it could then be harvested by ArkloneP extraction of infected cells and then propagated.

The majority of the UL/*b'* ORFs were successfully cloned into replication deficient Ad vectors. Due to time constraints, delays caused by overcoming problem constructs and local circumstances, a number of UL/*b'* ORFs were cloned into RAd vectors by other researchers from within the laboratory (Table 2.3). Dr B. McSharry had previously produced the ORF UL130 RAd, cloned into an Ad vector with a FLAG-tag in place of Streptag II using the AdMax system, and Dr V. Prod'homme cloned eight Strep-tagged UL/*b'* ORFs into Ad vectors using the AdEasy system (RAdUL128, RAdUL131A, RAdUL138, RAdUL140, RAdUL147A, RAdUL148A, RAdUL148C and RAdUL148D). With the exception of UL128 and UL131A, which did not produce RAd using the AdEasy system, all the UL/*b'* ORF RAd vectors successfully produced virus. With the contributions from Drs V. Prod'homme and B. McSharry to the bank of UL/*b'* RAds, it was possible to complete the characterisation of these UL/*b'* ORFs, and the production of UL128 and UL131A (Section 3.5) within the course of this project.

To test that each RAd encoded a UL/*b'* ORF of the appropriate size, adenoviral genomic DNA was extracted and the transgene insertion PCR-amplified using specific primers (Fig 3.2). By comparing predicted sizes for each ORF with those produced by

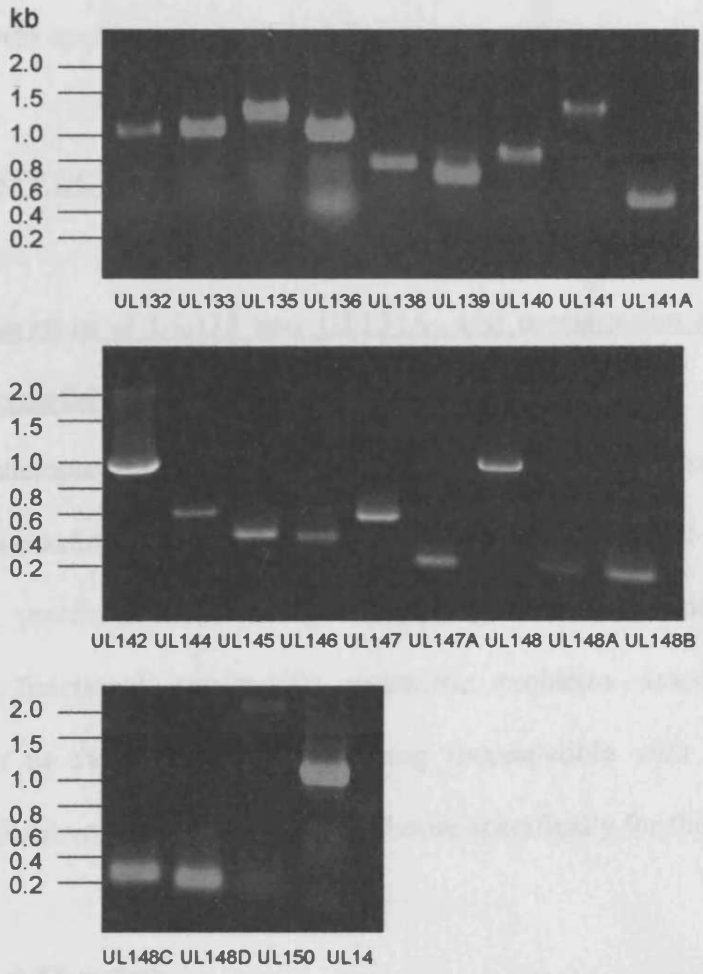

Figure 3.2 PCR analysis to test that each RAd encodes a UL/*b*' ORF
UL/*b*' ORFs were amplified by PCR from UL/*b*' ORF RAd DNA with their respective specific primers and fragments analysed by 0.8% agarose gel electrophoresis to check that each RAd encoded for the appropriately sized UL/*b*' ORF.

PCR amplification, all RAds that were made were shown to contain a UL/*b'* gene product of the appropriate size (Fig 3.2).

3.4 CONSTRUCTION OF RECOMBINANT ADENOVIRUSES VIA THE AdZ SYSTEM

3.4.1 Generation of UL128 and UL131A, and propagation of UL132 and UL148 was unsuccessful using the AdEasy system

Multiple attempts to generate the UL128 and UL131A RAds using the AdEasy system were unsuccessful. In addition, although RAds UL132 and UL148 were both produced (Fig 3.2), problems arose during the propagation of the viruses with low yields curtailing functional assays. To overcome problems associated with transgene expression in the helper cell line being incompatible with vector replication, an inducible RAd vector was developed in-house specifically for this application.

3.4.2 The AdZ system

It became clear during the course of this study that the production of large numbers of RAds using the AdEasy-1 vector was labour-intensive, unreliable and time-consuming. A high efficiency Ad vector system was therefore developed by Dr R. Stanton that eliminated the need for all conventional cloning steps; called AdZ, or Ad production with zero cloning steps (Fig 2.4; Stanton *et al.*, unpublished). This system makes use of *E.coli* strain SW102 (kindly donated by Dr N. Copeland), which contain a defective phage that expresses the lambda red genes. These genes are temperature-sensitive, and mediate homologous recombination between arms of homology as short as 50bp when incubated at 42°C. The Ad vector present in SW102 bacteria, designated pAL942, contains the entire Ad genome from the AdEasy system as a single copy vector. It also contains the CMV promoter, two tetracycline (Tet) operator sites, polyA tail, and

incorporates a C-terminal Streptag II into the reading frame. Ampicillin resistance, *SacB* encoding sensitivity to sucrose, and *LacZα* to enable blue white screening are also included in the vector to enable analysis of clones. The 50bp arms of homology to the CMV promoter region and polyA region are incorporated into PCR primers, permitting a system whereby the PCR product, amplified with regions of homology, can be directly ligated into the Ad vector by homologous recombination, without the need for multiple cloning and subcloning steps. This type of cloning has been termed "recombineering". The presence of Tet operator sites enables expression of the transgene to be regulated during virus production. Binding of the Tet repressor, which is constitutively expressed by 293 T-REx™ cells, to the Tet operator sites suppresses gene expression, enabling RAd to be produced in 293 T-REx™ without potentially toxic transgene expression.

3.4.3 Cloning of UL128, UL131A, UL132 and UL148 into Tet regulated recombinant Ad vectors via the AdZ system

UL128, UL131A, UL132 and UL148 were PCR-amplified from HCMV strain Merlin template DNA using transgene-specific primers (Table 2.2), yet the primers also contain sequence homology with the CMV promoter and polyA regions in the Ad vector (pAL942) to enable direct insertion by recombineering. The Amp-LacZ-SacB cassette is replaced by the UL/*b'* ORF upon successful recombination and clones were plated onto chloramphenicol selection plates containing sucrose and X-gal. Growth on sucrose becomes possible with the loss of the negative selectable marker (SacB), and positive colonies also do not stain blue on X-gal with loss of LacZ. Colonies containing the appropriate transgene insertion were thereby readily selected, yet still needed to be sequenced in order to check for PCR-generated errors in the insert. Plasmid was purified from correct clones, and transfected into 293 T-REx™ cells. The AdZ vector is self-excising, thus obviating any need to scale up plasmid purification, or to excise the

Ad genome (e.g. by *Pac*I digestion) before transfection. Expression of the UL/*b*' ORF under the Tet operator element is repressed in T-REx cells, thus enabling production of the RAd encoding potentially toxic gene products.

RAdUL148 was remade using the AdZ system, and has produced a good high titre stock. Currently, only low titre stocks of RAdUL132 are available. UL132 has yet to be inserted into the AdZ system during this project, however the results obtained with UL148 indicate this approach is valid. RAdUL128 and RAdUL131A were successfully produced using the AdZ system, and their generation has completed the bank of RAds encoding the entire UL/*b*' region.

4. ANALYSIS OF ADENOVIRUS RECOMBINANTS ENCODING UL/*b'* ORFS

Each UL/*b'* ORF was cloned into a RAd vector with a C-terminal Streptag in order to allow expression of each ORF to be followed and characterised. Expression of most of these ORFs has not previously been investigated, so in addition to validating expression from the vectors the studies had potential to provide novel insights into the properties of the expressed proteins. Three distinct techniques were exploited to characterise their expression: western blotting, flow cytometry and immunofluorescence.

4.1 CHARACTERISATION OF UL/*b'* ORFS BY WESTERN BLOT

To analyse transgene expression in western blot, a Streptag II-specific mAb was used. RAd592 is an AdEasy vector that lacks an insert, and was used throughout as a negative control that could distinguish non-specific interactions. In contrast, RAdIL10 was used as a robust positive control. RAdIL10 encodes a C-terminal Strep-tagged HCMV vIL10 (UL111A) fusion protein that has consistently provided good expression and a strong positive signal with the Streptag II-specific mAb.

For expression analysis, immortalised human foetal foreskin fibroblasts (HFFF-htert) were initially infected with individual RAds encoding Strep-tagged UL/*b'* ORFs. To maximise expression, HFFF-htert were infected with RAds at a high MOI (100pfu/cell), cells were cultured in the presence of forskolin to boost protein expression from the HCMV IE promoter (Wilkinson & Akrigg, 1992) and extracts prepared at 72hpi. In these preliminary experiments, expression from only a limited number of constructs could be detected (pUL14, pUL135, pUL141, pUL145 and pUL150), with detection of pUL141, pUL145 and pUL150 being inconsistent (data not shown).

Ad5 normally uses the CAR (Cocksackie and adenovirus receptor) as a primary receptor and αv integrin as a secondary receptor to gain entry into cells. Whilst human fibroblasts are routinely used in HCMV research, they have low levels of cell surface CAR. The study was repeated using HFFF-htert transduced with a retrovirus encoding CAR (designated HFFF-hCAR), which renders them more than 10-fold susceptible to Ad5 infection (Dr B. McSharry, personal communication). Where HFFF-htert were infected with each UL/*b*' ORF RAd at a MOI of 100 pfu/cell, the MOI was reduced for the new HFFF-hCAR cell line to 10 pfu/cell. At 24hpi, RAd infected HFFF-hCAR were supplemented with forskolin to boost protein expression and harvested at 72hpi.

Detection of expressed Strep-tagged proteins from HFFF-hCAR cells proved to be significantly more efficient than using the parental HFFF-htert (Fig 4.1). After multiple attempts, the expression of 8/22 ORFs could not be detected by western blot: UL132, UL133, UL139, UL142, UL144, UL146, UL148 and UL148C (Fig 4.1). Each RAd was demonstrated to encode correct insert by both PCR and DNA sequence analysis (Fig 3.2); thus indicating that the problem in detecting these proteins lies with expression or western blot detection. There are a number of explanations why the Streptag mAb may not have detected expression. Potentially, a protein may have been processed in such a way that the C-terminus and therefore the Streptag have been cleaved, to release an untagged mature protein. A protein may have folded in such a way as to distort the Streptag, or conceal it from antibody recognition. This may happen when the protein is denatured prior to electrophoresis, or the protein may undergo partial refolding after western blotting. Potentially, expression of the tagged protein may be influenced by a function of a gene product itself. It had originally been envisaged that the shared epitope tag would enable the relative level of expression of each of these proteins to be estimated by western blot. Although infection conditions were identical and comparable amounts of cell extract loaded, the signal strength of each protein varies dramatically.

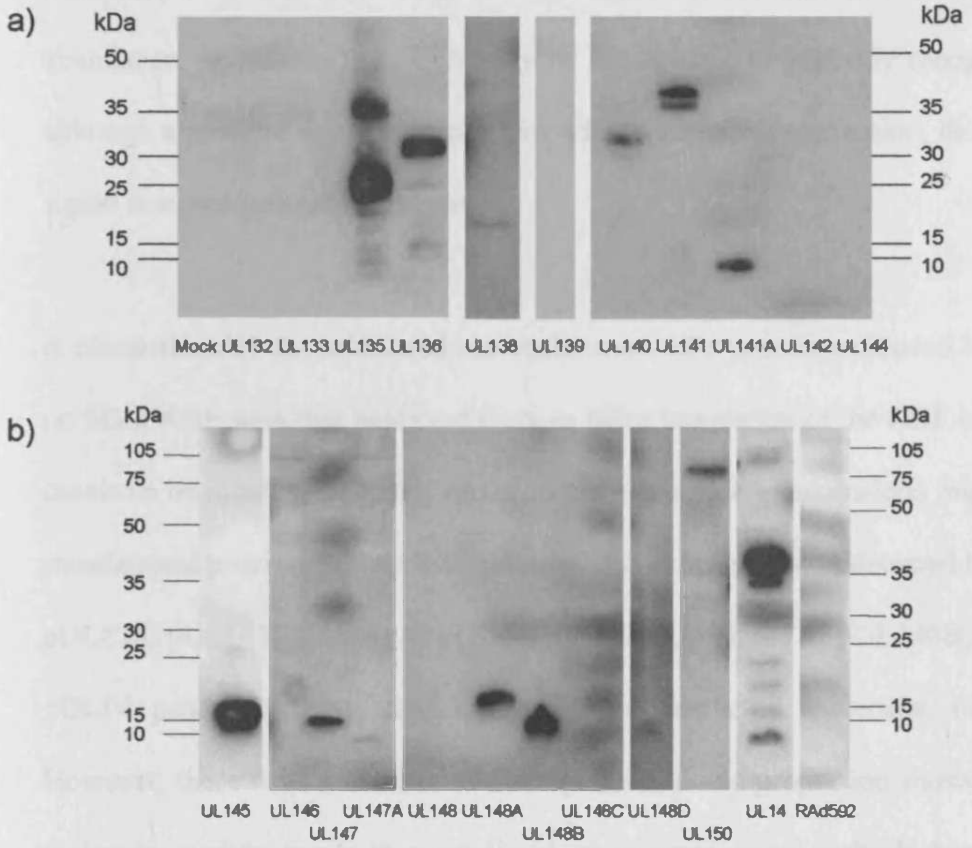

Figure 4.1 Western blot detection of UL/*b*' ORFs by Streptag antibody. HFFF-hCAR cells were infected with UL/*b*' RAds at a MOI of 10, cell extracts prepared at 72hpi and proteins separated by SDSPAGE and transferred to nitrocellulose. Strep-tagged proteins were detected by Streptag monoclonal antibody. a) Mock control, plus RAd infected cell extracts RAdUL132 through to RAdUL144, and b) Rad592 control, plus RAd infected cell extracts RAdUL145 through to RAdUL150 and RAdUL14.

However, it is not clear whether this represents a direct measurement of protein abundance, or reflects the availability of the epitope to antibody recognition. Indeed, although a positive signal detection provides evidence of expression, the lack of such a signal does not preclude expression.

A comparison of the calculated molecular mass of a protein estimated by its migration on SDSPAGE with that predicted from *in silico* translation of the ORF is important as a check on its identity, although variation can occur due to anomalous migration or post-translational processing. Of those genes whose expression was detected by western blot, pUL138, pUL141, pUL141A, pUL145, pUL147, pUL147A, pUL148B, pUL148D and pUL14 produced bands that matched their predicted molecular mass (Fig 4.1). However, there were a number of discrepancies, and a proportion showed either higher molecular weight bands than predicted or in some cases multiple bands. pUL135 is predicted to have a mass of 33kDa, but blots show 2 bands, the first of approximately 25kDa, and the second of approximately 35kDa that may account for the predicted mass (Fig 4.1). The 25kDa band appears to be the more dominant band, and may be a breakdown product or the result of cleavage of the full length pUL135. pUL136 produces a major band of ~33kDa, which is slightly larger than its predicted 27kDa (Fig 4.1). UL136 is not predicted to be glycosylated, or to possess any other post-translational motifs that may have resulted in this higher molecular weight protein. pUL140 is predicted to have a molecular mass of 21.5kDa, yet RAdUL140 encodes a protein estimated at 33kDa, giving an increase in predicted mass of approximately 12kDa (Fig 4.1). UL140 is predicted to encode two N-glycosylation sites, which may contribute to a higher molecular mass, though this type of modification has not been confirmed. UL140 is also predicted to contain a number of low probability SUMO modification sites. SUMOylation is the covalent modification of an 11kDa, ubiquitin-

like molecule that may account for this increase in predicted mass. Although UL140 is predicted to contain a number of low probability sites, co-immunoprecipitation studies with an anti-SUMO antibody did not reveal pUL140 to be SUMOylated (data not shown). pUL14 and pUL141 were both observed with bands of approximately their predicted mass, but produced a double banding pattern (Fig 4.1). UL14 and UL141 are both predicted to contain N-glycosylation sites (Table 3.2), and the incomplete glycosylation of some of the cellular protein may explain the double banding pattern produced by pUL14 and pUL141, where the upper band represents fully glycosylated protein and the lower band the incomplete or un-glycosylated product. (The glycosylation of these two proteins will be examined further in Chapter 6). pUL148A and pUL148B are both predicted to be approximately 9kDa. pUL148B produced a band of ~10kDa, corresponding to its *in silico* prediction, but pUL148A produced a higher mass of ~18kDa (Fig 4.1). Interestingly, pUL148A is predicted to contain a SUMO modification site of high probability, which may account for this ~10kDa increase in mass. However, similar to pUL140, pUL148A was not observed to co-immunoprecipitate with an α-SUMO antibody (data not shown). At 70.1kDa, UL150 is predicted to encode the largest protein of the UL/*b'* ORFs. pUL150 was detected at an actual mass of slightly larger (75kDa) that may be the result of extensive O-glycosylation predicted for this protein (Table 3.2). In addition, UL150 is predicted to contain a high probability SUMO modification site, although the increase in mass observed is not in agreement with the 11kDa size of SUMO, and similar to pUL140 and pUL148A, pUL150 was not observed to co-immunoprecipitate with an α-SUMO antibody (data not shown). It is important to note here that immunoprecipitation using the SUMO antibody can be very difficult, and optimisation of this immunoprecipitation will be necessary before forming a definitive conclusion concerning SUMO modification.

Not all of the UL/*b'* RAd constructs were available for western blot analyses. UL128 and UL131A Ad recombinants could not be generated using the AdEasy system. Whilst they have recently been generated using the AdZ system, they were not available for this study.

4.2 DETECTING EXPRESSION OF UL/*b'* ORFS BY FACS

In flow cytometry (FACS) experiments, an antibody-independent assay based on a StrepTactin-PE conjugate was used to detect the expression of Strep-tagged proteins. StrepTactin is an engineered version of the streptavidin protein that binds to the Streptag with 100x higher affinity than streptavidin. Conjugation of StrepTactin with PE makes it a very simple and efficient detection system for Strep-tagged protein by FACS and immunofluorescence. HFFF-hCAR were infected with RAds encoding the UL/*b'* ORFs for 72 hrs. Cells were then fixed and permeabilized before being incubated with the StrepTactin-PE conjugate. Expression of only 9/22 UL/*b'* proteins (pUL133, pUL135, pUL136, pUL140, pUL141, pUL148A, pUL148B, pUL148D and pUL14) was clearly apparent by FACS analysis (Fig 4.2). The expression of the UL/*b'* ORFs detected by FACS did not correspond to those detected by western blotting. For example, pUL145 is detected readily by the Streptag antibody in western blot, but was not detected by FACS with StrepTactin-PE. The proteins pUL147, pUL148D and pUL14 were detected readily by western blot, but only marginally detected using StrepTactin-PE. This may be due to the intracellular localisation of these proteins. For example, detection of the protein may be reduced if it is present in a vesicular structure. In contrast, pUL133 was detected by flow cytometry with StrepTactin-PE, but is not seen by Streptag antibody detection in western blotting. Again, this may be due to the nature of the protein, and indicates that the pUL133 may be partially re-folding during SDSPAGE to render the Streptag epitope inaccessible to the Streptag antibody.

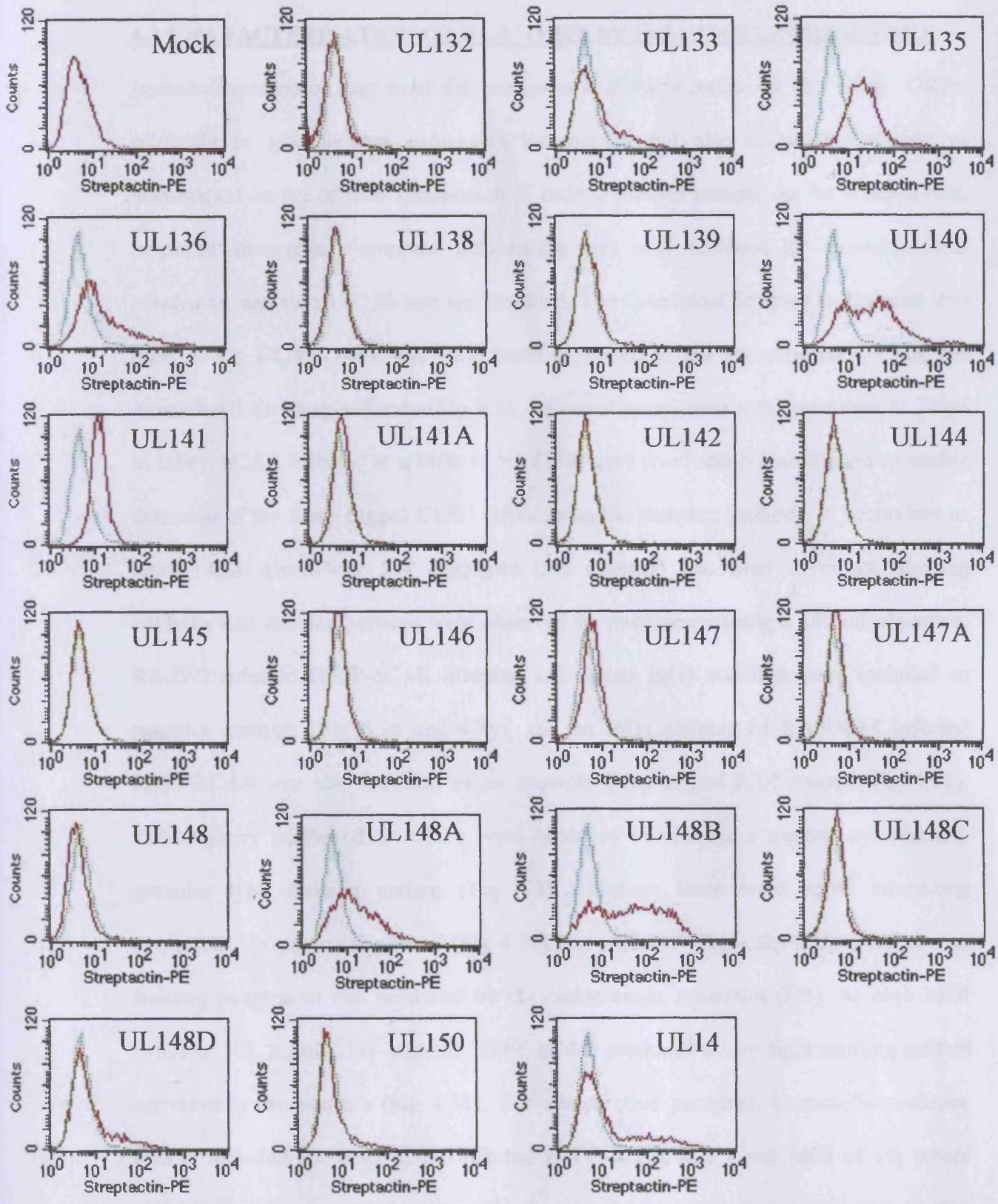

Figure 4.2 Intracellular detection of Strep-tagged UL/*b*' ORFs by flow cytometry
HFFF-hCAR were infected with UL/*b*' RAd at a MOI of 10. Infected cells were fixed at 72hpi and permeabilized to enable intracellular detection of the UL/*b*' proteins using StrepTactin-PE (1/100). StrepTactin-PE bound to Strep-tagged UL/*b*' ORFs was detected using flow cytometry (red line). RAd592 infected HFFF-hCAR was included as a negative staining control (dashed line).

4.3 CHARACTERISATION OF UL/*b'* ORFS BY IMMUNOFLUORESCENCE

Immunofluorescence was used for preliminary characterisation of the UL/*b'* ORFs, primarily to gain general expression information but also to provide qualitative information on the cellular localisation of each expressed protein. As for western blot, immunofluorescence expression information was only obtained for available RAd constructs, and thus UL128 was not included. The C-terminal Streptag engineered into each of the UL/*b'* ORFs was once more exploited to test for expression using the monoclonal Streptag antibody (Fig 4.3). Immunofluorescence was performed at 72hpi in HFFF-hCAR infected at a MOI of 50. Cells were fixed and permeabilized to enable detection of the Strep-tagged UL/*b'* ORFs using the Streptag antibody. A secondary α-mouse IgG AlexaFluor 594 conjugate (red channel) was used to detect Streptag antibody and staining patterns were observed by microscope using a x40 oil objective. RAd592 infected HFFF-hCAR Streptag and mouse IgG1 stainings were included as negative controls (Fig 4.3x and 4.3y), and an IgG1 staining of RAdUL14 infected HFFF-hCAR was also included as an example Strep-tagged RAd control (Fig 4.3y). The majority of the UL/*b'* ORFs were observed to produce a general cytoplasmic, granular type staining pattern (Fig 4.3), although there were some interesting exceptions. In particular pUL14 (Fig 4.3v) and pUL141 (Fig 4.3h) show very similar staining patterns to that produced by the endoplasmic reticulum (ER). At high MOI (MOI of 50), RAdUL141 infected HFFF-hCAR produced a very tight staining pattern surrounding the nucleus (Fig 4.3h). For comparative purposes, immunofluorescence data is included for RAdUL141 infected HFFF-hCAR at a lower MOI of 10, where pUL141 shows a more diffuse cytoplasmic-type staining pattern similar to pUL14 (Fig 4.3h). The localisation of pUL14 and pUL141 is investigated in further detail in Chapter 6, Figures 6.2 and 6.3.

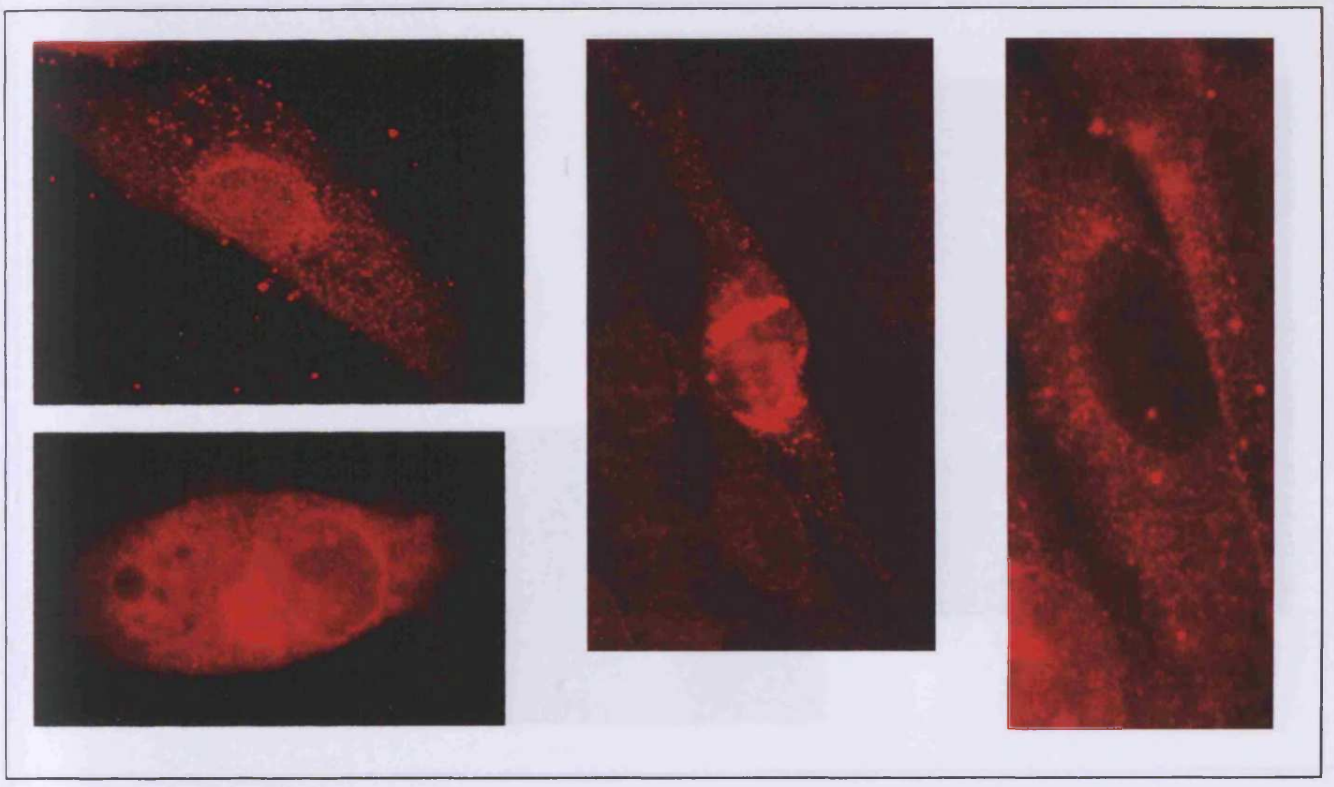

Fig 4.3a Immunofluorescence – RAdUL132

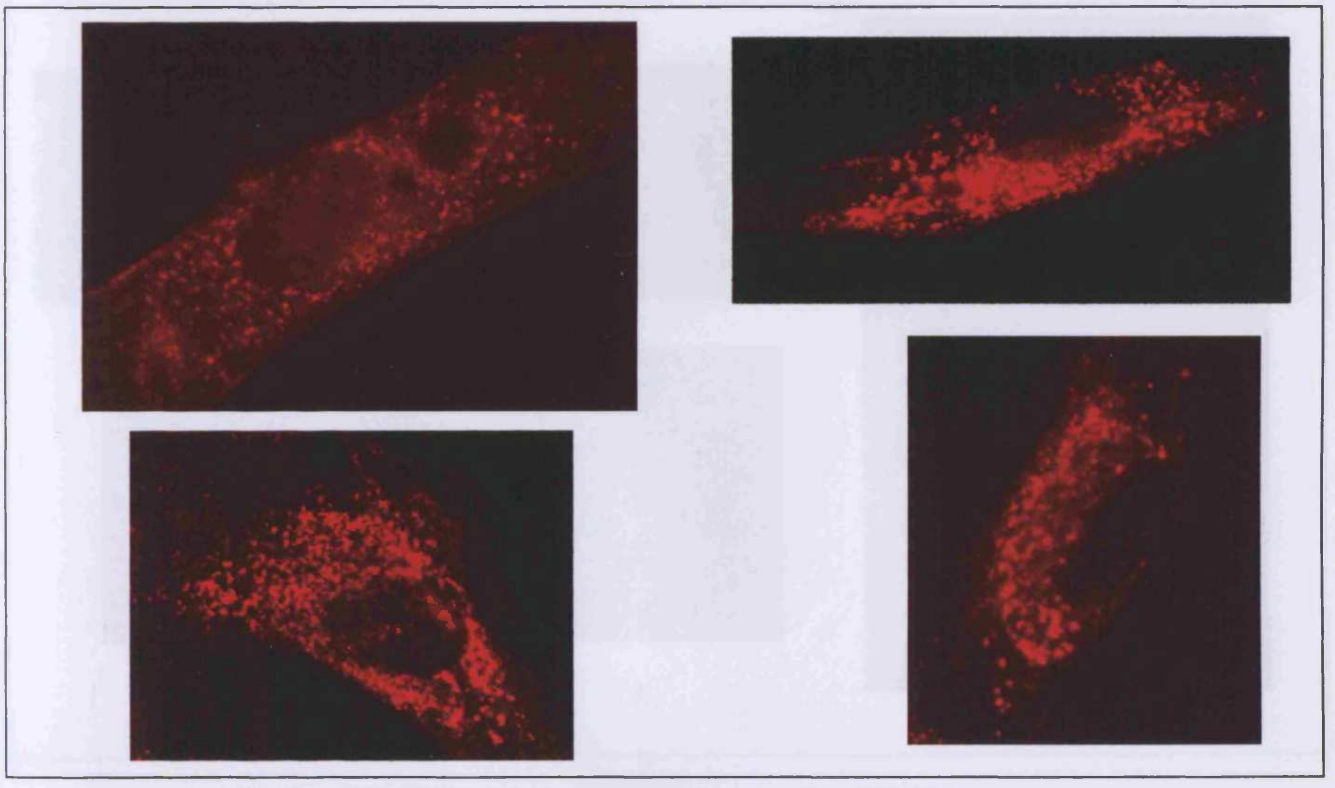

Fig 4.3b Immunofluorescence – RAdUL133.

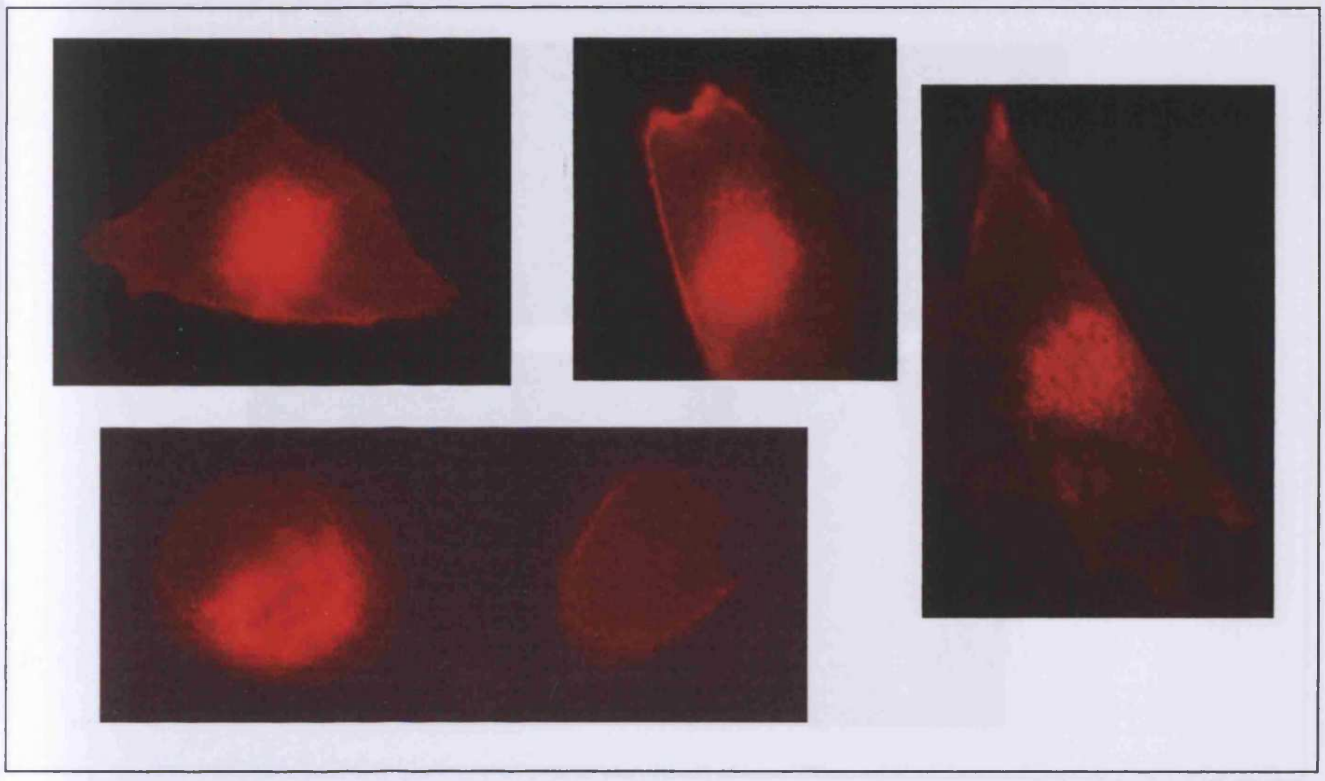

Figure 4.3c Immunofluorescence RAdUL135

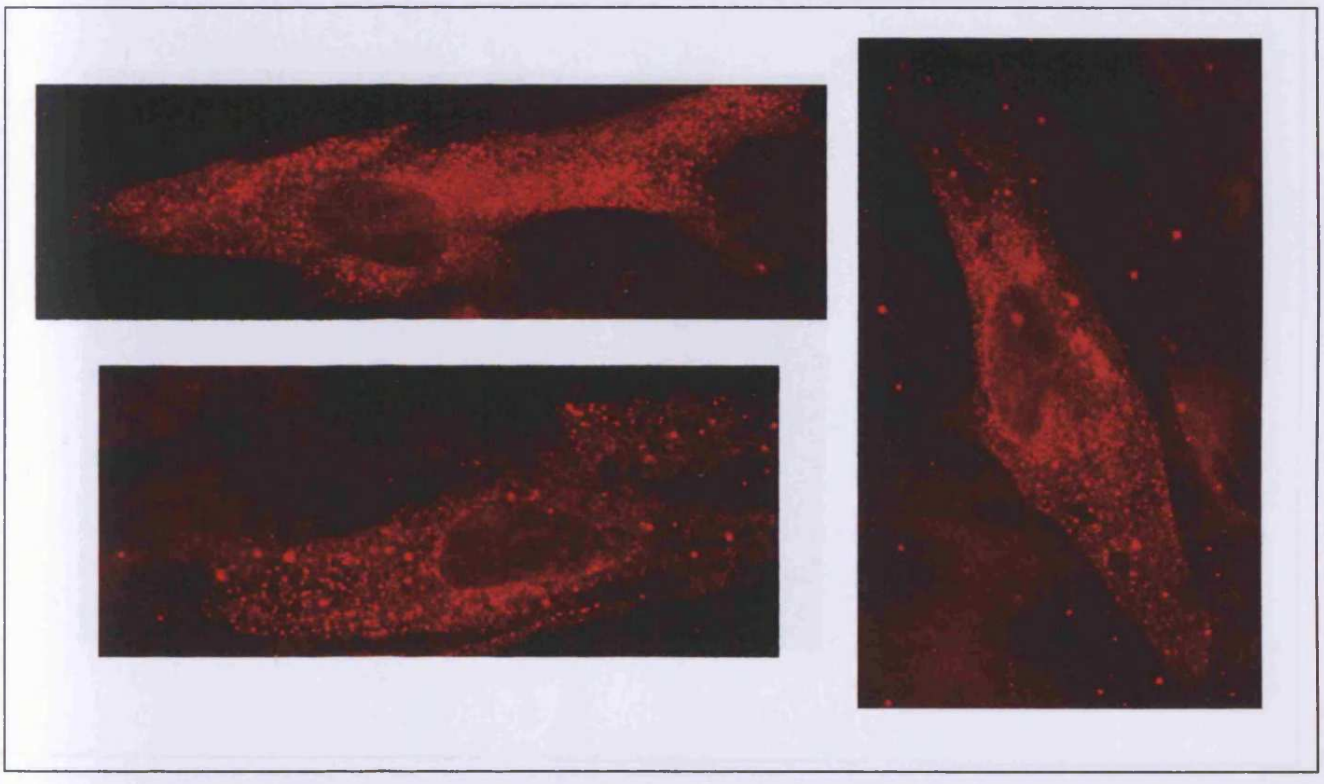

Figure 4.3d Immunofluorescence RAdUL136

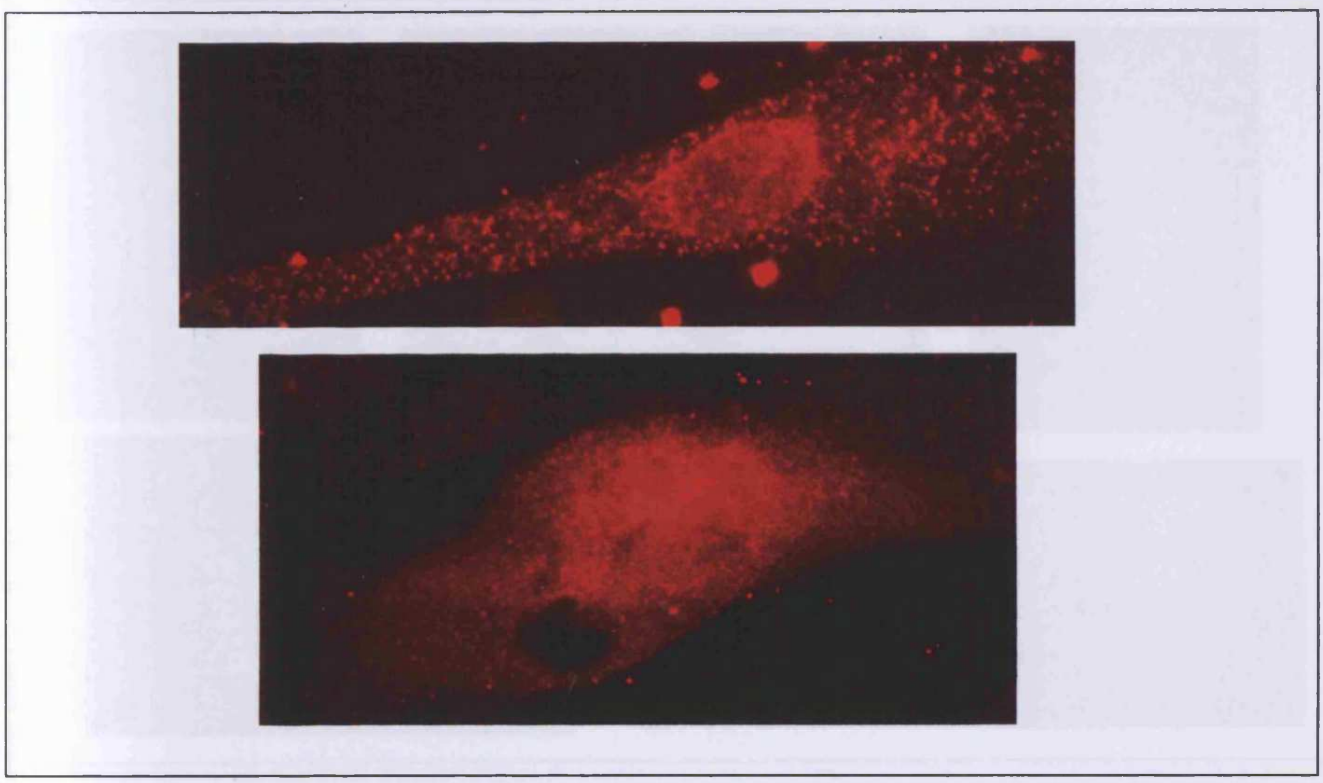

Figure 4.3e Immunofluorescence RAdUL138

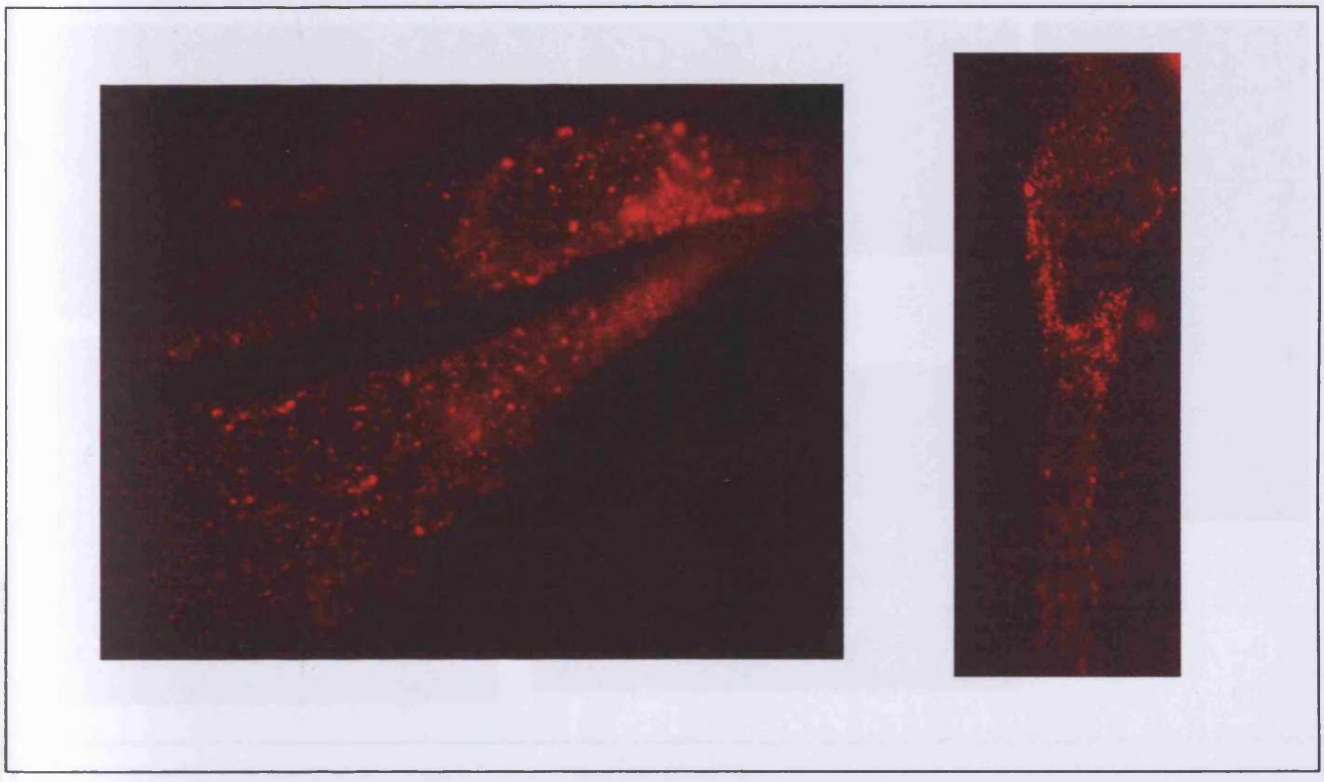

Figure 4.3f Immunofluorescence RAdUL139

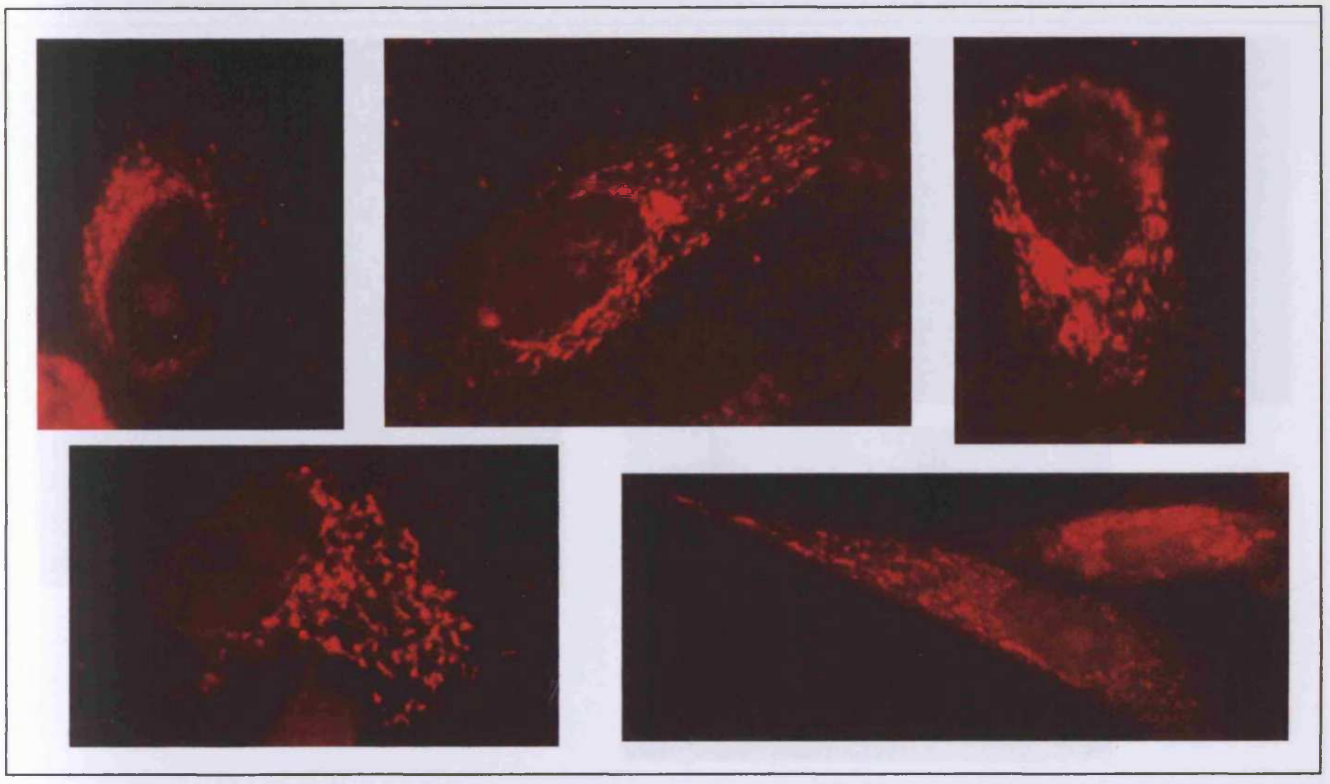

Figure 4.3g Immunofluorescence RAdUL140

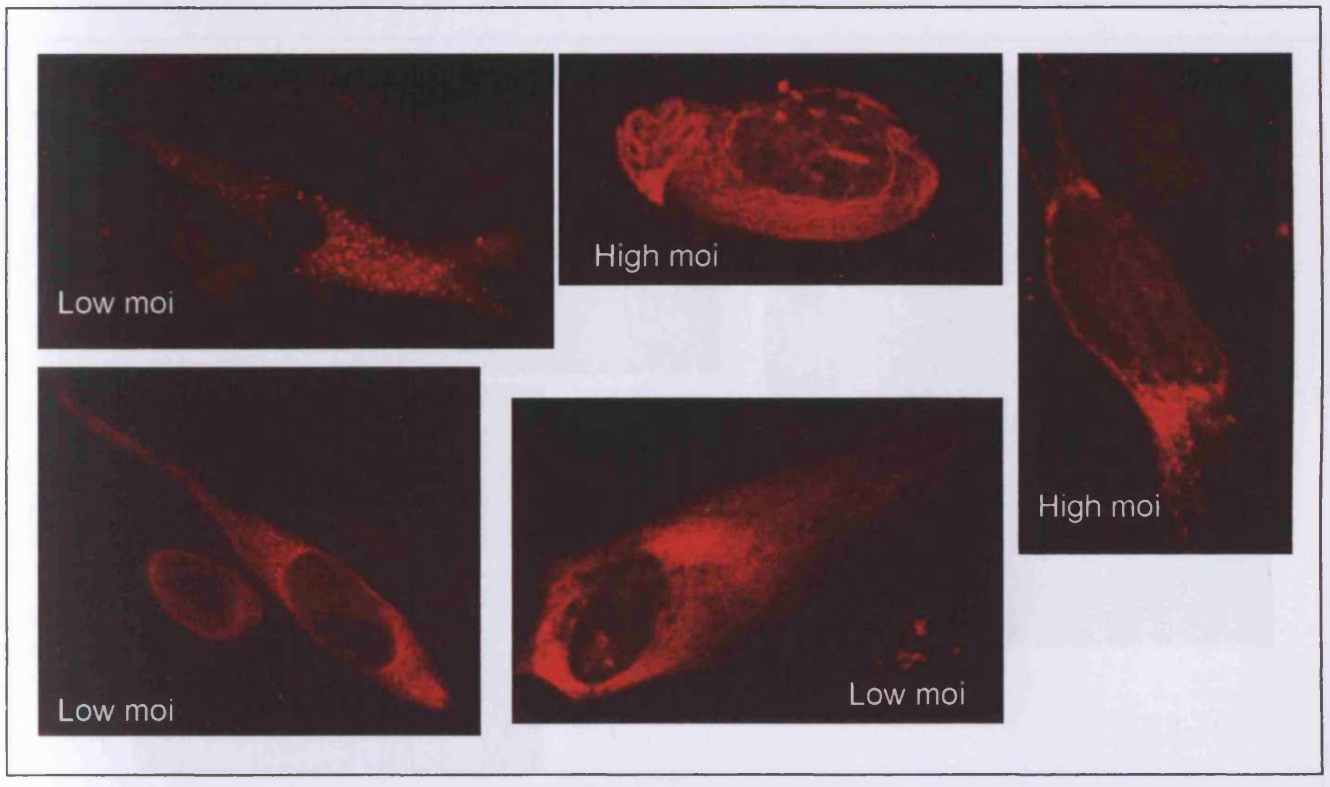

Figure 4.3h Immunofluorescence RAdUL141

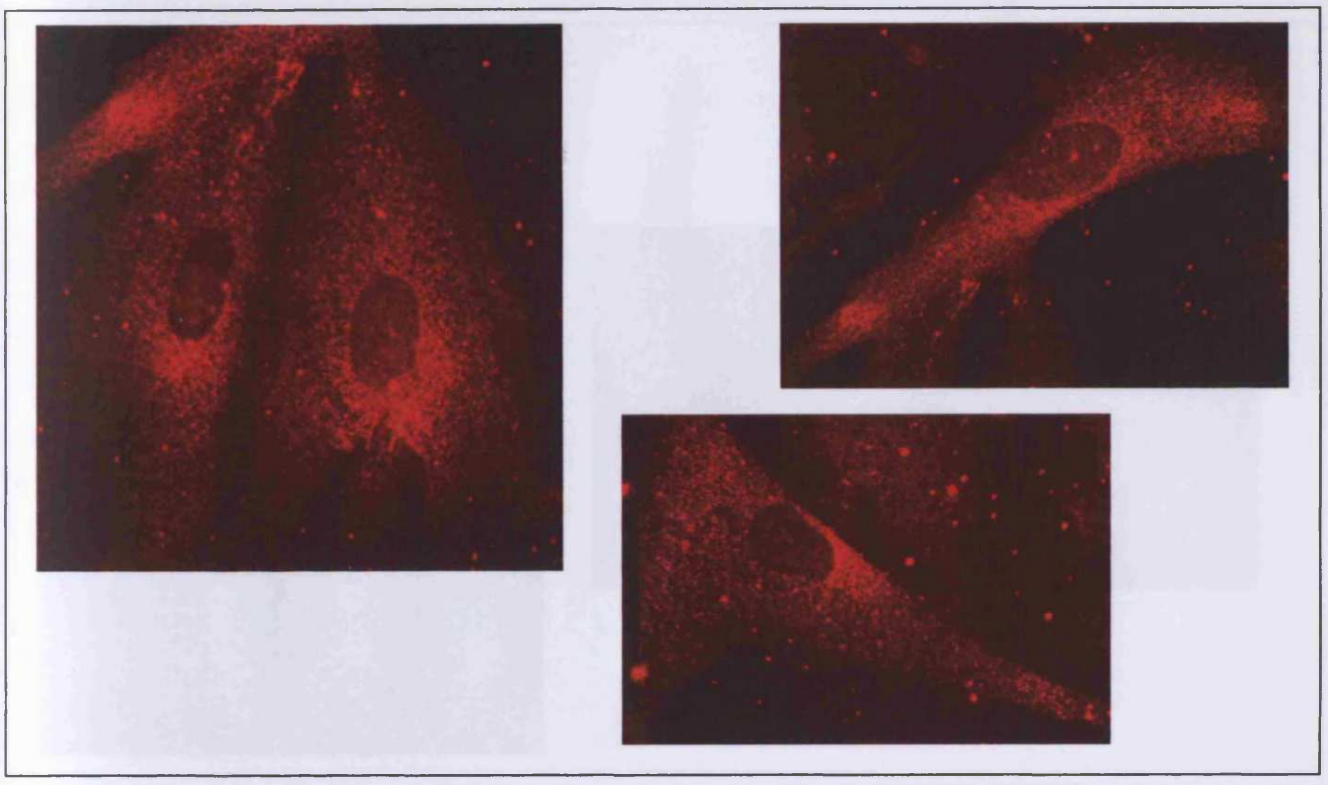

Figure 4.3i Immunofluorescence RAdUL141A

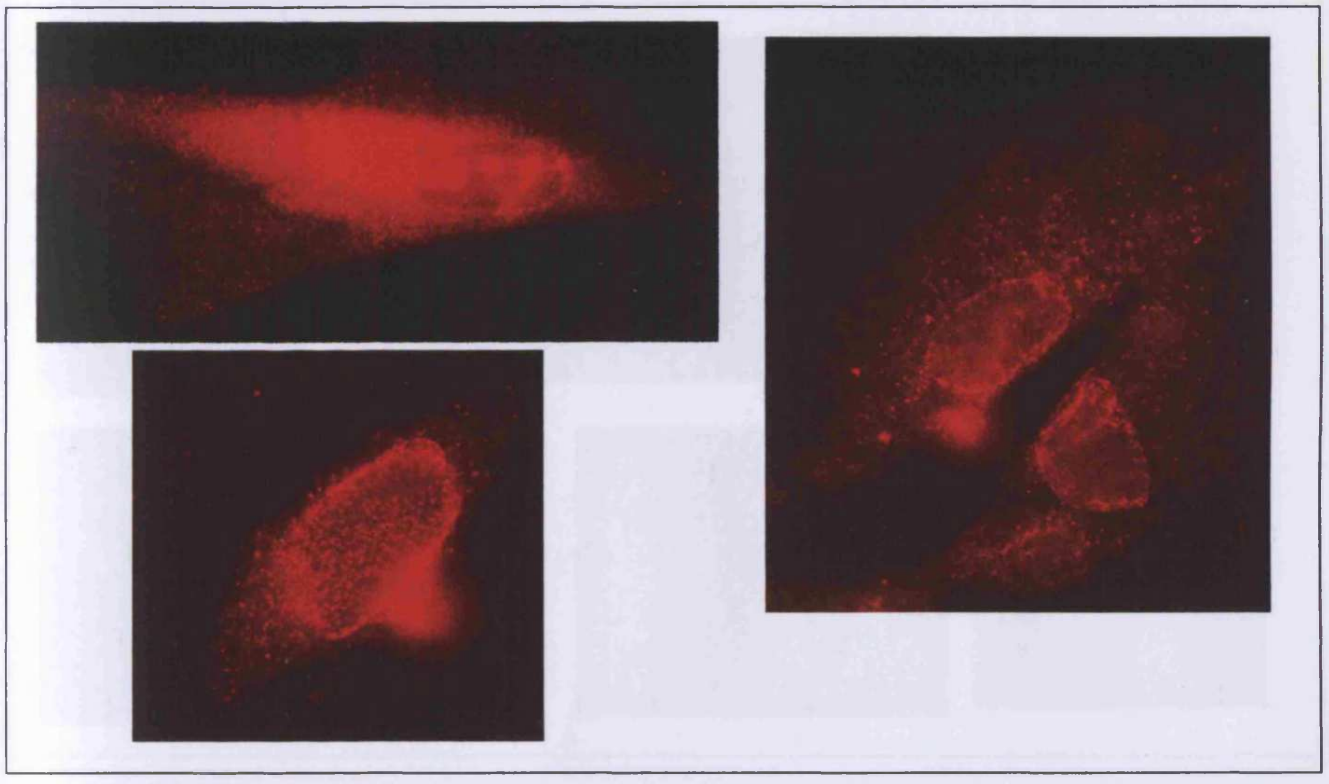

Figure 4.3j Immunofluorescence RAdUL142

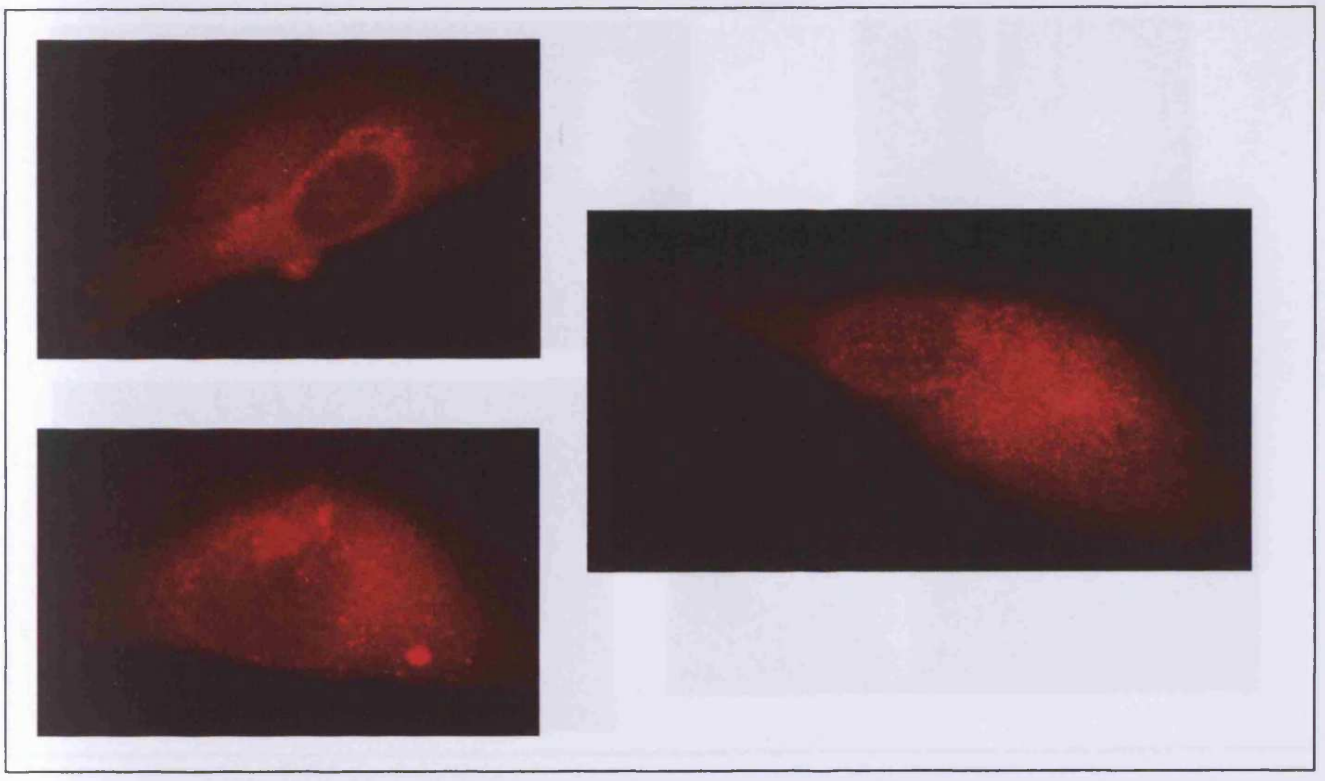

Figure 4.3k Immunofluorescence RAdUL144

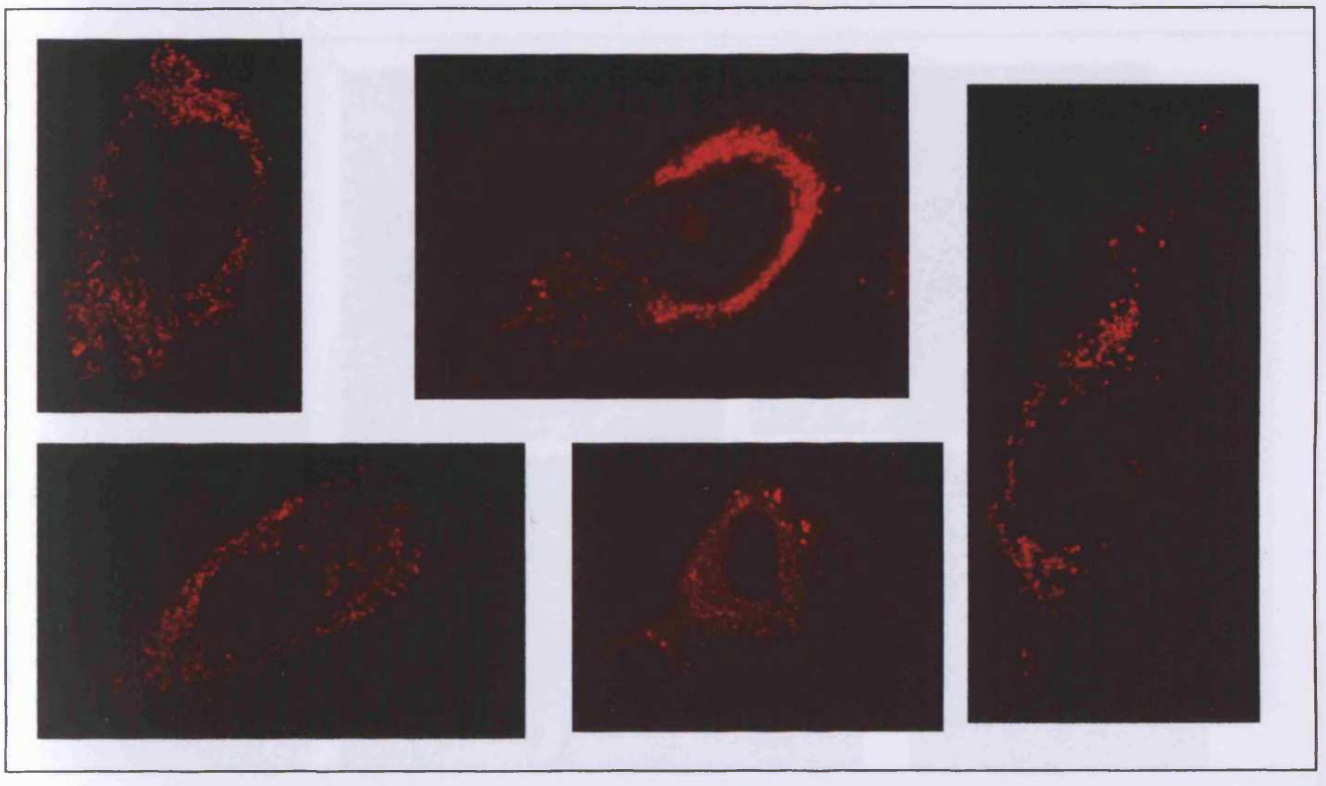

Figure 4.3l Immunofluorescence RAdUL145

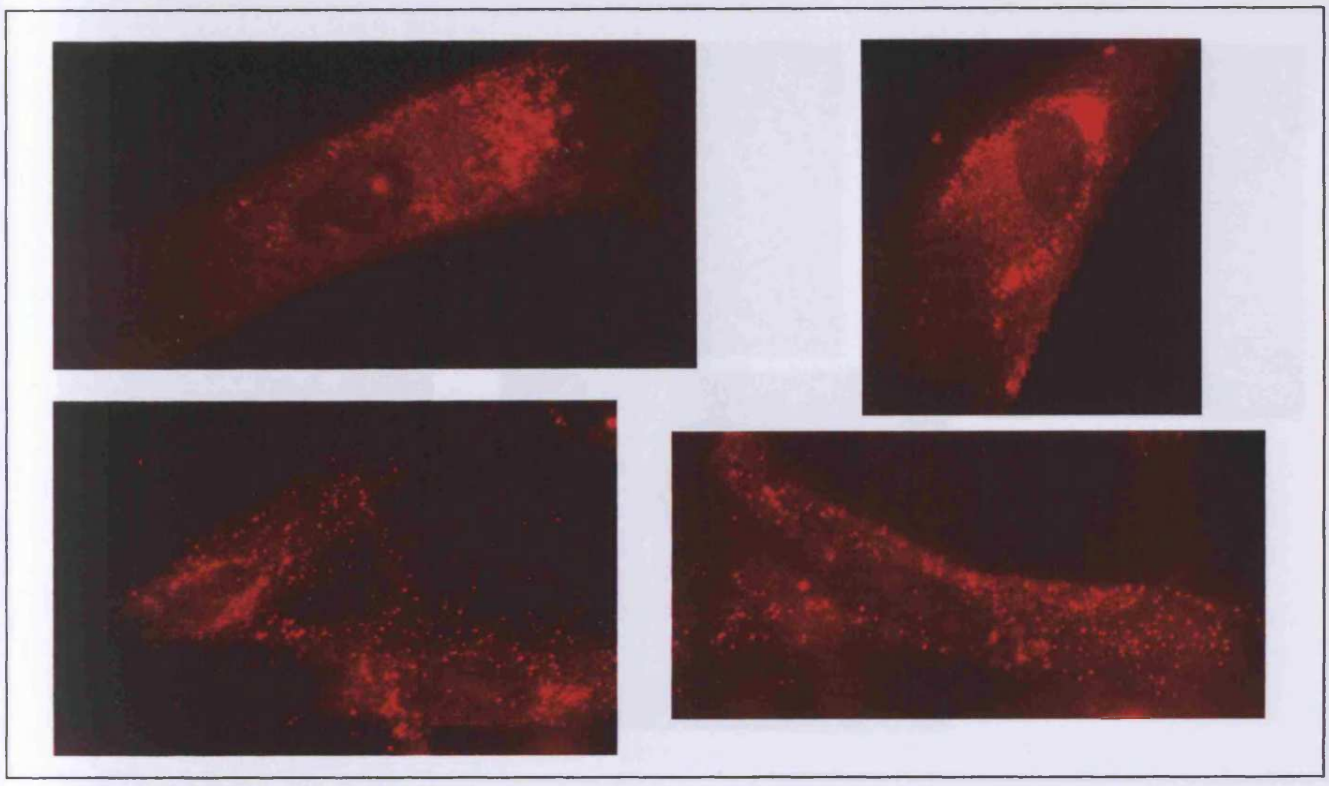

Figure 4.3m Immunofluorescence RAdUL146

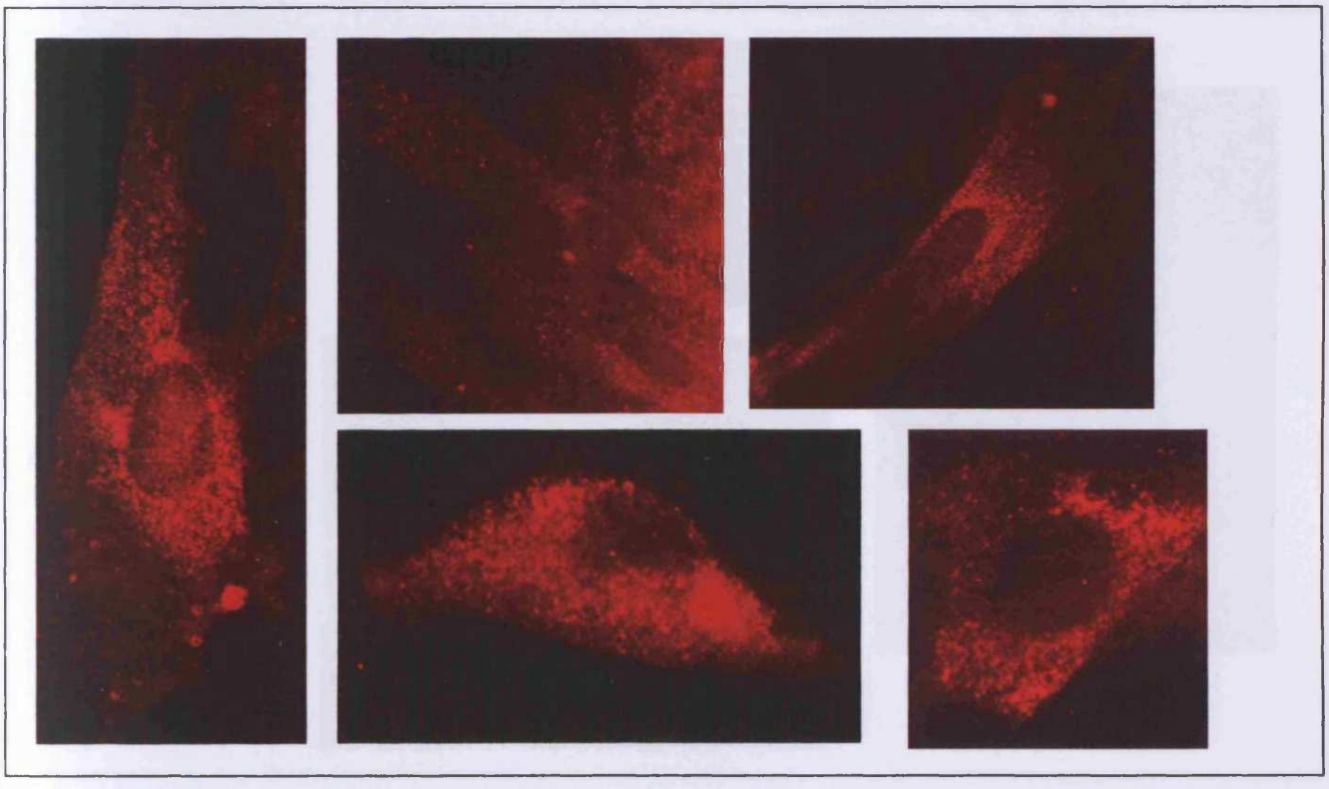

Figure 4.3n Immunofluorescence RAdUL147

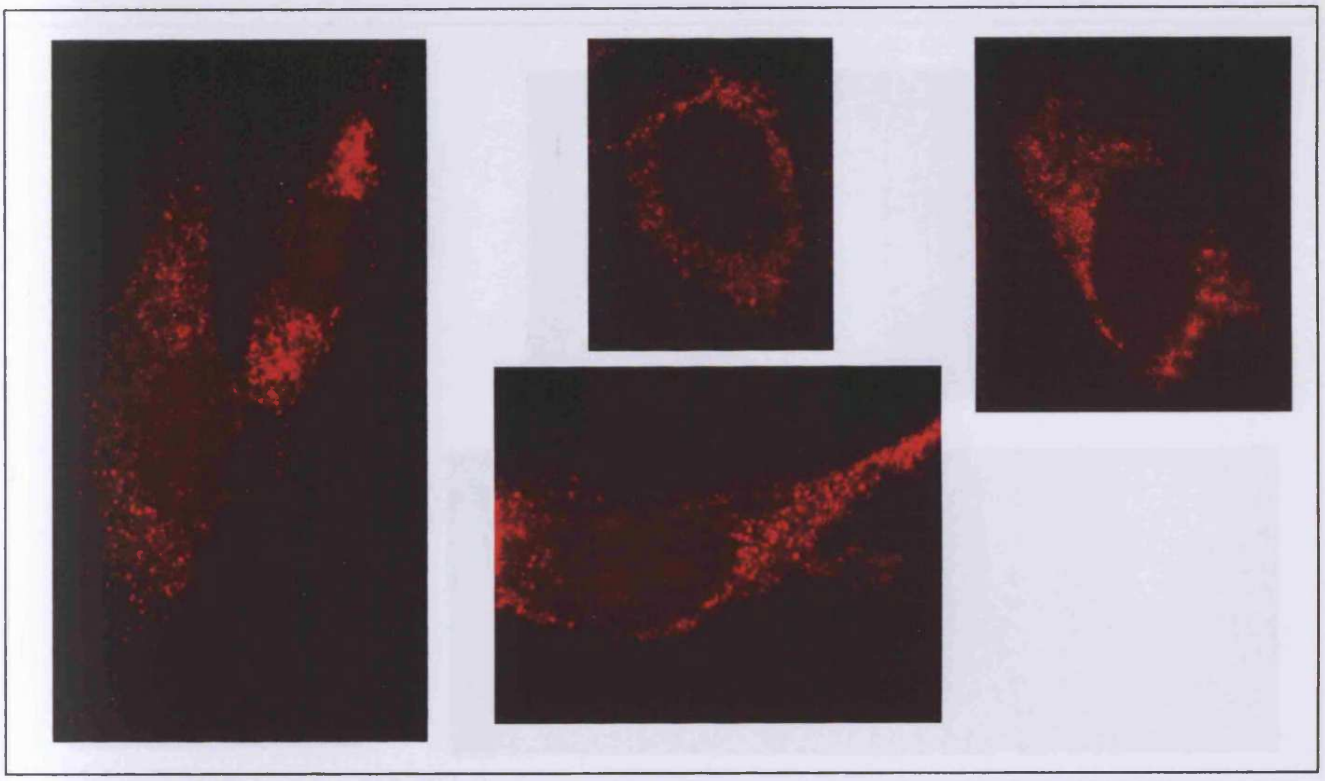

Figure 4.3o Immunofluorescence RAdUL147A

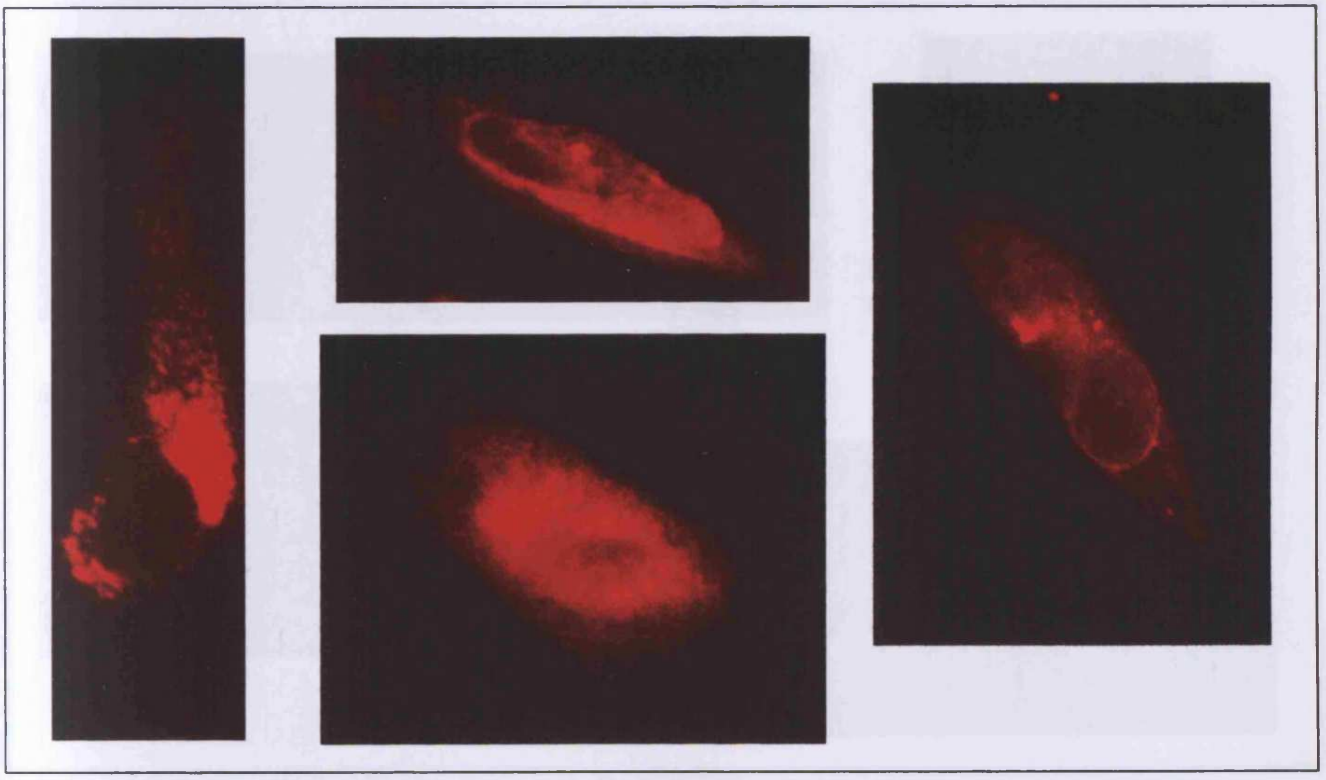

Figure 4.3p Immunofluorescence RAdUL148

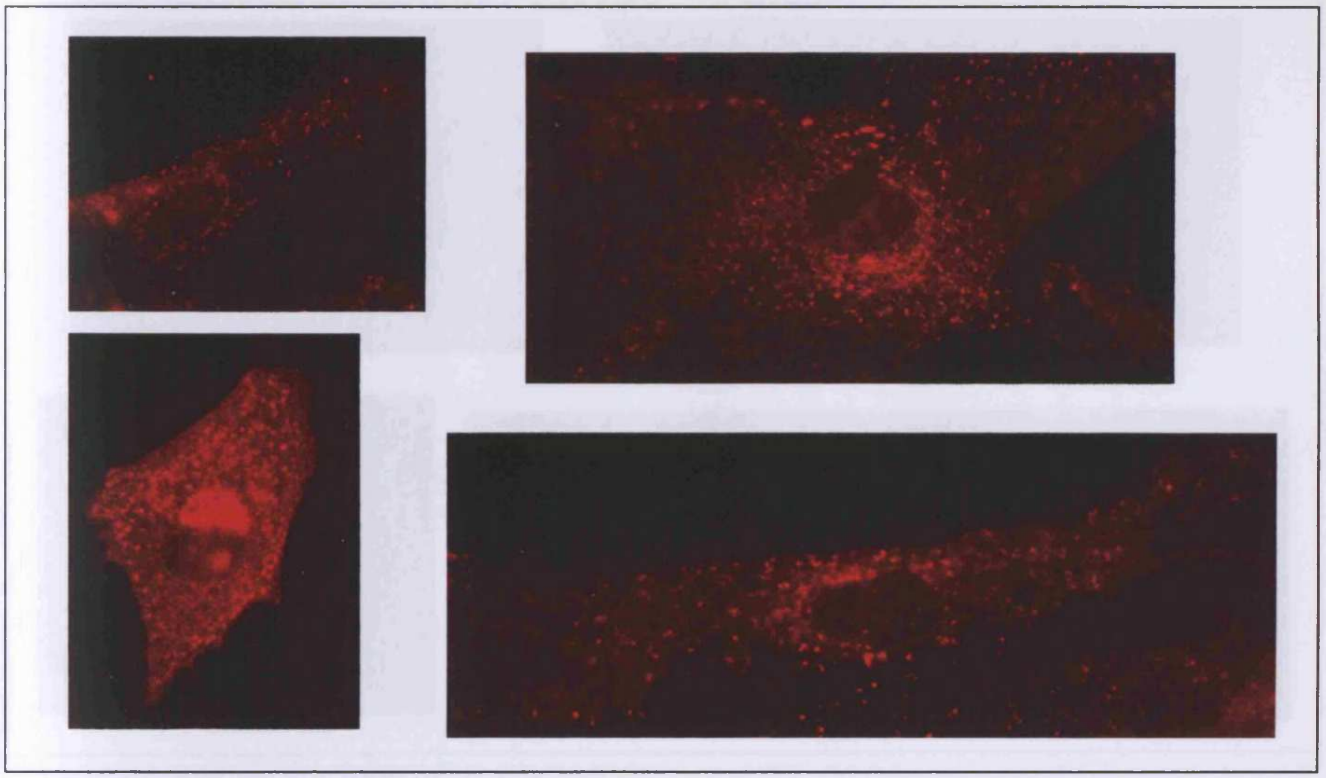

Figure 4.3q Immunofluorescence RAdUL148A

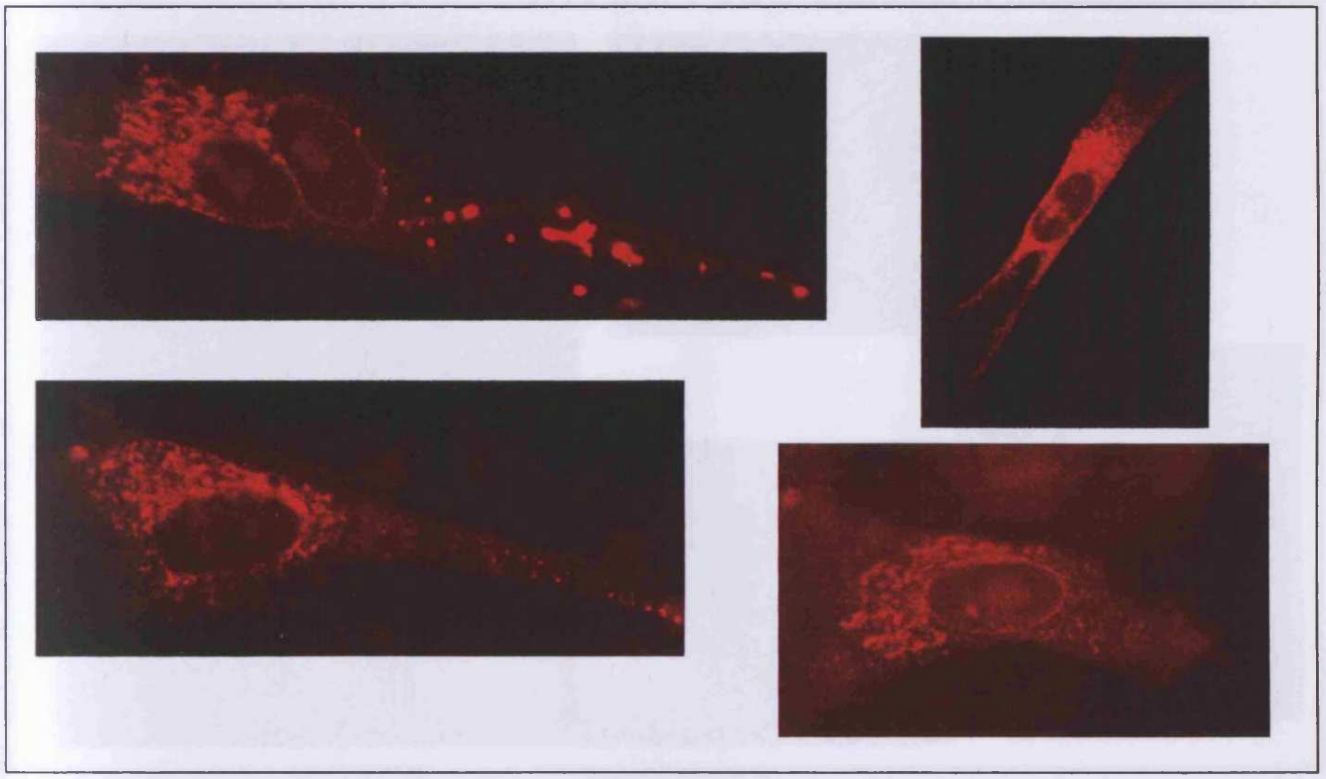

Figure 4.3r Immunofluorescence RAdUL148B

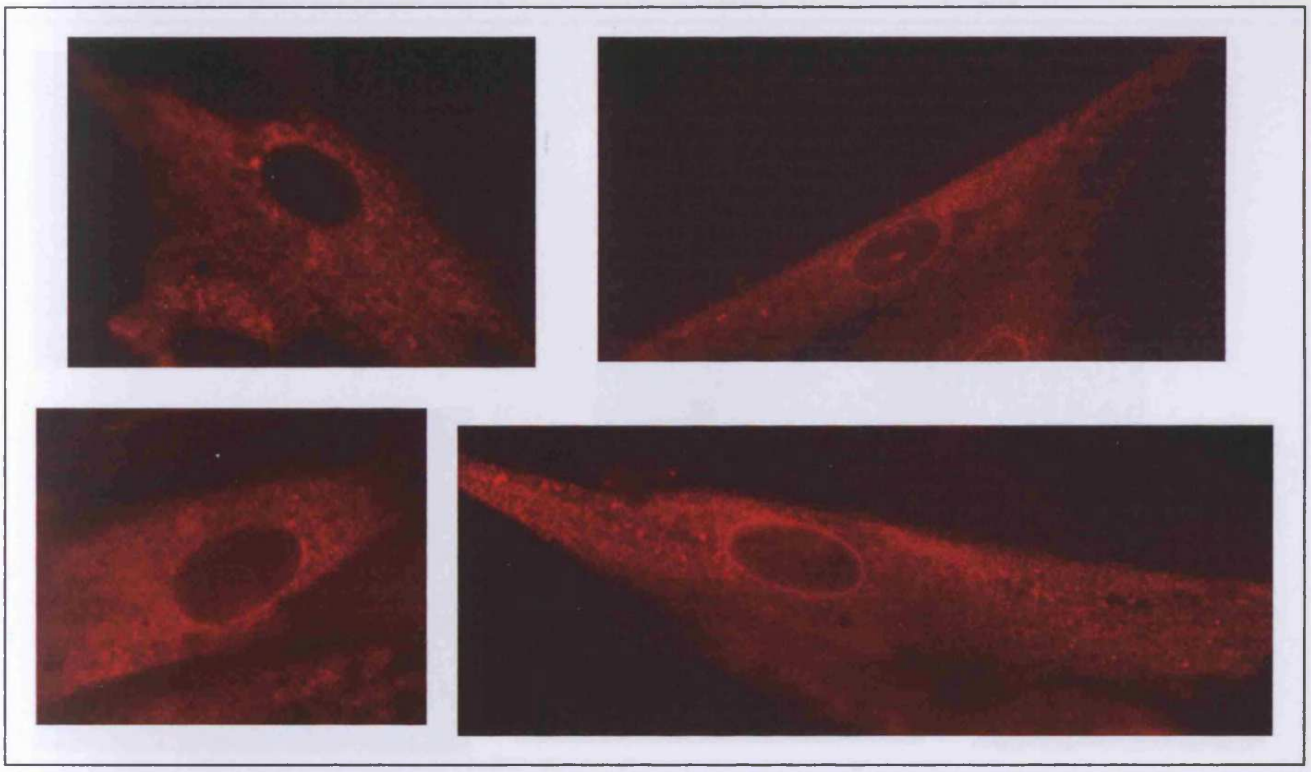

Figure 4.3s Immunofluorescence RAdUL148C

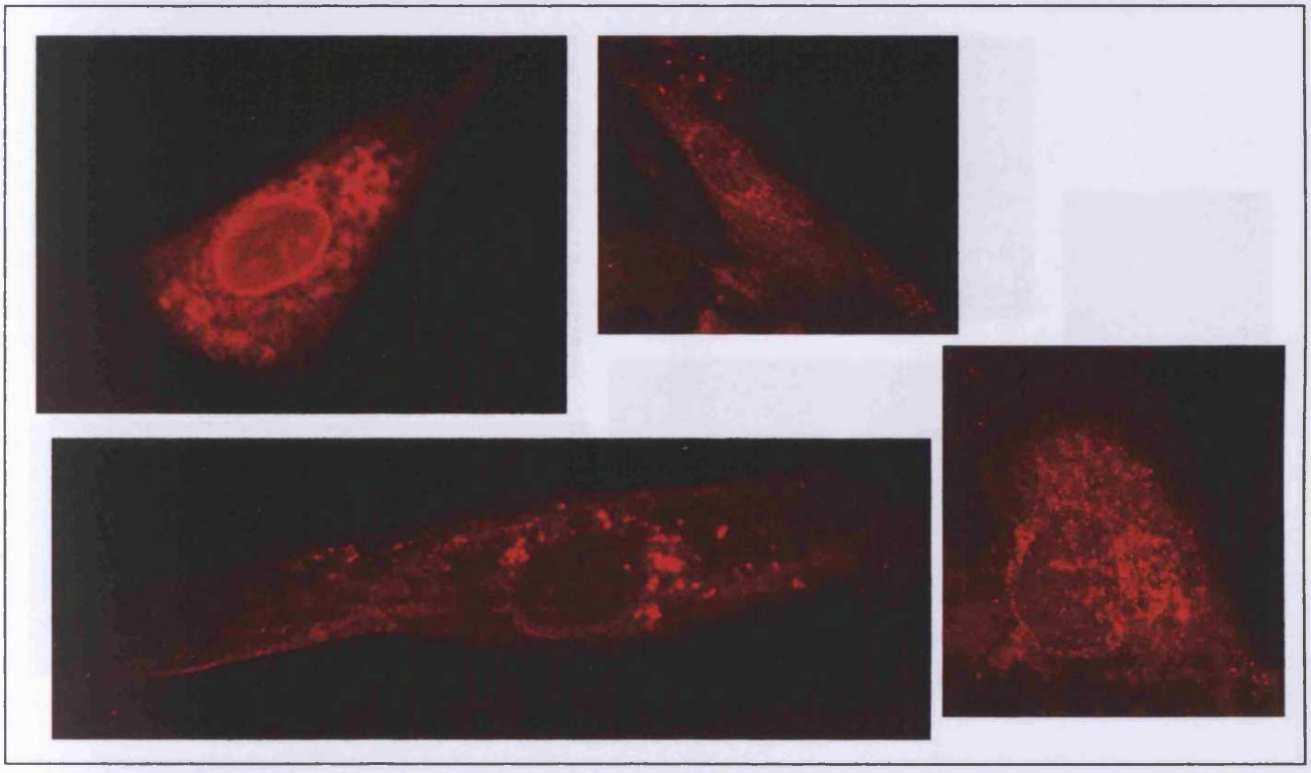

Figure 4.3t Immunofluorescence RAdUL148D

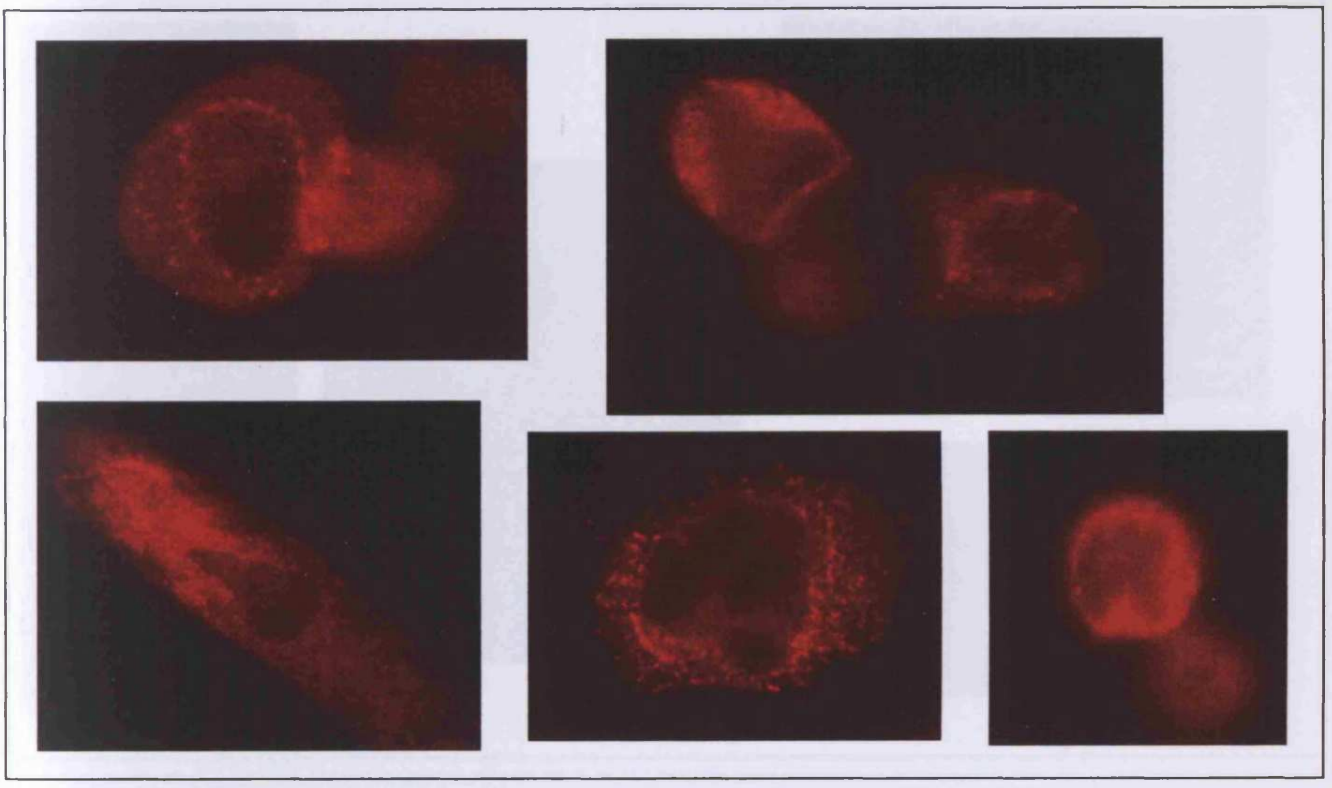

Figure 4.3u Immunofluorescence RAdUL150

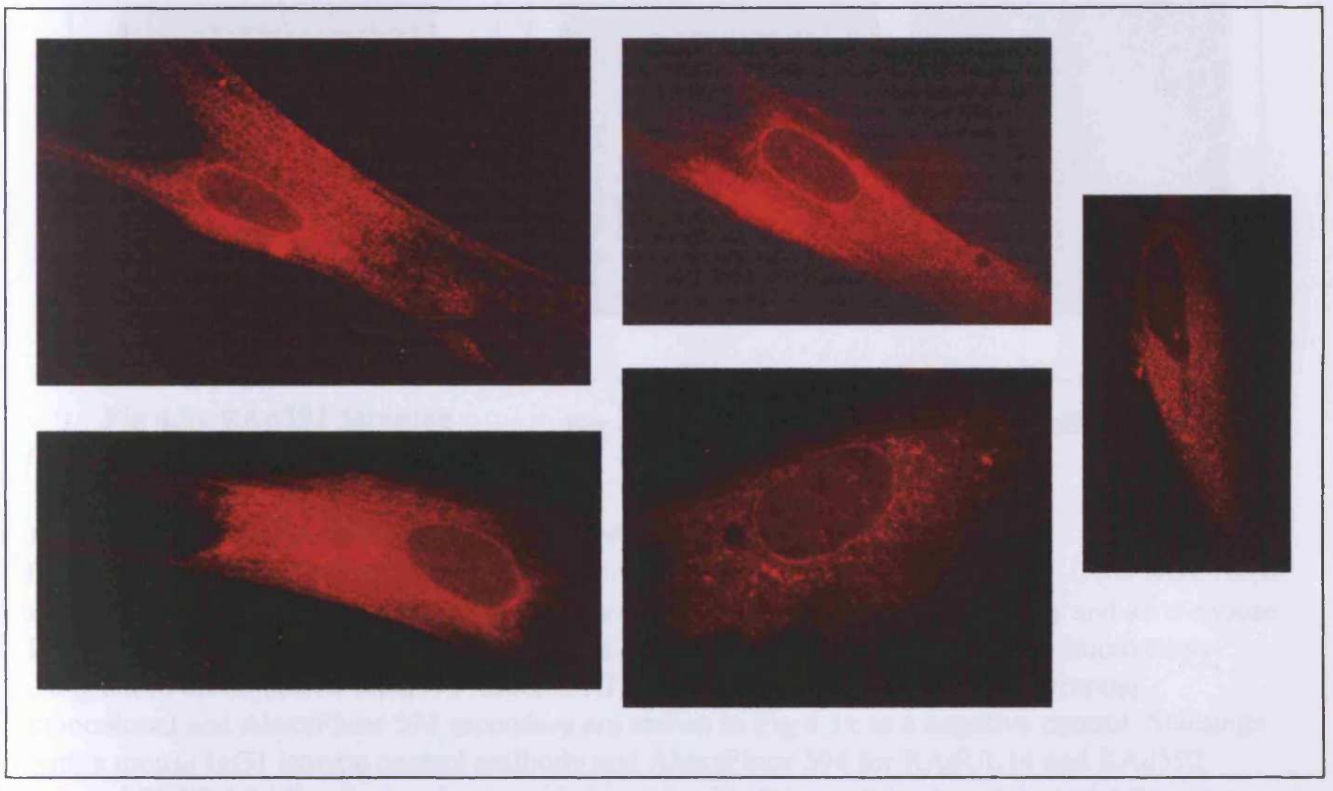

Figure 4.3v Immunofluorescence RAdUL14

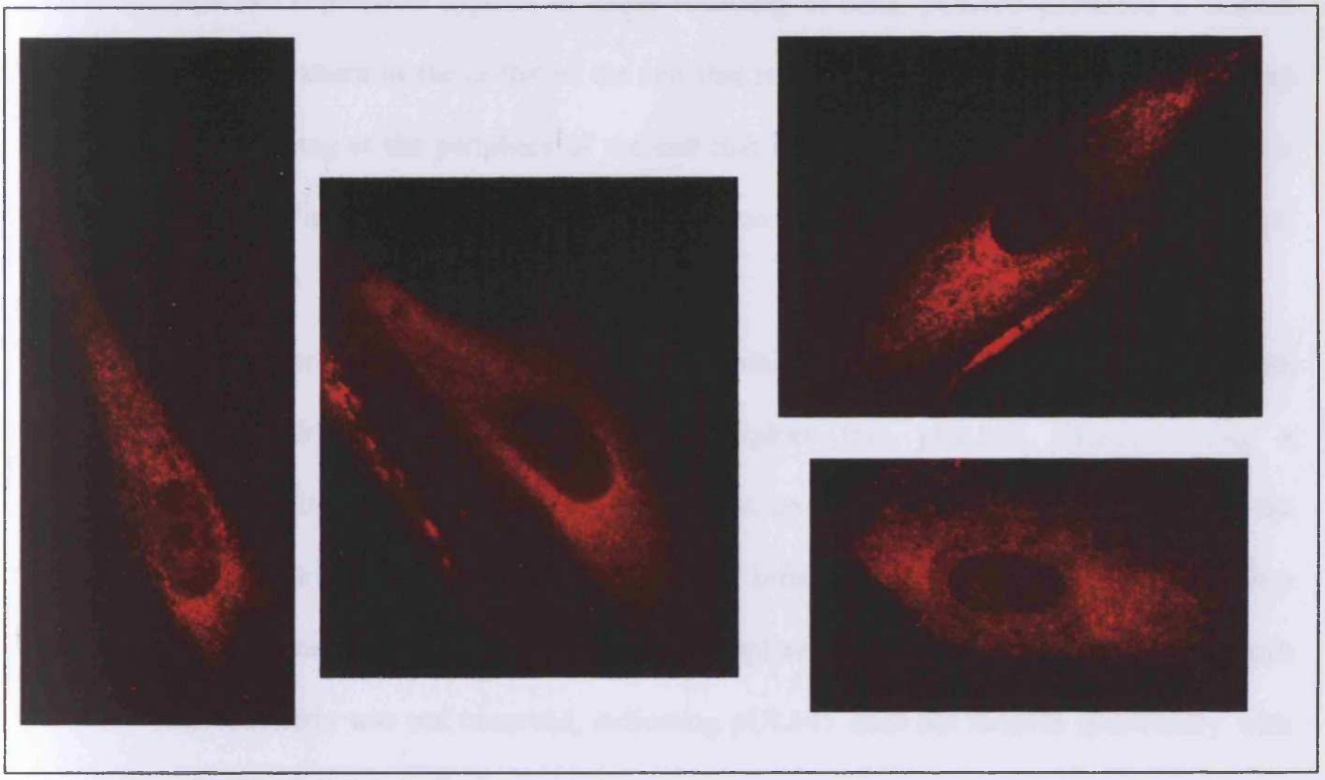

Fig 4.3w Immunofluorescence RAdUL131A

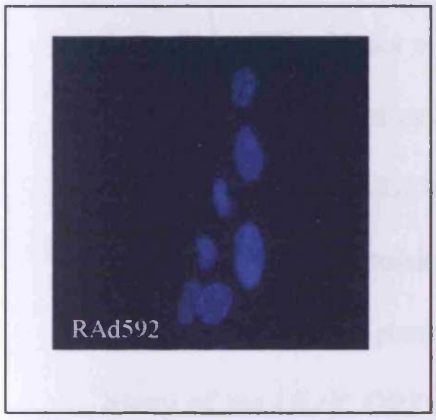

Fig 4.3x RAd592 Streptag immunofluorescence

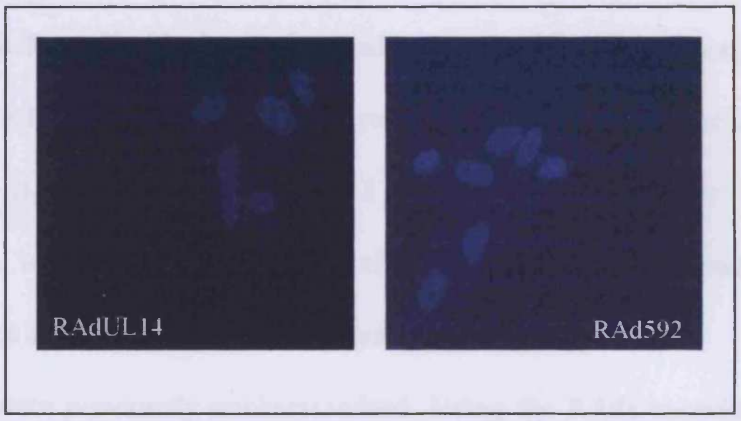

Fig 4.3y IgG isotype control immunofluorescence

Figure 4.3 Immunofluorescence detection of the UL/*b*' ORFs
HFFF-hCAR were infected with RAds encoding the UL/*b*' ORFs at a MOI of 50. Cells were fixed and permeabilized at 72hpi and UL/*b*' ORFs detected using the Streptag antibody and an α-mouse IgG AlexaFluor 594 secondary antibody. Immunofluorescence was visualised by microscopy using a x40 oil objective. RAd592 infected HFFF-hCAR cells stained with the Streptag monoclonal and AlexaFluor 594 secondary are shown in Fig 4.3x as a negative control. Stainings with a mouse IgG1 isotype control antibody and AlexaFluor 594 for RAdUL14 and RAd592 infected HFFF-hCAR cells are also provided in 4.3y. Nuclei are stained in 4.3x and 4.3y using Hoestch. (Figs 4.3x and 4.3y were provided by Dr V. Prod'Homme).

pUL135 expression appears to cause rounding of cells. pUL135 produced a distinct staining pattern in the centre of the cell that is not nuclear (DAPI staining not shown) with staining at the periphery of the cell that indicates pUL135 may be a cell surface protein (Fig 4.3c). UL135 expression is also studied in further detail in Chapter 6, Figure 6.7.

pUL145 produced an interesting punctate staining pattern, similar to that seen with mitochondrial staining (Fig 4.3l). To explore this, pUL145, detected using a Streptavidin-Alexa Fluor 594 conjugate, was co-stained with an antibody against the mitochondrial protein, Bcl-2, in RAdUL145 infected fibroblasts (Fig 4.4). Although a similar staining pattern was seen, complete co-localisation of pUL145 with mitochondria was not observed, indicating pUL145 does not localise specifically with mitochondria.

pUL150 exhibited a granular type staining pattern throughout the cell (Fig 4.3u). Infection of fibroblasts with RAdUL150 also had a tendency to round cells, although not to the same extent as RAdUL135. The immunofluorescence staining pattern for the FLAG-tagged RAdUL130 is included in Appendix I (kindly provided by Dr B. McSharry). Its expression was detected using an αFLAG monoclonal antibody, revealing pUL130 to produce a vesicular-type staining pattern.

Many of the UL/*b*' ORFs were previously uncharacterised. Using the RAds encoding each of the Strep-tagged UL/*b*' proteins, expression data has been gathered from flow cytometry, immunofluorescence and western blot to provide preliminary characterisation for the UL/*b*' ORFs. Many transcriptional and posttranscriptional processes contribute to dictating the efficiency of expression of any ORF, thus even when the same promoter, polyadenylation signal, vector and conditions are used, the efficiency of expression can be expected to vary. A number of ORFs exhibited overt cytotoxicity (e.g UL135 and UL150), and this could potentially also impact on

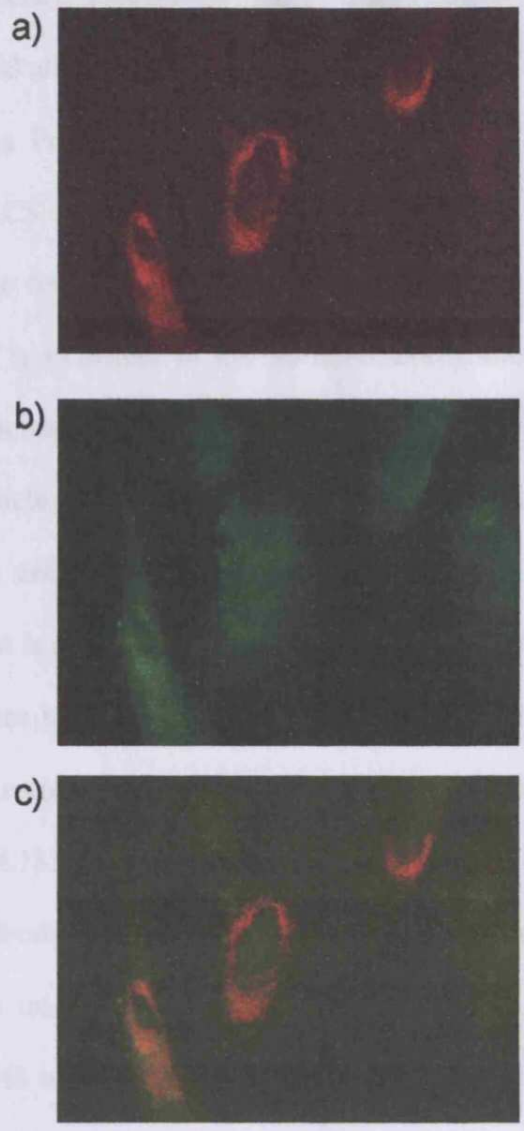

Figure 4.4 UL145 does not co-localise with the mitochondria Bcl-2 protein.
RAdUL145 infected HFFF-htert were fixed and permeabilised at 72hpi and stained with a) Streptavidin-Alexa Fluor 594 (1/100) to detect pUL145, and b) an α-Bcl-2 antibody (1/100) followed by an α-mouse IgG-FITC (1/1000) to detect the mitochondrial protein, Bcl-2. c) The Streptavidin-Alexa Fluor 594 and α-Bcl-2-FITC staining patterns were merged.

expression efficiency. Protein-folding, post-translational modification and intracellular localisation could all affect the capacity of the detection reagent to bind the Streptag in different systems. For example, a number of expressed ORFs that were not detected by intracellular FACS staining were detected by western blot and immunofluorescence. This may be the result of the location of a number of these proteins in intracellular vesicles, which is indicated in the immunofluorescence data. For example, pUL145 exhibited a punctate staining pattern that would be consistent with trafficking to a cytoplasmic vesicle or granule structure. Although pUL145 was detected by western blot, it was not detected by FACS staining. Conversely, pUL133 is not detected by western blot, but is seen by FACS staining and immunofluorescence. Protein-refolding following western blotting could potentially conceal/ hide the epitope tag in pUL133 from antibody recognition, whereas fixing pUL133 in its native state renders the Streptag of pUL133 accessible to detection by StrepTactin-PE and the Streptag II monoclonal antibody to yield FACS and immunofluorescence data. A number of other proteins remain undetected by western blot (pUL132, pUL139, pUL142, pUL144, pUL146, pUL148 and pUL148C), which may also be the result of protein-refolding during western blotting or of tag-removal during protein processing and modification. The nature of these proteins may also reflect on their expression levels. Other influences on expression detection may include protein secretion, as is predicted for the IL8 homologue, UL146, where if the majority of UL146 protein is secreted, a lower expression level is expected from the cell extract. UL147 on the other hand is readily detected by western blot, indicating that UL147 may not be secreted as for UL146, and that these two IL8 homologues may be functionally distinct.

The substantial number of genes studied in parallel limited the adoption of alternative strategies to optimise the detection of each ORF, e.g by using different epitope tags. As such, Streptag was chosen to study all these genes in parallel for these preliminary

experiments. The difference observed in the ability of these different techniques to detect expression from the UL/*b*' proteins illustrates the importance of using a variety of different methods in order to characterise these proteins.

4.4 ADDITIONAL CHARACTERISATION OF UL/*b*' EXPRESSION

4.4.1 Polyclonal antibody production

A device that has previously proved effective for the generation of polyclonal antibodies for expressed transgenes has been to directly immunise animals with an Ad recombinant (Tomasec *et al.*, 2000; Wilkinson *et al.*, 1998). Using this approach, specific polyclonal antibodies were sought against pUL135, pUL144, pUL146, pUL147 and pUL14 by inoculating three mice with 10^9pfu of each corresponding RAd (performed by Dr. C. Rickards). The mouse produces polyclonal antibodies against the gene encoded by the RAd. At 5-6 weeks pi, serum was taken from these mice and tested for the detection of each gene by immunofluorescence, western blot and flow cytometry. None of the polyclonal antibodies produced were successful in the detection of the UL/*b*' proteins by flow cytometry or immunofluorescence, only varying degrees of background staining comparable with control cells. However, the UL135-specific polyclonal antibody was successful in detecting pUL135 expression by western (Fig 4.5). RAdUL135 infected HFFF-hCAR cell extracts were separated by SDSPAGE and pUL135 detected by western blot using UL135 polyclonal serum (Fig 4.5). Blots were stripped and pUL135 reprobed using the Streptag antibody (Fig 4.5). Both the polyclonal and Streptag antibody detected specific UL135 bands of approximately 35kDa and 25kDa. In contrast to Figure 4.1, both antibodies detected the major UL135 band at its predicted ~35kDa mass, with the 25kDa band a lower intensity, indicating this lower band is likely to be a breakdown product (Fig 4.5). Polyclonal serum for the

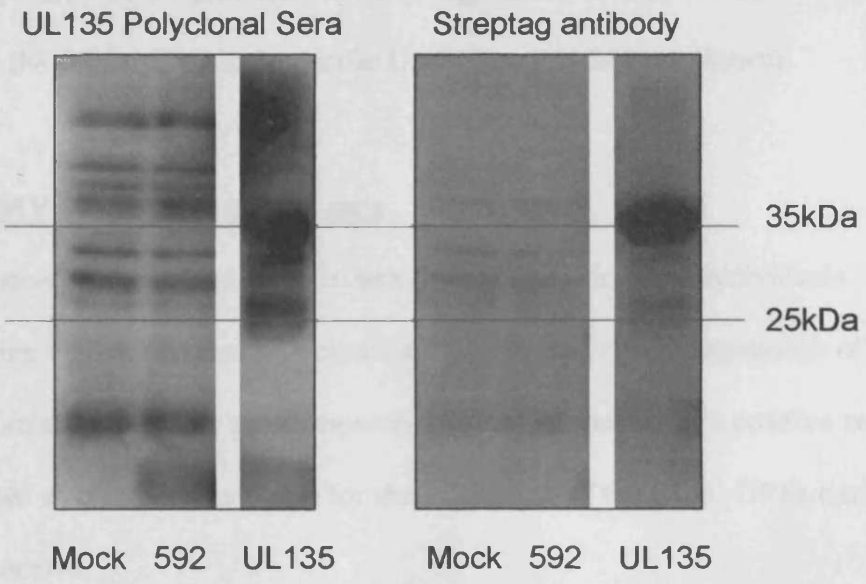

Figure 4.5 Detection of pUL135 with a UL135 polyclonal antibody
HFFF-hCAR were infected with RAdUL135 at a MOI of 10. Cell extracts were prepared at 72hpi, and proteins separated by SDSPAGE. pUL135 was detected by western blot using polyclonal UL135 sera obtained from three RAdUL135 inoculated mice (1/1000 each). The western blot was stripped and reprobed for pUL135 using the Streptag antibody (1/1000). Mock and RAd592 infected HFFF-hCAR were included as negative controls.

remaining UL/*b'* ORFs produced varying degrees of background by western blot that prevented the detection of each specific UL/*b'* protein (data not shown).

4.4.2 HCMV seropositive patient sera

An alternative source of antibody is sera from HCMV-infected individuals. We sought to determine whether human polyclonal antibody could detect expression of any of the UL/*b'* proteins encoded by their respective RAds. Furthermore, a positive result in this assay would also provide evidence for the expression of the UL/*b'* ORFs during HCMV infection *in vivo*.

Pooled serum from eight HCMV seropositive patients (kindly provided by Dr. L. Neale, Cardiff University) was used as a source of polyclonal antibodies in a western blot assay for the detection of the UL/*b'* proteins from UL/*b'* RAd infected HFFF-hCAR cell extracts (Fig 4.6). Cell extracts were also prepared from HCMV strain AD169 and Merlin infected HFFF-hCAR and were included in this experiment as positive controls (Fig 4.6). The mixed sera was unable to detect expression of any of the UL/*b'*-encoded proteins tested, yet a positive signal was observed against HCMV strain AD169 and Merlin proteins. Strain AD169 extracts produced 4 additional bands that were not seen in the strain Merlin infected cell extracts; at ~20kDa, ~35kDa, ~60kDa and ~100kDa. Strain Merlin infected cell extracts also produced a band at ~75-80kDa that is not seen in strain AD169 extracts, but it is unclear if this is a UL/*b'* protein as banding patterns for the UL/*b'* ORFs were not detected (Fig 4.6). Background staining was seen in RAdUL147, RAdUL147A, RAdUL148B, RAdUL150 and RAdUL14 infected cell extracts (Fig 4.6). Polyclonal serum would be expected to contain polyclonal antibodies against Ad, and these bands are likely to represent Ad background.

Additional serum (kindly provided by Dr R.Milne, Royal Holloway) was tested from a single HCMV infected patient as a source of polyclonal antibodies in a similar western

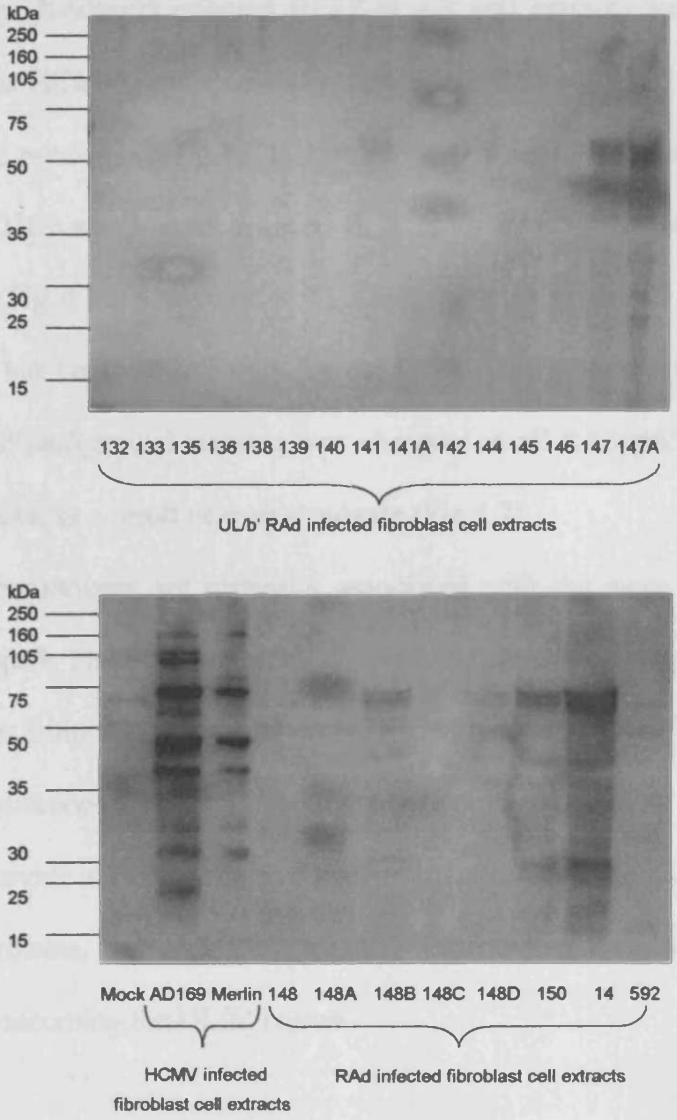

Figure 4.6 Detection of UL/*b*' ORFs with HCMV seropositive patient serum from eight individuals
Cell extracts from UL/*b*' RAd and HCMV strains AD169 and Merlin infected HFFF-hCAR were prepared at 72hpi. Proteins were separated by SDSPAGE and detected by western blot using serum (1/2000) pooled from eight HCMV seropositive individuals (kindly provided by Dr L. Neale).

blot assay. RAdpp65 infected HFFF-hCAR cell extracts were included as a positive control, as HCMV pp65 protein is highly immunogenic, and antibodies to this protein should be produced upon HCMV infection. As for the previous pooled serum, HCMV strain AD169 and Merlin infected fibroblast extracts both produced multiple banding patterns (Fig 4.7). A specific pp65 band was also produced in RAdpp65 infected cell extracts, but no specific bands for the UL/*b*' ORFs were produced (Fig 4.7). A large amount of background staining was observed in all RAdpp65 and UL/*b*' RAd infected cell extracts, as a result of over-exposure (Fig 4.7).

Major immunogens are primarily associated with the more abundant virion proteins, such as pp65. The detection of UL/*b*' proteins has proved unsuccessful using polyclonal antibodies from a number of sources, indicating that the UL/*b*' region does not encode major immunogens. The production of specific monoclonal antibodies for each ORF would provide a more definitive approach for the characterisation of expression of the UL/*b*' proteins, and their generation is expected to form an essential part of future studies concerning the UL/*b*' region.

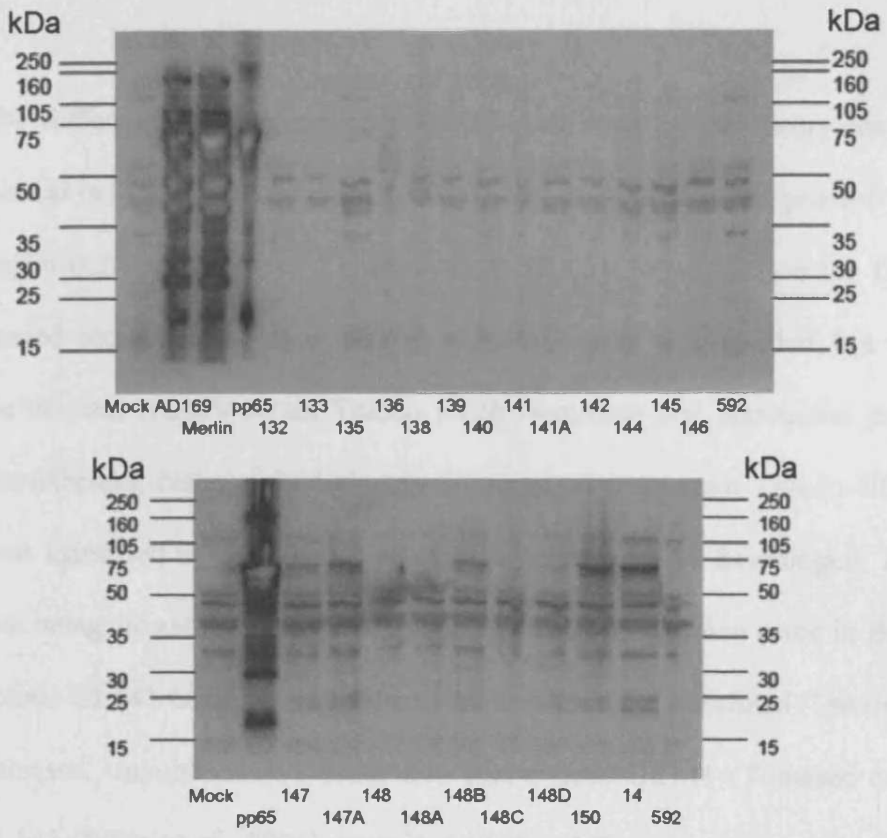

Figure 4.7 Detection of UL/*b*' ORFs with serum from one HCMV seropositive individual

Cell extracts from UL/*b*' RAd, HCMV strains AD169 and Merlin infected HFFF-hCAR were prepared at 72hpi. Proteins were separated by SDSPAGE and detected by western blot using polyclonal human serum (1:2000) from one HCMV seropositive individual (kindly provided by Dr R. Milne). RAdpp65 and RAd592 were included as positive and negative controls respectively.

5. NK SCREENING

The difference in susceptibility to NK cell lysis of laboratory-adapted strains and clinical isolates (Cerboni *et al.*, 2000; Wang *et al.*, 2002) lies primarily with the UL/*b'* region (Cha *et al.*, 1996; Tomasec *et al.*, 2005). Research into the UL/*b'* region was carried out in this laboratory before this PhD study was initiated, but was frustrated as the original HCMV strain Toledo UL/*b'* sequence and annotation proved unreliable. Nevertheless, research had already commenced into strain Toledo UL142, which had been identified by Davison *et al.* (2003a) to be a UL18 homologue. The UL141 ORF was being investigated in parallel to UL142 as a sequence error in the original strain Toledo UL141 ORF had been identified, and the ORF redefined (Davison, *et al.*, 2003a; Tomasec, unpublished). During this study, both UL141 (Tomasec *et al.*, 2005) and UL142 (Wills *et al.*, 2005) were identified as NK evasion genes. A mechanism of NK inhibition by UL142 was recently identified by Chalupny *et al.* (2006) who describe UL142 to downregulate an allele of MICA, a ligand of the NKG2D NK activating receptor. UL141 was found to encode a particularly potent inhibitor of NK cell lysis, and has been shown to prevent the cell surface expression of CD155, the cellular ligand of the ubiquitous NK activating receptor, DNAM-1, effectively preventing activation of the NK cell (Tomasec *et al.*, 2005).

Based upon these findings, the decision was made to screen the entire UL/*b'* region for novel NK evasion functions. Using the HCMV clinical isolate, Merlin, as the prototypic HCMV strain (Dolan *et al.*, 2004), RAds encoding each of the UL/*b'* ORFs were created for use in functional NK assays. The construction and generation of titred virus stocks for 24 RAds was a substantial undertaking, and some of the more problematic constructs have only recently been generated. As a result, NK cytolysis and CD107a

mobilisation assays were performed on the UL/*b'* ORF RAd constructs as they became available, and thus the results detailed below were restricted to the available constructs.

5.1 FUNCTIONAL SCREEN OF UL/*b'* ORFS USING THE NKL CELL LINE IN CYTOXICITY ASSAYS

5.1.1 Culture of NKL and assay preparation

NKL is a transformed human NK cell line, characterised by Robertson *et al.* (1996). NKLs were used to screen the available UL/*b'* ORF RAds in parallel as a means to compare each gene in multiple assays with the same NK cell phenotype. NKL are recognised to have a limited NK activating/inhibitory receptor repertoire. The screen can therefore only be expected to detect functions that impact on mechanisms encoded by NKL, and this will be restrictive. However, if an NK modulating function can be identified, this limited receptor repertoire of NKL may also be invaluable in characterising the mechanism of action. NKL cells can be expanded efficiently in media containing 10% FCS and 1000IU/ml IL2. However, in order to activate NKL killing over a 10 day period, serum was gradually decreased to 1-2% serum and IL2 to 125-250IU/ml IL2 (Robertson *et al.*, 1996). Activated NKL (effector cells) were then used in a chromium release assay against RAd-infected fibroblasts (HFFF-hCAR) (target cells).

The chromium release assay is a method of measuring specific lysis of a target cell by an effector cell. Briefly, target cells are incubated with radioactive sodium chromate, followed by incubation with the effector cells. If lysis of the target cell occurs, sodium chromate is released into the culture medium, and the amount released can be measured by scintillation counting. This measurement gives a percentage specific lysis of the

target cells, which can be used to distinguish activation or inhibition of target cell lysis when compared to assay controls.

Infection of human fibroblasts with any recombinant Ad vector has the potential to activate NK cell lysis in comparison with mock infection (Tomasec *et al.*, 2007). A suitable negative control was required, thus an Ad vector that does not encode a transgene (RAd592) was included in all assays. Values of NK cell-mediated cytolysis of fibroblasts infected with RAd encoding UL/*b'* ORFs were measured against this RAd592 control. A difference of 10% specific lysis between the RAd592 control and the test construct was considered significant (Wills *et al.*, 1996), as this was greater than 3 standard deviations of the mean percentage specific lysis of a plate read 4 times on the scintillation counter. As a positive control for NK activation, the NK susceptible cell line, K562, was included in all assays. An NKL culture was considered activated when there was an excess of 10% specific lysis of K562.

5.1.2 Screen of UL/*b'* ORFs with NKL by chromium release assay

RAds were used to infect HFFF-hCAR at a MOI of 10, and prepared for chromium release assay at 72hpi. These infected cells were used as targets, alongside the control cell line, K562, with the activated NKL cells at effector:target (E:T) ratios of 40:1 to 2.5:1 (Fig 5.1). The average percentage specific lysis at each E:T ratio is plotted for each UL/*b'* ORF from a minimum of 2 individual experiments. As the positive control, K562 cells were used as a target in all assays, with up to 55% specific lysis at an E:T ratio 40:1 (Fig 5.1a) demonstrating that the NKL were activated to kill. As the negative control, RAd592 infected fibroblasts also show up to 40% specific lysis at an E:T ratio 40:1 (Fig 5.1a). It was against this background that NKL lysis of the UL/*b'* RAds was compared.

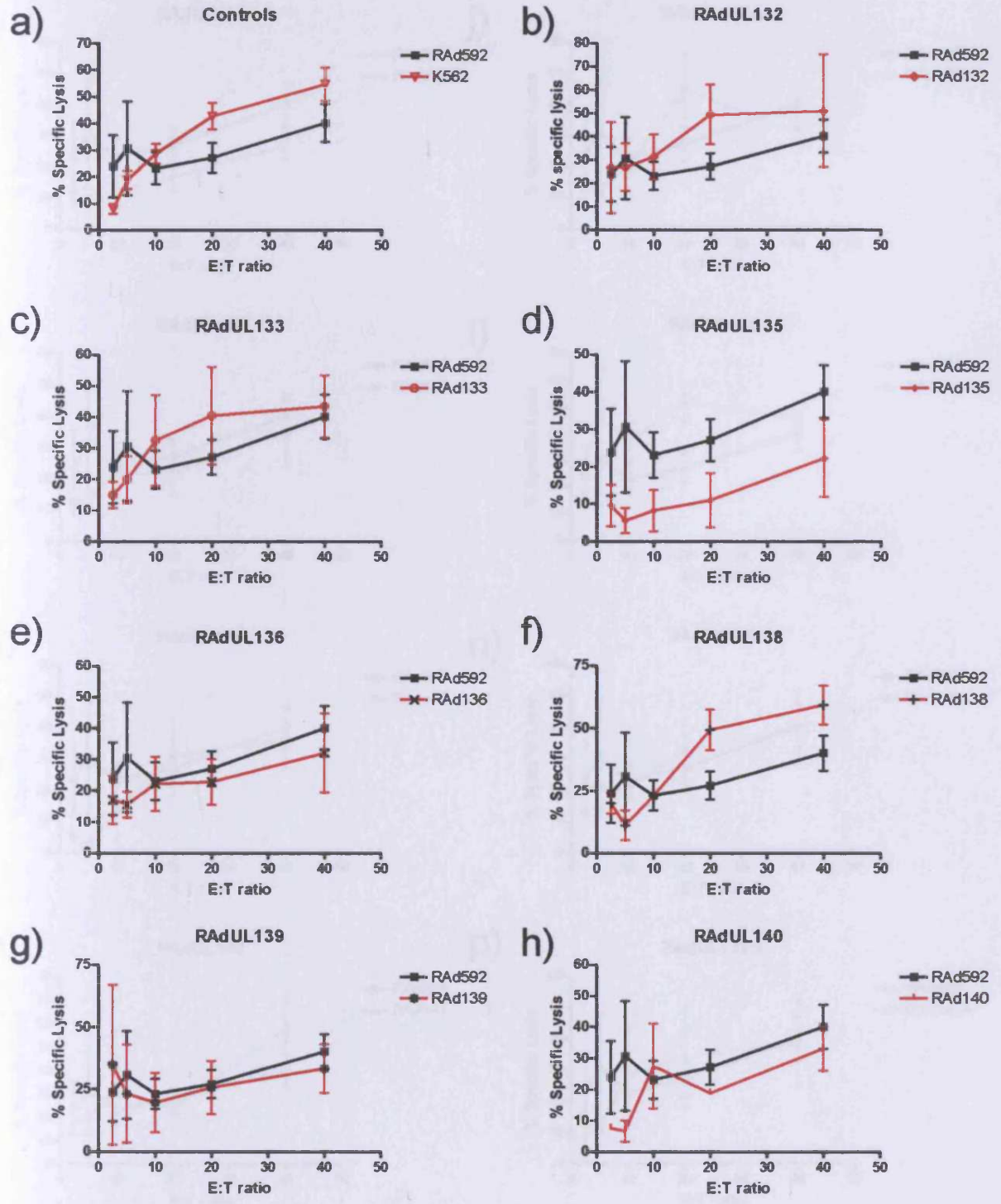

Figure 5.1 NKL screen of UL/*b*' ORFs

Chromium release assays were performed with UL/*b*' ORF RAd infected HFFF-hCAR (MOI of 10) as target cells at 72hpi and the activated, transformed NK cell line, NKL as effector cells at an E:T ratio 40:1 through to 2.5:1. The NK susceptible cell line, K562, was included as a control for NKL activation. RAd592 infected HFFF-hCAR at 72hpi were included for comparative purposes.

a) % specific lysis of the negative control, RAd592, and positive control cell line, K562, in response to NKLs

b) – h) % specific lysis of UL/*b*' ORF RAd infected fibroblasts in response to NKLs. All assays in duplicate with the exception of d) which was performed in triplicate.

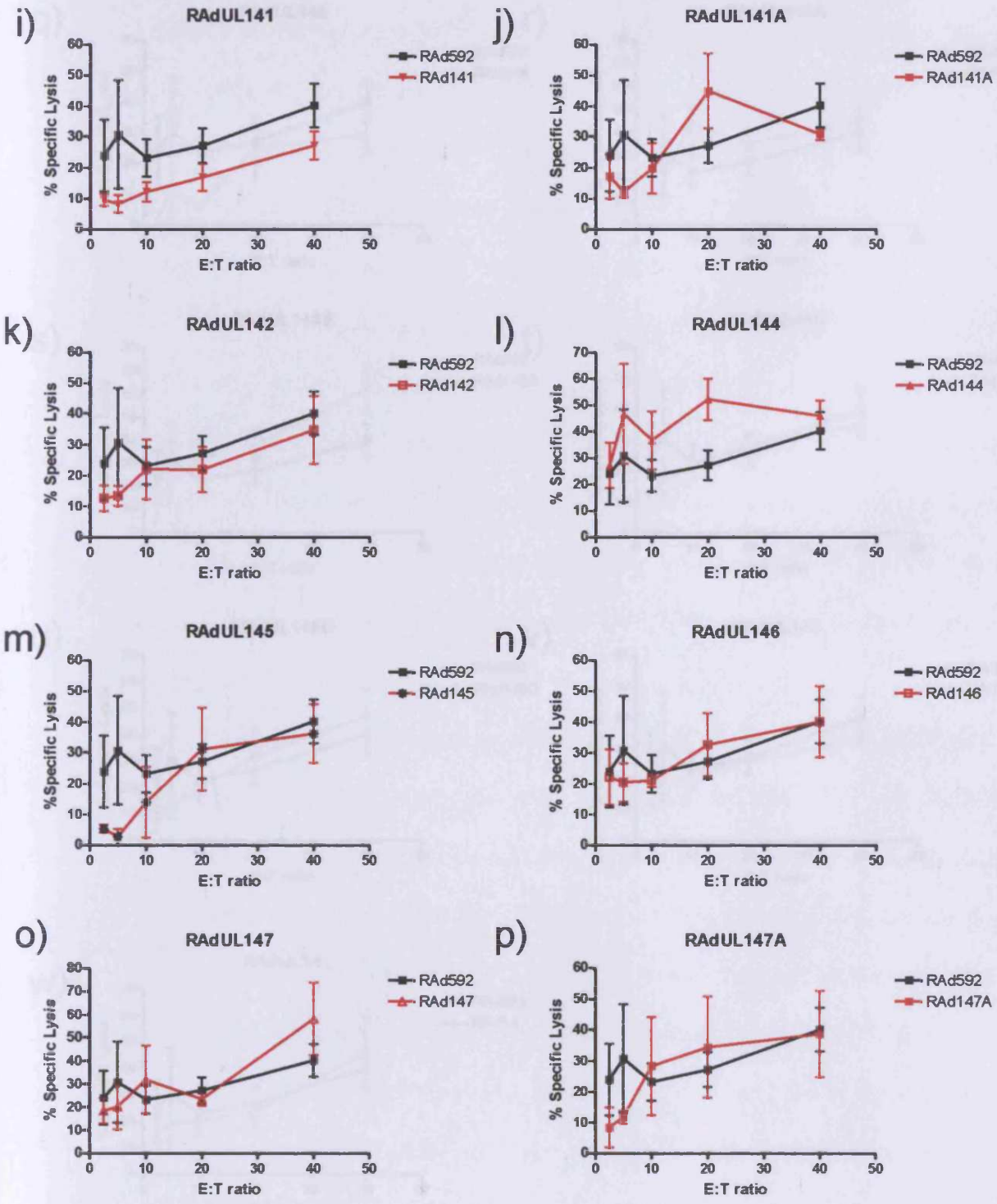

i) – p) % specific lysis of UL/*b'* ORF RAd infected fibroblasts in response to NKLs. All assays in duplicate with the exception of n) and o) which were performed in triplicate, and i) which was performed in quadruplicate.

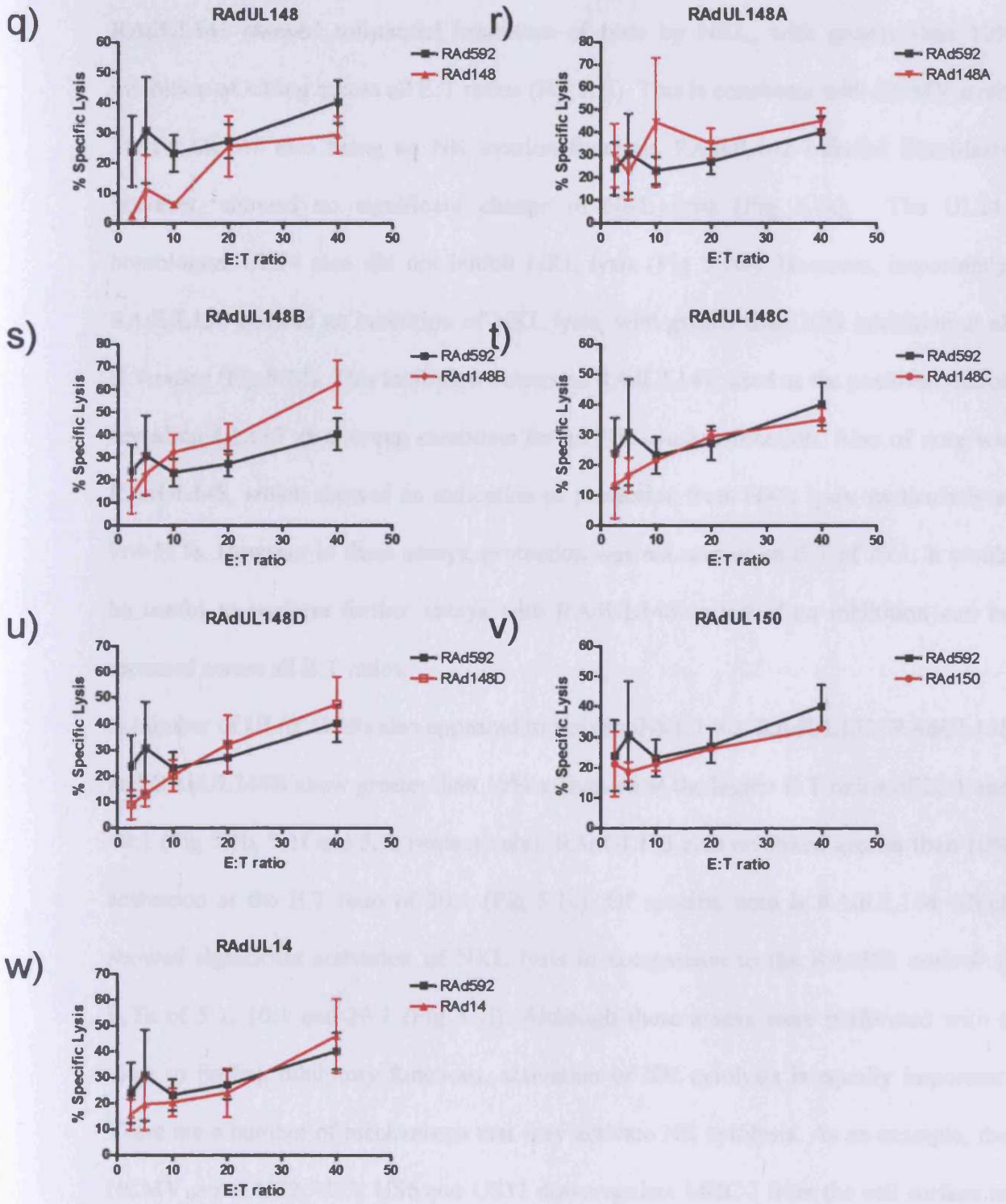

q) – w) % specific lysis of UL/*b*' ORF RAd infected fibroblasts in response to NKLs. All assays in duplicate with the exception of v) which was performed in triplicate, and w) which was performed in quadruplicate.

RAdUL141 showed substantial inhibition of lysis by NKL, with greater than 10% inhibition of killing across all E:T ratios (Fig 5.1i). This is consistent with HCMV strain Merlin UL141 also being an NK evasion function. RAdUL142 infected fibroblasts, however, showed no significant change in NKL lysis (Fig 5.1k). The UL141 homologue, UL14 also did not inhibit NKL lysis (Fig 5.1w). However, importantly, RAdUL135 showed an inhibition of NKL lysis, with greater than 10% inhibition at all E:T ratios (Fig 5.1d). This inhibition outscored RAdUL141, used as the positive control, revealing UL135 as a strong candidate for an NK evasion function. Also of note was RAdUL148, which showed an indication of protection from NKL lysis, particularly at low E:Ts. However in these assays, protection was not seen at an E:T of 20:1. It would be useful to perform further assays with RAdUL148 to test if an inhibition can be repeated across all E:T ratios.

A number of UL/*b*' ORFs also appeared to activate NKL lysis. RAdUL132, RAdUL138 and RAdUL148B show greater than 10% activation at the higher E:T ratios of 20:1 and 40:1 (Fig 5.1b, 5.1f and 5.1s respectively). RAdUL133 also exhibited greater than 10% activation at the E:T ratio of 20:1 (Fig 5.1c). Of specific note is RAdUL144 which showed significant activation of NKL lysis in comparison to the RAd592 control at E:Ts of 5:1, 10:1 and 20:1 (Fig 5.1l). Although these assays were performed with a view to finding inhibitory functions, activation of NK cytolysis is equally important. There are a number of mechanisms that may activate NK cytolysis. As an example, the HCMV genes US2, US3, US6 and US11 downregulate MHC-I from the cell surface in order to prevent lysis by CTL. Removal of the MHC-I inhibitory signal confers susceptibility to NK killing. Similarly, the UL/*b*' ORFs UL132, UL133, UL138, UL144 and UL148B may also be downregulating an NK inhibitory receptor ligand, or conversely upregulating an NK activating ligand as a result of their action within the

cell. Further assays will be required to determine whether this affect is reproducible for these ORFs.

The remaining UL/*b'* ORFs showed no significant difference between lysis of the UL/*b'* ORF RAd infected target and RAd592 infected target control.

5.2 FUNCTIONAL SCREEN OF UL/*b'* ORFS USING POLYCLONAL NK BULK CULTURES IN CYTOTOXICITY ASSAYS

5.2.1 Generation of polyclonal NK bulk cultures

In contrast to NKL, freshly isolated polyclonal NK cells are a heterogeneous population that express a broad range of NK cell receptors that are representative of the entire population in circulation. They allow analysis of the effect of NK modulatory functions against a physiologically representative NK cell population, and were therefore used for preliminary analysis of NK cell lysis by the UL/*b'* ORFs. Polyclonal NK cells were obtained from fresh peripheral blood mononuclear cells (PBMC) from consenting laboratory donors or from buffy coats obtained from the Blood Transfusion Service (Rhydlafa, Lllantrisant, UK). The NK cells were enriched from fresh PBMC by $CD3^+$depletion, and as there is little NK activity in the absence of stimulation, the NK cultures were stimulated overnight with 1000IU/ml of IFNα and 200IU/ml IL2 to induce cytotoxicity (Borysiewicz *et al.*, 1985). Polyclonal bulk cultures were used in both allogeneic and autologous assays.

5.2.2 Chromium release NK cytotoxicity assay with UL14, UL141 and UL135

Experiments with NKL indicated that HCMV strain Merlin UL141 was an NK evasion function, consistent with the function initially described for this gene in strain Toledo (Tomasec *et al.*, 2005) (Fig 5.1). UL141 is a member of the UL14 gene family. UL14's homology to UL141 thus makes it a likely candidate for an NK evasion gene. UL14

expression did not elicit protection from NKL cell-mediated cytolysis, yet this does not necessarily mean that UL14 is not an NK evasion gene. Further experiments with UL14 were performed using the more general polyclonal NK bulk culture population. Results obtained using RAdUL14 and RAdUL141 in a chromium release assay with polyclonal NK bulk cultures from four different donors are shown in Figure 5.2. Donors 1, 2 and 531Z are polyclonal bulk cultures obtained from buffy coat and were used in an allogeneic assay with HFFF-htert fibroblasts. Polyclonal NK bulk culture from donor 9 was obtained from a consenting donor, and was used in an autologous assay. RAdUL135 was included in assays with polyclonal bulk cultures from donors 9 and 531Z. UL14 and UL141 inhibited NK cell cytolysis with polyclonal NK bulk culture in 3 of the donors, as indicated by inhibition of NK killing by >10% compared with the RAd592-infected control. RAdUL135 also showed significant inhibition of lysis in donor 531Z (Fig 5.2). The polyclonal NK bulk culture from donor 9 was not inhibited by RAdUL141 or RAdUL135, which may be explained by the low specific kill of RAd592 seen with this donor. Conversely, RAdUL14 shows a significant activation of donor 9, as indicated by activation of NK killing by >10% compared with the RAd592 control. These chromium release results provide further evidence for NK evasion functions encoded by the strain Merlin UL141 ORF and the UL135 ORF. These results also indicate that UL14 encodes an NK evasion function, as it significantly inhibited polyclonal NK bulk culture from 3 donors. It is interesting to note that although both UL14 and UL141 induced inhibition of polyclonal NK bulk cultures, unlike UL141, UL14 did not inhibit cytolysis from NKL. This is consistent with UL14 and UL141 being functionally distinct, and indicates that UL14 is targeting a receptor that is not found on NKL. Also of interest is the activatory effect seen with UL14. The induction of NK killing with donor 9 indicates that in addition to its inhibitory function, UL14 has a stimulatory effect on NK killing in some donors.

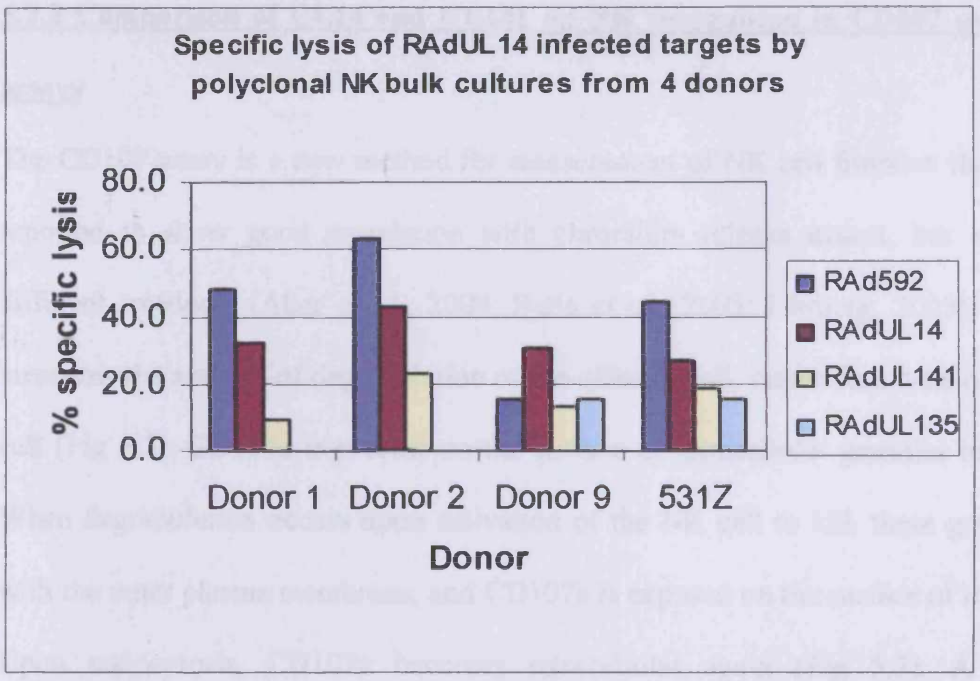

Figure 5.2 Chromium release assay screen of RAdUL14, RAdUL141 and RAdUL135 with polyclonal NK bulk cultures from multiple donors
NK chromium release assays were performed using polyclonal NK bulk cultures from four different donors with RAdUL14 infected fibroblasts at 72hpi. RAdUL141 and RAd592 were included for comparative purposes. Donors 1, 2 and 531Z are polyclonal NK bulk cultures obtained from buffy coat and were used in allogeneic assays. Polyclonal NK bulk culture from donor 9 was obtained from consenting donor PBMC and was used in an autologous assay system. RAdUL135 was included in assays with donor 9 and 531Z.

5.2.3 Comparison of UL14 and UL141 on NK recognition in CD107 mobilisation assays

The CD107 assay is a new method for measurement of NK cell function that has been reported to show good correlation with chromium release assays, but measures a different 'readout' (Alter *et al.*, 2004; Betts *et al.*, 2003; Uhrberg, 2005). The assay measures the amount of degranulation of the effector cell, rather than lysis of the target cell (Fig 5.3). CD107a is present on the surface of intracellular granules in NK cells. When degranulation occurs upon activation of the NK cell to kill, these granules fuse with the outer plasma membrane, and CD107a is exposed on the surface of the NK cell. Upon endocytosis, CD107a becomes intracellular again (Fig 5.3). A αCD107a monoclonal antibody is added to the NK/target cell incubation. When NK cells degranulate, the αCD107a binds to CD107a on the NK cell surface and is then internalized. After their incubation time, the amount of αCD107a antibody that has bound to the NK cell can be measured by flow cytometry, enumerating the proportion of NK cells stimulated to degranulate in response to a specific target. The CD107 assay has many advantages over the chromium release assay. CD107 negates the use of radioactivity, requires only small working volumes and cell numbers, and is a measurement of the effector cell response, rather than the target cell. All CD107 assays were performed by Dr V. Prod'homme. In chromium release assays, a 10% difference between the control and target was considered significant, as this was greater than 3 standard deviations of the mean percent specific lysis of a plate read 4 times on the 1450 Microbeta Trilux Liquid Scintillation Counter. With CD107 assays, much less than 10% difference in total anti-CD107a$^+$ cells between a target and control can be meaningful. As duplicates were not performed for targets with all donors, standard statistical analyses cannot be performed with this data. Instead, in order to compare results from across multiple assays, the percentage anti-CD107a of the target was described as a

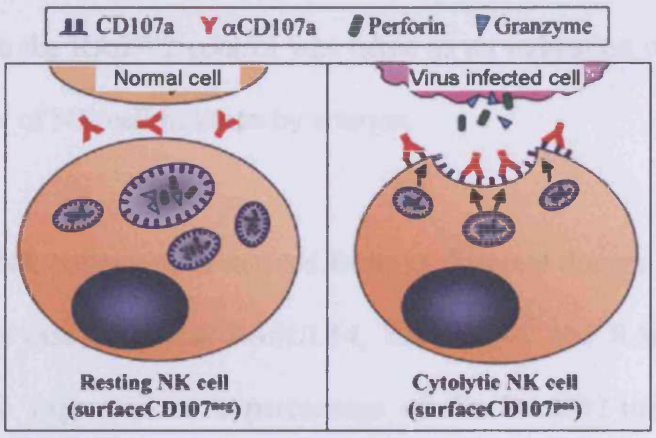

Fig 5.3 The CD107a assay principle
CD107a is a glycoprotein that lines the surface of lytic granules. CD107a is not detectable on the cell surface in resting NK cells (left planel). Upon NK activation, lytic granules move to the cell surface and fuse with the plasma membrane (right panel). Lytic granule contents, perforin and granzyme, are exocytosed and the CD107a molecule is temporarily present on the cell surface. Degranulating NK cells can be detected by flow cytometry using an αCD107a monoclonal antibody (right panel). Figure from Uhrberg (2005).

percentage of the RAd592 control. In these cases, a difference of 20% or greater when compared to the RAd592 control was taken as an indication of a substantial inhibition or activation of NK cell function by a target.

Polyclonal NK bulk cultures derived from 13 different donors were all tested in CD107 mobilisation assays against RAdUL14, RAdUL141 and RAd592-infected cells. The results were expressed as a percentage of the RAd592-infected control (Fig 5.4). Primary data can be found in Appendix II. NK assays for donors 7, 8 and 9 were performed in an autologous setting using corresponding donor skin fibroblasts. The remaining PBMC are from buffy coat, and were tested in an allogeneic system, using HFFF-htert targets. UL141 induced inhibition of NK degranulation in 9/13 donors tested, with no change being observed in the other 4. UL14 induced inhibition of NK degranulation in 5/13 donors tested (Fig 5.4). UL14 also induced NK killing in donor 8 and 004W polyclonal bulk cultures (Fig 5.4). The data from these CD107 assays, and the chromium release assays described above, suggests that although UL14 does not affect cytolysis by NKL, UL14 does induce protection from NK cytolysis in 5/13 different donors, identifying UL14 as a potential NK evasion gene. However, as was seen in chromium release assays, UL14 was also found to stimulate NK killing in some donors. This is an interesting effect, and suggests that UL14 may impact on an NK recognition pathway that can impair NK recognition, but also in some cases stimulate it.

5.2.4 CD107 mobilisation assays with polyclonal NK bulk cultures and UL/*b'* ORFs

In addition to UL14, the effect of expressing all UL/*b'* ORFs available as Ad recombinants on NK recognition was also investigated in CD107 assays using polyclonal NK bulk cultures from multiple donors. In order to compare results from different assays, the percentage degranulation for each UL/*b'* RAd has been presented

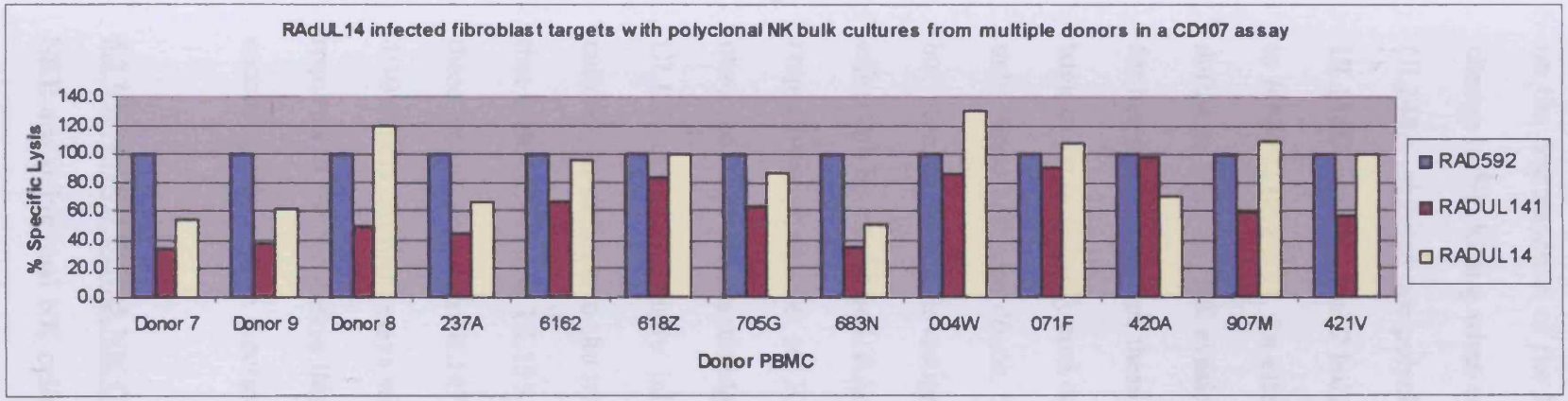

Figure 5.4 Screen of RAdUL14-infected fibroblast targets with polyclonal NK bulk cultures from different donors in a CD107 assay.

For autologous assays, RAdUL14, RAdUL141 or RAd592-infected donor skin fibroblasts were used 72hpi in a CD107 assay with polyclonal NK bulk cultures obtained from multiple donor PBMC (donors 7, 8 and 9). For allogeneic assays, RAdUL14, RAdUL141 or RAd592-infected HFFF-htert were used 72hpi in a CD107 assay with the remaining polyclonal NK bulk cultures, obtained from multiple donor buffy coats. Assays were performed by Dr V. Prod'homme

as a percentage of the RAd592-infected control (Fig 5.5), and primary data also provided in full in Appendix III. The majority of the UL/*b'* ORFs had no obvious effect on the degranulation of the NK cells: ORFs UL139, UL148C and UL150 showed no change in NK killing when compared to RAd592; UL130, UL140, UL145, UL147 and UL148A inhibited one polyclonal NK bulk culture and UL141A, UL146, UL148B and UL148D inhibited 1 or 2 bulk cultures, but also activated 1 or 2 bulk cultures compared to RAd592 (Fig 5.5). An effect on only 1 or 2 donors was not considered sufficient to define an ORF as 'NK evasion function' or 'NK activatory function', but does warrant further investigation of these ORFs with additional donors, as it is not possible to go back to the same buffy coat donor. A similar situation was applied to UL144, which was only tested with one donor. This donor was inhibited compared to RAd592 (Fig 5.5), but requires further investigation with more polyclonal bulk cultures before an NK effect can be considered. RAdUL14l and RAdUL135 inhibited 11/17 and 13/15 donors respectively compared to RAd592 in different assays, with no change in killing observed with the remaining donors (Fig 5.5). This suggests that both UL141 and UL135 can substantially inhibit NK cytolysis from multiple polyclonal NK bulk cultures, in addition to the transformed NK cell line, NKL, providing further evidence that both UL141 and UL135 encode robust NK evasion functions. Also of interest in these assays was RAdUL147A, which showed an inhibition of NK degranulation in 4/10 donors. Further assays with polyclonal bulk cultures from additional donors will be required to further define this function, but the data indicates that UL147A may also encode an NK evasion function (Fig 5.5).

5.3 UL14 AND UL135 NK CLONE ASSAYS

NKL and polyclonal NK cells were used in CD107 and chromium release assays as a screening method to identify novel NK evasion functions. The UL141 proteins encoded

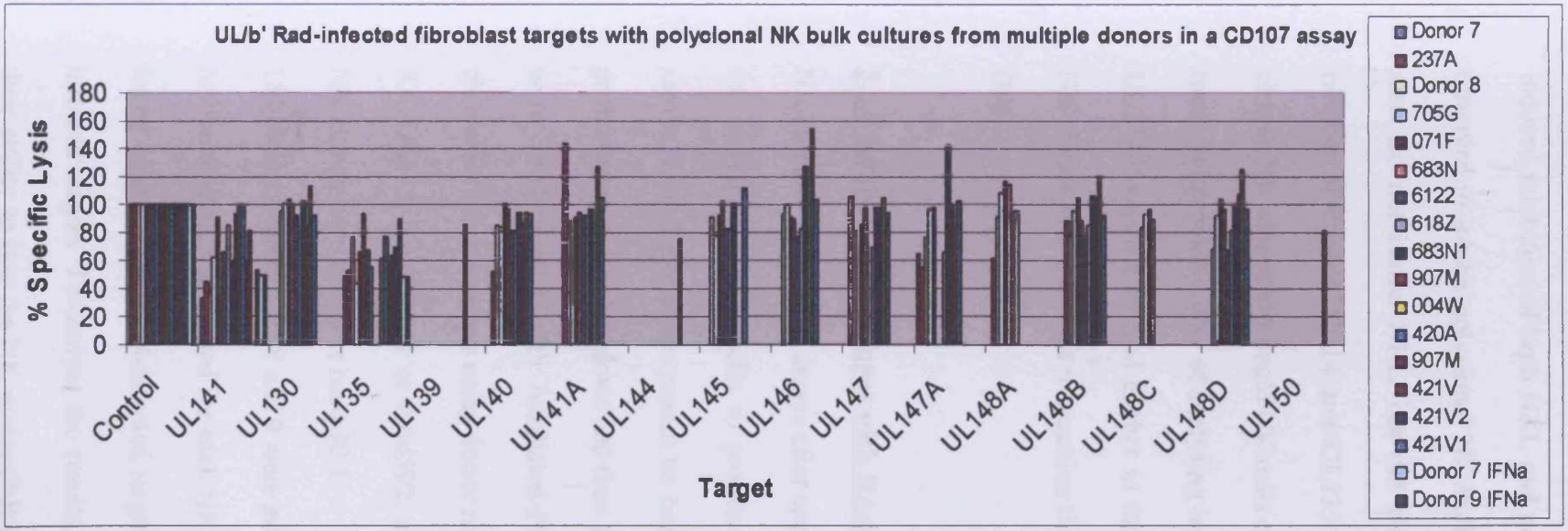

Figure 5.5 Screen of UL/*b*' RAd-infected fibroblast targets with polyclonal NK bulk cultures from different donors in a CD107 assay.

UL/*b*' RAd infected HFFF-hterts were used as targets in a CD107 mobilisation assay with a number of polyclonal NK bulk cultures from different donors. For comparison across multiple experiments, lysis of UL/*b*' RAd infected cells was expressed as a percentage of the RAd592-infected control. CD107 assays were performed by Dr V. Prod'homme.

by HCMV strains Toledo and Merlin both suppress NK recognition, whilst UL135, UL14 and UL147A were identified as potential novel NK evasion functions. UL135 induced inhibition of both NKL and polyclonal NK bulk cultures, whereas UL14 was observed to inhibit polyclonal NK bulk cultures, not NKL. Similar to UL14, UL147A also did not inhibit NKL, but did show inhibition of NK bulk populations from a number of donors. UL14 and UL135 were analysed in further detail using NK cell clones. NK clones are single NK cells cultured from donor PBMC over a long period of time, and provide a way of analysing individual NK cell phenotypes with a given target. UL147A was not studied further in this project, but should be analysed in depth with NK clones at some stage to examine the potential NK evasion function encoded by this ORF.

5.3.1 Analysis of NK clones with RAdUL14 and RAdUL135

NK clones were used in assays after approximately 5 weeks in culture, the time required for individual cloned cells to proliferate to sufficient numbers to enable functional assays. Clonal expansion cannot be continued indefinitely, and after this time, NK cell proliferation invariably slows and then stops. 10 days prior to inclusion in assays, clones were re-stimulated with irradiated-PBMC. NK clones were used in autologous chromium release assays using donor matched skin fibroblasts infected with RAdUL14, RAdUL135, RAdUL141 or RAd592, at an MOI of 500. Targets were used 72hpi and NK clones were used at a ratio 30:1.

112 clones from donors 8 and 9 were generated and used in NK cytotoxicity assays. The numbers of cells generated for each NK clone constrained some assays. All clones were tested against RAdUL14-infected targets, and 98 against RAdUL135 and RAdUL141-infected targets. To analyse the results, clones were first and foremost categorised on their ability to lyse the NK susceptible cell line, K562. For NK clones to be considered

activated, K562 targets must be lysed at or greater than 10%. Two clones from each donor were not activated and were therefore considered null and removed from further analysis, leaving 97 clones that were analysed with RAdUL135 and RAdUL141 and 108 clones that were analysed with RAdUL14. Clones were then categorised according to their ability to induce or inhibit cytolysis of RAdUL14, RAdUL135 or RAdUL141-infected fibroblasts in comparison with control Ad recombinant, RAd592. The categories were kill activation, kill inhibition, kill no change or no kill no change. For a clone to kill, RAd592 had to be lysed greater than 10% specific lysis. For a clone to be activated or inhibited there had to be greater than 10% difference in specific lysis between the UL/*b*' RAd and RAd592 control. Kill no change occurred when RAd592 was lysed greater than 10%, but there was less than 10% difference between lysis of the UL/*b*' RAd and lysis of RAd592. No kill no change indicates a clone that did not lyse RAd592 or UL/*b*' RAd more than 10%. An additional category, no kill activated, is included to describe clones that lysed RAd592 infected fibroblasts less than 10%, but RAdUL14, UL135 or UL141 infected fibroblasts were lysed greater than 10%.

Data for individual clone responses is included in Appendix IV. The overall responses from these assays are shown in Table 5.1. Table 5.1a shows the percentage of clones from donor 9 that were activated, inhibited or unchanged with each target. Table 5.1b shows the same data with clones from donor 8, and Table 5.1c shows the results from both donors 8 and 9 combined. Clone data from donors 8 and 9 combined (Table 5.1c) is also graphically depicted in Figure 5.6, showing the proportions of total activation and inhibition of all the clones tested in response to RAdUL14, RAdUL141 and RAdUL135-infected targets. UL141 inhibited approximately 25% of clones. Of the remaining clones ~60% had a no change response in comparison to RAd592, and 16% were activated (Table 5.1, Fig 5.6). UL135 on the other hand showed no activation of

Table 5.1 Summary of percentage of clones activated, inhibited or unchanged in response to RAdUL14, RAdUL135 and RAdUL141

a) Percentage of donor 8 clones activated, inhibited or unchanged by RAdUL14, RAdUL135 and RAdUL141-infected targets

	Activated (%)	Inhibited (%)	Kill no change (%)	No kill no change (%)	No kill Activated (%)
RAdUL14	44.2	17.3	26.9	11.5	0.0
RAdUL135	0.0	64.7	17.6	17.6	0.0
RAdUL141	23.5	23.5	39.2	13.7	0.0

b) Percentage of donor 9 clones activated, inhibited or unchanged by RAdUL14, RAdUL135 and RAdUL141-infected targets

	Activated (%)	Inhibited (%)	Kill no change (%)	No kill no change (%)	No kill Activated (%)
RAdUL14	28.1	12.3	12.3	26.3	21.1
RAdUL135	0.0	38.3	17.0	44.7	0.0
RAdUL141	8.5	25.5	19.1	46.8	0.0

c) Percentage of all clones from donors 8 and 9 activated, inhibited or unchanged by RAdUL14, RAdUL135 and RAdUL141-infected targets

	Activated (%)	Inhibited (%)	Kill no change (%)	No kill no change (%)	No kill Activated (%)
RAdUL14	35.8	14.7	19.3	19.3	11.0
RAdUL135	0.0	52.0	17.3	30.6	0.0
RAdUL141	16.3	24.5	29.6	29.6	0.0

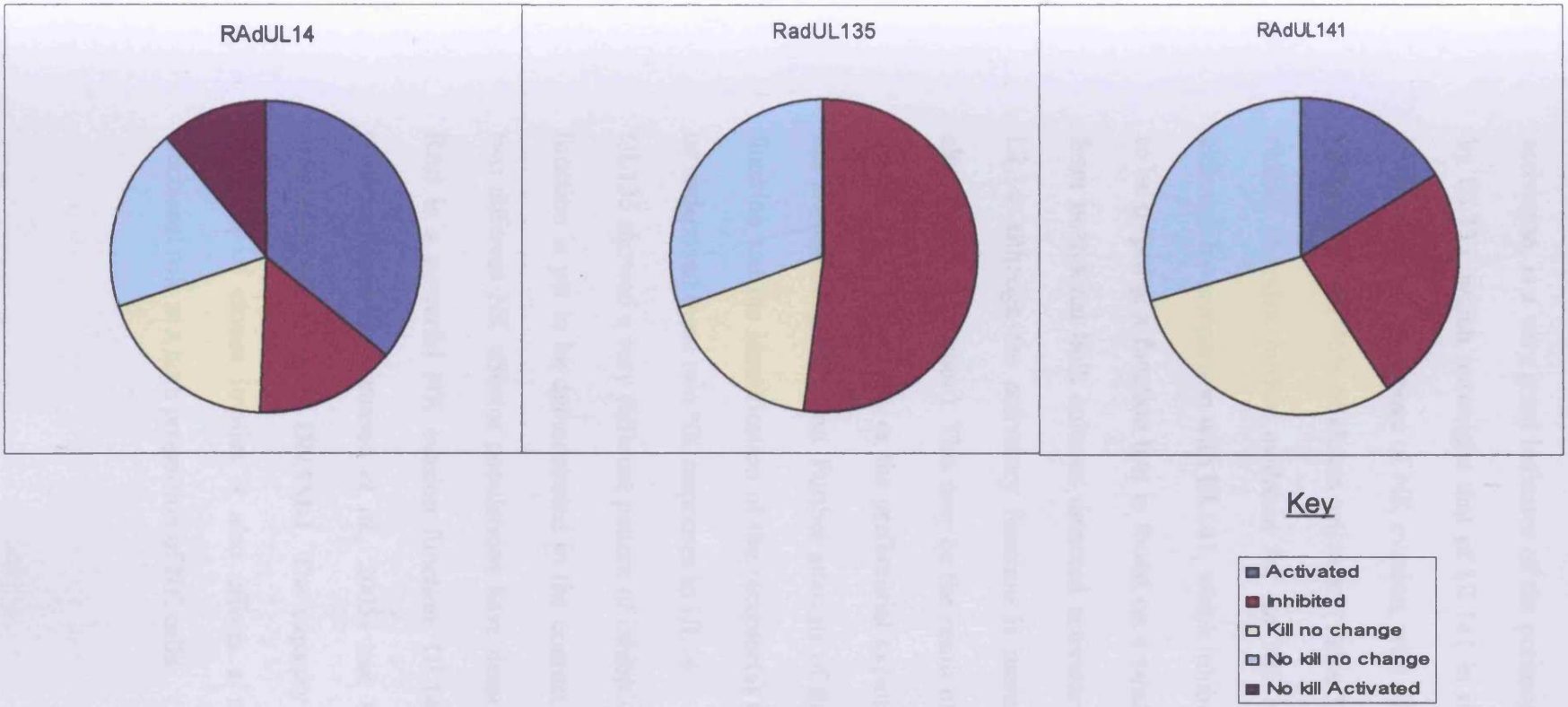

Figure 5.6 Percent activation, inhibition and no change of NK clones tested against RAdUL14, RAdUL135 and RAdUL141-infected targets

Charts show percentages of clones generated from both donors 8 and 9 that were classed as activated, inhibited, kill no change, no kill no change or no kill activated when assayed with RAdUL14, RAdUL135 or RAdUL141-infected targets at 72hpi. 97 clones from donors 8 and 9 were tested with RAdUL135 and RAdUL141, and 108 clones from donors 8 and 9 were tested with RAdUL14.

the 97 clones tested. Instead, either no change in killing (48%), or inhibition of clones (52%) was observed (Table 5.1, Fig 5.6). The extent of clone inhibition, and the lack of activation, is a very good indicator of the potency of the NK evasion function encoded by UL135, which outweighs that of UL141 in these experiments. UL14 on the other hand, had a smaller range of NK evasion, with 15% of clones inhibited, 38% of clones unchanged, and 46% of clones activated (Table 5.1, Fig 5.6). Inhibition of 15% of NK clones provides further evidence for an NK evasion function encoded by UL14, although by comparison with UL141, which inhibited 25% of clones, UL14 does appear to be targeting a function that is found on a smaller sub-population of NK cells. Data from polyclonal bulk cultures detected activatory as well as inhibitory functions for UL14, although the activatory function is more frequently represented in expanded clones (46% activation). This may be the result of 'culturing' out of the NK phenotype that UL14 functions on, or the preferential expansion of the NK phenotype that UL14 has a stimulating effect on. Further analysis of the mechanism of UL14's NK evasion function and the identification of the receptor(s) that UL14 may be targeting will help us understand these two NK responses to UL14.

UL135 showed a very different pattern of inhibition to UL14. Although an NK evasion function is yet to be demonstrated in the context of an HCMV infection, clones from two different NK effector populations have demonstrated that UL135 encoded by the RAd is a powerful NK evasion function. UL141 is an exceptionally powerful NK evasion function (Tomasec *et al.*, 2005) that targets the ligand (CD155) for the ubiquitous NK receptor DNAM-1. The capacity for UL135 to inhibit such a broad spectrum of clones implies it also affects a mechanism that plays an important functional role in a high proportion of NK cells.

6. PRELIMINARY CHARACTERISATION OF HCMV UL14 AND UL135 NK EVASION FUNCTIONS

The systematic screen of the UL/*b'* region using Ad recombinants ultimately identified 4 novel NK evasion functions: UL14, UL135, UL141 (Tomasec *et al.*, 2005) and UL142 (Wills *et al.*, 2005). UL147A may yet be added to this list when further characterised. In order to gain insight into their potential mechanism of action, the expression characteristics of the products of the UL14 and UL135 ORFs (e.g intracellular localisation; glycosylation) were further investigated. HCMV research has contributed much to our understanding of how NK cell function is regulated. In investigating UL14 and UL135 function, it was considered prudent first to screen known NK ligands or potential candidate adhesion molecules whose dysregulation could impact on NK cell recognition.

6.1 CHARACTERISATION OF UL14 EXPRESSION

6.1.1 UL14 is observed to localise to the ER

In order to detect expression of UL14, fibroblasts infected with RAd encoding the UL14-strep were stained using the α-Streptag monoclonal antibody. Multiple images of RAdUL14 infected fibroblasts are provided in Figures 4.3v and 6.1a-c (control stainings are provided in Fig 4.3x and 4.3y). Each cell presents a cytoplasmic staining pattern for the UL14 gene product that resembles ER staining. Figure 6.1d shows a close up of part of the image from Figure 6.1c, where the staining appears very granular. The ER-like staining pattern of pUL14 was further investigated by co-localisation studies with an ER protein, calnexin. To overcome technical issues of dual labelling with murine primary antibodies, a UL14-GFP TOPO construct was used to transfect HFFF-htert. Transfected cells were fixed and stained for calnexin using a calnexin monoclonal antibody (Fig

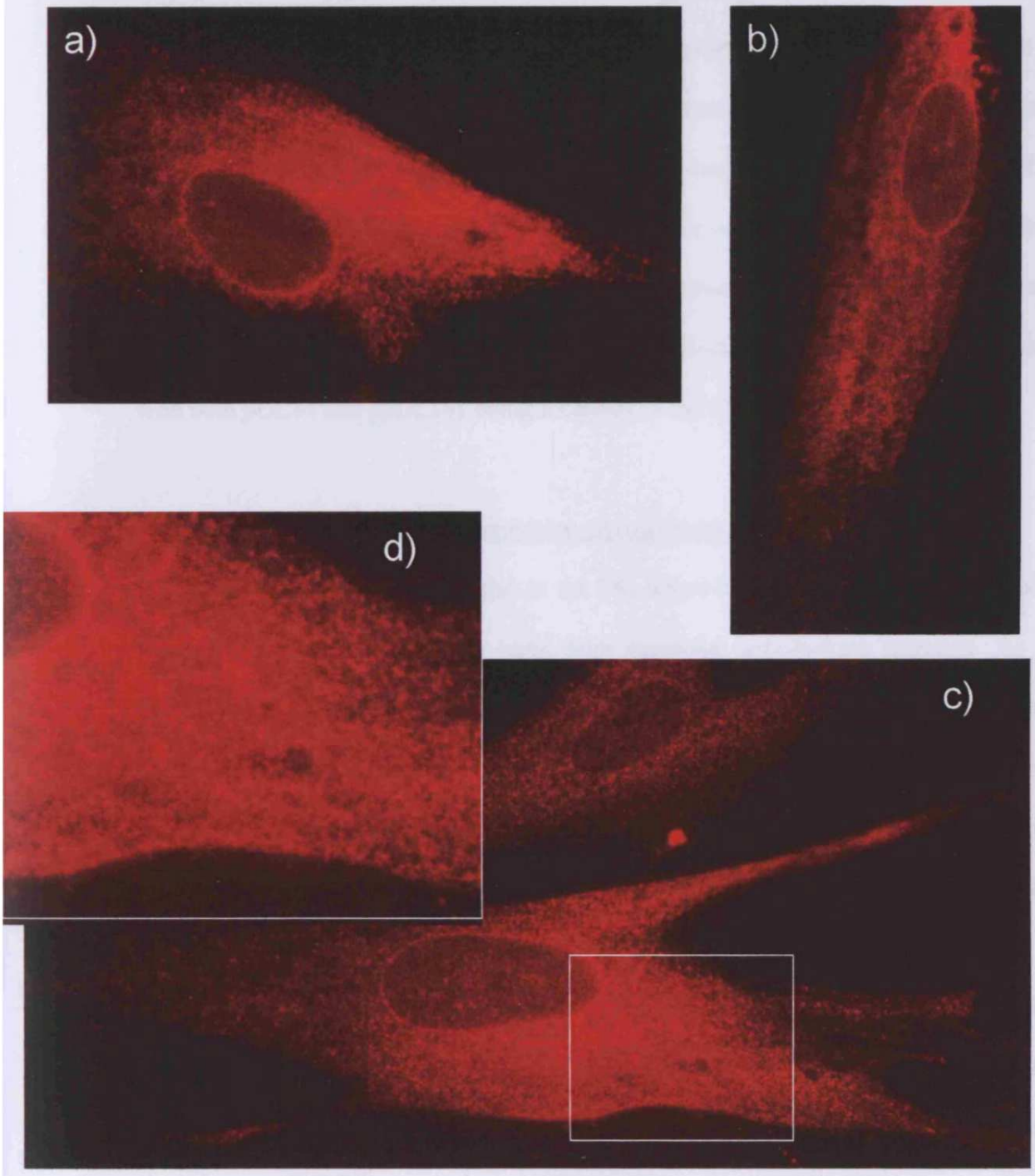

Figure 6.1 UL14-strep localisation in fibroblasts
The localisation of Strep-tagged UL14 in recombinant adenovirus infected HFFF-htert is shown in a)-d). Immunofluorescence was performed at 72hpi using the Streptag monoclonal antibody and an α-mouse Alexa Fluor 594 secondary. d) shows an enlargement of the boxed portion of the cell in c).

6.2). UL141 inserted into the same vector encoding as a GFP fusion (kindly provided by Dr P. Tomasec) was also transfected into fibroblasts for comparative purposes (Fig 6.2). Although both proteins exhibited a widespread granular distribution across the cell (excluding the nucleus), there was good co-localisation between calnexin and the UL14 and UL141 proteins as indicated by the yellow colour on the overlayed images. A direct interaction between calnexin and the UL14 gene product or gpUL141 is not anticipated, and consequently some disparity is expected. The observed co-localisation is consistent with both pUL14 and gpUL141 being localised to the ER.

6.1.2 UL14 encodes an EndoH sensitive glycoprotein

The process of glycosylation begins in the ER, where carbohydrate chains are added at N-glycosylation sites to form a basic high mannose carbohydrate structure. As the glycoprotein continues its maturation through the Golgi, additional carbohydrate side chains are added to form a complex carbohydrate. The deglycosylase enzyme, PNGase F, cleaves all carbohydrate structure from glycoproteins, and can be observed as a decrease in mass by SDS-PAGE. Endoglycosylase H (EndoH) is specific for high mannose type carbohydrates. Sensitivity to EndoH indicates that the protein has not been subject to further post-translation modification in the Golgi, and is therefore evidence for ER retention. gpUL141 is an EndoH-sensitive, ER resident, glycoprotein (Tomasec *et al.*, 2005). The UL14 gene product is also localised to the ER (Fig 6.2), and has been predicted to contain 2 N-glycosylation sites (Table 3.2). To investigate whether UL14 also encodes an EndoH-sensitive glycoprotein, cell extracts prepared from RAdUL14 infected fibroblasts were subjected to PNGase F or EndoH treatment and analysed by western blot after SDS-PAGE. UL141 was included as a positive control, and expression of both proteins detected by exploiting the C-terminal Streptag (Fig 6.3a). A gpUL141-specific monoclonal antibody was also used because recognition

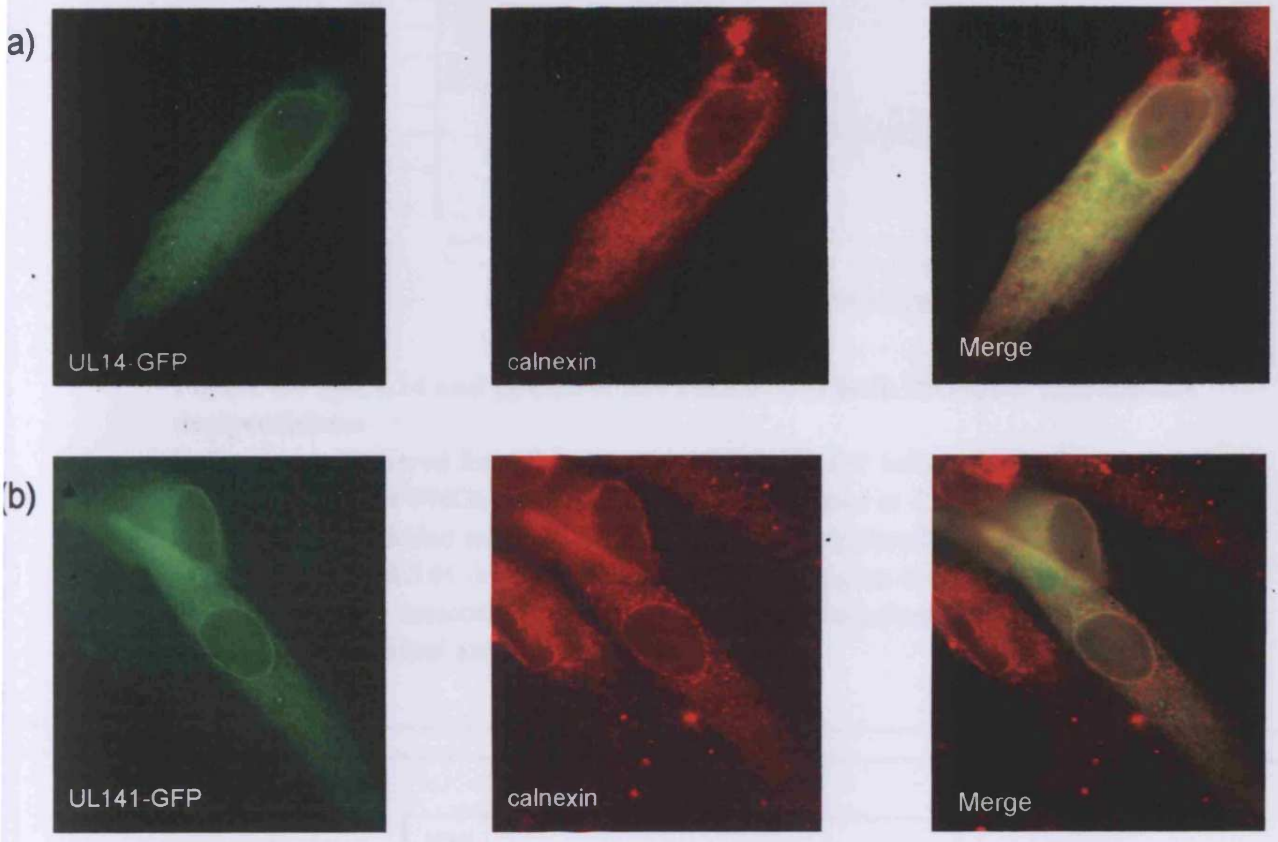

Figure 6.2 UL14 co-localises with the ER protein, calnexin.
a) UL14-GFP TOPO plasmid transfected fibroblasts were stained with an α-calnexin monoclonal antibody followed by α-mouse Alexa Fluor 594. A merge of the GFP and calnexin staining patterns indicates UL14-GFP co-localises with the ER protein calnexin. b) UL141-GFP (kindly provided by Dr P. Tomasec) transfected fibroblasts were included for comparative purposes, and were also observed to co-localise with calnexin.

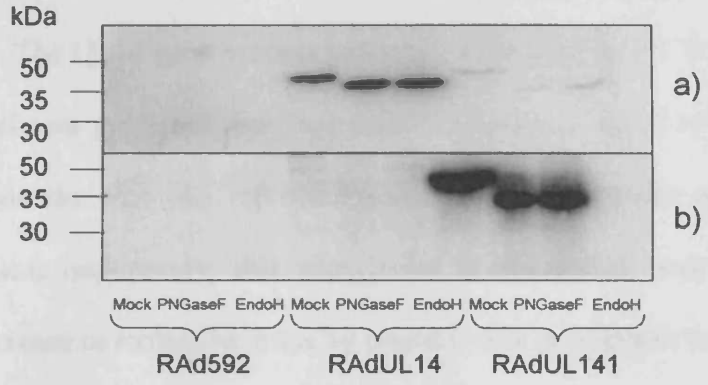

Figure 6.3 gpUL14 and gpUL141 are sensitive to both PNGaseF and EndoH deglycosidases
Cell extracts prepared from RAdUL14 and RAdUL141 infected HFFF-hCAR were treated with either PNGase F or EndoH deglycosidases at 72hpi. Mock treated extracts were included as a control. Proteins were separated by SDSPAGE, and gpUL14 and gpUL141 detected by western blot using an α-Streptag monoclonal antibody (a). The membrane was then stripped and reprobed for gpUL141 using an α-UL141 monoclonal antibody (b).

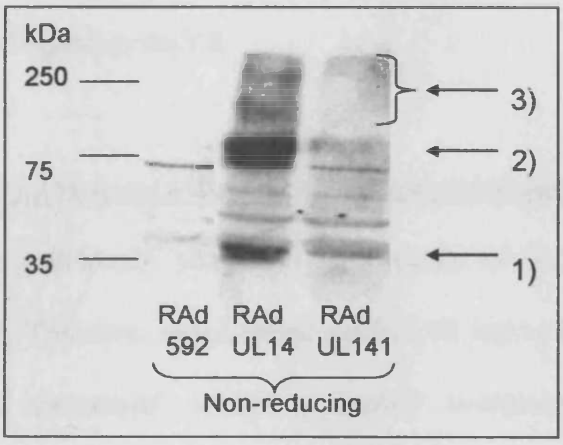

Figure 6.4 gpUL14 and gpUL141 form dimers under non-reducing conditions
Non-reduced cell extracts were prepared from RAdUL14 and RAdUL141 infected HFFF-htert at 72hpi and proteins separated by SDSPAGE. gpUL14 and gpUL141 were detected using the anti-Streptag monoclonal antibody. Arrows indicate 1) the UL14 and UL141 monomer band, 2) the dimer band and 3) bands that may potentially be due to higher molecular weight complexes.

of the Streptag with the monoclonal can exhibit variability between and within experiments. The UL14 gene product was readily detected by the Streptag antibody, yet in this experiment gpUL141 was less readily visualized. gpUL141 was more readily detected when the blot was reprobed with the UL141-specific antibody (Fig 6.3b). However, most importantly, this experiment revealed that both UL14 and UL141 exhibit a decrease in molecular mass by western blot in response to both PNGaseF and EndoH, indicating that UL14 also encodes an EndoH-sensitive glycoprotein. This result, taken together with the observation that UL14 co-localises with an ER resident protein, indicates that gpUL14 is potentially retained in the ER in a similar fashion to gpUL141. gpUL141, as an ER resident protein, retains CD155 to prevent its expression at the cell surface and subsequent interaction with the NK activating receptor, DNAM-1 (Tomasec *et al.*, 2005). The localisation of gpUL14 to the ER may therefore be related to its function and it is possible that like its homologue, gpUL14 may also be retaining an NK activating receptor ligand in the ER.

6.1.3 UL14 and UL141 form a dimer and higher molecular weight complexes

UL141 has been previously shown to be capable of forming a disulphide-linked homodimer (Dr P. Tomasec, unpublished data). Cell extracts from RAdUL14-infected fibroblasts were generated using a buffer containing no dithiothreitol or mercaptoethanol. Without these reducing agents, intra and intermolecular disulphide bonds are not reduced. Subunits of a protein therefore migrate by SDSPAGE together according to their secondary structure. By retaining these protein interactions, complex structures may be observed by western blot. Non-reduced RAdUL14 infected cell extracts were separated by SDSPAGE, and gpUL14 detected using the α-Streptag monoclonal antibody (Fig 6.4). Non-reduced RAdUL141 cell extracts were included in this experiment for comparison. gpUL14 was found to migrate as a species with

approximately double its predicted mass under non-reducing conditions (Fig 6.4). Higher molecular weight bands were also formed in non-reduced gpUL14 samples, and indicate that gpUL14 may also form higher molecular weight complexes. In comparison with gpUL14, the dimer band formed by gpUL141 appears weaker than that produced by gpUL14, and no higher molecular weight bands were observed. gpUL141 was detected in this blot using the Streptag monoclonal. As there have been problems associated with this tag in the detection of gpUL141, this may explain the weaker signal produced by this protein. Importantly however, these results indicate that UL14 is also likely to form a dimer, and, potentially, higher molecular weight complexes.

6.2 INVESTIGATING POTENTIAL LIGAND MODULATION BY gpUL14

The members of the UL14 gene family, UL14 and UL141, both encode NK evasion functions. They are also biochemically similar, encoding EndoH-sensitive, ER localised glycoproteins, with each potentially forming a dimer or higher molecular weight complex. It is therefore possible that gpUL14 may have a mechanism of NK evasion similar to that of gpUL141, and is also sequestering an NK activating ligand within the ER. Using this hypothesis, investigations were focussed on identifying the cell ligand that may be modulated by the expression of gpUL14. A co-immunoprecipitation experiment was performed to identify any cellular ligands that may interact with gpUL14. The Streptag monoclonal antibody was used to pull down gpUL14 from ^{35}S-methionine labelled RAdUL14 infected cells, with a number of other antibodies included as isotype controls (UL141 specific monoclonal, mouse IgG and CD66a). RAdUL141 infected fibroblasts were also included for comparative purposes. Although both gpUL14 and gpUL141 were successfully immunoprecipitated using the Streptag antibody and UL141-specific monoclonal respectively, neither gpUL14 nor gpUL141 appears to have co-immunoprecipitated with any other distinct proteins (data not

shown). Of particular note, gpUL141 was not observed to co-precipitate with CD155, an ~80kDa protein. The failure to observe co-precipitating ligands with UL141 and UL14 may be the result of a weak or transient interaction of these proteins with their binding ligands rather than a direct binding. Alternative methods will be required to observe modulation of a cellular ligand by UL14 expression. Western blot is a particularly valuable technique that can be used to visualize changes to the expression of a specific cell protein. As a basis for this screen, there are a number of molecules that HCMV is known to modulate in infected cells, and a number of orphan NK inhibiting and activating ligands that have been identified. Using antibodies for these molecules, the expression pattern of these ligands in RAdUL14-infected cells was screened by western blot. To aid further investigation of cell ligand modulation by gpUL14 expression, an HCMV strain AD169 UL14 deletion mutant was created by Dr R. Stanton. Briefly, the UL14 deletion mutant was made using a self excisable AD169 BAC, to generate an AD169-Δ14-BAC. When this construct is transfected into HFFF-htert fibroblasts, self-excision of the BAC results in the production of an AD169-Δ14 mutant virus. The deletion mutant provides a very useful tool with which to study the effect of gpUL14 expression in an HCMV background.

6.2.1 UL14 does not affect expression of nectin-2 or nectin-3

UL141 evades NK cell lysis by downregulating the DNAM-1 receptor, CD155, from the HCMV infected cell surface. CD155 is also known as PVR, or Nectin-like molecule 5 (Necl-5). UL14 does not affect the expression of CD155 (Dr P. Tomasec, personal communication), but it was hypothesised that UL14 may interact with other nectin or Necl molecules. Nectins and necls make up a branch of the Ig superfamily, and are involved in cell-cell adhesion, and interaction with F-actin via afadin binding domains. Like CD155, nectin-2 has also been identified as a ligand for DNAM-1 (Bottino *et al.*,

2003). CD155 also forms intercellular bridges with nectin-3, recruiting the complex to cell-cell junctions along with vitronectin, a component of the ECM, and αv-integrin (Lange *et al.*, 2001; Mueller & Wimmer, 2003; Sato *et al.*, 2004).

In order to screen for modulation of nectins by UL14, the expression of nectins 1 to 4 were analysed in RAdUL14-infected fibroblasts by western blot. RAdUL141, RAdUL16, RAd592, HCMV strain AD169 and Merlin plus mock infected fibroblasts were included for comparative purposes. Nectin-1 and nectin-4 expression could not be detected in fibroblasts with the monoclonal antibodies used (data not shown). Nectin-2 was detected as a doublet band at approximately 70-75kDa (Fig 6.5a). Nectin-2 expression was not downregulated by UL14, when protein loading efficiency was taken into account (Fig 6.5a). In support of this finding, nectin-2 expression was comparable in cells infected with the strain AD169-ΔUL14 deletion mutant, strain AD169 and strain Merlin (Fig 6.5a). These results indicate that UL14 does not modulate nectin-2 expression.

Whilst the 95kDa nectin-3 protein was also not overtly affected by UL14 (Fig 6.5b), it was observed to reduce in abundance in both HCMV strain AD169 and Merlin infected cell extracts (Fig 6.5b). To control for protein loading of RAd infected cell extracts, blots were stripped and reprobed with an actin antibody. Whilst the Ad vector exerted no affect on actin, HCMV strain AD169 and Merlin infection cause a modest reduction in its expression (Fig 6.5b). Nevertheless, nectin-3 expression was downregulated by HCMV to an even greater degree than the actin (Fig 6.5b), thus indicating that HCMV infection downregulates nectin-3 expression.

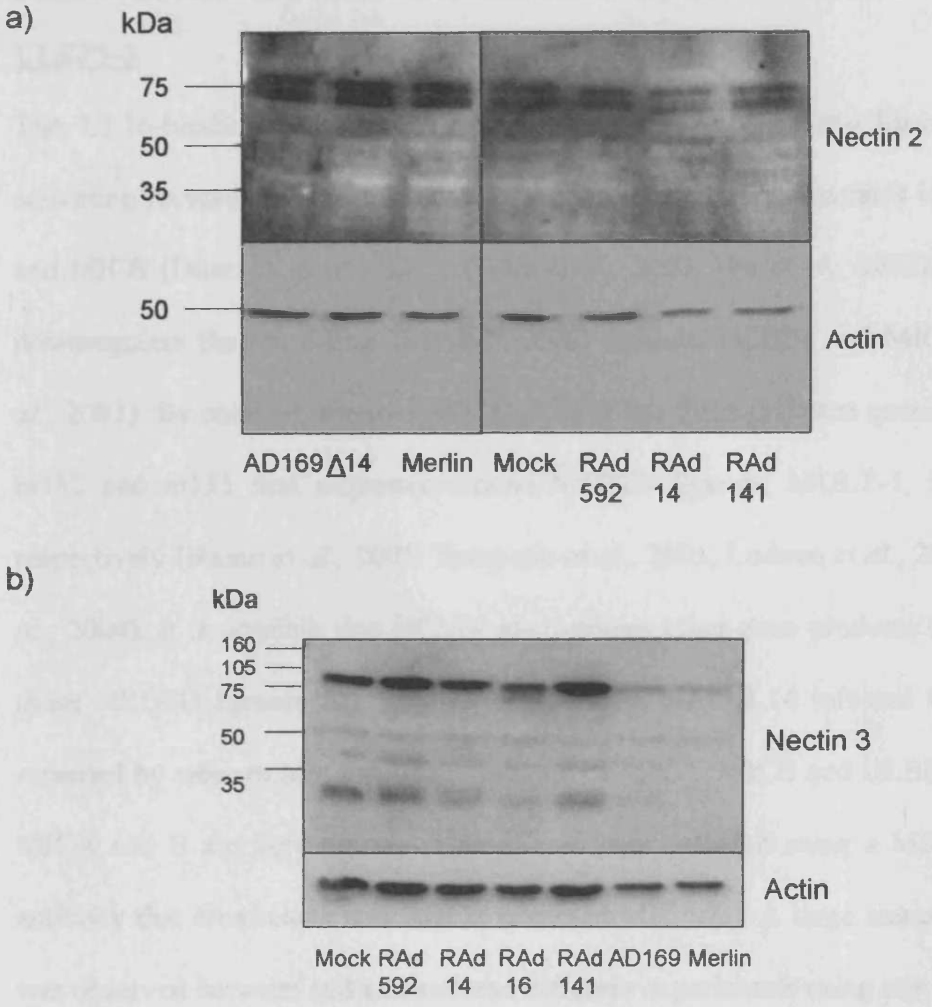

Figure 6.5 Nectin-2 and nectin-3 expression is not altered in RAdUL14-infected fibroblasts

Cell extracts were prepared from RAdUL14 infected HFFF-htert at 72hpi and proteins separated by SDSPAGE. Proteins were transferred to nitrocellulose and nectin-2 expression was detected by monoclonal antibody (a). Mock, RAd592 and RAdUL141 infected HFFF-htert cell extracts were included for comparative purposes. HCMV strain AD169, Merlin and AD169-ΔUL14 infected fibroblasts were also included. Blots were stripped and reprobed for actin as a protein loading control. Nectin-3 expression was detected in RAdUL14 infected HFFF-htert cell extracts by western blot using a nectin-3-specific monoclonal antibody (b). Mock, RAd592, RAdUL16 and RAdUL141 infected fibroblasts were included for comparison. HCMV strain AD169 and Merlin were also included. Blots were stripped and reprobed for actin as a protein loading control.

6.2.2 UL14 does not modulate the expression of NKG2D ligands MICA, MICB or ULBP1-3

The UL16-binding proteins, ULBP1-3 and MICA and B are ligands of the NK activating receptor NKG2D. The HCMV gene, UL16, downregulates ULBP1, ULBP2, and MICB (Dunn C. *et al.*, 2003, Welte *et al.*, 2003, Wu *et al.*, 2003), but it does not downregulate the remaining known NKG2D ligands, ULBP3 and MICA (Dunn C. *et al.*, 2003). By contrast, mouse CMV (MCMV) has three different gene products m145, m152 and m155 that sequester mouse NKG2D ligands, MULT-1, Rae-1 and H60 respectively (Hasan *et al.*, 2005; Krmpotic *et al.*, 2005; Lodoen *et al.*, 2003; Loedoen *et al.*, 2004). It is possible that HCMV also utilizes other gene products to downregulate those NKG2D ligands not affected by gpUL16. RAdUL14 infected fibroblasts were screened by western blot for the modulation of MICA, MICB and ULBP1-3 expression. MICA and B are very closely related, and were detected using a MICA monoclonal antibody that crossreacts with MICB (denoted MICA/B). A large amount of variability was observed between cell extracts and different experiments using this antibody and as a result data has not been shown. At the time of these experiments, a specific monoclonal antibody for each protein that does not cross react with the other MIC molecule was unavailable. Recent acquisition of these antibodies enabled further analysis of specific MICA and MICB expression which was performed by FACS in U373 cells (Fig 6.6). These cells are homozygous for MICA*005, a full length version of MICA. MICA has 53 different alleles, 6 of which are truncated on the intracellular portion of the transmembrane protein (Robinson *et al.*, 2001). Of these truncated alleles is MICA*008, the most common allele found in the Caucasian population. Full length MICA expression was observed to decrease in RAdUL142 infected U373 cells (Fig 6.6), corresponding with results from Chalupny *et al.* (2006), and providing further evidence for the expression of gpUL142 encoded by RAdUL142. Full length MICA

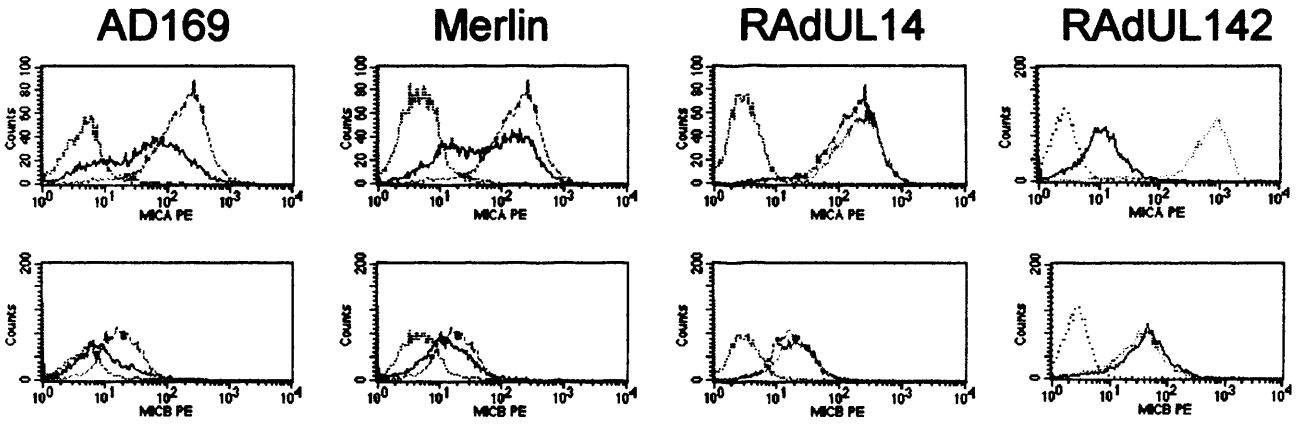

Figure 6.6 UL14 does not modulate the expression of MICA or MICB
U373s were infected with HCMV strain AD169 (red line), HCMV strain Merlin (blue line) or RAdUL14 (light blue line) and RAdUL142 (red line). MICA (top row) and MICB (bottom row) cell surface expression was detected using a MICA and a MICB monoclonal antibody respectively. For comparison with HCMV infected cells, cell surface expression of MICA and MICB in mock infected cells is shown in green and the IgG control as a dashed black line. For comparison with RAdUL14 and RAdUL142 infected cells, cell surface expression of MICA and MICB in RAd592 infected cells is shown in green and the IgG control as a dashed black line.

surface expression was also observed to decrease in HCMV strain AD169 and Merlin infected U373 cells, but not in RAdUL14 infected cells (Fig 6.6), indicating that HCMV infection downregulates full length MICA*005 which is not a result of gpUL14. These results are consistent with findings from Zou *et al.* (2005), who reported that full length MICA is downregulated from the cell surface by HCMV strain AD169, but truncated forms of MICA are not. The HCMV genes UL1-UL20 and US1-US11 were shown not responsible for the downregulation of full length MICA (Zou *et al.*, 2005), providing further evidence that gpUL14 does not affect MICA expression. MICB surface expression in U373 cells was also analysed by FACS (Fig 6.6) and is seen to decrease from the cell surface in AD169 and Merlin infected U373's, but not in RAdUL14 or RAdUL142 infected U373's, indicating that neither gpUL14 nor gpUL142 affect MICB expression.

The expression of the NKG2D ligands ULBP1 and ULBP2 were compared by western blot in fibroblasts infected with HCMV strain AD169, RAdUL14, RAdUL141 and RAd592 (Fig 6.7a). The 28kDa ULBP1 protein was detected in all infected cell extracts, with the exception of AD169, where a band of much lower mass (~23kDa) was detected (Fig 6.7a). This lower molecular weight form of ULBP1 was presumed to represent the immature form of ULBP1, which is sequestered in the ER by gpUL16. The expression of gpUL14 does not appear to modulate ULBP1 expression (Fig 6.7a). The 30kDa ULBP2 protein was also detected at a lower molecular weight (~25kDa) in AD169 infected cell extracts (Fig 6.7a). As is the case for ULBP1, this lower molecular weight form of ULBP2 is likely to represent the gpUL16-sequestered immature form of ULBP2. Upregulation of ULBP2 in strain AD169 infected cells (Fig 6.7a) may be due to gpUL16-stabilisation of a protein that is normally rapidly turned over. Additionally, transcriptional upregulation has been reported due to an HCMV-induced cell stress response to infection (Rolle *et al.*, 2003), but because gpUL16 sequesters ULBP1 and

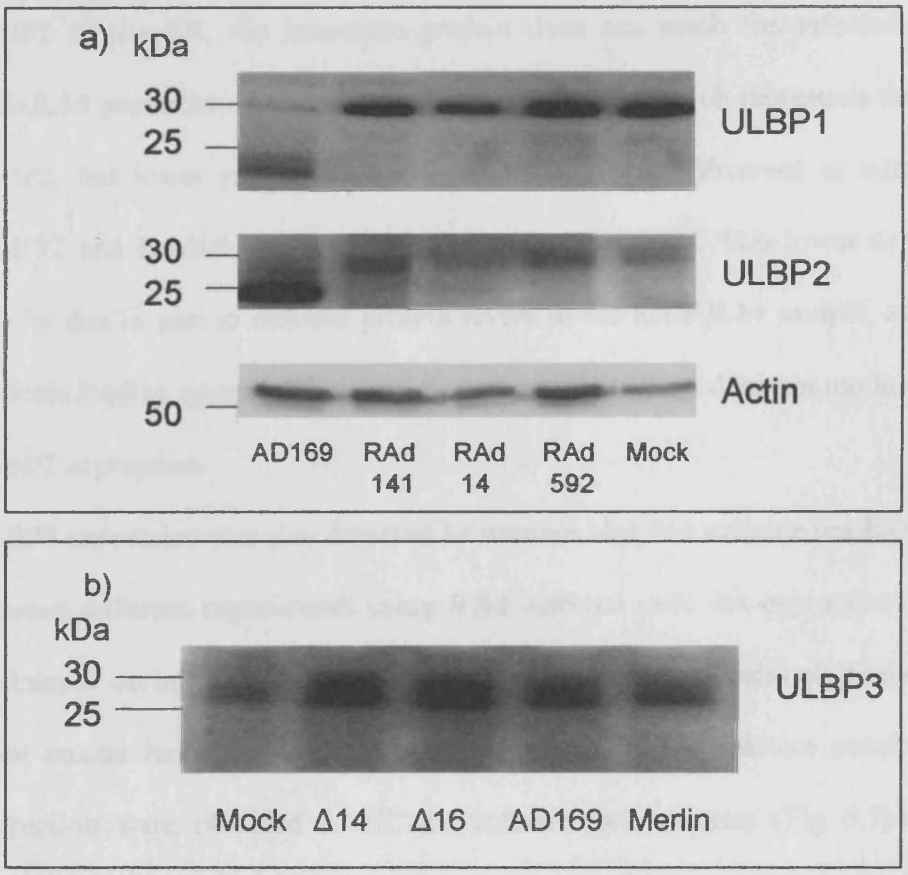

Figure 6.7 Expression of ULBP1, ULBP2 and ULBP3 in HCMV strain AD169 and RAdUL14 infected cells

a) Cell extracts were prepared from RAdUL14 infected HFFF-htert at 72hpi and proteins separated by SDSPAGE. ULBP1 and ULBP2 were detected by western blot using a ULBP1-specific and ULBP2-specific monoclonal antibody respectively. HCMV strain AD169, RAdUL141 and RAd592 infected cell extracts were included for comparative purposes. Blots were stripped and reprobed for actin as a protein loading control. b) Cell extracts were prepared from mock, AD169-ΔUL14, AD169-ΔUL16 and HCMV strain Merlin infected HFFF-hterts at 72hpi and proteins separated by SDSPAGE. ULBP3 was detected by western blot using a ULBP3-specific monoclonal antibody.

ULBP2 in the ER, the immature protein does not reach the infected cell surface. RAdUL14 produced a band of approximately 30kDa, which represents the full form of ULBP2, but lower expression levels of ULBP2 were observed in comparison with RAd592 and RAdUL141 adenovirus controls (Fig 6.7a). This lower expression level may be due in part to reduced protein levels in the RAdUL14 sample, as indicated by the actin loading control. These results indicate that UL14 does not modulate ULPB1 or ULBP2 expression.

ULBP3 expression was also detected by western blot, but variable results were obtained between different experiments using RAd infected cells. Its expression appears to be modulated during cell growth and with the formation of cell-cell contacts. As such, these results have not been shown. However, more consistent results for ULBP3 expression were obtained in HCMV infected cell extracts (Fig 6.7b). The 28kDa ULBP3 was detected at approximately 25-30kDa in mock infected cells (Fig 6.7b). The expression level of ULBP3 was observed to increase in all HCMV infected cells in comparison with mock infected extracts, consistent with results from Rolle *et al.* (2003) who describe ULBP3 upregulation upon HCMV infection. In addition, ULBP3 was detected as a doublet at approximately 25-30kDa in all HCMV infected cells (Fig 6.7b). No difference was detected in expression between the UL16 and UL14 deletion mutants and HCMV strain AD169 infected cell extracts, indicating that the increased levels of ULBP3 are not due to either gpUL14 or gpUL16 expression. Consistent with these results, no change in ULBP3 surface expression was detected in RAdUL14 infected fibroblasts by FACS (FACs performed by Dr V. Prod'homme, data not shown). The appearance of an upper band detected for ULBP3 in HCMV strain AD169 and the deletion mutants may be the result of increased glycosylation due to HCMV infection in these cells. Less protein was detected in the upper band of the doublet in HCMV strain Merlin infected cells in comparison with HCMV strain AD169 and the deletion mutants

(Fig 6.7b). It is possible that expression of a UL/*b'* protein may be responsible for this effect, and the modulation of ULBP3 glycosylation by HCMV strain Merlin may represent an additional mechanism by which HCMV escapes immune surveillance by the NK activating receptor, NKG2D.

6.2.3 UL14 does not affect the expression of E-cadherin or CEACAM-1 (CD66a)

Killer cell lectin-like receptor G1 (KLRG1) is an inhibitory NK receptor. E-cadherin has recently been shown to bind KLRG1, an interaction which prevents lysis of E-cadherin expressing target cells (Ito *et al.*, 2006). To study the effect of HCMV on this interaction, it was necessary to use cadherin-expressing ARPE cells. In western blot analysis, no effect on cadherin was seen in strain AD169 or Merlin infected ARPE cells, indicating that HCMV does not modulate cadherin expression (Fig 6.8). This was confirmed by FACS analysis, which showed no modulation of E-cadherin cell surface expression upon HCMV infection (FACS performed by Dr V. Prod'homme, data not shown).

The homophilic interaction of carcinoembryonic antigen adhesion molecule 1 (CEACAM-1 or CD66a) has been reported as an NK inhibitory mechanism (Markel *et al.*, 2002), as has the heterophilic interaction of carcinoembryonic antigen (CEA) with CEACAM-1 (Stern *et al.*, 2005). The affect of HCMV infection on the expression of CEACAM-1 is unknown, but it is hypothesised that an increase in CEACAM-1 expression on the infected cell surface may represent an additional mechanism by which HCMV evades NK cell lysis. Attempts to detect CEACAM-1 in RAd and HCMV infected fibroblasts by western blot were unsuccessful. However, FACS analysis of CEACAM-1 surface expression in HCMV strain AD169, Merlin and AD169ΔUL14 infected fibroblasts was successful with an increase in CEACAM-1 surface expression observed in all HCMV infected fibroblasts in comparison to mock infected control cells

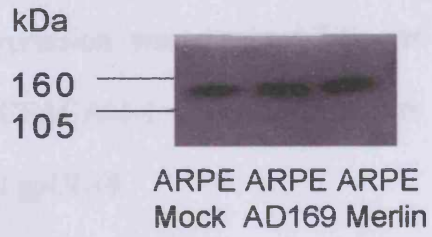

Figure 6.8 Expression of cadherin is not modulated by HCMV strain AD169 or Merlin
Cell extracts were prepared from mock, HCMV strain AD169 or Merlin infected ARPE cells at 72hpi and proteins separated by SDSPAGE. Cadherin expression was detected by western blot with an α-cadherin antibody.

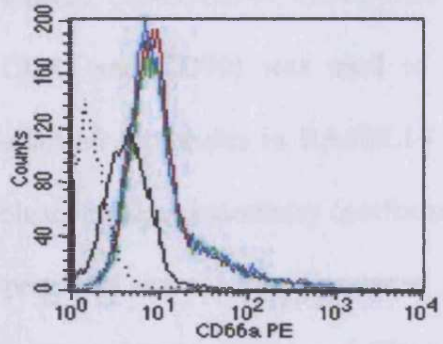

Figure 6.9 CEACAM-1 (CD66a) surface expression is upregulated in HCMV-infected fibroblasts
HCMV infected fibroblasts were fixed at 72hpi and stained for cell surface CEACAM-1 (CD66a) expression with an αCD66a monoclonal antibody. CEACAM-1 expression in mock infected cells is shown by a solid black line. HCMV strain Merlin (green line), AD169 (red line) and AD169ΔUL14 (blue line) infected cells show an increased cell surface expression of CEACAM-1. IgG control is shown by a dashed black line.

(Fig 6.9). This increase in CEACAM-1 cell surface expression represents a novel mechanism that may be employed by HCMV to inhibit NK lysis. No difference in CEACAM-1 expression was detected between HCMV strains, indicating that the modulation of CEACAM-1 observed in Figure 6.9 is the result of an AD169 gene function, but not gpUL14.

6.2.4 UL14 does not affect the expression of a panel of adhesion molecules

In addition to its role as DNAM-1 receptor, CD155 is also involved in cell-cell contacts and migration of cells. Downregulation of CD155 by gpUL141 can be expected to impact on CD155's normal cellular functions, and thus has the potential to impair migration of HCMV-infected cells. To examine whether UL14 acts to modulate a cell adhesion molecule, a panel of 25 antibodies (CD1a, CD2, CD11b, CD14, CD29, CD31, CD34, CD36, CD41, CD42b, CD43, CD44, CD48, CD50, CD54, CD56, CD58, CD162, CD49a, b, c, d, e, CD55 and CD99) was used to screen for changes in surface expression of these adhesion molecules in RAdUL14 and HCMV strain AD169 and Merlin infected fibroblasts by flow cytometry (performed by Dr V. Prod'homme, data not shown). Where possible, these antibodies were also screened by western blot (CD29, CD31, CD43, CD44, CD54, CD56 and CD58). For the majority of adhesion molecules tested, no definitive change in cell surface expression was observed in RAdUL14 infected fibroblasts. However, some interesting observations were made for CD44 and CD99 expression in HCMV infected cells. NK cells can express high levels of CD44, and signalling via CD44 can direct NK killing on IL2 activated NK cells (Sague *et al.*, 2004). The main ligand for CD44 is hyaluronan (HA), but it can interact homotypically with CD44 present on other cells (Droll *et al.*, 1995; Sconocchia *et al.*, 1997). Consequently, the downregulation of CD44 may represent an additional NK evasion mechanism. However, Ito *et al.* (1995) describe CD44 expression to increase

upon HCMV infection of fibroblasts, indicating that CD44 may play a role in modulating cell adhesion and migration during infection. CD44 is an 81.5kDa protein, and strong expression levels are observed in mock, RAd592 and RAdUL14 infected fibroblasts (Fig 6.10). No difference in expression level was observed between RAdUL14 and the RAd592 adenovirus vector control. However, in contrast to results published by Ito *et al.* (1995), HCMV strain AD169 and Merlin infected cells showed much reduced expression levels of CD44 (Fig 6.10), indicating that HCMV infection downregulates CD44 expression. This downregulation of CD44 may represent an additional NK evasion mechanism.

CD99R is an isoform of CD99, a cell surface membrane glycoprotein that is highly expressed on hematopoietic cells. CD99 is reported to interact homotypically and has been implicated in many cell processes such as cell-cell adhesion (Bernard *et al.*, 1995; Bernard *et al.*, 2000; Hahn *et al.*, 1997) and regulation of MHC class I transport from the Golgi complex to the cell surface (Sohn *et al.*, 2001). CD99R is a 32kDa protein and was detected by western blot in mock infected fibroblasts, but not in HCMV infected cells (Fig 6.11). A band of approximately 45-50kDa was also detected in all cell extracts. As no isoform of CD99 is reported at this molecular weight, this band is likely to represent background staining (Fig 6.11). These results suggest that CD99R expression is completely abrogated upon HCMV infection, though the functional significance of CD99R downregulation by HCMV remains unknown. No difference in CD99 expression was observed between AD169-ΔUL14 and HCMV strain AD169 infected cell extracts (Fig 6.11), indicating that UL14 does not affect the expression of CD99.

Although modulation of a cell ligand by gpUL14 was not identified by this screen, a number of novel cell ligand modulations were identified in HCMV infected cells

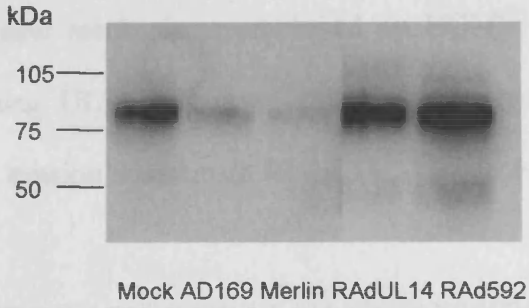

Figure 6.10 Expression of CD44 is downregulated in HCMV-infected fibroblasts
Cell extracts were prepared from HCMV strain AD169 and Merlin, and RAdUL14 and RAd592 infected HFFF-hterts at 72hpi and proteins separated by SDSPAGE. CD44 expression was detected by western blot with an α-CD44 monoclonal antibody.

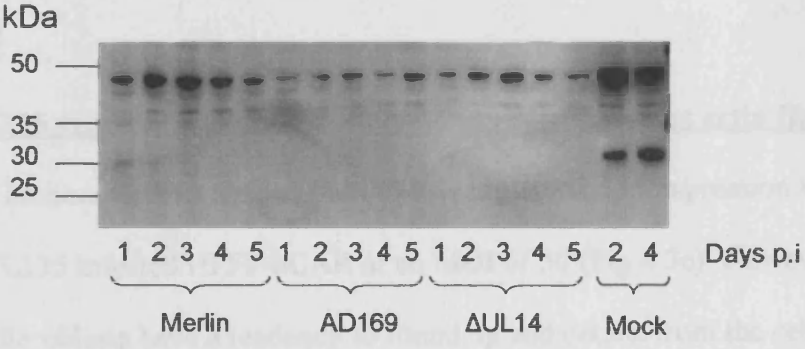

Figure 6.11 CD99R expression is downregulated in HCMV-infected fibroblasts
Cell extracts were prepared from HCMV strain Merlin, AD169 and AD169ΔUL14 infected HFFF-hterts at 72hpi and proteins separated by SDSPAGE. CD99R expression was detected by western blot with an αCD99R monoclonal antibody.

(Nectin-3, CD44, CEACAM-1 and CD99). The modulation of these ligands by HCMV may represent new mechanisms employed by HCMV to enhance virulence. Future studies concerning UL14 will now utilise a proteomics approach in an attempt to identify the NK evasion mechanism for UL14.

6.3 CHARACTERISATION OF UL135 EXPRESSION

6.3.1 UL135 is not N-glycosylated

UL135 is predicted to contain protein sequence motifs for both N- and O-glycosylation (Table 3.2). To establish whether pUL135 is N-glycosylated, RAdUL135 infected cell extracts were treated with PNGase F and Endo H overnight before separating proteins by SDSPAGE. pUL135 was detected by western blot using the Streptag monoclonal antibody (Fig 6.12). No change in mass was observed, consistent with pUL135 not being N-glycosylated. UL135 is also predicted to be heavily O-glycosylated, but this was not followed up during this study.

6.3.2 UL135 expression alters cell morphology by disrupting actin filamentation

Previous immunofluorescence studies to investigate UL135 expression were performed in RAdUL135 infected HFFF-hCAR at an MOI of 50 (Fig 4.3c). However, RAdUL135 infected fibroblasts have a tendency to round up and detach from the cell surface at this MOI, which may be the result of pUL135 toxicity, or possibly an indirect effect on a cellular adhesion molecule. The cellular localisation of pUL135 was further examined using RAdUL135 infected HFFF-hCAR at a range of MOIs (data not shown). At an approximate MOI of 30, cell detachment from the coverslip surface was prevented, whilst still maintaining good expression levels (Fig 6.13). In each of the cell pictures shown, pUL135 appears with cell surface staining in addition to heavy staining near the

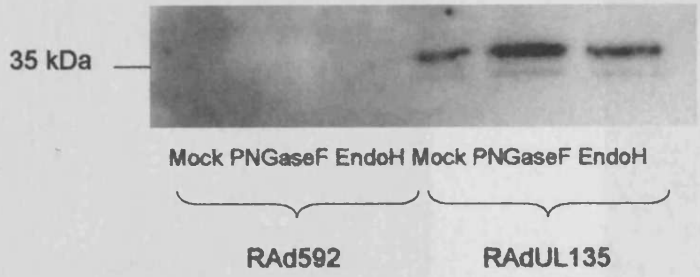

Figure 6.12 pUL135 is not sensitive to deglycosidases PNGaseF or EndoH
Cell extracts were prepared from RAdUL135 infected HFFF-htert at 72hpi and treated with either PNGaseF, EndoH, or untreated as a mock control overnight. Proteins were separated by SDSPAGE and UL135 detected using an α-Streptag monoclonal antibody.

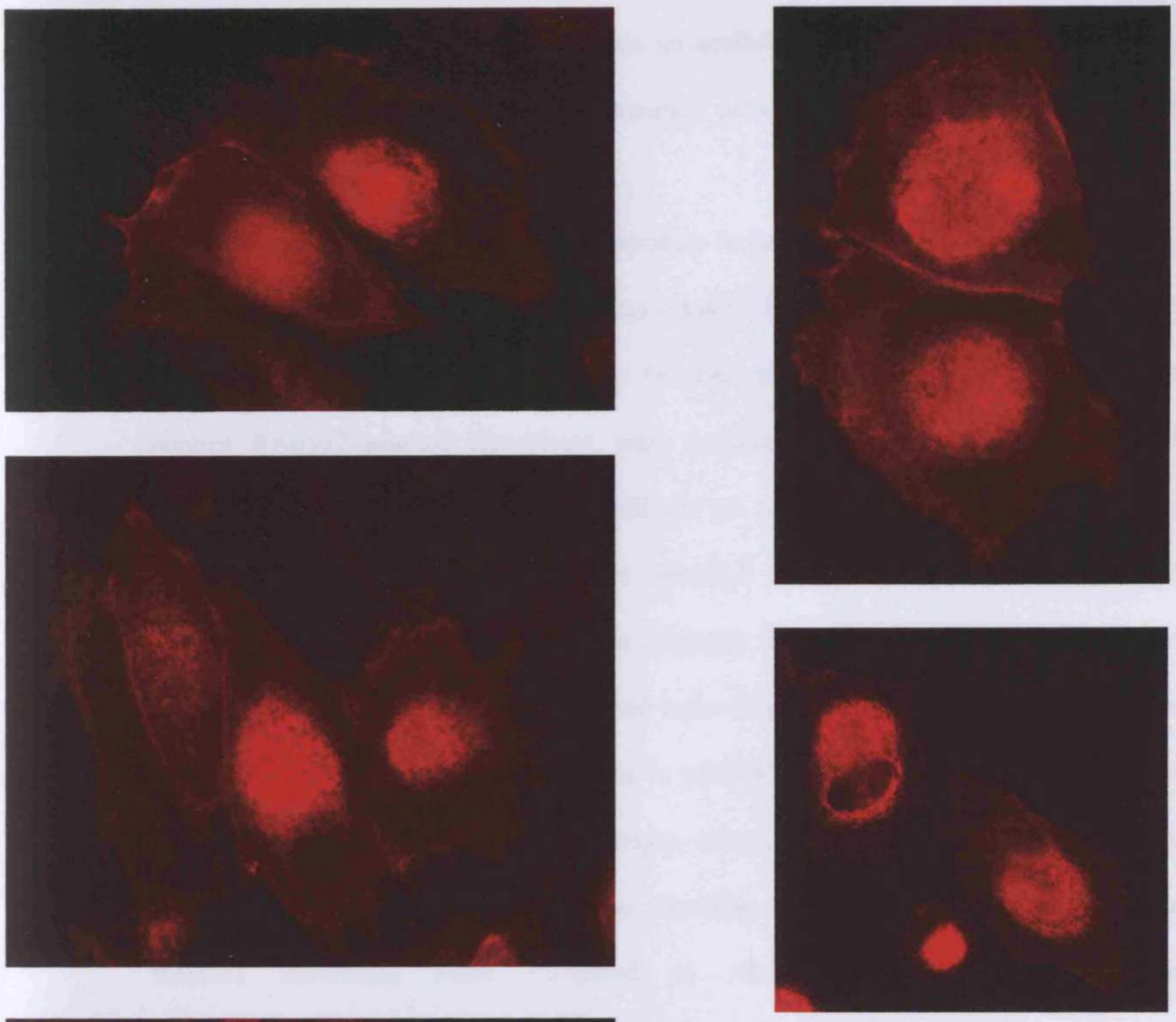

Figure 6.13 pUL135 cellular localisation Immunofluorescence was performed at 72hpi in HFFF-htert infected with RAdUL135 at an MOI of 30. An α-Streptag monoclonal antibody and secondary α-mouse Alexa Fluor 594 were used to visualize Strep-tagged UL135 expression by microscopy.

centre of the cell (Fig 6.13). This central localisation was not nuclear, but could potentially represent Golgi staining. This intracellular distribution of pUL135 to two discrete sites was unusual, and may ultimately provide insight into the mechanism of action of this protein.

To study the dramatic effect pUL135 appears to have on cell morphology, the actin structure of RAdUL135 infected cells was visualised using coumarin phallacidin which stains F-actin filaments, as opposed to G-actin monomer pools. Actin filaments in control RAd592-infected fibroblasts were predominately observed as longitudinal fibres, with individual cells being difficult to distinguish (Fig 6.14e). However, RAdUL135 infected cells show the rounded cell phenotype with a general disappearance of long intracellular actin filaments from the cytoplasm of the cell, but with the appearance of cell surface based actin (Fig 6.14a-d). This effect may be the result of a change in cell adhesion due to pUL135 expression, or a direct effect of pUL135 on actin filamentation. Interestingly, changes in cell morphology are also seen in HCMV infected cells, with a greater rounding of cells observed in Merlin strain infected fibroblasts when compared to AD169-infected cells (unpublished observations). Of particular interest, cells infected with HCMV strain Toledo show less adhesion to NK cells than AD169 infected cells (Dr P. Tomasec, personal communication). UL135 may potentially contribute to the differential cpe seen in clinical and laboratory strains of HCMV.

Whilst both UL135 and UL14 are important novel NK evasion functions, only UL14 was selected for further analysis of its NK evasion mechanism. Further investigation of pUL135 expression and its potential mechanism of NK evasion is currently underway by other members of the laboratory.

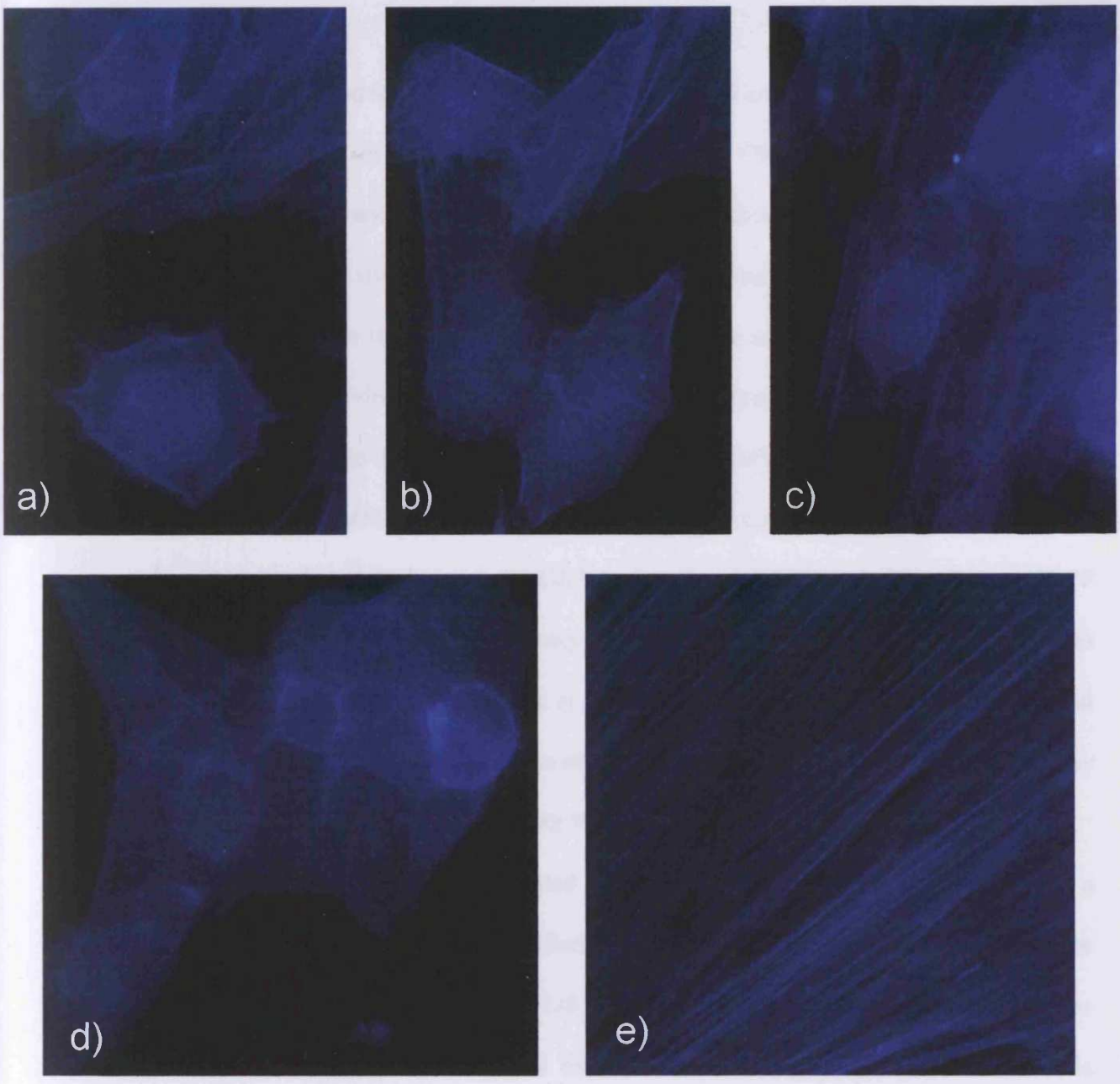

Figure 6.14 F-actin staining pattern visualised by coumarin phallacidin in RAdUL135 infected fibroblasts

a) – d) RAdUL135 infected HFFF-htert were stained for F-actin with coumarin phallacidin at 72hpi. RAd592 control adenovirus infected fibroblasts at 72hpi were stained for F-actin with coumarin phallacidin as a control (e).

7. DISCUSSION

HCMV is predicted to encode 165 ORFs, yet only ~45 are essential for virus replication *in vitro* (Dunn W. *et al.*, 2003). The remaining ~122 ORFs (73% of the gene content) are anticipated to encode for functions that are specifically associated with promoting virus survival *in vivo*, potentially 'virulence functions'. When such 'non-essential' HCMV genes have been characterised, they have been associated either with extending the tropism of the virus or modulating the immune response (Section 1.5 and 1.6.4). Of particular interest to this study is the interaction of HCMV with NK cells. The increased susceptibility of cells infected with HCMV laboratory-adapted strains to NK cell attack has been attributed to loss of the UL/*b'* sequence, a 13-15kb region of the HCMV genome that had been lost by laboratory strains during serial culture *in vitro* (Cerboni *et al.*, 2000; Cha *et al.*, 1996; Tomasec *et al.*, 2005; Wang *et al.*, 2002). This observation led to the hypothesis that one or more additional NK evasion functions were encoded by the UL/*b'* region (Cerboni *et al.*, 2000; Wang *et al.*, 2002).

The UL/*b'* sequence was first defined in strain Toledo (where it is inverted), but a comparable element has been identified in all sequenced clinical isolates. Prior to the commencement of this project, all UL/*b'* ORFs originally predicted in the strain Toledo UL/*b'* were amplified by PCR and expressed as GFP fusion proteins in 293 cells (Tomasec, unpublished). This analysis identified a small number of sequencing errors in the strain Toledo sequence that had a profound effect on ORF assignment (Tomasec, unpublished data; Davison *et al.*, 2003). In addition to general limitations of the original annotation of the strain Toledo UL/*b'* sequence, the genetic integrity of strain Toledo genome is compromised by the inversion. A strategic decision was therefore made to adopt the Merlin strain as the prototype virus. Additionally, the use of stable 293 cells as targets for NK cell assays proved to be extremely restrictive, whereas when

replication deficient adenovirus vectors are used a range of target cells can readily be employed. Before the decision was made to change strain, the strain Toledo ORFs UL141 and UL142 were cloned into an Ad vector. UL142 had been identified independently by Dr A. Davison (Glasgow) as a UL18 homologue (Davison *et al.*, 2003) and Dr M. Wills (Univ. of Cambridge) as exhibiting structural similarity to MHC-1. UL141 was selected because its original definition in strain Toledo was shown to be erroneous (Tomasec, personal communication). As the aim of this project was to analyse all ORFs in the strain Merlin UL/*b'* region, RAd encoding UL141 and UL142 were generated and included in the analysis. As a result of this overall approach, the two HCMV strain Toledo UL/*b'* resident ORFs; UL141 (Tomasec *et al.*, 2005) and UL142 (Wills *et al.*, 2005) were identified to encode NK evasion functions at an early stage. Further analysis of the strain Merlin UL/*b'* region using recombinant adenoviruses generated during this study has identified two additional novel NK evasion functions: UL135, located within the UL/*b'* region, and UL14, a homologue of UL141.

7.1 GENERATION OF RAds ENCODING THE UL/*b'* ORFS

The UL/*b'* region of strain Merlin is predicted to encode 23 ORFs. An additional putative ORF, UL141A (proposed by Dr P. Tomasec), was also included in this study along with UL14, a homologue of the UL/*b'* resident ORF, UL141. UL14 and the UL/*b'* ORFs were cloned into RAd vectors using the AdEasy system. The AdEasy system permitted the generation of a number of recombinant adenoviruses that could not be generated using the AdMax system (Microbix), and was thus considered the most efficient available for the generation of the 25 recombinant viruses.

The AdEasy system involves a series of cloning and sub-cloning steps to produce Ad recombinants (RAds). Each gene was normally first amplified by PCR before being 'TA-cloned into a TOPO vector, where it was sequenced to check for PCR errors. After

the initial cloning step, the gene was sub-cloned into a transfer vector to place under the control of the HCMV major IE promoter and flanked with Ad vector sequences. The transfer and AdEasy vector were fused by recombination in *E.coli*, thus placing the gene in context with the Ad vector genome. The recombinant adenovirus genome then has to be excised from the large, low copy bacterial plasmid by *Pac*I digestion and transfected into 293 or 911 packaging cells to produce the recombinant adenovirus. The generation of 25 discrete RAds using the AdEasy system required a large number of DNA manipulations and proved very time-consuming.

Whilst the majority of recombinants were readily generated following DNA transfection of 911 cells, 9 were not (UL128, UL131A, UL132, UL133, UL138, UL145, UL148 and UL148B). 7 were made by changing cell type and transfecting 293 cells (UL132, UL133, UL138, UL145, UL148 and UL148B). Of these 7, UL132 and UL148 were made, but the RAd produced would not grow to high titre, and UL128 and UL131A did not make at all. A subset of the UL/*b'* ORFs was either incompatible with, or compromised the growth of the RAd vector in the helper cell lines. It became clear during the execution of this study that the Ad vector system could be further developed to be more compatible with the high throughput cloning of HCMV ORFs. To this end, a new Ad vector system (AdZ) was developed by Dr. R. Stanton (Stanton *et al.*, unpublished) that exploits "recombineering" technology and results in a process whereby the gene of interest can be directly ligated into the Ad vector by homologous recombination, obviating the need for multiple cloning steps. The vector is also self-excising, removing the need for *Pac*I digestion before transfection of packaging cells. This results in a highly efficient, one-step method for the generation of RAds (Fig 2.4). Although the AdEasy and AdZ systems use different technologies, the genetic composition of the Ad vector is identical. The AdZ system uses a truncated HCMV IE promoter and its own polyadenylation signal, whereas the pAdEasy-1 vector contains a

'longer' version of the IE promoter and an SV40 polyadenylation site. The AdZ system was used to successfully generate RAds for both UL128 and UL131A that were not made with the AdEasy system. The AdZ system was also used to produce a UL148 RAd, which was generated using the AdEasy system but only produced a low titre stock. RAdUL148 generated using the AdZ system successfully produced a high titre virus stock. A tetracycline regulated system was used with the AdZ system to produce these RAds. This regulation limits the expression of potentially toxic gene products during RAd production in 293 TREx cells. It is therefore probable that the toxicity of UL128, UL131A, UL148 and UL132 gene products prevented the successful generation of recombinants using the AdEasy system, but that this problem was removed with the AdZ system.

Using the AdEasy and AdZ vector systems, the 24 UL/*b'* ORFs and UL14 were successfully cloned into RAd vectors, providing a "bank" of the entire UL/*b'* region. Using the newly developed AdZ system, there is great potential to expand this bank to incorporate RAds encoding for the complete HCMV genome, enabling further characterisation and functional analysis of the entire HCMV proteome.

7.2 CHARACTERISATION OF THE UL/*b'* REGION

The majority of the UL/*b'* genes were uncharacterised at the start of this study. By incorporating an epitope tag, Streptag II, expression of the UL/*b'* proteins could be detected, localised within cells by immunofluorescence and the molecular mass of the expressed protein determined by western blot analysis. Immunofluorescence proved the most successful detection system and has enabled an initial characterisation of UL14 and all the UL/*b'* ORFs. For most of these proteins, the data presented in this thesis is the first characterisation of these ORFs. However, numerous problems were experienced with detection of the Strep-tagged UL/*b'* ORFs by western blot. It was

expected that the epitope tag would provide a means with which to monitor expression of the UL/*b'* ORFs encoded by the RAds. However, a number of UL/*b'* ORFs were not detected by the Streptag II monoclonal antibody by western blot. It is unlikely that the lack of detection is due to a RAd not encoding an ORF, as PCR analysis confirmed the presence of each ORF in their respective RAds (Fig 3.2). Other explanations included the possibility that potential toxicity of the expressed ORF influenced the level of expression, and therefore the level of detection; the protein may be have been processed so that the tag is cleaved, or re-folded in such a way as to make the tag inaccessible. It is a surprise that the denatured protein is not accessible to the monoclonal antibody in western blotting, and indicates that some of the proteins may be refolding during SDSPAGE, rendering the Streptag undetectable. Further evidence that this may be the case was seen with detection of Strep-tagged UL141, which was variable between experiments. On occasions where no, or very low expression was observed using the Streptag monoclonal, detection of UL141 was clearly observed using the UL141-specific monoclonal antibody.

In an alternative approach to validate expression of the UL14 and UL/*b'* ORFs, numerous attempts were made to detect expression of the UL14 and UL/*b'* ORFs using polyclonal sera obtained from HCMV infected patients. Detection was unsuccessful, indicating that the proteins encoded by this region are unlikely to be major immunogens. Attempts were made to generate polyclonal antibodies against UL144, UL14, UL146, UL147 and UL135 by direct murine immunisation with the Ad recombinants with a view to validating expression. The UL135 polyclonal antibody successfully detected expression of pUL135 from the RAd, but did not detect expression in strain Merlin infected cells. The expression of these proteins using the RAd does not provide evidence of their expression by HCMV infection. Thus although expression of all the ORFs was detected by immunofluorescence, further studies are

required to determine whether these ORFs are used within the context of an HCMV infection.

A summary of the characterisation data obtained for each UL/*b*' ORF is provided in Table 7.1. It is important to bear in mind the lack of expression detected for some of the ORFs throughout this study, and this data should be taken into account when looking at functional data for the ORFs (Chapter 5, Table 7.1). However, the reliability of the Streptag system was disappointing in this study, and as research into each UL/*b*' ORF continues it is expected that expression characterisation for these ORFs will improve. For example, UL142 appears functional both in the downregulation of MICA, and in NK polyclonal bulk culture assays (performed by Dr V. Prod'Homme) despite the lack of expression detected by western blot, immunofluorescence and FACS. For ORFs such as UL142, the development of a specific monoclonal antibody would be highly useful. Indeed, to expand on the characterisation of this region, the production of specific antibodies for each gene using the RAds would be an invaluable reagent. Dr R. Strong's laboratory recently initiated a research programme aimed at expressing UL14 and each of the UL/*b*' ORFs in *E.coli* in order to produce soluble proteins for use in crystallographic studies. A by-product of this endeavour will be substantial amounts of purified soluble proteins, suitable for the production of polyclonal or monoclonal antibodies. Specific antibody reagents will greatly assist in characterising the expression of UL/*b*' ORFs from both RAds and HCMV. Until specific antibodies are generated, the epitope-tag incorporated into the expressed ORFs will be invaluable in monitoring expression from the RAds generated in this project.

UL128, UL130 and UL131A are involved in HCMV cell tropism, and are essential for HCMV infection of endothelial cells, leukocytes (Grazia Revello *et al.*, 2001; Hahn *et*

Table 7.1 Summary of expression and functional data for each UL/*b*' ORF RAd

UL/*b*' ORF Rad	Expression characterisation[c]			Functional characterisation			
	Western Blotting	FACS	Immunofluorescence	NKL assays[d]	NK bulk culture[e]	NK clones[f]	Other
UL128[a]	nd	nd	nd	nd	nd	nd	
UL130[b]	nd	nd	(++)	nd	1/10 inhibited	nd	
UL131A[a]	nd	nd	++	nd	nd	nd	
UL132	-	-	++	Activated	nd	nd	
UL133	-	+/-	++	Activated	nd	nd	
UL135	++	++	++	Inhibited	14/17 inhibited	52% inhibited	
UL136	++	+	++	No affect	nd	nd	
UL138	+	-	++	Activated	nd	nd	
UL139	-	-	++	No affect	No affect	nd	
UL140	++	+	++	No affect	1/11 inhibited	nd	
UL141	+/-	++	++	Inhibited	14/21 inhibited	25% inhibited, 16% activated	
UL141A	++	-	++	No affect	1/10 inhibited, 2/10 activated	nd	
UL142	-	-	++	No affect	nd	nd	Downregulated MICA
UL144	-	-	++	Activated	1/1 inhibited	nd	Activated NFκB
UL145	++	-	++	No affect	1/8 inhibited	nd	
UL146	-	-	++	No affect	1/9 inhibited, 1/9 activated	nd	
UL147	++	+/-	++	No affect	1/10 inhibited	nd	
UL147A	+	-	++	No affect	4/10 inhibited, 1/10 activated	nd	
UL148	-	-	++	No affect	nd	nd	
UL148A	++	+	++	No affect	1/6 inhibited	nd	
UL148B	++	+	++	Activated	2/11 inhibited, 1/11 activated	nd	
UL148C	-	-	++	No affect	No affect	nd	
UL148D	+	+/-	++	No affect	2/10 inhibited	nd	
UL150	++	-	++	No affect	No affect	nd	
UL14	++	+/-	++	No affect	8/17 inhibited, 3/17 activated	15% inhibited, 46% activated	

nd Not done

a RAds were only recently generated and expression/ functional characterisation was not performed in all assays.

b Generated by Dr B. McSharry with a FLAG tag. Expression detected by immunofluorescence using FLAG tag by Dr B. McSharry (Appendix I)

c Level of expression graded using ++ (high level expression detected), + (good level expression detected), +/- (low or variable expression detected) and - (no expression detected).

d Affect of UL/*b*' ORF RAd on NKL lysis of infected cells: Activated, Inhibited or No affect

e Number of polyclonal bulk cultures activated or inhibited

f % clones inhibited or activated

al., 2004) and dendritic cells (Gerna *et al.*, 2005). They are thought to play a role in the entry process (Hahn *et al.*, 2004) and recent studies have revealed that UL128, UL130 and UL131A are virion constituents. UL130 was cloned into a RAd vector by Dr B. McSharry with a FLAG tag before the start of this study. gpUL130 has been recently characterized by Patrone *et al.*, (2005) as an ER luminal glycoprotein, where it accumulates intracellularly before associating with virions as they mature through the Golgi, becoming incorporated into the virion envelope as a Golgi-matured glycoprotein. Consistent with this report, gpUL130 was found to have a cytoplasmic, vesicular type staining pattern (Dr B. McSharry, unpublished; Appendix I). UL128 and UL131A are spliced genes (Akter *et al.*, 2003), that could not be cloned into the Ad vector using the AdEasy system. RAds encoding UL128 and UL131A were only recently generated, when the inducible AdZ system became available. Consequently, characterisation of the RAdUL128 and RAdUL131A is limited. gpUL131A produced a cytoplasmic staining pattern similar to that of gpUL130 (Fig 4.3w). It is possible therefore that gpUL131A is also a luminal protein that becomes incorporated into the virion in a similar way to gpUL130, where it forms a complex with gH and plays a role in cell entry (Adler *et al.*, 2006). The production of RAds encoding UL128, UL130 and UL131A provides valuable tools for the further investigation of these proteins to define their roles and protein-protein interactions. For example, it is possible that UL128, UL130 and UL131A may interact together, and the RAds could be used to co-express these proteins in order to examine potential interactions. These genes also appear toxic to both recombinant adenovirus and HCMV replication; mutations occur in at least one of the genes upon the first passage of HCMV in fibroblasts (Akter *et al.*, 2003; Hahn *et al.*, 2004) and difficulties in the production of RAds encoding UL128 and UL131A were rectified by the use of an inducible system. They perhaps induce an IFN or apoptosis response upon infection, and the RAds could be used to evaluate these responses with

each gene in isolation or co-expressed together. The generation of the RAds will be invaluable for the direct analysis of each protein, and also for the study of cell responses to the individual proteins, for example by microarray.

UL132 produced a granular type staining pattern in RAdUL132 infected fibroblasts (Fig 4.3a). Consistent with this result, HCMV UL132 was recently characterised by Spaderna *et al.* (2005) and shown to encode an N-linked glycoprotein that was localised to the trans-Golgi network, as well as in extracellular virions. Deletion of UL132 from laboratory strain AD169 and low-passage strain PAN resulted in an impaired virus growth phenotype in fibroblasts, and virus yield was reduced by 100-fold (Spaderna *et al.*, 2005). Quantitative PCR also showed that the number of HCMV genome copies in the supernatants of UL132 deletion mutant infected cells was reduced in parallel to the reduction in infectious titres (Spaderna *et al.*, 2005). These data indicate a role for gpUL132 in the production of infectious progeny and the viral replication cycle (Spaderna *et al.*, 2005). The AD169 UL132 deletion mutant was also used to analyse whether gpUL132 was involved in the attachment or penetration of fibroblasts. By comparison with AD169 wild type, deletion of UL132 from AD169 did not affect the translocation of pp65 to the nucleus upon entry, indicating that deletion of UL132 from the virus particle has no major impact on HCMV entry (Spaderna *et al.*, 2005).

There is no published expression data available for the HCMV ORFs UL133, UL136, UL138, UL139 and UL140, and functions for these genes remain to be defined. UL139 genome variability has been recently studied by Qi *et al.* (2006). Using Toledo as a reference strain, the authors found that a large number of nucleotide insertions or substitutions occurred in the UL139 ORF across a number of low passage HCMV strains, and that these UL139 variants were not distributed randomly, but fell into three groups (G1, G2 and G3) (Qi *et al.*, 2006). UL139 was also described by these authors as a CD24 homologue, consistent with findings from bioinformatic analysis performed

during this study (Qi *et al.*, 2006; Table 3.2). The RAds produced in this study encoding for the UL133, UL136, UL138, UL139 and UL140 ORFs have been successfully used to provide initial characterisation for each of these genes. pUL136 was detected by western blot with a molecular weight of 33kDa, approximately equal to its predicted molecular weight (Fig 4.1). pUL140 was also detected by western blot, but at a higher molecular weight than predicted, indicating that UL140 may undergo a post-translational modification such as N-glycosylation, which is yet to be confirmed (Fig 4.1). Strep-tagged UL133, UL138 and UL139 were not detected by western blot. pUL133 and pUL136 and pUL139 each produced punctate, granular type staining patterns by immunofluorescence (Fig 4.3b, 4.3d, 4.3f respectively). pUL138 also produced a granular type staining in the majority of RAdUL138 infected cells, though a more diffuse cytoplasmic staining pattern was also observed (Fig 4.3e). pUL140 appeared to produce a large granular staining pattern located close to the nucleus that may represent Golgi staining (Fig 4.3g). Further investigations using the RAds and organelle markers will help define the localisation of these proteins.

During the early stages of this study, HCMV strain Toledo UL141 ORF was found to encode an NK evasion function (Tomasec *et al.*, 2005) As a result of research by Tomasec and co-workers, a monoclonal antibody was raised and gpUL141 expression characterised from the RAd encoding strain Toledo UL141 and from HCMV. UL141 was characterised as an EndoH-sensitive glycoprotein that was localised to the ER, where it retains the NK activating ligand, CD155 and inhibits NK cell recognition. The strain Merlin UL141 ORF was also cloned into a RAd vector, and work presented in this thesis showed it too encodes an ER-resident, EndoH-sensitive glycoprotein (Fig 6.2, 6.3). HCMV strain Merlin UL141 is also an NK evasion function (Fig 5.1).

UL141A is a small ORF that was identified overlapping with the 3' end of UL141 (Table 3.1). UL141A exhibits a granular staining pattern (Fig 4.3i) and produced a band

of approximately its predicted molecular weight of 11kDa (Fig 4.1). As this ORF has only recently been identified and its existence is disputed, the production of a specific antibody for UL141A would be particularly valuable for its detection in the context of an HCMV infection to help define its inclusion as an HCMV gene.

During the course of this study HCMV strain Toledo UL142 was also identified by Wills *et al.* (2005) to be an NK evasion function. Whilst UL142 is a member of the UL18 gene family, Wills' interest in UL142 was derived from an independent observation that gpUL142 exhibited structural homology to MHC class I. Chalupny *et al.* (2006) subsequently demonstrated that strain Toledo UL142 acts to downregulate a full-length allele of MICA, an NKG2D ligand. Sequestration of full-length MICA alleles represents an additional mechanism by which HCMV evades NK cell recognition. Using the RAd encoding strain Merlin UL142 that was generated during this study, gpUL142 expression could be detected by immunofluorescence with a cytoplasmic staining pattern (Fig 4.3j) that is consistent with the characterisation of strain Toledo gpUL142 by Wills *et al.* (2005). gpUL142 expression could not be detected by western blot using RAdUL142. However, as a function has been established for Toledo UL142, it was possible to characterise gpUL142 expression by functional assay. Indeed, RAdUL142-infected fibroblasts showed significant inhibition of NK lysis in polyclonal bulk culture NK assays (Dr V. Prod'homme, personal communication), indicating strain Merlin UL142 also encodes an NK evasion function. In addition, FACS analysis of MICA surface expression also confirms that HCMV strain Merlin UL142 downmodulates full length MICA (Fig 6.6), consistent with results from Chalupny *et al.* (2006). However, downregulation of full length MICA does not appear to represent the only NK evasion mechanism encoded by UL142. Functional NK assays performed during this study utilised HFFF-htert fibroblasts, which were genotyped recently by Dr A. Little (Anthony Nolan Institue) to possess full length

MICA*016*027, and skin fibroblasts from donors 7, 8 and 9 which were all genotyped as homozygous for the truncated MICA*008 allele. UL142 was functional as an NK evasion gene when expressed in both HFFF-htert and donor skin fibroblasts. As truncated MICA alleles are not downregulated by UL142 (Chalupny *et al.*, 2006), this data indicates that an unknown additional NK evasion mechanism is also employed by gpUL142.

UL144 is a homologue of the herpes simplex virus entry mediator (HVEM), a member of the TNFR superfamily (Benedict *et al.*, 1999). UL144 expression was detected by immunofluorescence with an intracellular staining pattern. Benedict *et al.* (1999) also indicated that UL144 is an intracellular protein, as they could not detect pUL144 at the cell surface or in cell culture supernatants. UL144 was found to inhibit T cell proliferation by binding the B and T cell attenuator (BTLA) (Cheung *et al.*, 2005). Recent analysis by Poole *et al.* (2006) revealed an additional function for UL144, showing UL144 activates NFκB-induced transcription. An outcome of this activation was the enhanced expression of CCL22, a chemokine which attracts Th2 and regulatory T cells. By attracting Th2 cells, it is thought that an efficient antiviral Th1 response will not be induced (Poole *et al.*, 2006). Interestingly, RAdUL144-infected fibroblasts activated NKL-mediated cytolysis (Fig 5.1l). It is possible that CCL22 or another product of the enhanced NFκB signalling generated by gpUL144 expression may influence NK cell activation. The CCL22 receptor, CCR4, is present on NK cells (Inngjerdingen *et al.*, 2000). As a result of enhanced CCL22 expression, it is possible HCMV UL144 also affects the chemotaxis and activation of NK cells during an infection. Similar to UL142, the expression of gpUL144 was not detected by western blot. Activation of NFκB-induced transcription by UL144 provided a means with which to test functionally for gpUL144 expression. Indeed, NFκB activation in RAdUL144 infected cells was detected using a luciferase reporter assay (Dr E. Poole, personal

communication), suggesting UL144 is both expressed in RAdUL144 infected fibroblasts and is functional.

UL145 was observed to produce an interesting punctate staining pattern, suggestive of mitochondrial staining (Fig 4.3l). However, lack of co-localisation with the mitochondrial marker protein, Bcl-2, indicated that UL145 does not traffick to mitochondria (Fig 4.4). The function of UL145 has yet to be determined; further analysis of its subcellular localisation may provide insight into its role in virus infection. There is potential to expand this screen to include additional cytoplasmic domains, for example endosomes or lysosomes. Indeed, an extensive, systematic analysis could readily be performed to localise expression of all the expressed UL/*b'* proteins.

UL146 and UL147 are IL-8 chemokine homologues, with strain Toledo UL146 defined as a functional neutrophil chemotactic protein (Penfold *et al.* 1999). UL146 and UL147 sequences are highly variable between different HCMV strains (He *et al.*, 2006), although the chemokine motif is conserved throughout (He *et al.*, 2006). Expression results using the Streptag were surprisingly poor for these proteins. Whilst it was anticipated that the Streptag would also be useful for purifying UL146 and UL147, attempts to concentrate UL146 from the supernatant of RAdUL146-infected cells using Streptactin affinity columns produced very poor yields. Recent studies within this laboratory have made use of strain Merlin UL146 soluble protein, produced in *E.coli* (kindly provided by Dr R. Strong). Using this soluble UL146 in a neutrophil chemotaxis assay that measures calcium mobilisation revealed that strain Merlin UL146 is functional as a neutrophil chemotactant (Dr R. Aicheler, personal communication). Although neither UL146 nor UL147 exhibited any direct effect in NK functional assays, NK cells do possess the IL8-receptors CXCL1 and CXCL2. Further analysis using RAdUL146 and RAdUL147 could determine whether the HCMV virokines were capable of promoting calcium mobilisation in, or chemotaxis by NK cells.

By immunofluorescence, pUL147A, pUL148A, pUL148D and pUL150 each displayed a cytoplasmic, granular type staining pattern. pUL148, pUL148B and pUL148C produced more vesicular staining patterns (Fig 4.3). With the exception of pUL148 and pUL148C, these proteins were also detected by western blot. pUL148A showed an increase in mass of approximately 15kDa. SUMOylation (an 11kDa molecule) was considered as a potential post-translational modification for pUL148A, as UL148A is predicted to contain a high probability SUMO modification site. Co-immunoprecipitation experiments were unsuccessful, but as pull down of SUMO is difficult, repetition of this experiment may be required to optimize experimental conditions. The remaining proteins, pUL147A, pUL148B, pUL148D and pUL150, produced bands of molecular weights (~10kDa for pUL147A, pUL148B and pUL148D, and ~75kDa for pUL150) that were approximately equal those molecular weights predicted for these genes.

7.3 IDENTIFICATION OF TWO NOVEL NK EVASION FUNCTIONS

The aim of this project was to set up a system to screen the UL/*b'* region for novel NK evasion functions. The UL/*b'* ORFs were screened in functional NK assays using NK cells from various sources: the NK cell line NKL, polyclonal NK bulk cultures obtained from PBMC and NK clones. The most comprehensive screen was performed with NKL. Whilst the majority of the UL/*b'* genes did not modulate NKL lysis, the NKL screen identified that both RAdUL141 and RAdUL135 infected fibroblasts exhibited enhanced resistance to NKL-mediated cytolysis, indicating that HCMV strain Merlin UL141 and strain Toledo UL141 both encode an NK evasion function, and most importantly that UL135 encodes a potentially novel NK evasion gene (Fig 5.1). NKL cells are an atypical immortalised NK cell line established from a patient with large granular lymphocyte leukaemia and characterized by an extremely limited NK receptor

repertoire (Robertson *et al.*, 1996). The capacity of UL135 to inhibit NKL, with its restricted receptor usage, was remarkable. It was important to determine if UL135 was capable of acting on a more physiologically-relevant effector cell population. Polyclonal NK bulk cultures obtained from multiple donors were used in both autologous and allogeneic functional assays against target cells infected with RAds encoding all available UL/*b*' ORFs. Polyclonal NK bulk cultures are generated by overnight stimulation with interferon, and thus their NK receptor usage reflects that of the donor. Screening with polyclonal NK bulk cultures provided further evidence for an NK evasion function encoded by UL135, which inhibited polyclonal NK bulk cultures from 14/17 donors (Fig 5.4 and 5.5). NK clones were also generated from fresh PMBC from two different donors and used in autologous functional assays with RAdUL135 infected targets. Remarkably, UL135 inhibited 50% of 97 NK clones assayed, and did not activate any clones (Fig 5.6). For comparison, UL141 was used as a positive control in these NK clone assays as a potent NK evasion gene. UL141 inhibited 25% but also activated a proportion of clones (16%) (Fig 5.6). From this functional data, it appears UL135 encodes for an NK evasion function that affects most NK sub-populations, indicating that UL135 could be targeting either a ubiquitous NK receptor or another vital aspect of NK activation such as target cell attachment.

UL135 encodes a 35kDa protein (Fig 4.1) that localises both at/near the cell surface as well as in an intracellular compartment, indicating that pUL135 may encode a cell surface protein (Fig 4.3c and 6.13). However, pUL135 does not appear to be N-glycosylated (Fig 6.12), suggesting that pUL135 is cytosolic, and that its' predicted leader sequence is not functional. Immunofluorescence indicates there are two forms of the UL135 protein, and it is possible that some of the pUL135 may be trafficking through the ER, but glycosylation is not detected. There are a number of different potential mechanisms for the pUL135 NK evasion function. If pUL135 is a cell surface

molecule, it may interact directly with an NK cell receptor to inhibit NK activation. If pUL135 is intracellular, it may bind and retain a cell surface NK activating ligand within the cell. Cell rounding and detachment was also observed upon pUL135 expression in fibroblasts, indicating that pUL135 may be targeting a cell adhesion molecule. This cell rounding effect led to an investigation of the actin structure of RAdUL135 infected cells. Upon pUL135 expression, actin filamentation can no longer be visualised by coumarin phallacidin (Fig 6.14), indicating that pUL135 may be directly involved in actin remodelling or targeting a receptor involved in actin remodelling. It is also possible that the changes in actin structure are a secondary effect of pUL135 disruption of a cell adhesion molecule. Destroying the cellular architecture would intuitively be expected to stimulate NK cell recognition. The effect of UL135 expression appears to override this ability to recognise target cells. From the data obtained during this study, a number of models can be hypothesised for the function of UL135. In the first model, pUL135 is trafficked through the ER and is expressed at the cell surface, as indicated by immunofluorescence data, where it may directly interact with an NK cell receptor to inhibit NK activation. An alternative model may be the downregulation of a cell adhesion molecule that also plays a role in NK activation or NK cell binding. A secondary effect of this downregulation may be the disruption of the actin structure. pUL135 may also be directly involved in disrupting actin filamentation, which in turn may then disrupt the effective binding of NK cells to the infected target cell, preventing NK activation. Future studies may investigate the effect of chemically-induced actin depolymerisation (for example by cytochalasin B treatment) on NK cell recognition in order to test this theory.

Research is now focussed on identifying cellular ligands that may alter upon pUL135 expression by a similar screening method to that used with UL14. It is important also to examine the role of UL135 in the context of a HCMV infection. This is problematic in

the strain Merlin wild type virus as the Merlin BAC technology is still in development, and there are a number of other NK evasion functions that may mask the effect of UL135. An alternative potential strategy would be to insert UL135 into strain AD169 using existing BACs. This would enable the analysis of the UL135 NK evasion function in a HCMV context, but without the interference of UL141 and UL142 NK evasion genes. Polyclonal sera were generated during this project that were successful in the detection of pUL135 expressed using an Ad recombinant, but were unable to detect UL135 expression from HCMV. This probably reflects the relative levels of UL135 expression from the two viruses, rather than any defect in expression from HCMV. The generation of a UL135 specific monoclonal antibody would be invaluable for further characterisation of UL135 expression during productive HCMV infection.

Functional data obtained in this study indicates that HCMV UL14 also encodes an NK evasion gene. Like UL141, HCMV UL14 encodes an EndoH-sensitive glycoprotein that localises to the ER. In context with its role as an NK evasion gene, the sub-cellular location of gpUL14 may be of functional importance; potentially gpUL14 may have a similar mechanism of action to gpUL141 in sequestering an NK activating molecule within the ER.

RAdUL14 infected fibroblasts inhibited polyclonal NK bulk cultures from 8/17 donors. In NK clone assays to further analyse the NK evasion function encoded by UL14, approximately 15% of NK clones were inhibited. However, UL14 was also observed to activate NK lysis in approximately 50% of the 108 clones assayed. A comparable situation was observed in recent investigations of UL18 (Griffin *et al.*, 2005; Prod'homme *et al.*, 2007). gpUL18 inhibits LIR-1^{+} NK cell function, and this effect was observed in autologous and allogeneic assays using a range of effector cells including NKL, bulk cultures, and a single LIR-1^{high} NK clone. LIR-1^{+} NK cells generally do not thrive during *in vitro* culture, and are thus greatly underrepresented in expanded

populations of NK clones. A similar situation may exist for UL14; NK clones inhibited by UL14 may also be underrepresented in expanded NK clones, whereas UL14-activated NK clones are overrepresented. The existence of UL14-inhibited clones supports the definition of UL14 as an NK evasion function. However, UL14 is also capable of stimulating NK recognition, as indeed is UL18. Whilst UL18 promotes inhibition by LIR-1$^+$ NK cells, it also stimulated recognition by LIR-1$^-$ NK cells, clearly by a LIR-1-independent mechanism (Prod'homme *et al.*, 2007). The interacting receptor for gpUL14 is unknown. The proposed working model for UL14 is unlike UL18, i.e. gpUL14 interacts directly with and sequesters a ligand for an NK activating receptor. It is possible that a ligand sequestered by UL14 is perceived as an activating ligand by a receptor of certain NK subsets, and an inhibitory ligand by others. The identification of the ligand(s) modulated by gpUL14 would clearly be invaluable in appreciating the role of UL14 during HCMV infection.

7.4 HCMV MODULATES NECTIN-3, CD44, CEACAM-1 AND CD99 EXPRESSION

A systematic investigation of likely potential targets for UL14 was undertaken. Although this screen did not identify a cellular target for gpUL14, it did reveal a number of molecules that were altered by HCMV infection. The modulation of these ligands may represent novel mechanisms by which HCMV enhances virulence or escapes immune surveillance.

Nectin-3 and CD99R were downregulated by both strains AD169 and Merlin infection (Figs 6.5b and 6.11). Nectin-3 is a cell adhesion molecule which interacts with afadin at adherin junctions (Reymond *et al.*, 2000) and forms intracellular interactions with CD155 at cell contacts with the ECM (Lange *et al.*, 2001; Mueller & Wimmer, 2003; Sato *et al.*, 2004). Suppression of nectin-3 may serve to impair intercellular

communications and thus promote virus transmission. CD99 interacts homotypically and is involved in cell-cell adhesion (Bernard *et al,* 1995; Bernard *et al,* 2000; Hahn *et al.,* 1997) and regulation of MHC class I transport from the Golgi complex to the cell surface (Sohn *et al.,* 2001). Downregulation of CD99R by HCMV may modulate, for example, cell adhesion and migration during infection, or may represent an additional mechanism encoded by HCMV to help prevent MHC-I transport to the cell surface and avoid immune surveillance by CTLs. There is currently no evidence that either nectin-3 or CD99R influences NK recognition, yet this possibility could be investigated using blocking antibodies in a functional assay. Certainly, if the Ad expression library initiated in this project were to be expanded to include all HCMV ORFs, then it will be possible to map these functions on the HCMV genome.

HCMV was also found to modulate the expression of CEACAM-1 and CD44, both of which are implicated in NK function, and hence their modulation may represent potentially novel NK evasion mechanisms encoded by HCMV. The homophilic interaction of CEACAM-1 has been reported as an NK inhibitory mechanism (Markel *et al.,* 2002). Therefore the upregulation CEACAM-1 cell surface expression that is seen in HCMV infection (Fig. 6.9) may enhance NK inhibitory signals, resulting in the evasion of NK cytolysis. Thus the modulation of CEACAM-1 represents a novel NK evasion mechanism that may be employed by HCMV. Similarly, the downregulation of CD44 expression by HCMV (Fig 6.10) is also particularly interesting as CD44 functions as an NK activating receptor upon interaction with its cell ligand, hyaluronan (Sague *et al.,* 2004; Nolte-t'Hoen *et al.,* 2007). However, as well as its heterotypic interaction with hyaluronan, CD44 can also interact homotypically (Droll *et al.,* 1995; Sconocchia *et al.,* 1997). Thus, the downregulation of CD44 expression indicates that HCMV may be able to evade NK cytolysis by removing the CD44 NK activating stimulus. Interestingly, this is in direct conflict with findings from Ito *et al.* (1995), who

show an upregulation of CD44 at the cell surface following HCMV infection of fibroblasts, and further experiments will be necessary to confirm the affect of HCMV on CD44 expression. Future investigations are likely to focus on further examination of the roles of these molecules during HCMV infection and on the NK cell response. For example, blocking antibodies in functional assays will be invaluable in determining the role of enhanced CEACAM-1 expression on NK cell activation during an HCMV infection, as well as confirming a role for reduced CD44 expression in NK evasion. As this project has demonstrated, the opportunity now also exists to generate a bank of RAds that encode for the entire HCMV genome. This will provide the scope to screen the HCMV genome in order to map the genes responsible for the modulation of CEACAM-1 and CD44, and provide the tools to further characterise these novel HCMV NK evasion functions.

8. REFERENCES

- Abate, D.A., Watanbe, S. & Mocarski, E.S. (2004) Major human cytomegalovirus structural protein pp65 (ppUL83) prevents interferon response factor 3 activation in the interferon response. J Virol, 78:10995-06.
- Adler, B., Scrivano, L., Ruzcics, Z., Rupp, B., Sinzger, C. & Koszinowski U. (2006) Role of human cytomegalovirus UL131A in cell type-specific virus entry and release. J Gen Virol, 87:2451-60
- Adler, S.P. (1983) Transfusion-associated cytomegalovirus infections. Rev Infect Dis, 5:977-93.
- Ahn, J.H. & Hayward, G.S. (1997) The major immediate early proteins IE1 amd IE2 of human cytomegalovirus colocalize with and disrupt PML-associated nuclear bodies at very early times in infected permissive cells. J Virol, 71:4599-13.
- Ahn, J.H. & Hayward, G.S. (2000) Disruption of PML-associated nuclear bodies by IE1 correlates with efficient early stages of viral gene expression and DNA replication in human cytomegalovirus infection. Virology, 274:39-55.
- Ahn, J.H., Brignole, E.J. III, & Hayward, G.S. (1998) Disruption of PML subnuclear domains by the acidic IE1 protein of human cytomegalovirus is mediated through interaction with PML and may modulate a RING finger-dependent cryptic transactivator function of PML. Mol Cell Biol, 18:4899-13
- Ahn, J.H., Jang, W.J. & Hayward, G.S. (1999) The human cytomegalovirus IE2 and UL112-113 proteins accumulate in viral DNA replication compartments that initiate from the periphery of promyelocytic leukemia proteinassociated nuclear bodies (PODs or ND10). J Virol, 73:10458-71.
- Ahn, K., Angulo, A., Ghazal, P., Peterson, P.A., Yang, Y. & Fruh, K. (1996) Human cytomegalovirus inhibits antigen presentation by a sequential multistep process. Proc Natl Acad Sci USA, 93:10990-95.
- Ahn, K., Gruhler, A., Galocha, B., Jones, T.R., Wiertz, E.J., Ploegh, H.L., Peterson, P.A., Yang, Y. & Fruh, K. (1997) The ER-luminel domain of the HCMV glycoprotein US6 inhibits peptide translocation by TAP. Immunity, 6:613-21.
- Akrigg, A., Wilkinson, G.W. & Oram, J.D. (1985) The structure of the major IE gene of human cytomegalovirus strain AD169. Virus Res, 2:107-21
- Akter, P., Cunningham, C., McSharry, B.P., Dolan, A., Addison, S., Dargan, D.J., Hassan-Walker, A.F., Emery, V.C., Griffiths, P.D., Wilkinson, G.W. & Davison, A.J. (2003) Two novel spliced genes in human cytomegalovirus. J Gen Virol, 84:1117-22.
- Alcami, A. (2003) Viral mimicry of cytokines, chemokines and their receptors. Nat Rev Immunol, 3:36-50.
- Aldemir, H., Prod'homme, V., Dumaurier, M.J., Retiere, C., Poupon, G., Cazareth, J., Bihl, F. & Braud, V.M. (2005) Cutting edge: lectin-like transcript 1 is a ligand for the CD161 receptor. J Immunol, 175:7791-95.
- Allal, C., Buisson-Brenac, C., Marion, V., Claudel-Renard, C., Faraut, T., Dal Monte, P., Streblow, D., Record, M. & Davignon, J.L. (2004) Human cytomegalovirus carries a cell-derived phosholipase A2 required for infectivity. J Virol, 78:7717-26.

- Alter, G., Malenfant, J.M. & Altfeld, M. (2004) CD107a as a functional marker for the identification of natural killer cell activity. J Immunol Methods, 294:15-22
- Altschul, S.F., Gish, W., Miller, W., Myers, E.W. & Lipman, D.J. (1990) Basic local alignment search tool. J Mol Biol, 215:403-10
- Anders, D.G., Kacica, M.A., Pari, G. & Punturieri, S.M. (1992) Boundaries and structure of human cytomegalovirus oriLyt, a complex origin for lytic-phase DNA replication. J Virol, 66:3373-84.
- Antolovic, D., Koch, M., Bohlmann, I., Kienle, P., Buchler, M. & Weitz, J. (2005) Short descripition of an alternative simplified method for screening recombinant clones within the "AdEasy system" by duplex PCR. BMC Biotechnol, 5:1.
- Appay, V. & Rowland-Jones, S.L. (2001) RANTES: A vesatile and controversial chemokine. Trends Immunol, 22:83-87.
- Appay, V., Brown, A., Cribbes, S., Randle, E. & Czaplewski, L. G. (1999) Aggregation of RANTES is responsible for its inflammatory properties. Characterisation of nonaggreagating, noninflammatory RANTES mutants. J Biol Chem, 274:27505-12.
- Arnon, T.I., Achdout, H., Lieberman, N., Gazit, R., Gonen-Gross, T., Katz, G., Bar-Ilan, A., Bloushtain, N., Lev, M., Joseph, A., Kedar, E., Porgador, A. & Mandelboim, O. (2004) The mechanisms controlling the recognition of tumor- and virus-infected cells by NKp46. Blood, 103:664-72.
- Arnon, T.I., Archdout, H., Levi, O., Markel, G., Saleh, N., Katz, G., Gazit, R., Gonen-Gross, T., Hanna, J., Nahari, E., Porgador, A., Honigman, A., Plachter, B., Mevorach, D., Wolf, D.G. & Mandelboim, O. (2005) Inhibition of the NKp30 activating receptor by pp65 of human cytomegalovirus. Nat Immunol, 6:515-23.
- Arnon, T.I., Lev, M., Katz, G., Chernobrov, Y., Porgador, A. & Mandelboim O. (2001) Recognition of viral hemagglutinins by NKp44 but not by NKp30. Eur J Immunol, 31:2680-89.
- Arvin, A.M., Fast, P., Myers, M., Plotkin, S. & Rabinovich, R. (2004) Vaccine development to prevent cytomegalovirus disease: report from the National Vaccine Advisory Committee. Clin Infect Dis, 39:233-39.
- Atalay, R., Zimmermann, A., Wagner, M., Borst, E., Benz, C., Messerle, M. & Hengel, H. (2002) Identification and expression of human cytomegalovirus transcription units coding for two distinct Fcgamma receptor homologs. J Virol, 76:8596-08.
- Azizkhan, J.C., Jensen, D.E., Pierce, A.J. & Wade, M. (1993) Transcription from TATA-less promoters: Dihydrofolate reductase as a model. Crit Rev Eukaryot Gene Expr, 3:229-54.
- Bairoch, A., Bucher, P. & Hofmann, K. (1997) The PROSITE database, its status in 1997. Nucleic Acids Res, 25:217-21
- Baldick, C.J. Jr & Shenk, T. (1996) Proteins associated with purified human cytomegalovirus particles. J Virol, 70:6097-05
- Barry, M. & Bleackley, R.C. (2002) Cytotoxic T lymphocytes: all roads lead to death. Nat Rev Immunol, 2:401-09.
- Bauer, S., Groh, V., Wu, J., Steinle, A., Phillips, J.H., Lanier, L.L. & Spies, T. (1999) Activation of NK cells and T cells by NKG2D, a receptor for stress-inducible MICA. Science, 285:730-31.

- Baum, E.Z., Bebernitz, G.A., Hulmes, J.D., Muzithras, V.P., Jones, T.R. & Gluzman, Y. (1993) Expression and analysis of the human cytomegalovirus UL80-encoded protease: Identification of autoproteolytic sites. J Virol, 67:497-06.
- Baxter, M.K. & Gibson, W. (2001) Cytomegalovirus basic phosphoprotein (pUL32) binds to capsids in vitro through its amino one-third. J Virol, 75:6865-73.
- Beck, S. & Barell, B.G. (1988) Human cytomegalovirus encodes a glycoprotein homologous to MHC class-I antigens. Nature, 331:269-72.
- Beersma, M.F.C., Bijlmakers, M.J.E. & Ploegh, H.L. (1993) Human cytomegalovirus down-regulates HLA class I expression by reducing the stability of class I H chains. J Immunol, 151:4455-64.
- Bendstenn, J.D., Nielsen, H., von Heijne, G. & Brunak, S. (2004) Improved prediction of signal peptides: SignalP 3.0. J Mol Biol, 340:783-95.
- Benedict, C.A., Butrovich, K.D., Lurain, N.S., Corbeil, J., Rooney, I., Schneider, P., Tschopp, J. & Ware, C.F. (1999) Cutting edge: A novel viral TNF receptor superfamily member in virulent strains of human cytomegalovirus. J Immunol, 162:6967-70.
- Benihoud, K., Yeh, P. & Perricaudet, M. (1999) Adenovirus vectors for gene delivery. Curr Opin Biotechnol, 10:440-47.
- Benko, D.M., Haltiwanger, R.S., Hart, G.W. & Gibson, W. (1988) Virion basic phosphoprotein from human cytomegalovirus contains O-linked N-acetylglucosamine. Proc Natl Acad Sci USA, 85:2573-77.
- Bernard, G., Raimondi, V., Alberti, I., Pourtein, M., Widjenes, J., Ticchioni, M. & Bernard A. (2000) CD99 (E2) up-regulates alpha4beta1-dependent T cell adhesion to inflamed vascular endothelium under flow conditions. European J Immunol, 30: 3061-65
- Bernard, G., Zoccola, D., Deckert, M., Breittmayer, J.P., Aussel, C. & Bernard A. (1995) The E2 molecule (CD99) specifically triggers homotypic aggregation of CD4+ CD8+ thymocytes. J Immunol, 154:26-32
- Betts, M.R., Brenchley, J.M., Price, D.A., De Rosa, S.C., Douek, D.C., Roederer, M. & Koup, R.A. (2003) Sensitive and viable identification of antigen-specific CD8+ T cells by a flow cytometric assay for degranulation. J Immunol Methods, 281:65-78.
- Bhella, D., Rixon, F.J. & Dargan, D.J. (2000) Cryomicroscopy of human cytomegalovirus virions reveals more densely packed genomic DNA than in herpes simplex virus type I. J Mol Biol, 295: 155-61.
- Biassoni, R., Cantoni, C., Pende, D., Sivori, S., Parolini, S., Vitale, M., Bottino, C. & Moretta, A. (2001) Human natural killer cell receptors and coreceptors. Immunol Rev, 181:203-14.
- Billstrom, M.A., Johnson, G.L., Avdi, N.J. & Worthen, G.S. (1998) Intracellular signaling by the chemokine receptor US28 during human cytomegalovirus infection. J Virol, 72:5535-44.
- Biron, C.A. (1997) Activation and function of natural killer cell responses during viral infections. Curr Opin Immunol, 9:24-34.
- Biron, C.A., Byron, K.S & Sullivan, J.L. (1989) Severe herpesvirus infections in an adolescent without natural killer cells. N Engl J Med, 320:1731-35.

- Biron, C.A., Nguyen, K.B., Pien, G.C., Cousens, L.P. & Salazar-Mather, T.P. (1999) Natural killer cells in antiviral defense: function and regulation by innate cytokines. Annu Rev Immunol, 17:189-220.
- Bluman, E.M., Bartynski, K.J., Avalos, B.R. & Caligiuri, M.A. (1996) Human natural killer cells produce abundant macrophage inflammatory protein-1α in response to moncyte-derived cytokines. J Clin Invest, 97:2722-27.
- Bodaghi, B., Jones, T.R., Zipeto, D., Vita, C., Sun, L., Laurent, L., Arenzana-Seisdedos, F., Virelizier, J.L. & Michelson, S. (1998) Chemokine sequestration by viral chemoreceptors as a novel viral escape strategy: Withdrawal of chemokines from the environment of cytomegalovirus-infected cells. J Exp Med, 188:855-66
- Boehme, K.W. & Compton, T. (2006) Virus entry and activation of innate immunity. In Cytomegalovirus Molecular Biology and Immunology, Ed. Reddehase, M.J., Caister Academic Press, 6:111-30.
- Bogner, E., Radsak, K. & Stinski, M.F. (1998) The gene product of human cytomegalovirus open reading frame UL56 binds the pac motif and has specific nuclease activity. J Virol, 72:2259-64.
- Bolovan-Fritts, C.A., Mocarski, E.S. & Wiedeman, J.A. (1999) Peripheral blood CD14+ cells from healthy subjects carry a circular conformation of latent cytomegalovirus genome. Blood, 93:394-98.
- Booy, F.P., Newcomb, W.W., Trus, B.L., Brown, J.C., Baker, T.S. & Steven, A.C. (1991) Liquid-crystalline, phage-like packaging of the encapsidated DNA in herpes simplex virus. Cell, 64:1007-15.
- Borysiewicz, L.K., Rodgers, B., Morris, S., Graham, S. & Sissons, J.G. (1985) Lysis of human cytomegalovirus infected fibroblasts by natural killer cells: demonstration of an interferon-independent component requiring expression of early viral proteins and characterization of effector cells. J Immunol, 134:2695-01.
- Boshart, M., Weber, F., Jahn, G., Dorsch-Hasler, K., Fleckenstein, B. & Schaffner, W. (1985) A very strong enhancer is located upstream of an immediate early gene of human cytomegalovirus. Cell, 41:521-30.
- Bottino, C., R. Castriconi, D. Pende, P. Rivera, M. Nanni, B. Carnemolla, C. Cantoni, J. Grassi, S. Marcenaro, N. Reymond, *et al* (2003) Identification of PVR (CD155) and Nectin-2 (CD112) as cell surface ligands for the human DNAM-1 (CD226) activating molecule. J Exp Med, 198:557
- Boyle, K.A. & Compton, T. (1998) Receptor-binding properties of a soluble form of human cytomegalovirus glycoprotein B. J Virol, 72:1826-33.
- Braud, V. M., Allan, D.S., O'Callaghan, C.A., Soderstrom, K., D'Andrea, A., Ogg, G.S., Lazetic, S., Young, N.T., Bell, J.I., Phillips, J.H., *et al.* (1998) HLA-E binds to natural killer cell receptors CD94/NKG2A, B and C. Nature, 391:795.
- Braud, V.M., Tomasec, P. & Wilkinson, G.W. (2002) Viral evasion of natural killer cells during human cytomegalovirus infection. Curr Top Microbiol Immunol, 269:117-29.
- Bresnahan, W.A. & Shenk, T.E. (2000) A subset of viral transcripts packaged within human cytomegalovirus particles. Science, 288:2373-76.
- Britt, W.J. & Mach, M. (1996) Human cytomegalovirus glycoproteins. Intervirology, 39:401-12.

- Browne, E.P. & Shenk, T. (2003) Human cytomeglaovirus UL83-coded pp65 virion protein inhibits antiviral gene expression in infected cells. Proc Natl Acad Sci USA, 100:11439-44.
- Browne, H., Smith, G., Beck, S. & Minson, T. (1990) A complex between the MHC class I homologue encoded by human cytomegalovirus and β2 microglobulin. Nature, 347:770-72.
- Bukowski, J.F., Woda, B.A. & Welsh, R.M. (1984) Pathogenesis of murine cytomegalovirus infection in natural killer cell-depleted mice. J Virol, 52:119-28
- Butcher, S.J., Aitken, J., Mitchell, J., Gowan, B. & Dargan, D.J. (1998) Structure of the human cytomegalovirus B capsid by electron cryomicroscopy and image reconstruction. J Struct Biol, 124:70-76.
- Cerboni, C., Mousavi-Jazi, M., Linde, A., Soderstrom, K., Brytting, M., Wahren, B., Karre, K. & Carbone, E. (2000) Human cytomegalovirus strain-dependent changes in NK cell recognition of infected fibroblasts. J Immunol, 164:4775-82.
- Cha, T.A., Tom, E., Kemble, G.W., Duke, G.M., Mocarski, E.S. & Spaete, R.R. (1996) Human cytomegalovirus clinical isolates carry at least 19 genes not found in laboratory strains. J Virol, 70:78-83.
- Chalupny, N.J., Rein-Weston, A., Dosch, S. & Cosman, D. (2006) Down-regulation of the NKG2D ligand MICA by the human cytomegalovirus glycoprotein UL142. Biochem Biophys Res Commun, 346:175-81.
- Chang, C.P., Vesole, D.H., Nelson, J., Oldstone, M.B. & Stinski, M.F. (1989) Identification and expression of a human cytomegalovirus early glycoprotein. J Virol, 63:3330-37.
- Chapman, T.L., Heikeman, A.P. & Bjorkman, P.J. (1999) The inhibitory receptor LIR-1 uses a common binding interaction to recognize class I MHC molecules and the viral homolog UL18. Immunity, 11:603-13.
- Chartier, C., Degryse, E., Gantzer, M., Dieterle, A., Pavirani, A. & Mehtali, M. (1996) Efficient generation of recombinant adenovirus vectors by homologous recombination in Escherichia Coli. J Virol, 70:4805-10.
- Chee, M.S., Bankier, A.T., Beck, S., Bohni, R., Brown, C.M., Cerny, R., Horsnell, T., Hutchinson, C.A., Kouzarides, T., Martignetti, J.A., Preddie, E., Satchwell, S.C., Tomlinson, P., Weston, K.M. & Barrell, B.G. (1990a). Analysis of the protein coding content of the sequence of human cytomegalovirus strain AD169. Curr Top Microbiol Immunol, 154:125-69
- Chee, M.S., Satchwell, S.C., Preddie, E., Weston, K.M. & Barrell, B.G. (1990b) Human cytomegalovirus encodes three G protein-coupled receptor homologues. Nature, 344:774-77.
- Chen, D.H., Jiang, H., Lee, M., Liu, F. & Zhou, Z.H. (1999) Three dimensional visualization of tegument/ capsid interactions in the intact human cytomegalovirus. Virology, 260:10-16.
- Cherrington, J.M., Khoury, E.L. & Mocaski, E.S. (1991) Human cytomegalovirus ie2 negatively regulates α gene expression via a short target sequence near the transcription start site. J Virol, 65:887-96.
- Cheung, T.C., Humphreys, I.R., Potter K.G., Norris, P.S., Shumway, H.M., Tran, B.R., Patterson, G., Jean-Jacques, R., Yoon, M., Spear, P.G., Murphy, K.M., Lurain, N.S., Benedict, C.A. & Ware, C.F. (2005) Evolutionarily

divergent herpesviruses modulate T cell activation by targeting the herpesvirus entry mediator cosignaling pathway. Proc Natl Acad Sci USA, 102:13218-23

- Child, S.J., Hakki, M., De Niro, K.L. & Geballe, A.P. (2004) Evasion of cellular antiviral responses by human cytomegalovirus TRS1 and IRS1. J Virol, 78:197-05.
- Ciccone, E., Pende, D., Viale, O., Di Donato, C., Orengo, A.M., Biassoni, R., Verdiani, S., Amoroso, A., Moretta, A. & Moretta, L. (1992) Involvement of HLA class I alleles in natural killer (NK) cell-specific functions: expression of HLA-Cw3 confers selective protection from lysis by alloreactive NK clones displaying a defined specificity (specificity 2). J Exp Med, 176:963-71
- Colberg-Poley, A.M. (1996) Functional roles of immediate early proteins encoded by the human cytomegalovirus UL36-38, UL115-UL119, TRS1/IRS1 and US3 loci. Intervirology, 39:350-60.
- Colonna, M., Borsellino, G., Falco, M., Ferrara, G.B. & Strominger, J.L. (1993) HLA-C is the inhibitory ligand that determines dominant resistance to lysis by NK1- and NK2-specific natural killer cells. Proc Natl Acad Sci USA, 90:1200-04.
- Compton, T., Nowlin, D.M. & Cooper, N.R. (1993) Initiation of human cytomegalovirus infection requires initial interaction with cell surface heparan sulfate. Virology, 193:834-41.
- Cosman, D., Fanger, N. & Borges, L. (1999) Human cytomegalovirus, MHC class I and inhibitory signalling receptors: more questions than answers. Immunol Rev, 168:177-85.
- Cosman, D., Fanger, N., Borges, L., Kubin, M., Chin, W., Peterson, L. & Hsu, M.L. (1997) A novel immunoglobulin superfamily receptor for cellular and viral MHC class I molecules. Immunity, 7:273-82.
- Cosman, D., Mullberg, J., Sutherland, C.L., Chin, W., Armitage, R., Fanslow, W., Kubin, M. & Chalupny, N.J. (2001) ULBPs, novel MHC class I-related molecules, bind to CMV glycoprotein UL16 and stimulate NK cytotoxicity through the NKG2D receptor. Immunity, 14:123-33
- Coux, O., Tanaka, K. & Goldberg, A.L. (1996) Structure and functions of the 20S and 26S proteosomes. Annu Rev Biochem, 65:801-47.
- Craighead, J.E., Kanich, R.E. & Almeida, J.D. (1972) Nonviral microbodies with viral antigenicity produced in cytomegalovirus-infected cells. J Virol, 10:766-75.
- Cranage, M.P., Kouzarides, T., Bankier, A.T., Satchwell, S., Weston, K., Tomlinson, P., Barrell, B., Hart, H., Bell, S.E., Minson, A.C. & Smith, G.L. (1986) Identification of the human cytomegalovirus glycoprotein B gene and induction of neutralizing antibodies via its expression in recombinant vaccinia virus. EMBO J, 5:3057-63
- Crnkovic-Mertens, I., Messerle, M., Milotic, I., Szepan, U., Kucic, N., Krmpotic, A., Jonjic, S. & Koszinowski, U.H. (1998) Virus attenuation after deletion of the cytomegalovirus Fc receptor gene is not due to antibody control. J Virol, 72:1377-82.
- Dargan, D.J., Jamieson, F.E., MacLean, J., Dolan, A., Addison, C. & McGeoch, D.J. (1997) The published DNA sequence of human cytomegalovirus strain AD169 lacks 929 base pairs affecting genes UL42 and UL43. J Virol, 71: 9833-36.

- Davis, B.D., Dulbecco R., Elsen, H.N. & Ginsberg, H.S. (1990) The nature of viruses. Microbiology, Lippincott, pp 769-94.
- Davis, S.J., Ikemizu, S., Wild, M.K. & van der Merwe, P.A. (1998) CD2 and the nature of protein interactions mediating cell-cell recognition. Immunol Rev, 163: 217-24
- Davison, A., Dolan, A., Akter, P., Addison, C., Dargan, D.J., Alcendor, D.J., McGeoch, D.J. & Hayward, G.S. (2003a) The human cytomegalovirus revisited: comparison with the chimpanzee cytomegalovirus genome. J Gen Virol, 84:17-28.
- Davison, A.J., Akter, P., Cunningham, C., Dolan, A., Addison, C., Dargan, D.J., Hassan-Walker, A.F., Emery, V.C., Griffiths, P.D. & Wilkinson, G.W. (2003b) Homology between the human cytomegalovirus RL11 gene family and human adenovirus E3 genes. J Gen Virol, 84:657-63
- Davis-Poynter, N.J., Lynch, D.M., Vally, H., Shellam, G.R., Rawlinson, W.D., Barrell, B.G. & Farrell, H.E. (1997) Identification and characterization of a G protein-coupled receptor homolog encoded by murine cytomegalovirus. J Virol, 71:1521-29.
- Dolan, A., Cunningham, C., Hector, R.D., Hassan-Walker, A.F., Lee, L., Addison, C., Dargan, D.J., McGeoch, D.J., Gatherer, D., Emery, V.C., Griffiths, P.D., Singzer, C., McSharry, B.P., Wilkinson, G.W.G. & Davison, A.J. (2004) Genetic content of a wild type human cytomegalovirus. J Gen Virol, 85:1301-12
- Dowler, K. W. & Veltri, R.W. (1984) In vitro neutralisation of HSV-2: inhibition by binding of normal IgG and purified Fc to virion Fc receptor (FcR). J Med Virol, 13:251-59
- Droll, A., Dougherty, S.T., Chiu, R.K., Dirks, J.F., McBride, W.H., Cooper, D.L. & Dougherty, G.J. (1995) Adhesive interactions between alternatively spliced CD44 isoforms. J Biol Chem, 270:11567-73.
- Dubin, G., Socolof, E., Frank, I. & Friedman, H.M. (1991) Herpes simplex virus type 1 Fc receptor protects infected cells from antibody-dependent cellular cytotoxicity. J Virol, 65:7046-50
- Dunn, C., Chalupny, N.J., Sutherland, C.L., Dosch, S., Sivakumar, P.V., Johnson, D.C. & Cosman, D. (2003) Human cytomegalovirus glycoprotein UL16 causes intracellular sequestration of NKG2D ligands, protecting against natural killer cell cytotoxicity. J Exp Med, 197:1427-39
- Dunn, W., Chou, C., Li, H., Hai, R., Patterson, D., Stolc, V., Zhu, H. & Liu, F. (2003) Functional profiling of a human cytomegalovirus genome. Proc Natl Acad Sci USA, 100:14223-28
- Elek, S.D. & Stern, H. (1974) Development of a vaccine against mental retardation caused by cytomegalovirus infection in utero. Lancet, 1:1-5
- Fahnestock, M.L., Johnson, J.L., Feldman, R.M., Neveu, J.M., Lane, W.S. & Bjorkman, P.J. (1995) The MHC class I homolog encoded by human cytomegalovirus binds endogenous peptides. Immunity, 3:583-90.
- Fallaux, F.J., Kranenburg, O., Cramer, S.J., Houweling, A., van Ormondt, H., Hoeben, R.C. & van der Eb, A.J. (1996) Characterisation of 911: a new helper cell line for the titration and propagation of early region 1-deleted adenoviral vectors. Hum Gene Ther, 7:215-22.

- Feire, A.L., Koss, H. & Compton, T. (2004) Cellular integrins function as entry receptors for human cytomegalovirus via a highly conserved disintegrin-like domain. Proc Natl Acad Sci USA, 101:15470-75
- Frank, I. & Friedman, H.M. (1989) A novel function of the herpes simplex virus type 1 Fc receptor: participation in bipolar bridging of antiviral immunoglobulin G. J Virol, 63:4479-88
- Friedman, H. M., Cohen, G.H., Eisenberg, R.J., Siedel, C.A. & Clines D.B. (1984) Glycoprotein C of herpes simplex virus 1 acts as a receptor for the complement component C3b on infected cells. Nature, 309:633-35
- Fuchs, A., Cella, M., Giurisato, E., Shaw, A.S. & Colonna, M. (2004) Cutting edge: CD96 (tactile) promotes NK cell-target cell adhesion by interacting with the poliovirus receptor (CD155). J Immunol, 172:3994-8.
- Gao, J.L. & Murphy, P.M. (1994) Human cytomegalovirus open reading frame US28 encodes a functional β chemokine receptor. J Biol chem, 269:28539-42.
- Gerna, G., Percivalle, E., Baldanti, F., Sozzani, S., Lanzarini, P., Genini, E., Lilleri, D. and Revello, M.G. (2000) Human cytomegalovirus replicates abortively in polymorphonuclear leukocytes after transfer from infected endothelial cells via transient microfusion events. J Virol, 74: 5629-38
- Gerna, G., Percivalle, E., Lilleri, D., Lozza, L., Fornara, C., Hahn, G., Baldanti, F. & Revello, M.G. (2005) Dendritic-cell infection by human cytomegalovirus is restricted to strains carrying functional UL131-128 genes and mediates efficient viral antigen presentation to CD8+ T cells. J Gen Virol, 86:275-84
- Gibson, W. (1996) Structure and assembly of the virion. Intervirology, 39:389-400.
- Gibson, W., Baxter, M.K. & Clopper, K.S. (1996a) Cytomegalovirus "missing" capsid protein identified as heat-aggregable product of human cytomegalovirus UL46. J Virol, 70:7454-61.
- Gibson, W., Clopper, K.S., Britt, W.J. & Baxter, M.K. (1996b) Human cytomegalovirus (HCMV) smallest capsid protein identified as product of short open reading frame located between HCMV UL48 and UL49. J Virol, 70:5680-83.
- Gibson, W., Marcy, A.I., Comolli, J.C. & Lee, J. (1990) Identification of precursor to cytomegalovirus capsid assembly protein and evidence that processing results in loss of its carboxy-terminal end. J Virol, 64:1241-49.
- Gibson, W., van Breemen, R., Fields, A., LaFemina, R. & Irmiere, A. (1984) D,L-α-difluoromethylornithine inhibits human cytomegaloviurs replication. J Virol, 50:145-54.
- Goldmacher, V.S., Bartle, L.M., Skaletskaya, A., Dionne, C.A., Kedersha, N.L., Vater, C.A., Han, J.W., Lutz, R.J., Watanabe, S., Cahir McFarland, E.D., Keiff, E.D., Mocarski, E.S. & Chittenden, T. (1999) A cytomegalovirus-encoded mitochondria-localized inhibitor of apoptosis structurally unrelated to Bcl-2. Proc Natl Acad Sci USA, 96:12536-41
- Graham, F.L., Smiley, J., Russel, W.C. & Nairn, R. (1977) Characteristics of a human cell line transformed by DNA from human adenovirus type 5. J Gen Virol, 36:59-72.
- Grazia Revello, M., Baldanti, F., Percivalle, E., Sarasini, A., De-Giuli, L., Genini, E., Lilleri, D., Labo, N. & Gerna, G. (2001) In vitro selection of

human cytomegalovirus variants unable to transfer virus and virus products from infected cells to polymorphonuclear leukocytes and to grow in endothelial cells. J Gen Virol, 82:1429-38

- Greenaway, P.J. & Wilkinson, G.W. (1987) Nucleotide sequence of the most abundantly transcribed early gene of human cytomegalovirus strain AD169. Virus Res, 7:17-31.
- Greijer, A.E., Dekkers, C.A. & Middeldorp, J.M. (2000) Human cytomegalovirus virions differentially incorporate viral and host cell RNA during the assembly process. J Virol, 74:9078-82.
- Gretch, D.R., Kari, B., Rasmussen, L., Gehrz, R.C. & Stinksi, M.F. (1988) Identification and characterisation of three distinct families of glycoprotein complexes in the envelopes of human cytomegalovirus. J Virol, 62:875-81.
- Griffin, C., Wang, E.C., McSharry, B.P., Rickards C., Browne, H., Wilkinson, G.W. & Tomasec, P. (2005) Characterisation of a highly glycosylated form of the human cytomegalovirus HLA class I homologue gpUL18. J Gen Virol, 86:2999-08
- Groh, V., Bahram, S., Bauer, S., Herman, A., Beauchamp, M. & Spies, T. (1996) Cell stress-regulated human major histocompatibility complex class I gene expressed in gastroepithelium. Proc Natl Acad Sci USA, 93:12445-50.
- Grundy, J.E., McKeating, J.A., Ward, P.J., Sanderson, A.R. & Griffiths, P.D. (1987) B2 microglobulin enhances the infectivity of cytomegalovirus and when bound to the virus enables class I HLA molecules to be used as a virus receptor. J Gen Virol, 68:793-803
- Hahn, G., Grazia-Revello, M., Patrone, M., Percivalle, E., Campanini, G., Sarasini, A., Wagner, M., Gallina, A., Milanesi, G., Koszinowski, U., Baldanti, F. & Gern, G. (2004) Human cytomegalovirus UL131-128 genes are indispensable for virus growth in endothelial cells and virus transfer to leukocytes. J Virol, 78:10023-33
- Hahn, G., Jores, R. & Mocarski, E.S. (1998) Cytomegalovirus remains latent in a common precursor of dendritic and myeloid cells. Proc Natl Acad Sci USA, 95:3937-42.
- Hahn, J.H., Kim, M.K., Choi, E.Y., Kim, S.H., Sohn, H.W., Ham, D.I., Chung, D.H., Kim, T.J., Lee, W.J., Park, C.K., Ree, H.J. & Park SH. (1997) CD99 (MIC2) regulates the LFA-1/ICAM-1-mediated adhesion of lymphocytes, and its gene encodes both positive and negative regulators of cellular adhesion. J Immunol, 159: 2250-58
- Hamzeh, F.M., Lietman, P.S., Gibson, W. & Hayward, G.S. (1990) Identification of the lytic origin of DNA replication in human cytomegalovirus by a novel approach utilizing ganciclovir-induced chain termination. J Virol, 64:6184-95.
- Hasan, M., Krmpotic, A., Ruzsics, Z., Bubic, I., Lenac, T., Halenius, A., Loewendorf, A., Messerle, M., Hengel, H., Jonjic, S. & Koszinowski U.H. (2005) Selective down-regulation of the NKG2D ligand H60 by mouse cytomegalovirus m155 glycoprotein. J Virol, 79:2920-30
- Hassan-Walker, A.F., Okwuadi, S., Lee, L., Griffiths, P.D. & Emery, V.C. (2004) Sequence variability of the alpha chemokine UL146 from clinical strains of human cytomegalovirus. J Med Virol, 74:573-79.
- Hayhurst, G.P., Bryant, L.A., Caswell, R.C., Walker, S.M. & Sinclair, J.H. (1995) CCAAT box-dependent activation of the TAT-less human DNA

polymerase α promoter by the human cytomegalovirus 72-kilodalton major immediate-early protein. J Virol, 69:182-88

- He, R., Ruan, Q., Qi, Y., Ma, Y.P., Huang, Y.J., Sun, Z.R. and Ji, Y.H. (2006) Human cytomegalovirus-encoded alpha -chemokines exhibit high sequence variability in congenitally infected newborns. J Infect Dis, 193:788-91.
- He, T.C., Zhou, S., Da Costa, L.T., Yu, J., Kinzler, K.W. & Vogelstein, B. (1998) A simplified system for generating recombinant adenoviruses. Proc Natl Acad Sci, 95:2509-14.
- Heemels, M-T. & Ploegh, H.L. (1995) Generation, translocation and presentation of MHC class I-restricted peptides. Annu Rev Biochem, 64:463-91.
- Hegde, N.R. & Johnson, D.C. (2003) Human cytomegalovirus US2 causes similar effects on both major histocompatibility complex class I and II proteins in epithelial and glial cells. J Virol, 77:9287-94.
- Hengel, H., Brune, W. & Koszinowski, U.H. (1998) Immune evasion by cytomegalovirus - survival strategies of a highly adapted oppurtunist. Trends Microbiol, 6:190-97.
- Hengel, H., Flohr, T., Hammerling, G.J., Koszinowski, U.H. & Momberg, F. (1996) Human cytomegalovirus inhibits peptide translocation into the endoplasmic reticulum for MHC class I assembly. J Gen Virol, 77:2287-96.
- Hengel, H., Koopman, J.O., Flohr, T., Muranyi, Y., Goulmy, E., Hammerling, G.J., Koszinowski, U.H. & Momburg, F. (1997) A viral ER-resident glycoprotein inactivates the MHC-encoded peptide transporter. Immunity, 6:623-32.
- Hermiston, T.W., Malone, C.L., Witte, P.R. & Stinksi, M.F. (1987) Identification and characterization of the human cytomegalovirus immediate-early region 2 that stimulates gene expression from an inducible promoter. J Virol, 61:3214-21.
- Hewitt, E.W., Gupta, S.S. & Lehner, P.J. (2001) The human cytomegalovirus gene product US6 inhibits ATP binding by TAP. EMBO J, 20:387-96.
- Hirai, K. & Watanabe, Y. (1976) Induction of α type DNA polymerases in human cytomegalovirus-infected WI-38 cells. Biochim Biophs Acta, 447:328-39.
- Hoffman, K. & Stoffel, W. (1993) TMbase - A database of membrane spanning protein segments. Biol Chem, 374:166
- Hofmann, H., Sindre, H. & Stamminger, T. (2002) Functional interaction between the pp71 protein of human cytomegalovirus and the PML-interacting protein human Daxx. J Virol, 76:5769-83.
- Hollenbach, A.D., McPherson, C.J., Mientjes, E.J., Lyengar, R. & Grosveld, G. (2002) Daxx and histone deacetylase II associate with chromatin through an interaction with core histones and the chromastin-associated protein Dek. J Cell Sci, 115:3319-30
- Homman-Loudiyi, M., Hultenby, K., Britt, W. & Soderberg-Naucler, C. (2003) Envelopment of human cytomegalovirus occurs by budding into Golgi-derived vacuole compartments positive for gB, Rab 3, trans-golgi network 46, and mannosidase II. J Virol, 77:3191-203.
- Horwitz, M.S. (2001) Adenoviruses. In Fields Virology, eds Knipe, B.N., Howley, D.M., Chanock, R.M., Melnick, J.L., Monath, T.P., Rolzman, B. & Straws, S.E. Lippincott, Philadelphia, pp2301-2326.

- Hosfield, T. & Eldridge, L. (2000) Generate adenovirus vectors in *E.coli* by homologous recombination with the AdEasy adenoviral vector system. Strategies Newsletter, 13:100-102.
- Houchins, J. P., Lanier, L.L., Niemi, E.C., Phillips, J.H. & Ryan, J.C. (1997) Natural killer cell cytolytic activity is inhibited by NKG2-A and activated by NKG2-C. J Immunol, 158:3603.
- Hsu, K.C., Chida, S., Geraghty, D.E. & Dupont, B. (2002) The killer cell immunoglobulin-like receptor (KIR) genomic region: gene-order, haplotypes and allelic polymorphism. Immunol Reviews, 190:40-52.
- Huber, M.T. & Compton, T. (1998) The human cytomegalovirus UL74 gene encodes the third component of the glycoprotein H-glycoprotein L-containing envelope complex. J Virol, 72:8191-97.
- Ibanez, C.E., Schrier, R., Ghazal, P., Wiley, C. & Nelson, J.A. (1991) Human cytomegalovirus productively infects primary differentiated macrophages. J Virol, 65:6581-88.
- Inngjerdingen, M., Damaj, B. & Maghazachi, A.A. (2000) Human NK Cells Express CC Chemokine Receptors 4 and 8 and Respond to Thymus and Activation-Regulated Chemokine, Macrophage-Derived Chemokine, and I-309. J Immunol, 164: 4048-54.
- Irmiere, A. & Gibson, W. (1983) Isolation and characterisation of a noninfectious virion-like particle released from cells infected with human strains of cytomegalovirus. Virology, 130:118-33.
- Irmiere, A. & Gibson, W. (1985) Isolation of human cytomegalovirus intranuclear capsids, characterization of their protein constituents, and demonstration that the B-capsid assembly protein is also abundant in noninfectious enveloped particles. J Virol, 56:277-83
- Ishov, A.M., Stenberg, R.M. & Maul, G.G. (1997) Human cytomegalovirus immediate early interaction with host nuclear structures: Definition of an immediate transcript environment. J Cell Biol, 138:5-16.
- Ishov, A.M., Vladimirova, O.V. & Maul, G.G. (2002) Daxx-mediated accumulation of human cytomegalovirus tegument protein pp71 at ND10 facilitates initiation of viral infection at these nuclear domains. J Virol, 76:7705-12.
- Ito, M., Maruyama, T., Saito, N., Koganei, S., Yamamoto, K. & Matsumoto, N. (2006) Killer cell lectin-like receptor G1 binds three members of the classical cadherin family to inhibit NK cell cytotoxicity. J Exp Med, 203(2):289-95
- Ito, M., Watanabe, M., Ihara, T., Kamiya, H. and Sakurai, M. (1995) Increased expression of adhesion molecules (CD54, CD29 and CD44) on fibroblasts infected with cytomegalovirus. Microbiol Immunol, 39:129-33.
- Iwayama, S., Yamamoto, T., Furuya, T., Kobayashi, R., Ikuta, K. & Hirai, K. (1994) Intracellular localization and DNA-binding activity of a class of viral early phosphoproteins in human fibroblasts infected with human cytomegalovirus (Towne strain). J Gen Virol, 75:3309-18.
- Jenkins, C., Abendroth, A. and Slobedman, B. (2004) A novel viral transcript with homology to human IL-10 is expressed during latent human cytomegalovirus infection. J Virol, 78:1440-1447.

- Jenkins, D.E., Martens, C.L. & Mocarski, E.S. (1994) Human cytomegalovirus late protein encoded by ie2: A transactivator as well as a repressor of gene expression. J Gen Virol, 75:2337-48.
- Johnson, D.C. & Hegde, N. R. (2002) Inhibition of the MHC class II antigen presentation pathway by human cytomegalovirus. Curr Top Microbiol Immunol, 269:101-15.
- Jones, T.R. & Muzithras, V.P. (1992) A cluster of dispensable genes within the human cytomegalovirus genome short component: IRS1, US1 through US5, and the US6 family. J Virol, 66:2541-46.
- Jones, T.R. & Sun, L. (1997) Human cytomegalovirus US2 destabilizes major histocompatibility complex class I heavy chains. J Virol, 71:2970-79.
- Jones, T.R., Hanson, L.K., Sun, L., Slater, J.S., Stenberg, J.M. & Campbell, A.E. (1995) Multiple independent loci within the human cytomegalovirus unique short region downregulate expression of major histocompatibility complex class I heavy chains. J Virol, 69:4830-41
- Jones, T.R., Wiertz, E.J., Sun, L., Fish, K.N., Nelson, J.A. & Ploegh, H.L. (1996) Human cytomegalovirus US3 impairs transport and maturation of major histocompatibility complex class I heavy chains. Proc Natl Acad Sci USA, 93:11327-33.
- Jorgensen, J.L., Reay, P.A., Ehrich, E.W. & Davis, M.M. (1992) Molecular components of T-cell recognition. Annu Rev Immunol, 10:835-73.
- Julenius, K., Molgaard, A., Gupta, R. & Brunak, S. (2005) Prediction, conservation analysis and structural characterisation of mammalian mucin-type O-glycosylation sites. Glycobiology, 15:153-64.
- Kahl, M., Siegel-Axel, D., Stenglein, S., Jahn, G. & Singzer, C. (2000) Efficient lytic infection of human arterial endothelial cells by human cytomegalovirus strains. J Virol, 74:7628-35.
- Kari, B., Cooper, J., Goertz, R. & Radeke, B. (1994) The human cytomegalovirus UL100 gene encodes the gGII glycoproteins recognized by group 2 monoclonal antibodies. J Gen Virol, 75:3081-86.
- Karlin, S., Mocarski, E.S. & Schachtel, G.A. (1994) Molecular evolution of herpesviruses: Genomic and protein sequence comparisons. J Virol, 68:1886-902.
- Katz, F.E., Tindle, R., Sutherland, D.R. & Greaves, M.F. (1985) Identification of a membrane glycoprotein associated with haemopoietic progenitor cells. Leuk Res, 9:191-98.
- Kaye, J.F., Gompels, U.A. & Minson, C.A. (1992) Glycoprotein H of human cytomegalovirus (HCMV) forms a stable complex with the HCMV UL115 gene product. J Gen Virol, 73:2693-98.
- Keay, S. & Baldwin, B. (1991) Anti-idiotype antibodies that mimic gp86 of human cytomegalovirus inhibit viral fusion but not attachment. J Virol, 65:5124-28.
- Kelly, C., Van Driel, R. & Wilkinson, G.W. (1995) Disruption of PML-associated nuclear bodies during human cytomegalovirus infection. J Gen Virol, 76:2887-93.
- Kemble, G.W. & Mocarski, E.S. (1989) A host cell protein binds to a highly conserved sequence element (pac-2) within the cytomegalovirus a sequence. J Virol, 63:4715-28.

- Kiehl, A., Huang, L., Franchi, D. & Anders, D.G. (2003) Multiple 5' ends of human cytomegalovirus UL57 transcripts identify a complex, cycloheximide-resistant promoter region that activates oriLyt. Virology, 314:410-22.
- Kim, J.S., Choi, S.E., Yun, I.H., Kim J.Y., Ahn, C., Kim, S.J., Ha, J., Hwang, E.S., Cha, C.Y., Miyagawa, S. & Park, G.C. (2004) Human cytomegalovirus UL18 alleviated human NK-mediated swine endothelial cell lysis. Biochem Biophys Res Commun, 315:144-50
- Kledal, T.N., Rosenkilde, M.M. & Schwarttz, T.W. (1998) Selective recognition of the membrane-bound CXC3 chemokine, fractalkine, by the human cytomegalovirus-encoded broad-spectrum receptor US28. FEBS Lett, 441:209-14.
- Kondo K., Xu, J. & Mocarski, E.S. (1996) Human cytomegalovirus latent infection of granulocyte-macrophage progenitors. Proc Natl Acad Sci USA, 93:11137-42.
- Korioth, F., Maul, G.G., Plachter, B., Stamminger, T. & Frey, J. (1996) The nuclear domain 10 (ND10) is disrupted by the human cytomegalovirus gene product IE1. Exp Cell Res, 229:155-58.
- Kotenko, S.V., Saccani, S., Izotova, L.S., Mirochnitchenko, O.V. & Pestka, S. (2000) Human cytomegalovirus harbours its own unique IL-10 homolog (cmvIL-10). Proc Natl Acad Sci USA, 97:1695-700.
- Krmpotic, A., Hasan, M., Loewendorf, A., Saulig, T., Halenius, A., Lenac, T., Polic, B., Bubic, I., Kriegeskorte, A., Pernjak-Pugel, E., Messerle, M., Hengel, H., Busch, D.H., Koszinowski, U.H. & Jonjic, S. (2005) NK cell activation through the NKG2D ligand MULT-1 is selectively prevented by the glycoprotein encoded by mouse cytomegalovirus gene m145. J Exp Med, 201:211-20
- Krogh, A., Larsson, B., von Heijne, G. & Sonnhammer, E.L.L. (2001) Predicting transmembrane protein topology with a hidden Markov model: Application to complete genomes. J Mol Biol, 305:567-80.
- Krosky, P.M., Baek, M.C., Jahng, W.J., Barrera, I., Harvey, R.J., Biron, K.K., Coen, D.M. & Sethna, P.B. (2003) The human cytomegalovirus UL44 protein is a substrate for the UL97 protein kinase. J Virol, 77:7720-7.
- Kubin, M., Cassiano, L., Chalupny, J., Chin, W., Cosman, D., Fanslow, W., Mullberg, J., Rousseau, A.M., Ulrich, D. & Armitage, R. (2001) ULBP1, 2, 3: novel MHC class I-related molecules that bind to human cytomegalovirus glycoprotein UL16, activate NK cells. Eur J Immunol, 31:1428-37
- Kuhn, D.E., Beall, C.J. & Kolattukudy, P.E. (1995) The cytomegalovirus US28 protein binds multiple CC chemokines with high affinity. Biochem Biophys Res Commun, 211:325-30.
- LaFemina, R.L., Pizzorno, M.C., Mosca, J.D. & Hayward, G.S. (1989) Expression of the acidic nuclear immediate-early protein (IE1) of human cytomegalovirus in stable cell lines and its preferential association with metaphase chromosomes. Virology, 172:584-600
- Landini, M.P., Lazzarotto, T., Xu, J., Geballe, A.P. & Mocarski, E.S. (2000) Humoral immune response to proteins of human cytomegalovirus latency-associated transcripts. Biol Blood Marrow Transplant, 6:100-08.
- Landini, M.P., Severi, B., Furlini, G. & Badiali, D.G.L. (1987) Human cytomegalovirus structural components: Intracellular and intraviral

localization of p28 and p65-69 by immunoelectron microscopy. Virus Res, 8:15-23.

- Lang, D. & Stamminger, T. (1993) The 86-kilodalton IE-2 protein of human cytomegalovirus is a sequence-specific DNA-binding protein that interacts directly with the negative autoregulatory response element located near the cap site of the IE-1/2 enhancer/promoter. J Virol, 67:323-31
- Lange, R., Peng, X., Wimmer, E., Lipp, M. & Bernhardt, G. (2001) The poliovirus receptor CD155 mediates cell-to-matrix contacts by specifically binding to vitronectin. J Virol, 285(2):218-27
- Lanier, L.L. (1998) NK receptors. Annu Rev Immunol, 16:359-93.
- Lanier, L.L. (2005) NK cell recognition. Annu Rev Immunol, 23:225-74.
- Larsson, S., Soderberg-Naucler, C., Wang, F.Z. & Moller, E. (1998) Cytomegalovirus DNA can be detected in peripheral blood mononuclear cells from all seropositive and most seronegative healthy blood donors over time. Transfusion, 38:271-78.
- Lee, J.Y., Irmiere, A. & Gibson, W. (1988) Primate cytomegalovirus assembly: Evidence that DNA packaging occurs subsequent to B capsid assembly. Virology, 167:87-96.
- Lee, N., Llano, M., Carretero, M., Ishitani, A., Navarro, F., Lopez-Botet, M. & Geraghty, D.E. (1998) HLA-E is a major ligand for the natural killer inhibitory receptor CD94/NKG2A. Proc Natl Acad Sci USA, 95:5199-204.
- Lehner, P.J., Karttunen, J.T., Wilkinson, G.W. & Cresswell, P. (1997) The human cytomegalovirus US6 glycoprotein inhibits transporter associated with antigen processing-dependent peptide translocation. Proc Natl Acad Sci, 94:6904-09.
- Leong, C.C., Chapman, T.L., Bjorkman, P.J., Formankova, D., Mocarski, E.S., Phillips, J.H. & Lanier, L.L. (1998) Modulation of natural killer cell cytotoxicity in human cytomegalovirus infection: the role of endogenous class I major histocompatibility complex and a viral class I homolog. J Exp Med, 187:1681-87
- Lepin, E.J., Bastin, J.M., Allan, D.S., Roncador, G., Braud, V.M., Mason, D.Y., van der Merwe, P.A., McMichael, A.J., Bell, J.I., Powis, S.H. & O'Callaghan, C.A. (2000) Functional characterisation of HLA-F and binding of HLA-F tetramers to ILT2 and ILT4 receptors. Eur J Immunol, 30:3552-61
- Li, C.R., Greenberg, P.D., Gilbert, M.J., Goodrich, J.M. & Riddell, S.R. (1994) Recovery of HLA-restricted cytomegalovirus (CMV)-specific T-cell responses after allogeneic bone marrow transplant: Correlation with CMV disease and effect of ganciclovir prophylaxis. Blood, 83:1971-79
- Li, L., Nelson, J.A. & Britt, W.J. (1997) Glycoprotein H-related complexes of human cytomegalovirus: identification of a thrid protein in the gCIII complex. J Virol, 71:3090-97.
- Lilley, B.N. & Ploegh, H.L. (2004) A membrane protein is required for dislocation of misfolded proteins from the ER. Nature, 429:834-40.
- Lilley, B.N., Ploegh, H. & Tirabassi, R.S. (2001) Human cytomegalovirus open reading frame TRL11/IRL11 encodes an immunoglobulin G Fc-binding protein. J Virol, 75:11218-21.
- Liu, B. & Stinski, M.F. (1992) Human cytomegalovirus contains a tegument protein that enhances transcription from promoters with upstream ATF and AP-1 cis-acting elements. J Virol, 66:4434-44.

- Liu, B., Hermiston, T.W. & Stinksi, M.F. (1991) A cis-acting element in the major immediate-early (IE) promoter of human cytomegalovirus is required for negative regulation by IE2. J Virol, 65:897-903.
- Ljunggren H-G. & Karre, K. (1990) In search of the "missing self": MHC molecules and NK cell recognition. Immunol Today, 11:237-44.
- Lockridge, K.M., Zhou, S.S., Kravtiz, R.H., Johnson, J.L., Sawai, E.T., Blewett, E.L. & Barry, P.A. (2000) Primate cytomegaloviruses encode and express and IL-10-like protein. Virology, 268:272-80.
- Lodoen, M., Ogasawara, K., Hamerman, J.A., Arase, H., Houchins, J.P., Mocarski, E.S. & Lanier, L.L. (2003) NKG2D-mediated natural killer cell protection against cytomegalovirus is impaired by viral gp40 modulation of retinoic acid early inducible 1 gene molecules. J Exp Med, 197:1245-53
- Lodoen, M.B., Abenes, G., Umamoto, S., Houchins, J.P., Liu, F. & Lanier, L.L. (2004) The cytomegalovirus m155 gene product subverts natural killer cell antiviral protection by disruption of H60-NKG2D interactions. J Exp Med, 200:1075-81
- Long, E.O. (1999) Regulation of immune response through inhibitory receptors. Annu Rev Immunol, 17:875-904.
- Lucin, P., Jonjic, S., Messerle, M., Polic, B., Hengel, H. & Koszinowski, U.H. (1994) Late phase inhibition of murine cytomegalovirus replication by synergistic action of interferon-γ and tumour necrosis factor. J Gen Virol, 75:101-10.
- Lunetta, J.M. & Weideman, J.A. (2000) Latency-associated sense transcripts are expressed during in vitro human cytomegalovirus productive infection. Virology, 278:467-76.
- MacCormac, L.P. & Grundy J.E. (1996) Human cytomegalovirus induces an Fcγ receptor (Fc γR) in endothelial cells and fibroblasts that is distinct from the human cellular Fc γRs. J Infect Dis, 174:1151-61.
- MacCormac, L.P. & Grundy, J.E. (1999) Two clinical isolates and the Toledo strain of cytomegalovirus contain endothelial cell tropic variants that are not present in the AD169, Towne or Davis strain. J Med Virol, 74:7720-29.
- MacDonald, M.R., Burney, M.W., Resnick, S.B. & Virgin, H.W.I. (1999) Spliced mRNA encoding the murine cytomegalovirus chemokine homolog predicts a β chemokine of novel structure. J Virol, 73:3682-91.
- MacDonald, M.R., Li, X.Y. & Virgin, I.H.W. (1997) Late expression of a β chemokine homolog by murine cytomegalovirus. J Virol, 71:1671-78.
- Mach, M., Kropff, B., Dal Monte, P. & Britt, W. (2000) Complex formation by human cytomegalovirus glycoproteins M (gpUL100) and N (gpUL73). J Virol, 74:11881-92.
- Mandelboim, O., Lieberman, N., Lev, M., Paul, L., Arnon, T.I., Bushkin, Y., Davis, D.M., Strominger, J.L., Yewdell, J.W. & Porgador, A. (2001) Recognition of haemagglutinins on virus-infected cells by NKp46 activated lysis by human NK cells. Nature, 409:1055-60
- Mar, E.C., Patel, P.C. & Huang, E.S. (1981) Human cytomegalovirus-associated DNA polymerase and protein kinase activities. J Gen Virol, 57:149-56.
- Markel, G., Lieberman, N., Katz, G., Arnon, T.I., Lotem, M., Drize, O., Blumberg, R.S., Bar-Haim, E., Mader, R., Eisenbach, L. & Mandelboim, O. (2002) CD66a interactions between human melanoma and NK cells: a novel

class I MHC-independent inhibitory mechanism of cytotoxicity. J Immunol, 168(6):2803-10

- Masse, M.J., Karlin, S., Schachtel, G.A. & Mocarski, E.S. (1992) Human cytomegalovirus origin of DNA replication (oriLyt) resides within a highly complex repetitive region. Proc Natl Acad Sci USA, 89:5246-50.
- Mathew, S.O., Kumaresan, P.R., Lee, J.K., Huynh, V.T. & Mathew, P.A. (2005) Mutational analysis of the human 2B4 (CD244) /CD48 interaction: Lys68 and Glu70 in the V domain of 2B4 are critical for CD48 binding and functional activation of NK cells. J Immunol, 175:1005-13.
- McGavran, M.H. & Smith, M.G. (1965) Ultrastructural, cytochemical and microchemical observations on cytomegalovirus (salivary gland virus) infection of human cells in tissue culture. Exp Mol Pathol, 4:1-10.
- McGeoch, D.J., Dalrymple, M.A., Davison, A.J., Dolan, A., Frame, M.C., McNab, D., Perry, L.J., Scott, J.E. & Taylor P. (1988) The complete DNA sequence of the long unique region in the genome of herpes simplex virus type I. J Gen Virol, 69:1531-74.
- McSharry, B.P., Jones, C.J., Skinner, J.W., Kipling, D. & Wilkinson, G.W. (2001) Human telomerase reverse transcriptase-immortalized MRC-5 and HCA2 human fibroblasts are fully permissive for human cytomegalovirus. J Gen Virol, 82:855-63
- McSharry, B.P., Tomasec, P., Neale, M.L. & Wilkinson, G.W. (2003) The most abundantly transcribed human cytomegalovirus gene (beta 2.7) is non-essential for growth in vitro. J Gen Virol, 84:2511-16.
- McVoy, M.A., Nixon, D.E., Adler, S.P. & Mocarski, E.S. (1998) Sequences within the herpesvirus-conserved pac1 and pac2 motifs are required for cleavage and packaging of the murine cytomegalovirus genome. J Virol, 72:48-56
- Meier, J.L. & Stinski, M.F. (1996) Regulation of human cytomegalovirus immediate-early gene expression. Intervirology, 39:331-42.
- Mendelson, M., Monard, S., Sissons, P. & Sinclair, J. (1996) Detection of endogenous human cytomegalovirus in CD34+ bone marrow progenitors. J Gen Virol, 77:3099-102.
- Metcalf, D. (1989) The molecular control of cell division, differentiation commitment and maturation in haemopoietic cells. Nature, 339:27-30.
- Michelson, S., Alcami, J., Kim, S.J., Danielpour, D., Bachelerie, F., Picard, L., Bessia, C., Paya, C. & Viralizier, J.L. (1994) Human cytomegalovirus infection induces transcription and secretion of transforming growth factor beta 1. J Virol, 68:5730-37
- Miller, D.M. & Sedmak, D.D. (1999) Viral effects on antigen processing. Curr Opin Immunol, 11:94-99.
- Miller, D.M., Rahill, B.M., Boss, J.M., Lairmore, M.D., Durbin, J.E., Waldman, J.W. & Sedmak, D.D. (1998) Human cytomegalovirus inhibits major histocompatibility complex class II expression by disruption of the Jak/Stat pathway. J Exp Med, 187:675-83.
- Misaghi, S., Sun, Z.Y., Stern, P., Gaudet, R., Wagner, G. & Ploegh, H. (2004) Structural and functional analysis of human cytomegalovirus US3 protein. J Virol, 78:413-23.

- Mocarski, E.S. & Courcelle, T.C. (2001) Cytomegaloviruses and their replication. In Fields Virology, eds. D.M. Knipe and P.M. Howley. Philadelphia:Lippincott Williams and Wilkins, pp2629-73.
- Mocarski, E.S., Abenes, G.B., Manning, W.C., Sambucetti, L.C. & Cherrington, J.M. (1990) Molecular genetic analysis of cytomegalovirus gene regulation in growth, persistence and latency. Curr Top Microbiol Immunol, 154:47-74.
- Mocarski, E.S., Kemble, G.W., Lyle, J.M. & Greaves, R.F. (1996) A deletion mutant in the human cytomegalovirus gene encoding IE1 (491aa) is replication defective due to a failure in autoregulation. Proc Natl Acad Sci USA, 96:11321-26.
- Mocarski, E.S., Liu, A.C. & Spaete, R.R. (1987) Structure and variability of the a sequence in the genome of human cytomegalovirus (Towne strain). J Gen Virol, 68:2223-30
- Mocarski, E.S., Prichard, M.N., Tan, C.S. & Brown, J.M. (1997) Reassessing the organization of the UL42-UL43 region of the human cytomegalovirus strain AD169 genome. Virology, 239:169-75.
- Moretta, A., Bottino, C., Vitale, M., Pende, D., Biassoni, R., Mingari, M.C. & Moretta, L. (1996) Receptors for HLA-class I molecules in human natural killer cells. Annu Rev Immunol, 14:619-48.
- Moretta, A., Vitale, M., Bottino, C., Orengo, A.M., Morelli, L., Augugliaro, R., Barbaresi, M., Ciccone, E. & Moretta, L. (1993) p58 molecules as putative receptors for MHC class I molecules in human natural killer (NK) cells Anti-p58 antibodies reconstitute lysis of MHC class I protected cells in NK clones displaying different specificities. J Exp Med, 178:597-604
- Moretta, L., & Moretta, A. (2004) Unravelling natural killer cell function: triggering and inhibitory human NK receptors. EMBO J, 23:255-59.
- Morris, R.J., Chong, L.C., Wilkinson, G.W. & Wang, E.C. (2005) A high-efficiency system of natural killer cell cloning. J Immunol Methods. 307:24-33.
- Mueller, S. & Wimmer, E. (2003) Recruitment of nectin-3 to cell-cell junctions through trans-heterophilic interaction with CD155, a vitronectin and poliovirus receptor that localizes to alpha(v)beta3 integrin-containing membrane microdomains. J Biol Chem, 278:31251-60
- Murphy, E., Rigoutsos, I., Shibuya, T. & Shenk, T.E. (2003a) Reevaluation of human cytomegalovirus coding potential. Proc Natl Acad Sci USA, 100:13585-90.
- Murphy, E., Yu, D., Grimwood, J., Schmutz, J., Dickson, M., Jarvis, M.A., Hahn, G., Nelson, J.A., Myers, R.M. & Shenk, T.E. (2003b) Coding potential of laboratory and clinical strains of human cytomegalovirus. Proc Natl Acad Sci USA, 100:14976-81.
- Murphy, J.C., Fischle, W., Verdin, E. & Sinclair, J.H. (2002) Control of cytomegalovirus lytic gene expression by histone acetylation. EMBO J, 21:1112-20
- Myerson, D., Hackman, R.C., Nelson, J.A., Ward, D.C. & McDougall, J.K. (1984) Widespread presence of histologically occult cytomegalovirus. Hum Pathol, 15:430-39.

- Neote, K., DiGregorio, D., Mak, J.Y., Horuk, R. & Schall, T.J. (1993) Molecular cloning, functional expression and signaling characteristics of a C-C chemokine receptor. Cell, 72:415-25.
- Nowlin, D.M., Cooper, N.R. & Compton, T. (1991) Expression of a human cytomegalovirus receptor correlates with infectibility of cells. J Virol, 65:3114-21.
- Odeberg, J., Cerboni, C., Browne, H., Karre, K., Moller, E., Carbone, E. & Soderberg-Naucler, C. (2002) Human cytomegalovirus (HCMV)-infected endothelial cells and macrophages are less susceptible to natural killer lysis independent of the downregulation of classical HLA class I molecules or expression of the HCMV class I homologue, UL18. Scand J Immunol, 55:149-61
- Oien, N.L., Thomsen, D.R., Wathen, M.W., Newcomb, W.W., Brown, J.C. & Homa, F.L. (1997) Assembly of herpes simplex virus capsids using the human cytomegalovirus scaffold protein: critical role of the C terminus. J Virol, 71:1281-91.
- Oliva, A., Kinter, A.L., Vaccarezza, M., Rubbert, A., Catanzaro, A., Moir, S., Monaco, J., Ehler, L., Mizell, S., Jackson, R., Li, Y., Romano, J.W. & Fauci, A.S. (1998) Natural killer cells from human immunodeficiency virus (HIV)-infected individuals are an important source of CC-chemokines nad suppress HIV-1 entry and replication in vitro. J Clin Invest, 102:223-31
- Oram, J.D., Downing, R.G., Akrigg, A., Dollery, A.A., Duggleby, C.J., Wilkinson, G.W. & Greenaway, P.J. (1982) Use of recombinant plasmids to investigate the structure of the human cytomegalovirus genome. J Gen Virol, 59:111-29.
- Orange, J.S., Fassett, M.S., Koopman, L.A., Boyson, J.E. & Strominger, J.L. (2002) Viral evasion of natural killer cells. Nat Immunol, 3:1006-12.
- Pande, H., Terramani, T., Tressel, T., Churchill, M.A., Hawkins, G.G. & Zaia, J.A. (1990) Altered expression of fibronectin gene in cells infected with human cytomegalovirus. J Virol, 64:1366-69.
- Pari, G.S. & Anders, D.G. (1993) Eleven loci encoding trans-acting factors are required for transient complementation of human cytomegalovirus oriLyt-dependent DNA replication. J Virol, 67:6979-88.
- Pari, G.S., Kacica, M.A. & Anders, D.G. (1993) Open reading frames UL44, IRS1/TRS1 and UL36-38 are required for transient complementation of human cytomegalovirus oriLyt-dependent DNA synthesis. J Virol, 67:2575-82.
- Patrone, M., Secchi, M., Fiorina, L., Ierardi, M., Milanesi, G. & Gallina, A. (2005) Human cytomegalovirus UL130 protein promotes endothelial cell infection through a producer cell modification of the virion. J Virol, 79:8361-73
- Patterson, C.E. & Shenk, T. (1999) Human cytomegalovirus UL36 protein is dispensable for viral replication in cultured cells. J Virol, 73:7126-31.
- Pearson, W.R. (1990) Rapid and sensitive sequence comparison with FASTP and FASTA. Methods Enzymol, 183:63-98
- Pearson, W.R. & Lipman, D.J. (1988) Improved tools for biological sequence comparison. Proc Natl Acad Sci U S A, 85:2444-8.

- Penfold, M.E. & Mocarski, E.S. (1997) Formation of cytomegalovirus DNA replication compartments defined by localization of viral proteins and DNA synthesis. Virology, 239:46-61.
- Penfold, M.E., Dairaghi, D.J., Duke, G.M., Saederup, N., Mocarski, E.S., Kemble, G.W. & Schall, T.J. (1999) Cytomegalovirus encodes a potent alpha chemokine. Proc Natl Acad Sci, 96:9839-44.
- Pepperl-Klindworth, S., Besold, K., Frankenberg, N., Farkas, M., Kuball, J., Theobald, M. and Plachter, B. (2006) Cytomegalovirus interleukin-10 expression in infected cells does not impair MHC class I restricted peptide presentation on bystanding antigen-presenting cells. Viral Immunol, 19:92-101.
- Philips, A.J., Tomasec, P., Wang, E.C.Y., Wilkinson, G.W.G. & Borysiewicz, L.K. (1998) Human cytomegalovirus infection downregulates expression of the cellular aminopeptidases CD10 and CD13. Virology, 250:350-58.
- Pignatelli, S., Dal Monte, P., Rossini, G. & Landini M.P. (2004) Genetic polymorphisms among human cytomegalovirus (HCMV) wild type strains. Red Med Virol, 14:383-410.
- Pizzorno, M.C., O'Hare, P., Sha, L., LaFemina, R.L. & Hayward, G.S. (1988) Trans-activation and autoregulation of gene expression by the immediate-early region 2 gene products of human cytomegalovirus. J Virol, 62:1167-79.
- Plachter, B., Singzer, C. & Jahn, G. (1996) Cell types involved in replication and distribution of human cytomegalovirus. Adv Virus Res, 46:195-261.
- Plotkin, S.A., Furukawa, T., Zygraich, N. & Huygelen, C. (1975) Candidate cytomegalovirus strain for human vaccination. Infect Immun, 12:521-27.
- Poole, E., King, C.A., Sinclair, J.H. & Alcami, A. (2006) The UL144 gene product of human cytomegalovirus activates NFkappaB via a TRAF6-dependent mechanism. EMBO J, 25:4390-99.
- Prichard, M.N., Gao, N., Jairath, S., Mulamba, G., Krosky, P., Coen, D.M., Parker, B.O. & Pari, G.S. (1999) A recombinant human cytomegalovirus with a large deletion in UL97 has a severe replication deficiency. J Virol, 73:5663-70.
- Prichard, M.N., Jairath, S., Penfold, M.E., St Jeor, S., Bohlman, M.C & Pari, G.S. (1998) Identification of persistent RNA-DNA hybrid structures within the origin of replication of human cytomegalovirus. J Virol, 72:6997-7004.
- Prichard, M.N., Penfold, M.E., Duke, G.M., Spaete, R.R. & Kemble, G.W. (2001) A review of genetic differences between limited and extensively passaged human cytomegalovirus strains. Rev Med Virol, 11:191-200.
- Prince, V.E. & Pickett, F.B. (2002) Splitting pairs: the diverging fates of duplicated genes. Nat Rev Genet, 3:827-37.
- Prod'homme, V., Griffin, C., Aicheler, R.J., Wang, E.C.Y., McSharry, B.P., Rickards, C.R., Stanton, R.J., Borysiewicz, L.K., Lopez-Botet, M., Wilkinson, G.W.G. & Tomasec, P. (2007) The human cytomegalovirus MHC class I homologue UL18 inhibits LIR-1+ but activates LIR-1- NK cells. J Immunol, 178:4473-81
- Quinnan, G.V., Delery, M., Rook, A.H., Frederick, W.R., Epstein, J.S., Manischewitz, J.F., Jackson, L., Ramsey, K.M., Mittal, K., Plotkin, S.A. *et al.* (1984) Comparitive virulence and immunogenicity of the Towne strain and a nonattenuated strain of cytomegalovirus. Ann Intern Med, 101:478-83

- Quinnan, G.V., Kirmani, N., Rook, A.H., Manischewitz, J.F., Jackson, L., Moreschi, G., Santos, G.W., Saral, R. & Burns, W.H. (1982) Cytotoxic T cells in cytomegalovirus infection: HLA-restricted T lymphocyte and non-T lymphocyte cytotoxic responses correlate with recovery from cytomegalovirus in bone marrow transplant recipients. New Engl J Med, 307:6-13
- Redpath, S., Angulo, A., Gascoigne, N.R. & Ghazel, P. (1999) Murin cytomegalovirus infection down-regulates MHC class II expression on macrophages by induction of IL-10. J Immunol, 162:6701-6707.
- Reed, L.J. and Meunch, H.A. (1983) A simple method of estimating fifty percent endpoints. Am J Trop Med Hyg, 27: 493-97.
- Reeves, M.B., Coleman, H., Chadderton, J., Goddard, M., Sissons, J.G. & Sinclair, J.H. (2004) Vascular endothelial and smooth muscle cells are unlikely to be major sites of latency of human cytomegalovirus in vivo. J Gen Virol, 85:3337-41.
- Reeves, M.B., Lehner, P., Sissons, J.P.G. & Sinclair, J.H. (2005a) An in vitro model for the regulation of human cytomegalovirus latency and reactivation in dendritic cells by chromatin remodelling. J Gen Virol, 86:2949-54.
- Reeves, M.B., MacAry, P, P.A., Lehner, P.J., Sisson, J.G.P. & Sinclair, J.H. (2005b) Latency, chromating remodelling and reactivation of human cytomegalovirus in the dendritic cells of healthy carriers. Proc Natl Acad Sci USA, 102:4140-45.
- Reusser, P., Riddell, S.R., Meyers, J.D. & Greenberg, P.D. (1991) Cytotoxic T-lymphocyte response to cytomegalovirus after human allogeneic bone marrow transplantation: pattern of recovery and correlation with cytomegalovirus infection and disease. Blood, 78: 1373-80.
- Revello, M.G., Baldanti, F., Percivalle, E., Sarasini, A., De Giuli, L., Genini, E., Lilleri, D., Labo, N. & Gerna, G. (2001) In vitro selection of human cytomegalovirus variants unable to transfer virus and virus products from infected cells to polymorphonuclear leukocytes and to grow in endothelial cells. J Gen Virol, 82:1429-38
- Revello, M.G., Zavattoni, M., Sarasini, A., Percivalle, E., Simoncini, L. & Gerna, G. (1998) Human cytomegalovirus in blood of immunocompetent persons during primary infection: Prognostic implications for pregnancy. J Infect Dis, 177:1170-75.
- Reyburn, H.T., Mandelboim, O., Vales-Gomez, M., Davis, D.M., Pazmany, L. & Strominger, J.L. (1997) The class I MHC homologue of human cytomegalovirus inhibts attak by natural killer cells. Nature, 386:514-17.
- Reymond, N., Borg, J.P., Lecocq, E., Adelaide, J., Campadelli-Fiume, G., Dubreuil, P. & Lopez, M. (2000) Human nectin3/PRR3: a novel member of the PVR/PRR/nectin family that interacts with afadin. Gene, 255:347-55.
- Riddell, S.R. & Greenberg, P.D. (1997) T cell therapy of human CMV and EBV infection in immunocompromised hosts. Rev Med Virol, 7:181-92.
- Robertson, M.J., Cochran, K.J., Cameron, C., Le, J.M., Tantravahi, R. & Ritz, J. (1996) Characterization of a cell line, NKL, derived from an aggressive human natural killer cell leukemia. Exp Hematol, 24:406-15.
- Robinson, J., Perez-Rodriguez, M., Waller, M.J., Cuillerier, B., Bahram, S., Yao, Z., Albert, E.D., Madrigal, J.A. & Marsh, S.G. (2001) MICA sequences 2000. Immunogenetics, 53(2):150-69

- Roby, C. & Gibson, W. (1986) Characterization of phosphoproteins and protein kinase activity of virions, noninfectious enveloped particles and dense bodies of human cytomegalovirus. J Virol, 59:714-27.
- Rolle, A., Mousavi-Jazi, M., Eriksson, M., Odeberg, J., Soderberg-Naucler, C., Cosman, D., Karre, K. & Cerboni, C. (2003) Effects of human cytomegalovirus infection on ligands for the activating NKG2D receptor of NK cells: up-regulation of UL16-binding protein (ULBP)1 and ULBP2 is counteracted by the viral UL16 protein. J Immunol, 171:902-8.
- Romanowski, M.J., Garrido-Guerrero, E. & Shenk, T. (1997) pIRS1 and pTRS1 are present in human cytomegalovirus virions. J Virol, 71:5703-5705.
- Rook, A.H. (1988) Interaction of cytomegalovirus with the human immune system. Rev Infect Dis, S3:S460-67.
- Rost, B., Yachdav, G. & Liu, J. (2003) The PredictProtein server. Nucleic Acids Res, 31:3300-04
- Rowe, W.P., Hartley, J.W., Waterman, S., Turner, H.C. and Huebner, R.J. (1956) Cytopathic agent resembling human salivary gland virus recovered from tissues cultured of human adenoids. Proc Soc Exp Biol Med, 92:418-424
- Rubin, R.H. (1990) Impact of cytomegalovirus infection on organ transplant recipients. Rev Infect Dis, 12 (Suppl. 7), S754-66.
- Saederup, N., Lin, Y.C., Dairaghi, D.J., Schall, T.J. & Mocarski, E.S. (1999) Cytomegalovirus-encoded β chemokine promotes monocyte-associated viremia in the host. Proc Natl Acad Sci, 96:10881-86.
- Sague, S.L., Tato, C., Pure, E. & Hunter, C.A. (2004) The regulation and activation of CD44 by natural killer (NK) cells and its role in the production of IFN-gamma. J Interferon Cytokine Res, 24:301-9.
- Sambucetti, L.C., Cherrington, J.M., Wilkinson, G.W. and Mocarski, E.S. (1989) NF-kappa B activation of the cytomegalovirus enhancer is mediated by a viral transactivator and by T cell stimulation. EMBO J, 8:4251-8
- Sanchez, V., Greis, K.D., Sztul, E. & Britt, W.J. (2000b) Accumulation of virion tegument and envelope proteins in a stable cytoplasmic compartment during human cytomegalovirus replication: Characterization of a potential site of virus assembly. J Virol, 74:975-86
- Sanchez, V., Sztul, E. & Britt, W.J. (2000a) Human cytomegalovirus pp28 (UL99) localizes to a cytoplasmic compartment which overlaps the endoplasmic reticulum-Golgi-intermediate compartment. J Virol, 74:3842-51.
- Sarov, I. & Abady, I. (1975) The morphogenesis of human cytomegalovirus. Isolation and polypeptide charcaterization of cytomegalovirus and dense bodies. Virology, 66:464-73.
- Sato, T., Irie, K., Ooshio, T., Ikeda, W. & Takai, Y. (2004) Involvement of heterophilic trans-interaction of Necl-5/Tage4/PVR/CD155 with nectin-3 in formation of nectin- and cadherin-based adherens junctions. Genes Cells, 9:791-9
- Scalzo, A.A., Fitzgerald, N.A., Wallace, C.R., Gibbons, A.E., Smart, Y.C., Burton, R.C. & Shellam, G.R. (1992) The effect of the Cmv-1 resistance gene, which is linked to the natural killer cell gene complex, is mediated by natural killer cells. J Immunol, 149:581-9
- Sconocchia, G., Titus, J.A. & Segal, D.M. (1997) Signaling pathways regulating CD44-dependent cytolysis in natural killer cells. Blood, 90(2):716-25

- Sedarati, F. & Rosenthal, L.J. (1988) Isolation and partial characterization of nucleocapsid forms from cells infected with human cytomegalovirus strains AD169 and Towne. Intervirology, 29:86-100.
- Shamu, C.E., Flierman, D., Ploegh, H.L., Rapoport, T.A. & Chau, V. (2001) Polyubiquitination is required for US11-dependent movement of MHC class I heavy chain from endoplasmic reticulum into cytosol. Mol Biol Cell, 12(8):2546-55.
- Shamu, C.E., Story, C.M., Rapoport, T.A. & Ploegh, H.L. (1999) The pathway of US11-dependent degradation of MHC class I heavy chains involves a ubiquitin-conjugated intermediate. J Cell Biol, 147:45-58.
- Shenk, T (2006) Human cytomegalovirus genomics. In Cytomegalovirus Molecular Biology and Immunology, Ed. Reddehase, M.J. Caister Academic Press, 3:49-61.
- Shenk, T. (2001) Adenoviridae: The viruses and their replication. In Fields Virology, eds Knipe, B.N., Howley, D.M., Chanock, R.M., Melnick, J.L., Monath, T.P., Rolzman, B. and Straws, S.E. Lippincott, Philadelphia, pp2265-300.
- Shiroishi, M., Tsumoto, K., Amano, K., Shirakihara, Y., Colonna, M., Braud, V.M., Allan, D.S., Makadzange, A., Rowland-Jones, S., Willcox, B., Jones, E.Y., van der Merwe, P.A., Kumagai, I. & Maenaka, K. (2003) Human inhibitory receptors Ig-like transcript 2 (ILT2) and ILT4 compete with CD8 for MHC class I binding and bind preferentially to HLA-G. Proc Natl Acad Sci USA, 100:8856-61.
- Siebert, S., Amos, N., Fielding, C.A., Wang, E.C., Aksentijevich, I., Williams, B.D. & Brennan, P. (2005) Reduced tumor necrosis factor signaling in primary human fibroblasts containing a tumor necrosis factor receptor superfamily 1A mutant. Arthritis Rheum, 52:1287-92.
- Sinclair, J. & Sissons, P. (2006) Latency and reactivation of human cytomegalovirus. J Gen Virol, 87:1763-79.
- Sinzger, C., Grefte, A., Plachter, B., Gouw, A.S., The, T.H. & Jahn, G. (1995) Fibroblasts, epithelial cells, endothelial cells and smooth muscle cells are major targets of human cytomegalovirus infection in lung and gastrointestinal tissues. J Gen Virol, 76:741-50
- Sinzger, C., Kahl, M., Laib, K., Klingel, K., Rieger, P., Plachter, B. & Jahn, G. (2000) Tropism of human cytomegalovirus for endothelial cells is determined by a post-entry step dependent on efficient translocation to the nucleus. J Gen Virol, 81:3021-35
- Sinzger, C., Schmidt, K., Knapp, J., Kahl, M., Beck, R., Waldman, J., Hebart, H., Einsele, H. & Jahn, G. (1999) Modification of human cytomegalovirus tropism through propagation in vitro is associated with changes in the viral genome. J Gen Virol, 80:2867-77.
- Skaletskaya, A., Bartle, L.M., Chittenden, T., McCormick, A.L., Mocarski, E.S. & Goldmacher, V.S. (2001) A cytomegalovirus-encoded inhibitor of apoptosis that suppresses caspase 8 activation. Proc Natl Acad Sci, 98:7829-34.
- Soderberg-Naucler, C. & Nelson, J.Y. (1999) Human cytomegalovirus latency and reactivation - A delicate balance between the virus and its host's immune system. Intervirology, 42:314-21.

- Soderberg-Naucler, C., Fish, K.N. & Nelson, J.A. (1997) Reactivation of latent cytomegalovirus by allogeneic stimulation of blood cells from healthy donors. Cell, 91:119-26.
- Sohn, H.W., Shin, Y.K., Lee, I.S., Bae, Y.M., Suh, Y.H., Kim, M.K., Kim, T.J., Jung, K.C., Park, W.S., Park, C.S., Chung, D.H., Ahn, K., Kim, I.S., Ko, Y.H., Bang, Y.J., Kim, C.W. & Park, S.H. (2001) CD99 regulates the transport of MHC class I molecules from the Golgi complex to the cell surface. J Immunol, 166:787-94
- Spaderna, S., Blessing, H., Bogner, E., Britt, W. & Mach, M. (2002) Identification of glycoprotein gpTRL10 as a structural component of human cytomegalovirus. J Virol, 76:1450-60.
- Spaderna, S., Kropff, B., Kodel, Y., Shen, S., Coley, S., Lu, S., Britt, W. & Mach, M. (2005) Deletion of gpUL132, a structural component of human cytomegalovirus, results in impaired virus replication in fibroblasts. J Virol, 79: 11837-47.
- Spaete, R.R. & Mocarski, E.S. (1985) The a sequence of the cytomegalovirus genome functions as a cleavage/ packaging signal for herpes simplex virus defective genomes. J Virol, 54:817-24
- Spaete, R.R., Gehrz, R.C. & Landini, M.P. (1994) Human cytomegalovirus structural proteins. J Gen Virol, 75: 3287-308.
- Spaete, R.R., Perot, K., Scott, P.I., Nelson, J.A., Stinski, M.F. & Pachl, C. (1993) Coexpression of truncated human cytomegalovirus gH with the UL115 gene product or the truncated human fibroblast growth factor receptor results in transport of gH to the cell surface. Virology, 193:853-61
- Spear, G.T., Lurain, N.S., Parker, C.J., Ghassemi, M., Payne, G.H. & Saifuddin, M. (1995). Host cell-derived complement control proteins CD55 and CD59 are incorporated into the virions of two unrelated enveloped viruses. Human T cell leukemia/ lymphoma virus type I (HTLV-I) and human cytomegalovirus (HCMV). J Immunol, 155:4376-81
- Spector, D.H. (1996) Activation and regulation of human cytomegalovirus early genes. Intervirology, 39:361-77.
- Spiller, O.B., Hanna, S.M., Devine D.V. & Tufaro, F. (1997) Neutralization of virions: the role of complement. J Infect Dis, 176:339-47.
- Spiller, O.B., Morgan, B.P., Tufaro, F. & Devine, D.V. (1996) Altered expression of host-encoded complement regulators on human cytomegalovirus infected cells. Eur J Immunol, 26:1532-38.
- Stanier, P., Kitchen, A.D., Taylor, D.L. and Tyms, A.S. (1992) Detection of human cytomegalovirus in peripheral blood mononuclear cells and urine samples using PCR. Mol Cell Probes, 6:51-8
- Stannard, L.M. (1989) B2 microglobulin binds to the tegument of cytomegalovirus: an immunogold study. J Gen Virol, 70:2179-84.
- Stanton, R.J., McSharry, B.P., Armstrong, M.L., Tomasec, P. & Wilkinson, G.W. (2007) Direct recombineering into an efficient adenovirus vector system suitable for high throughput cloning. *unpublished.*
- Stenberg, R.M. (1996) The human cytomegalovirus major immediate early gene. Intervirology, 39:343-49.
- Stern, N., Markel, G., Arnon, T.I., Gruda, R., Wong, H., Gray-Owen, S.D. & Mandelboim, O. (2005) Carcinoembryonic antigen (CEA) inhibits NK killing

via interaction with CEA-related cell adhesion molecule 1. J Immunol, 174(11):6692-701

- Story, C.M., Furman, M.H. & Ploegh, H.L. (1999) The cytosolic tail of class I MHC heavy chain is required for its dislocation by the human cytomegalovirus US2 and US11 gene products. Proc Natl Acad Sci USA, 96 (15):8516-21.
- Streblow, D.N., Soderberg-Naucler, C., Vieira, J., Smith, P., Wakabayashi, E., Ruchti, F., Mattison, K., Altschuler, Y. & Nelson, J.A. (1999) The human cytomegalovirus chemokine receptor US28 mediates vascular smooth muscle cell migration. Cell, 99:511-20
- Talbot, P. & Almeida, J.D. (1977) Human cytomegalovirus: purification of enveloped virions and dense bodies. J Gen Virol, 36:345-49.
- Taylor-Weideman, J., Hayhurst, G.P., Sissons, J.G.P & Sinclair, J.H. (1993) Polymorphonuclear cells are not sites of persistence of human cytomegalovirus in healthy individuals. J Gen Virol, 74:265-68.
- Taylor-Weideman, J., Sissons, J.G.P., Borysiewicz, L.K. & Sinclair, J.H. (1991) Monocytes are a major site of persistance of human cytomegalovirus in peripheral blood mononuclear cells. J Gen Virol, 72:2059-64
- Terhurne, S.S., Schroer, J. & Shenk, T. (2004) RNAs are packaged into human cytomegalovirus virions in proportion to their intracellular concentration. J Virol, 78:10390-98.
- Thale, R., Lucin, P., Schneider, K., Eggers, M. & Koszinowski, U.H. (1994) Identification and expression of a murine cytomegalovirus early gene coding for an Fc receptor. J Virol, 68:7757-65.
- Thomsen, D.R., Stenberg, R.M., Goins, W.F. & Stinski, M.F. (1984) Promoter-regulatory reion of the major immediate early gene of human cytomegalovirus. Proc Natl Acad Sci USA, 81:659-63.
- Tomasec, P., Braud, V.M., Rickards, C., Powell, M.B., McSharry, B.P., Gadola, S., Cerundolo, V., Borysiewicz, L.K., McMichael, A.J. & Wilkinson, G.W. (2000) Surface expression of HLA-E, an inhibitor of natural killer cells, enhanced by human cytomegalovirus gpUL40. Science, 287:1031.
- Tomasec, P., Wang, E.C., Davison, A.J., Vojtesek, B., Armstrong, M., Griffin, C., McSharry, B.P., Morris, R.J., Llewellyn-Lacey, S., Rickards, C., Nomoto, A., Sinzger, C. & Wilkinson, G.W. (2005) Downregulation of natural killer cell-activating ligand CD155 by human cytomegalovirus UL141. Nat Immunol, 6:181-88.
- Tomasec, P., Wang, E.C., Groh, V., Spies, T., McSharry, B.P., Aicheler, R.J., Stanton, R.J. & Wilkinson, G.W. (2007) Adenovirus vector delivery stimulates natural killer cell recognition. J Gen Virol, 88:1103-08.
- Tomazin, R., Boname, J., Hegde, N.R., Lewinsohn, D.M., Altschuler, Y., Jones, T.R., Cresswell, P., Nelson, J.A., Riddell, S.R. & Johnson, D.C. (1999) Cytomegalovirus US2 destroys two components of the MHC class II pathway, preventing recognition by CD4+ T cells. Nat Med, 5:1039-43
- Tooze, J., Hollinshead, M., Reis, B., Radsak, K. & Kern, H. (1993) Progeny vaccinia and human cytomegalovirus particles utilize early endosomal cisternae for their envelopes. Eur J Cell Biol, 60:163-78.
- Townsend, A. & Bodmer, H. (1989) Antigen recognition by class I restricted T-lymphocytes. Annu Rev Immunol, 7:601-24.

- Trus, B.L., Gibson, W., Cheng, N. & Steven, A.C. (1999) Capsid structure of simian cytomegalovirus from cryoelectron microscopy: Evidence for tegument attachment sites. J Virol, 73:2181-92.
- Tugizov, S., Maidji, E., Xiao, J., Zheng, Z. & Pereira, L. (1998) Human cytomegalovirus glycoprotein B contains autonomous determinants for vectorial targeting to apical membranes of polarized epithelial cells. J Virol, 72:7374-86.
- Uhrberg, M. (2005) The CD107 mobilization assay: Viable isolation and immunotherapeutic potential of tumour-cytolytic NK cells. Leukemia, 19:707-09.
- Ulbrecht, M., Martinozzi, S., Grzeschik, M., Hengel, H., Ellwart, J.W., Pla, M. & Weiss, E.H. (2000) Cutting edge: The human cytomegalovirus UL40 gene product contains a ligand for HLA-E and prevents NK cell-mediated lysis. J Immunol, 164: 5019-22.
- Varnum, S.M., Streblow, D.N., Monroe, M.E., Smith, P., Aubrey, K.J., Pasa-Tolic, L., Wang, D., Camp, D.G. 2nd, Rodland, K., Wiley, S., Britt, W., Shenk, T., Smith, R.D. & Nelson, J.A. (2004) Identification of proteins in human cytomegalovirus (HCMV) particles: the HCMV proteome. J Virol, 78:10960-66
- Waldman, W.J., Sneddon, J.M., Stephens, R.E. & Roberts, W.H. (1989) Enhanced endothelial cytopathogenicity induced by a cytomegalovirus strain propagated in endothelial cells. J Med Virol, 28:223-30.
- Wang, D. & Shenk, T. (2005) Human cytomegalovirus virion protein complex required for epithelial and endothelial cell tropism. Proc Natl Acad Sci U S A, 102:18153-8
- Wang, D., Bresnahan, W. & Shenk, T. (2004) Human cytomegalovirus encodes a highly specific RANTES decoy receptor. Proc Natl Acad Sci USA, 101:16642-47.
- Wang, E.C., McSharry, B.P., Retiere, C., Tomasec, P., Williams, S., Borysiewicz, L.K., Braud, V.M. & Wilkinson, G.W. (2002) UL40-mediated NK evasion during productive infection with human cytomegalovirus. Proc Natl Acad Sci USA, 99: 7570-75.
- Wang, X., Kenyon, W.J., Li, Q., Mullberg, J. and Hutt-Fletcher, L.M. (1998) Epstein-Barr virus uses different complexes of glycoproteins gH and gL to infect B lymphocytes and epithelial cells. J Virol, 72:5552-58.
- Warren, A.P., Ducroq, D.H., Lehner, P.J. & Borysiewicz, L.K. (1994a) Human cytomegalovirus-infected cells have unstable assembly of major histocompatibility complex class I complexes and are resistant to lysis by cytotoxic T lymphocytes. J Virol, 68:2822-29
- Warren, A.P., Owens, C.N., Borysiewicz, L.K. & Patel, K. (1994b) Downregulation of integrin alpha 1/beta 1expression and association with cell rounding in human cytomegalovirus infected fibroblasts. J Gen Virol, 75:3319-25.
- Weiland, K.L., Oien, N.L., Homa, F. & Wathen, W. (1994) Functional analysis of human cytomegalovirus polymerase accessory protein. Virus Res, 34:191-206.
- Welte, S., Kuttruff, S., Waldhauer, I. & Steinle, A. (2006) Mutual activation of natural killer cells and monocytes mediated by NKp80-AICL interaction. Nat Immunol, 7:1334-42.

- Welte, S.A., Singzer, C., Lutz, S.Z., Singh-Jasuja, H., Sampaio, K.L., Eknigk, U., Rammensee, H-G. & Steinle, A. (2003) Selective intracellular retention of virally induced NKG2D ligands by the human cytomegalovirus UL16 glycoprotein. Eur J Immunol, 33:194-203.
- Westrate, M.W., Geelen, J.L. & van der Noordaa, J. (1980) Human cytomegalovirus DNA: physical maps for restriction endonucleases BglII, HindIII and XbaI. J Gen Virol, 49:1-21.
- Wiertz, E.J., Jones, T.R., Sun, L., Bogyo, M., Geuze, H.J. & Ploegh, H.L. (1996a) The human cytomegalovirus US11 gene product dislocates MHC class I heavy chains from the endoplasmic reticulum to the cytosol. Cell, 84:769-79.
- Wiertz, E.J., Tortorella, D., Bogyo, M., Yu, J., Mothes, W., Jones, T.R., Rapoport, T.A. & Ploegh, H.L. (1996b) Sec61-mediated transfer of a membrane protein from the endolasmic reticulum to the proteosome for destruction. Nature, 384:432-38.
- Wiertz, E.J.H.J., Mukherjee, S. & Ploegh, H.L. (1997) Viruses use stealth technology to escape from the host immune system. Mol Med Today, 3:116-23.
- Wilkinson, G.W. & Akrigg, A. (1992) Constitutive and enhanced expression from the CMV major IE promoter in a defective adenovirus vector. Nucleic Acids Res, 20:2233-39.
- Wilkinson, G.W., Kelly, C., Sinclair, J.H. & Rickards, C. (1998) Disruption of PML-associated nuclear bodies mediated by the human cytomegalovirus major immediate early gene product. J Gen Virol, 79:1233-45.
- Wilkinson, G.W.G., Akrigg, A. & Greenaway, P.J. (1984). Transcription of the immediate early genes of human cytomegalovirus. Virus Research, 1:101-16
- Willcox, B.E., Thomas, L.M. & Bjorkman, P.J. (2003) Crystal structure of HLA-A2 bound to LIR-1, a host and viral major histocompatibility complex receptor. Nat Immunol, 4:913-9.
- Wills, M.R., Ashiru, O., Reeves, M.B., Okecha, G., Trowsdale, J., Tomasec, P., Wilkinson, G.W., Sinclair, J. & Sissons, J.G. (2005) Human cytomegalovirus encodes an MHC class I-like molecule (UL142) that functions to inhibit NK cell lysis. J Immunol, 175:7457-65.
- Wills, M.R., Carmichael, A.J., Maynard, K., Xin, J., Weekes, M.P., Plachter, B. and Sissons, J.G. (1996) The human cytotoxic T-lymphocyte (CTL) response to cytomegalovirus is dominated by structural protein pp65: frequency, specificity and T-cell receptor usage of pp65-specific CTL. J Virol, 70: 7569-79
- Winkler, M. & Stamminger, T. (1996) A specific subform of the human cytomegalovirus transactivator proein pUL69 is contained within the tegument of virus particles. J Virol, 70:8984-87.
- Winkler, M., Schmolke, S., Plachter, B. & Stamminger, T. (1995) The pUL69 protein of human cytomegalovirus (HCMV), a homologue of the herpes simplex virus ICP27, is contained within the tegument of virions and activates the major immediate early enhancer of HCMV in synergy with the tegument protein pp71 (ppUL82). Scand J Infect Dis Suppl, 99:8-9

- Wolf, D.G., Honigman, A., Lazarovits, J., Tavor, E. & Panet, A. (1998) Characterization of the human cytomegalovirus UL97 gene product as a virion associated protein kinase. Arch Virol, 143:1223-32.
- Wood, L.J., Baxter, M.K., Plafker, S.M. & Gibson, W. (1997) Human cytomegalovirus capsid assembly protein precursor (pUL80.5) interacts with itself and with the major capsid protein (pUL86) through two different domains. J Virol, 71:179-90.
- Woodhall, D.L., Groves, I.J., Reeves, M.B., Wilkinson, G.W. & Sinclair, J.H. (2006) Human Daxx-mediated repression of human cytomegalovirus gene expression correlates with a repressive chromatin structure around the major immediate early promoter. J Biol Chem, 281:37652-60
- Wright, D.A., Staprans, S.I. & Spector, D.H. (1988) Four phosphoproteins with common amino termini are encoded by human cytomegalovirus AD169. J Virol, 62:331-40.
- Wright, H.T. Jr, Goodheart, C.R. & Lielausis, A. (1964) Human cytomegalovirus morphology by negative staining. Virology, 23:419-24.
- Wright, J.F., Kurosky, A., Pryzdial, E.L. & Wasi, S. (1995) Host cellular annexin II is associated with cytomegalovirus particles isolated from cultured human fibroblasts. J Virol, 69:4784-91.
- Wu, J., Chalupny, N.J., Manley, T.J., Riddell, S.R., Cosman, D. & Spies, T. (2003) Intracellular retention of the MHC class I-related chain B ligand of NKG2D by the human cytomegalovirus UL16 glycoprotein. J Immunol, 170:4196-200.
- Xu-Bin, Murayama, T., Ishida, K., & Furukawa, T. (1989) Characterisation of IgG Fc receptors induced by human cytomegalovirus. J Gen Virol, 70:893-900.
- Young, N.T., Uhrberg, M., Phillips, J.H., Lanier, L.L. & Parham, P. (2001) Differential expression of leukocyte receptor complex encoded Ig-like receptors correlates with the transition from effector to memory CTL. J Immunol, 166:3933-41.
- Yu, X., Shah, S., Atanasov, I., Lo, P., Liu, F., Britt, W.J. & Zhou, Z.H. (2005) Three-dimensional localization of the smallest capsid protein in the human cytomegalovirus capsid. J Virol, 79:1327-32.
- Zanghellini, F., Boppana, S.B., Emery, V.C., Griffiths, P.D. & Pass, R.F. (1999) Asymptomatic primary cytomegalovirus infection: Virologic and Immunologic features. J Infect Dis, 180:702-07.
- Zeng, M., Smith, S.K., Siegel, F., Shi, Z., Van Kampen, K.R., Elmets, C.A. & Tang, D.C. (2001) AdEasy system made easier by selecting the viral backbone plasmid preceding homologous recombination. Biotechniques, 31:260-62.
- Zhou, Z.H., Chen, D.H., Jakana, J., Rixon, F.J. & Chiu, W. (1999) Visualisation of tegument-capsid interactions and DNA in intact herpes simplex virus type I virions. J Virol, 73:3210-18.
- Zhu, H., Shen, Y & Shenk, T. (1995) Human cytomegalovirus IE1 and IE2 proteins block apoptosis. J Virol, 69:7960-70.
- Zinkernagel, R.M. (1996) Immunology taught by viruses. Science, 271:173-78.
- Zinkernagel, R.M. & Doherty, P.C. (1979) MHC-restricted cytotoxic T cells: studies on the biological role of polymorphic major transplantation antigens

determining T cell restricition-specificity, function and responsiveness. Adv Immunol, 27:51-57.

- Zlotnik, A. & Yoshie, O. (2000) Chemokines: a new classification system and their role in immunity. Immunity, 12:121-27.
- Zou, Y., Bresnahan, W., Taylor, R.T. & Stastny, P. (2005) Effect of human cytomegalovirus on expression of MHC class I-related chains A. J Immunol, 174(5):3098-104

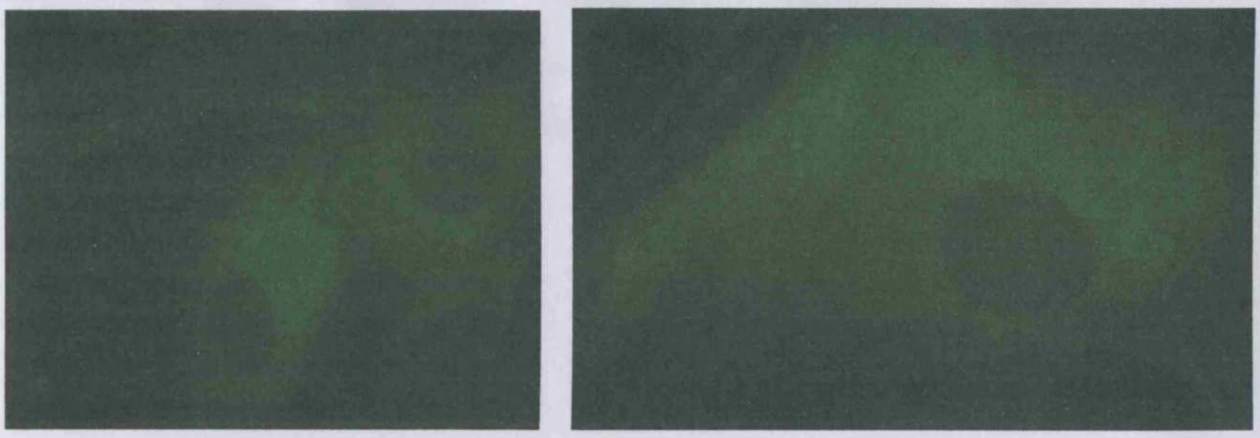

APPENDIX I Chapter 4: pUL130 produces a cytoplasmic staining pattern in RAdUL130 infected fibroblasts

RAdUL130 infected HFFF-htert (MOI of 100) were fixed and permeabilized at 72hpi. pUL130-FLAG tag was detected using α-FLAG-specific monoclonal antibody and an α-mouse IgG-FITC secondary. (Images kindly provided by Dr B. McSharry).

APPENDIX II Chapter 5: Screen of RAdUL14-infected fibroblasts with polyclonal NK bulk cultures from multiple donors in CD107 assays
(Assays performed by Dr V. Prod'homme)

	% anti-CD107a mAb			Specific Lysis as a percentage of RAd592 control		
Donor	**RAd592**	**RAdUL141**	**RAdUL14**	**RAd592**	**RAdUL141**	**RAdUL14**
Donor 7	11.8	3.9	6.4	100.0	33.5	54.0
Donor 9	31.6	12.0	19.6	100.0	37.8	62.1
Donor 8	7.9	3.9	9.4	100.0	49.7	119.0
237A	19.2	8.6	12.8	100.0	44.8	66.9
6162	20.7	13.7	19.7	100.0	66.3	95.2
618Z	26.3	21.8	26.3	100.0	82.8	99.7
705G	10.3	6.5	9.0	100.0	62.5	86.9
683N	11.4	4.0	5.8	100.0	35.5	51.2
004W	3.3	2.8	4.3	100.0	85.7	130.9
071F	11.0	9.9	11.8	100.0	90.1	107.5
420A	10.0	9.8	7.0	100.0	98.3	70.5
907M	22.0	13.0	23.8	100.0	59.1	108.2
421V	13.5	7.7	13.6	100.0	56.9	100.6

APPENDIX III Chapter 5: Screen of UL/*b'* RAd-infected fibroblasts with polyclonal NK bulk cultures from multiple donors in CD107 assays

(Assays performed by Dr V. Prod'homme. Lysis is given as a percentage of the RAd592 control which is taken as 100% lysed).

	% Specific Lysis as a percentage of RAd592 control																
Donor	**RAd592**	**UL141**	**UL130**	**UL135**	**UL139**	**UL140**	**UL141A**	**UL144**	**UL145**	**UL146**	**UL147**	**UL147A**	**UL148A**	**UL148B**	**UL148C**	**UL148D**	**UL150**
Donor 7	100	33.5		49.6								64.3					
237A	100	44.8		52.6		51.4	143.4				106.1	54.7	60.6	87.7			
Donor 8	100	37.8	95.1	76.1		84.3	78.9		91.1	92.8	81.4	76.4	90.8	77.9	83.1	67.8	
705G	100	62.5	101.1	43.3		83.0	88.7		77.5	100.0	81.4	96.3	108.6	95.5	93.4	91.2	
071F	100	90.1	104.0	66.0		101.1	90.5		92.1	90.7	86.2	98.1	116.9	104.5	96.2	103.6	
683N	100	35.5	100.2	93.3		96.7	93.7		101.8	89.5	97.1		114.7	88.5	89.5	96.5	
6122	100	66.3	92.2	66.5		80.7	92.0		82.9	76.1				78.0		66.8	
618Z	100	84.8	74.7	54.8		80.5	91.6		82.3	81.8	69.5	65.4	95.0	84.8		81.4	
683N1	100	58.8	101.9			93.6	96.8		101.6	127.4	97.1	141.9		105.9		99.0	
907M	100	93.2	84.4			87.0					97.4	100.5		104.3		107.4	
004W	100	98.5	112.5	61.0		93.7	127.1			154.4	104.8	83.6		120.5		124.8	
420A	100	98.3	91.8	76.0		92.5	104.3		112.2	103.8	94.3	101.9		91.5		96.2	
907M	100	59.1		58.5													
421V	100	81.1		63.9	86			75.5									80.9
421V2	100	56.9															
421V1	100			69.6													
Donor 7 IFNa	100	52.9		89.2													
Donor 9 IFNa	100	49.7		47.7													
	% anti-CD107a mAb																
Donor 7	11.8	3.9		5.8								7.6					
237A	19.2	8.6		10.1		9.8	27.5				20.3	10.5	11.6	16.8			
Donor 8	31.6	12.0	30.1	24.1		26.7	24.9		28.8	29.3	25.7	24.1	28.7	24.6	26.3	21.4	
705G	17.7	11.0	17.9	7.7		14.7	15.7		13.7	17.7	14.4	17.0	19.2	16.9	16.5	16.1	
071F	24.7	22.3	25.7	16.3		25.0	22.4		22.8	22.4	21.3	24.2	28.9	25.8	23.8	25.6	
683N	9.8	3.5	9.9	9.2		9.5	9.2		10.0	8.8	9.6		11.3	8.7	8.8	9.5	
6122	31.0	20.5	28.6	20.6		25.0	28.5		25.7	23.6				24.2		20.7	
618Z	29.0	24.6	21.7	15.9		23.4	26.6		23.9	23.7	20.2	19.0	27.6	24.6	24.7	23.6	
683N1	9.1	5.4	9.3			8.5	8.8		9.3	11.6	8.8	12.9		9.6		9.0	
907M	22.3	20.8	18.9			19.4					21.8	22.4		23.3		24.0	
004W	8.1	7.9	9.1	4.9		7.6	10.3			12.5	8.5	6.8		9.7		10.1	
420A	10.0	9.8	9.2	7.6		9.2	10.4		11.2	10.4	9.4	10.2		9.1		9.6	
907M	22.0	13.0		12.9													
421V	9.5	7.7		6.0	8.1			7.1									7.7
421V2	14.5	8.9															
421V1	14.8			10.3													
Donor 7 IFNa	3.7	2.0		3.3													
Donor 9 IFNa	7.9	3.9		3.8													

APPENDIX IV Chapter 5: Classification of individual NK clone responses from NK cytotoxicity assays with K562, RAdUL14, RAdUL141, RAdUL135 and RAd592-infected fibroblasts.

	% Specific Lysis					Classification		
Clone	K562	RAd592	RAdUL14	RAdUL135	RAdUL141	RAdUL14 Classified	RAdUL135 Classified	RAdUL141 Classified
RS9C4	11.2	32.8	11.4	23.5	29.8	Inhibited	Inhibited	No change
RS1B5	24.7	0.0	3.3	no exp	no exp	No kill no change		
RS1G3	9.3	0.0	1.4	no exp	no exp	NA		
RS10E11	30.7	0.0	19.6	no exp	no exp	Activated		
RS5F3	12.5	0.0	2.4	no exp	no exp	No kill no change		
RS3F11	42.3	0.0	15.7	no exp	no exp	Activated		
RS9D3	18.2	0.0	8.4	no exp	no exp	No kill no change		
LC10B8	14.4	0.0	10.2	no exp	no exp	No kill no change		
LC6GG	9.3	0.0	10.7	no exp	no exp	NA		
LC7E2	7.6	16.1	7.8	no exp	no exp	NA		
RS1E9	52.3	20.5	50.7	0.0	34.1	Activated	Inhibited	Activated
RS10F5	57.4	30.1	44.1	20.1	26.6	Activated	Inhibited	No change
RS9B3	50.9	16.4	42.6	0.0	21.8	Activated	Inhibited	No change
RS4F5	45.6	12.4	17.5	0.0	6.5	No change	Inhibited	No change
RS2D4	19.3	20.2	8.8	0.0	13.7	Inhibited	Inhibited	No change
RS5G2	42.7	21.8	24.8	7.8	14.3	No change	Inhibited	No change
RS2F10	55.5	40.9	17.9	0.0	10.9	Inhibited	Inhibited	Inhibited
RS10B2	68.3	23.0	27.5	10.2	7.6	No change	Inhibited	Inhibited
RS3D10	36.9	7.0	22.8	0.0	6.3	Activated	No kill no change	No kill no change
RS8F10	69.8	16.9	34.3	9.1	54.0	Activated	No change	Activated
RS5G5	55.6	29.9	23.8	0.0	19.7	No change	Inhibited	Inhibited
RS7E3	42.0	14.1	43.1	14.9	26.1	Activated	No change	Activated
RS10B4	77.9	35.0	63.5	19.6	16.9	Activated	Inhibited	Inhibited
RS3D9	67.2	16.2	37.9	9.1	2.7	Activated	No change	Inhibited
RS1D8	12.7	21.3	2.8	9.5	18.1	Inhibited	Inhibited	No change
RS5E10	34.7	14.2	1.8	7.5	4.5	Inhibited	No change	Inhibited
RS6E9	32.7	16.0	5.9	5.7	1.4	Inhibited	Inhibited	Inhibited
RS10D6	84.4	2.1	19.4	4.1	0.2	No Kill Activated	No kill no change	No kill no change
RS1B5	78.7	15.7	32.7	5.1	8.5	Activated	Inhibited	No change
RS9G9	84.9	23.8	37.8	5.6	7.3	Activated	Inhibited	Inhibited
RS6B9	72.2	13.8	22.6	6.4	5.6	No change	No change	No change
RS1B3	43.5	16.9	3.3	3.6	0.7	Inhibited	Inhibited	Inhibited
RS9B2	32.8	22.6	24.6	6.3	3.4	No change	Inhibited	Inhibited
RS9E7	63.7	20.2	14.6	8.2	2.8	No change	Inhibited	Inhibited
RS3E4	76.4	31.1	58.8	24.4	19.0	Activated	No change	Inhibited
RS6B8	54.4	0.0	11.6	9.7	0.0	No Kill Activated	No kill no change	No kill no change
RS8G5	40.0	0.0	11.7	6.2	3.4	No Kill Activated	No kill no change	No kill no change
RS1D2	17.2	0.0	1.1	no exp	no exp	No kill no change		
RS10D8	65.3	19.1	50.0	no exp	no exp	Activated		
RS2C7	12.4	5.3	10.4	0.3	6.5	No kill no change	No kill no change	No kill no change
RS10B6	17.6	2.2	8.0	no exp	no exp	No kill no change		
RS10D2	4.6	4.6	4.3	no exp	no exp	NA		

	% Specific Lysis					Classification		
Clone	K562	RAd592	RAdUL14	RAdUL135	RAdUL141	RAdUL14 Classified	RAdUL135 Classified	RAdUL141 Classified
RS1C10	67.0	19.8	73.1	12.4	41.0	Activated	No change	Activated
RS10G2	70.2	7.4	39.2	3.1	4.9	No Kill Activated	No kill no change	No kill no change
RS5D9	50.0	4.8	21.8	0.6	2.7	No Kill Activated	No kill no change	No kill no change
RS10E5	27.3	5.6	15.4	2.9	12.5	No kill no change	No kill no change	No kill no change
RS6B10	17.1	4.8	11.2	1.6	2.0	No kill no change	No kill no change	No kill no change
RS7D4	29.3	4.3	12.0	3.0	4.6	No kill no change	No kill no change	No kill no change
RS4F6	70.3	2.3	29.5	1.8	5.4	No Kill Activated	No kill no change	No kill no change
RS4F10	36.6	7.3	22.5	3.7	10.4	No Kill Activated	No kill no change	No kill no change
RS6D9	12.1	1.4	7.6	0.9	0.0	No kill no change	No kill no change	No kill no change
RS3C2	64.0	12.4	51.8	5.8	19.4	Activated	No change	No change
RS2E9	18.5	1.5	10.9	4.3	10.7	No kill no change	No kill no change	No kill no change
RS8B8	28.3	1.6	8.6	2.4	5.2	No kill no change	No kill no change	No kill no change
RS3F2	55.2	1.7	16.3	2.0	3.3	No Kill Activated	No kill no change	No kill no change
RS3G5	41.2	5.2	11.7	0.2	5.2	No kill no change	No kill no change	No kill no change
RS9D5	47.0	0.6	15.7	2.6	6.9	No Kill Activated	No kill no change	No kill no change
RS6B11	20.1	0.0	6.1	4.3	0.0	No kill no change	No kill no change	No kill no change
RS4E10	44.3	0.0	14.5	no exp	no exp	No Kill Activated		
RS7D7	59.3	0.0	22.7	2.2	0.0	No Kill Activated	No kill no change	No kill no change
RS7E8	64.1	0.0	31.9	5.1	5.8	No Kill Activated	No kill no change	No kill no change
LC8E3	49.1	15.1	27.9	12.5	16.0	Activated	No change	No change
LC5G2	39.3	35.6	43.5	17.6	44.5	No change	Inhibited	No change
LC2F2	55.6	80.2	65.6	34.6	37.4	Inhibited	Inhibited	Inhibited
LC8B10	60.6	22.4	65.5	7.7	41.2	Activated	Inhibited	Activated
LC5B8	45.4	18.2	52.6	3.5	26.7	Activated	Inhibited	No change
LC6D8	71.0	37.8	83.0	9.7	42.0	Activated	Inhibited	No change
LC6E11	50.7	36.8	49.8	15.1	34.4	Activated	Inhibited	No change
LC6B8	29.8	14.3	7.6	6.9	17.5	No change	No change	No change
LC8C11	43.2	29.4	20.5	5.8	27.8	No change	Inhibited	No change
LC8F10	48.1	49.6	46.1	10.2	31.6	No change	Inhibited	Inhibited
LC8G4	47.0	41.2	25.3	6.3	14.6	Inhibited	Inhibited	Inhibited
LC3G10	43.8	58.3	40.1	13.2	73.5	Inhibited	Inhibited	Activated
LC1C9	66.3	54.3	67.1	28.5	48.5	Activated	Inhibited	No change
LC8D1	57.5	36.3	58.4	18.6	65.8	Activated	Inhibited	Activated
LC7C11	40.7	29.1	25.1	15.3	40.0	No change	Inhibited	Activated
LC9C2	52.2	37.6	45.7	12.6	52.9	No change	Inhibited	Activated
LC10G11	29.8	28.3	14.3	13.4	33.8	Inhibited	Inhibited	No change
LC9F5	49.5	84.6	26.8	11.7	43.5	Inhibited	Inhibited	Inhibited
LC3B11	44.3	24.4	47.7	16.2	61.1	Activated	No change	Activated
LC8C9	51.1	20.3	30.8	15.3	47.3	Activated	No change	Activated
LC8G10	44.2	53.3	68.3	13.8	55.2	Activated	Inhibited	No change
LC9F4	33.4	23.8	23.1	4.9	13.3	No change	Inhibited	Inhibited
LC4G5	53.3	20.3	44.5	4.8	42.7	Activated	Inhibited	Activated

Appendix IV Chapter 5: continued

	% Specific Lysis					Classification		
Clone	K562	RAd592	RAdUL14	RAdUL135	RAdUL141	RAdUL14 Classified	RAdUL135 Classified	RAdUL141 Classified
LC9B4	36.0	13.2	26.8	9.1	35.1	Activated	Inhibited	Activated
LC8C3	36.1	17.8	24.8	11.1	22.1	No change	No change	No change
LC8C8	62.7	33.0	27.2	10.6	23.2	No change	Inhibited	Inhibited
LC4D2	35.0	16.2	6.7	5.8	6.7	Inhibited	Inhibited	Inhibited
LC7E4	55.7	19.4	32.6	0.0	18.8	Activated	Inhibited	No change
LC9B8	58.9	21.7	26.4	12.1	8.2	No change	No change	Inhibited
LC6B11	61.9	13.9	23.1	4.9	18.7	No change	No change	No change
LC6F11	41.8	2.6	26.2	6.2	20.7	Activated	No kill no change	Activated
LC6G10	53.0	10.6	30.2	8.6	13.0	Activated	No change	No change
LC5G10	54.5	5.1	6.5	5.4	20.2	No kill no change	No kill no change	Activated
LC8B2	44.9	10.5	35.0	0.9	18.5	Activated	Inhibited	No change
LC10C7	47.4	5.2	15.9	0.0	10.6	Activated	No kill no change	No kill no change
LC3D3	23.5	24.7	48.0	0.0	14.8	Activated	Inhibited	Inhibited
LC3E10	35.2	10.7	20.2	0.0	16.3	Activated	Inhibited	No change
LC3F3	30.9	19.3	3.8	0.0	9.1	Inhibited	Inhibited	Inhibited
LC1C5	16.0	10.8	5.3	0.0	5.6	No change	Inhibited	No change
LC7F4	33.3	5.5	14.4	0.0	6.4	No kill no change	No kill no change	No kill no change
LC7E2	49.0	14.8	22.4	0.0	14.4	No change	Inhibited	No change
LC7D9	30.9	4.4	8.6	6.4	0.9	No kill no change	No kill no change	No kill no change
LC10E5	53.7	15.1	22.7	16.5	12.0	No change	No change	No change
LC3G6	28.5	2.9	29.9	0.0	2.8	Activated	No kill no change	No kill no change
LC3B3	33.7	4.0	9.9	0.7	1.6	No kill no change	No kill no change	No kill no change
LC9D4	53.1	2.5	16.2	4.4	1.2	No kill	No kill no change	No kill no change
LC4B5	48.1	6.2	44.9	5.2	5.6	Activated	No kill no change	No kill no change
LC2G6	38.7	11.8	24.7	1.8	9.0	Activated	Inhibited	No change
LC4C8	17.9	17.4	0.0	4.9	8.5	Inhibited	Inhibited	Inhibited
LC2E10	59.4	18.7	35.1	2.3	28.7	Activated	Inhibited	Activated
LC8D7	19.2	23.3	8.4	4.3	8.6	Inhibited	Inhibited	Inhibited